frontiers

RESEARCH TOPICS

GLOBAL HOST PROTEOMIC RESPONSES TO VIRUS INFECTION

Topic Editors
Kevin Coombs and Ben Berkhout

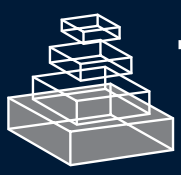

frontiers in MICROBIOLOGY

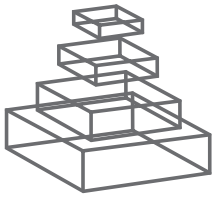

frontiers

Cover image provided by Ibbl sarl, Lausanne CH

ISSN 1664-8714
ISBN 978-2-88919-120-8
DOI 10.3389/978-2-88919-120-8

ABOUT FRONTIERS

Frontiers is more than just an open-access publisher of scholarly articles: it is a pioneering approach to the world of academia, radically improving the way scholarly research is managed. The grand vision of Frontiers is a world where all people have an equal opportunity to seek, share and generate knowledge. Frontiers provides immediate and permanent online open access to all its publications, but this alone is not enough to realize our grand goals.

FRONTIERS JOURNAL SERIES

The Frontiers Journal Series is a multi-tier and interdisciplinary set of open-access, online journals, promising a paradigm shift from the current review, selection and dissemination processes in academic publishing.
All Frontiers journals are driven by researchers for researchers; therefore, they constitute a service to the scholarly community. At the same time, the Frontiers Journal Series operates on a revolutionary invention, the tiered publishing system, initially addressing specific communities of scholars, and gradually climbing up to broader public understanding, thus serving the interests of the lay society, too.

DEDICATION TO QUALITY

Each Frontiers article is a landmark of the highest quality, thanks to genuinely collaborative interactions between authors and review editors, who include some of the world's best academicians. Research must be certified by peers before entering a stream of knowledge that may eventually reach the public - and shape society; therefore, Frontiers only applies the most rigorous and unbiased reviews.
Frontiers revolutionizes research publishing by freely delivering the most outstanding research, evaluated with no bias from both the academic and social point of view.
By applying the most advanced information technologies, Frontiers is catapulting scholarly publishing into a new generation.

WHAT ARE FRONTIERS RESEARCH TOPICS?

Frontiers Research Topics are very popular trademarks of the Frontiers Journals Series: they are collections of at least ten articles, all centered on a particular subject. With their unique mix of varied contributions from Original Research to Review Articles, Frontiers Research Topics unify the most influential researchers, the latest key findings and historical advances in a hot research area!
Find out more on how to host your own Frontiers Research Topic or contribute to one as an author by contacting the Frontiers Editorial Office: researchtopics@frontiersin.org

GLOBAL HOST PROTEOMIC RESPONSES TO VIRUS INFECTION

Topic Editors:
Kevin Coombs, University of Manitoba, Canada
Ben Berkhout, University of Amsterdam, Netherlands

The field of virology has seen explosive growth in the past few decades. A large amount of effort has gone into successfully delineating virus evolution, genetic diversity, immunology, pathogenesis, structure, vaccine development, viral gene expression and genomic replication strategies. In addition, considerable recent work has been focusing on cellular responses to infection as well as how viruses may induce transformation and oncogenesis. Viruses are obligate intracellular parasites and thus absolutely dependent upon host cells. Not surprisingly, they often cause profound changes in cells, including apoptosis, death and signalling, to name a few perturbations. Thus, the molecular signals for how viruses induce pathophysiological alterations in their hosts have been of growing recent interest.

Cellular and organismal responses, such as those induced by virus infection, are invariably mediated by changes in gene and protein expression and modification. Thus, there has been keen interest in understanding how gene and protein expressions and modifications are quantitatively and qualitatively affected by such challenges. From a historical perspective, most early work that examined host protein responses to virus infection employed "biased" approaches, in which investigators targeted a limited number, or only one cellular molecule of interest. Completion of many organisms' genome sequences has allowed the global "non-biased" simultaneous analysis of the entire repertoire of cellular mRNA species, the transcriptome, by gene micro-arrays. This has provided significant information about how cellular gene expressions are altered by virus-induced perturbations, but has not provided as much information about the encoded proteins. This results for several reasons, including, but not limited to the fact that gene expression levels cannot accurately predict protein expression levels, nor the types and extent of post-translational modifications, many genes encode multiple proteins through splice variants, and protein activity may be affected by a large number of conditions, including phosphorylation.

Recent technological and bioinformatic approaches make it now possible to begin to extend similar global analyses to probe the cellular proteome, the repertoire of the actual effector molecules. One general strategy has been to take advantage of improved separations technologies, as well as greatly improved mass spectrometry resolution, to quantitatively or

comparatively measure hundreds or thousands of proteins. Proteins from multiple conditions (i.e., mock-infected and infected) may be differentially labelled by various techniques, such as 2D-DIGE, ICAT, iTRAQ, SILAC, with 18O during peptide preparation, and/or by various other methods, and then compared to measure comparative alterations in the levels of proteins induced by the virus infection. Such analyses have also been extended by using "label-free" methods for more efficient multiplexing applications, and/or by examining specific protein modifications. In addition, concerted efforts to raise antibodies against all cellular proteins have resulted in the development of "antibody arrays," which are also generally used for quantitative or comparative assays. Finally, while assays, such as the above, are generally limited to delineating the absolute amount of specific proteins, newer technologies have been developed that allow the simultaneous probing of hundreds of proteins' functions. Assays, such as "Activity Based Protein Profiling", are designed to probe enzymatic activity, with current focus on broad-spectrum proteases and other enzymatic classes. This Research Topic will provide an overview of many of these methods, as well as numerous specific examples of each approach, and how they are used to better delineate the ways viruses affect cellular responses during infection.

Table of Contents

frontiers in
MICROBIOLOGY

EDITORIAL
published: 05 March 2013
doi: 10.3389/fmicb.2013.00031

Quantitative omics and its application to study virus-host interactions—a new frontier

Ben Berkhout[1] and Kevin M. Coombs[2]*

[1] Department of Medical Microbiology, Laboratory of Experimental Virology, University of Amsterdam, Amsterdam, Netherlands
[2] Department of Medical Microbiology, Manitoba Centre for Proteomics and Systems Biology, University of Manitoba, Winnipeg, MB, Canada
*Correspondence: kcoombs@cc.umanitoba.ca

Edited by:
Akio Adachi, The University of Tokushima Graduate School, Japan

Reviewed by:
Akio Adachi, The University of Tokushima Graduate School, Japan

Work during the past few decades has provided a good understanding of alterations that occur in viruses when they interact with host cells. This is generally possible because of the relative simplicity of virus systems, as compared to the more complex cellular systems. There has also been advancement made in delineating host genomic responses to virus infection because of the availability of gene arrays for diverse organisms. However, work that seeks to equally comprehend host responses to virus infection at the protein level (proteomics) has lagged behind because of technical challenges and the great complexity of the cellular proteome.

This series consists of six review articles, three original research papers and a single commentary that all focus on current research activities in the field of proteomics of virus-infected host cells, all designed to begin to fill these important gaps in our knowledge. The articles span quantitative proteomic analyses of host protein alterations induced upon virus infection of a range of host cells: archaeal, insect, and various animal systems. Several articles present results and reviews of new discovery-based functional assays to assess broad enzymatic groups within these experimental systems to complement the quantitative proteomics assays.

The review article by Enrique Santamaria and co-workers provides an overview of mass spectrometry (MS)-based proteomics and how this method has been useful for delineating some of the interactions between herpes simplex virus type 1 (HSV-1) and the host cells (Santamaria et al., 2012). HSV-1 has a unique and intimate relationship with its host, being capable of inducing either a lytic infection cycle or becoming dormant by establishment of the latent state, from which it can be reactivated at later times. As a relatively large and complex particle, HSV-1 virions would be expected to have myriad interactions with host cells. This article provides a broad overview of many of the strategies being used to elucidate proteomic profiling and interactome networks.

The review article by Lippé also presents work aimed at deciphering interactions between HSV and the host cells (Lippe, 2012). In particular, the focus is on specific host cell proteins that are packaged in virion particles and that may be important for viral replication. There is accumulating evidence that a variety of viruses package specific host cell proteins to modulate subsequent virus replication steps by interacting with components of the host cell or organism.

The review by Kramer and colleagues provides an update on another medically relevant human pathogen, the human immunodeficiency virus type 1 (HIV-1), with an emphasis on interactions between the virus and T cells (Kramer et al., 2012). A variety of current challenges and limitations in peptide and protein identification are highlighted, along with the description of new approaches to more rapidly identify potential targets with improved algorithms and by making use of label-free quantitative methodologies. Several authors within this volume highlight the need to couple these discovery-based methods with follow-up experimental validation, including the confirmation of biological relevance of positive hits via knockdown screens.

The review article by Shahiduzzaman and Coombs explores a relatively new area of proteomics and the application of activity-based protein profiling (ABPP) to study virus-host interactions (Shahiduzzaman and Coombs, 2012). ABPP has been used in several non-viral systems to identify and quantify the levels of different classes of enzymes. Thus, this approach offers a complementary set of analyses to those that examine the overall differential protein quantities. ABPP allows the assessment of relative functional activities of all enzymes within each of various broad classes.

The review by Monteiro and co-workers discusses some of the applications of proteomic analyses of baculoviruses (Monteiro et al., 2012). These viruses infect insects and have become a popular tool for the expression of eukaryotic proteins. Baculoviruses are amongst the more complex viral systems with large genomes. It is argued that the study of these viruses as well as the analysis of virus-host cell interactions is hampered by this complexity and the lack of genomic information on the host side. Nevertheless, advances are being made on several fronts to understand the complex interactions between this virus and the host.

Most of the original research and review articles presented above focus on individual virus-host model systems. The final review article by Zheng and colleagues provides a holistic overview of current approaches being undertaken to better define and functionally validate responses elicited within the host proteome by virus infection (Zheng et al., 2012). This includes a comprehensive overview of most of the quantitative approaches being undertaken and several of the functional validations being employed by the growing number of researchers in these areas.

In the first of three original research papers within this volume, Jiang and colleagues label HeLa cells with either normal isotopic amino acids or heavy forms of arginine and lysine in the SILAC approach (Jiang et al., 2012). They infect non-labeled cells

with a mammalian reovirus and compare the identities of proteins detected either without enrichment or after non-selective enrichment with Proteominer™ beads. These authors quantitatively compared host protein alterations and identified several thousand of such modifications by comparing the two situations (± enrichment). The proteins and cellular pathways that were either up- or down-regulated were identified. The authors conclude that enrichment does not provide a deeper mining of the host proteome. An accompanying commentary by Speijer points out some of the inherent assumptions and potential limitations of such a study (Speijer, 2012).

The research article by Milev and co-workers describes characterization of Staufen 1, a host protein that binds double-stranded RNA and that is associated with HIV-derived ribonucleoprotein complexes (Milev et al., 2012). This study uses tandem affinity approaches to identify more than 200 host proteins that interact with this viral complex and defines alterations induced in the complex by Staufen 1. The role of many of the identified host proteins is subsequently validated and the intracellular distribution is also determined. This provides a much more comprehensive picture of these important molecules and their intracellular interactions, which may pave the way toward the development of new therapeutic approaches.

The final article by Maaty and colleagues provides a global analysis of host responses to virus infection in an archaeal system (Maaty et al., 2012). Major potential benefits of this "primitive" experimental system relate to its unique placement in evolution. This study employs a multi-faceted omics set of approaches to delineate the fate of host cell RNA and protein after virus infection, both with respect to quantitative aspects and enzymatic activities. This study greatly advances a previously underappreciated area. Perhaps more importantly, comparison of the protein and functional activities that are altered by archaeal viruses to the quantitative and functional perturbations induced by "higher" animal viruses may eventually provide the evolutionary framework for a better understanding of the virus-host interaction in terms of conserved and divergent host genes and proteins.

In summary, these articles present overviews and ongoing original research in one of the "frontier" areas of virology—a better understanding of the complexity of various host omic responses to virus infection, with some examples of proteomic and functional genomic approaches.

ACKNOWLEDGMENTS

The co-editors thank each contributor for providing wide-ranging and interesting articles to this special topic.

REFERENCES

Jiang, J., Opanubi, K. J., and Coombs, K. M. (2012). Non-biased enrichment does not improve quantitative proteomic delineation of reovirus T3D-infected HeLa cell protein alterations. *Front. Microbiol.* 3:310. doi: 10.3389/fmicb.2012.00310

Kramer, G., Moerland, P. D., Jeeninga, R. E., Vlietstra, W. J., Ringrose, J. H., Byrman, C., et al. (2012). Proteomic analysis of HIV-T cell interaction: an update. *Front. Microbiol.* 3:240. doi: 10.3389/fmicb.2012.00240

Lippe, R. (2012). Deciphering novel host-herpesvirus interactions by virion proteomics. *Front. Microbiol.* 3:181. doi: 10.3389/fmicb.2012.00181

Maaty, W. S., Steffens, J. D., Heinemann, J., Ortmann, A. C., Reeves, B. D., Biswas, S. K., et al. (2012). Global analysis of viral infection in an archaeal model system. *Front. Microbiol.* 3:411. doi: 10.3389/fmicb.2012.00411

Milev, M. P., Ravichandran, M., Khan, M. F., Schriemer, D. C., and Mouland, A. J. (2012). Characterization of staufen1 ribonucleoproteins by mass spectrometry and biochemical analyses reveal the presence of diverse host proteins associated with human immunodeficiency virus type 1. *Front. Microbiol.* 3:367. doi: 10.3389/fmicb.2012.00367

Monteiro, F., Carinhas, N., Carrondo, M. J., Bernal, V., and Alves, P. M. (2012). Toward system-level understanding of baculovirus-host cell interactions: from molecular fundamental studies to large-scale proteomics approaches. *Front. Microbiol.* 3:391. doi: 10.3389/fmicb.2012.00391

Santamaria, E., Sanchez-Quiles, V., Ferdandez-Irigoyen, J., and Corrales, F. (2012). Contribution of MS-based proteomics to the understanding of Herpes Simplex virus type 1 interaction with host cells. *Front. Microbiol.* 3:107. doi: 10.3389/fmicb.2012.00107

Shahiduzzaman, M., and Coombs, K. M. (2012). Activity based protein profiling to detect serine hydrolase alterations in virus infected cells. *Front. Microbiol.* 3:308. doi: 10.3389/fmicb.2012.00308

Speijer, D. (2012). Penetrating insights? *Front. Microbiol.* 3:382. doi: 10.3389/fmicb.2012.00382

Zheng, J., Tan, B. H., Sugrue, R., and Tang, K. (2012). Current approaches on viral infection: proteomics and functional validations. *Front. Microbiol.* 3:393. doi: 10.3389/fmicb.2012.00393

Received: 02 February 2013; accepted: 04 February 2013; published online: 05 March 2013.

*Citation: Berkhout B and Coombs KM (2013) Quantitative omics and its application to study virus-host interactions—a new frontier. Front. Microbiol. **4**:31. doi: 10.3389/fmicb.2013.00031*

This article was submitted to Frontiers in Virology, a specialty of Frontiers in Microbiology.

frontiers in
MICROBIOLOGY

MINI REVIEW ARTICLE
published: 20 March 2012
doi: 10.3389/fmicb.2012.00107

Contribution of MS-based proteomics to the understanding of herpes simplex virus type 1 interaction with host cells

Enrique Santamaría[1], Virginia Sánchez-Quiles[2], Joaquín Fernández-Irigoyen[1] and Fernando Corrales[2]*

[1] *Proteomics Unit, Biomedical Research Centre, Navarra Health Service, Pamplona, Spain*
[2] *Proteomics Unit, Centre for Applied Medical Research, University of Navarra, Pamplona, Spain*

Edited by:
Kevin Coombs, University of Manitoba, Canada

Reviewed by:
Kevin Coombs, University of Manitoba, Canada
Roger Lippé, University of Montreal, Canada

****Correspondence:***
Fernando Corrales, Proteomics Unit, Centre for Applied Medical Research, University of Navarra, Pío XII Avenue, 55, 31008 Pamplona, Spain.
e-mail: fjcorrales@unav.es

Like other DNA viruses, herpes simplex virus type 1 (HSV-1) replicates and proliferates in host cells continuously modulating the host molecular environment. Following a sophisticated temporal expression pattern, HSV-1 encodes at least 89 multifunctional proteins that interplay with and modify the host cell proteome. During the last decade, advances in mass spectrometry applications coupled to the development of proteomic separation methods have allowed to partially monitor the impact of HSV-1 infection in human cells. In this review, we discuss the current use of different proteome fractionation strategies to define HSV-1 targets in two major application areas: (i) viral-protein interactomics to decipher viral-protein interactions in host cells and (ii) differential quantitative proteomics to analyze the virally induced changes in the cellular proteome. Moreover, we will also discuss the potential application of high-throughput proteomic approaches to study global proteome dynamics and also post-translational modifications in HSV-1-infected cells that will greatly improve our molecular knowledge of HSV-1 infection.

Keywords: HSV-1, fractionation, labeling, proteomics, mass spectrometry

INTRODUCTION

Herpes simplex virus type 1 (HSV-1) is a large, double stranded DNA virus with a genome of 152 kbp that replicates in the nucleus of the host cells and presents a unique genetic flexibility (Taylor et al., 2002). Its gene expression follows a temporal pattern including three stages: immediate early (IE), early (E), and late (L) genes (Clements et al., 1977). The process of infection begins when the virions bind heparin sulfate moieties present on host cell plasma membrane. Within the first 30 min of infection, the initial attachment triggers a cascade of molecular interactions involving multiple viral and host cell proteins and receptors, leading to penetration of the viral nucleocapsid and tegument proteins into the cytoplasm (Dohner et al., 2006). After penetration, viral capsids and associated tegument proteins interact with dynein and utilize the microtubule network to transit the cytosol to the nuclear envelope, where they dock with nuclear pores and release their genomes into the nucleus. The HSV-1 genome replication starts around 3–4 h post infection (hpi) reaching maximum efficiency between 8 and 16 hpi (Phelan and Barklie Clements, 1997).

A large amount of information is available about the cellular fate of viral proteins and their constitutive functions in infected cells (Taylor et al., 2002). However, little is known about host effectors involved in viral replication and their virally induced functions, a crucial issue to understand the molecular pathogenesis of HSV-1 in human cells. This biological information is critical to boost novel vaccines and treatments for the broad-spectrum of pathological disorders caused by HSV-1 infection (Al-Dujaili et al., 2011; Chisholm and Lopez, 2011;Rozenberg et al., 2011) and also to promote the development of conditionally replicating HSV-1 vectors expressing cellular genes as anticancer therapeutic agents (Argnani et al., 2011; Shen and Nemunaitis, 2006; Nguyen and Blaho, 2007). In spite of the different genomic approaches carried out to understand the molecular alterations induced by HSV-1 infection in different mammalian cells (Mossman et al., 2001; Higaki et al., 2002; Paludan et al., 2002; Taddeo et al., 2002; Ray and Enquist, 2004; Sun et al., 2004; Clement et al., 2008, 2009; Zeier et al., 2009), changes in mRNA abundance do not always correlate to changes at protein level (Tian et al., 2004). Proteomics, therefore, is expected to provide a more extensive and complementary description of the cellular mechanisms altered upon HSV-1 infection. In this review, we focus on various protein fractionation methods coupled to mass spectrometry (MS) previously used to decipher novel HSV-1 targets. The results discussed here anticipate the future impact of high-throughput proteomic applications in the field of HSV-1 biology.

HSV-1 PROTEIN INTERACTOME

In the last few years, LC–MS/MS analyses coupled to diverse purification steps has emerged as a powerful technique to elucidate viral proteins interactions with host proteome. In fact, some immediate-early viral-protein interactomes have been partially characterized (**Figure 1**). Using immunoprecipitation procedures coupled to MS and validation techniques, Fontaine-Rodriguez et al. (2004) identified eIF3 subunits p47 and p116, eIF4G, and poly A binding protein as cellular interactors of ICP27 viral protein in human epidermoid (Hep-2) cells, suggesting that ICP27 may interfere in viral or host mRNA translation. Using a similar approach, Taylor and Knipe (2004) analyzed the interaction partners of ICP8 in Hep-2 cells identifying over 50 cellular proteins (and also some viral proteins) that coimmunoprecipitate or localize with ICP8 in replication compartments. This potential

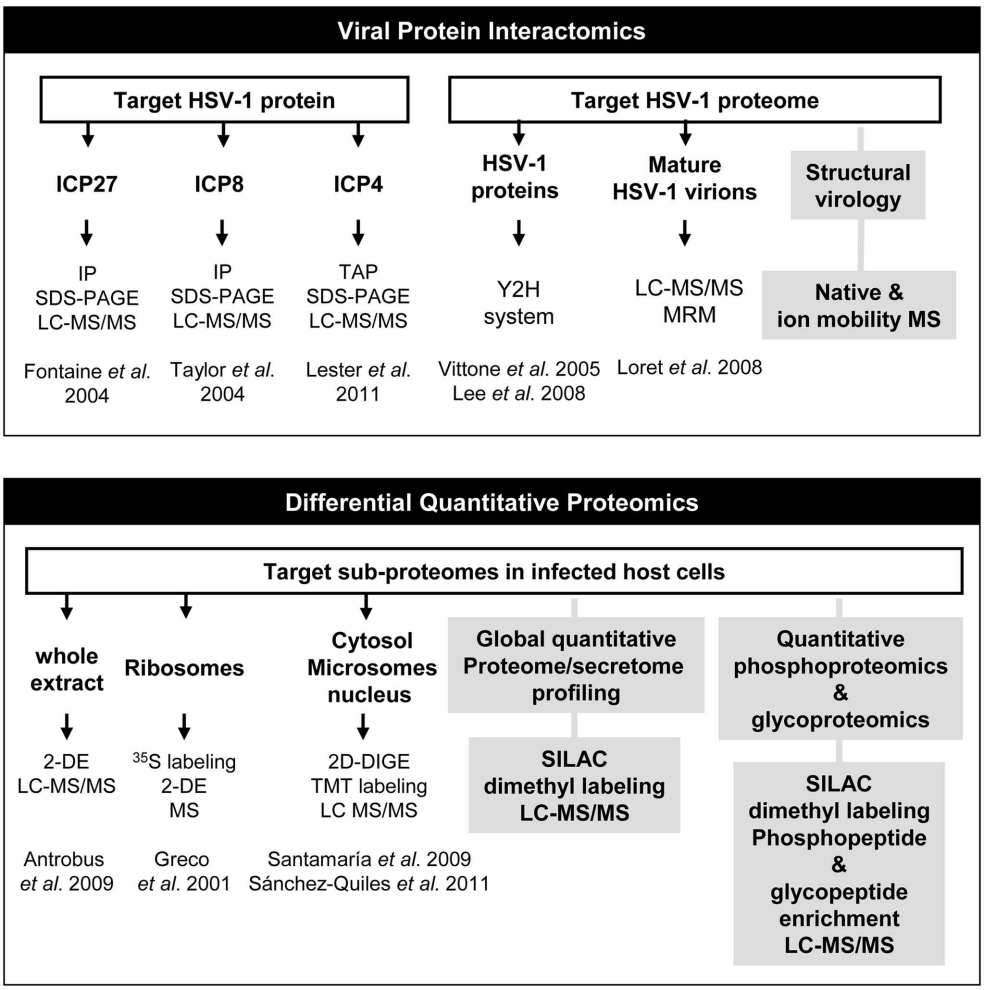

FIGURE 1 | Current and future applications of mass spectrometry to HSV-1 infection. Schematic representation of how proteomic technologies have been used to detect and identify HSV-1 targets in protein interactome experiments and also in differential quantitative protein expression studies. Gray boxes refer to alternative unexplored approaches that can be used to obtain more detailed information about the composition of HSV-1 particle (structural virology) and to analyze large-scale proteome perturbations and signaling pathways in host cells upon HSV-1 infection (Global and site specific quantitative glyco- and phosphoproteomics). IP, immunoprecipitation; LC–MS/MS, liquid chromatography coupled to tandem mass spectrometry; TAP, tandem affinity purification; Y2H, yeast two-hybrid system; MRM, multiple reaction monitoring; MS, mass spectrometry; 2-DE, two-dimensional electrophoresis; 2D-DIGE, two-dimensional fluorescence difference gel electrophoresis; TMT, Tandem mass tag isobaric labeling; SILAC, stable isotope labeling with amino acids in cell culture.

interactome was involved in different molecular function such as transcription, replication and recombination, chromatin remodeling, and RNA splicing (Taylor and Knipe, 2004). More recently, Lester and Deluca (2011) have isolated the ICP4-containing complexes from HeLa-infected cells using tandem affinity purification (TAP-ICP4) and protein fractionation by 1D gel SDS-PAGE, identifying more than 40 cellular proteins present in theses complexes by LC–MS/MS from which 11 and 4 proteins were components of the transcription factor TFIID and the mediator complex respectively. In this case, proteomic data were functionally validated by immunofluorescence and chromatin immunoprecipitation experiments showing that TFIID and mediator are recruited to viral promoters as a function of ICP4 during infection (Lester and Deluca, 2011). On the other hand, more than 40 binary interactions have been detected between capsid, envelope, and tegument viral proteins using protein–protein interaction yeast two-hybrid system (Bernhard et al., 2005; Vittone et al., 2005; Lee et al., 2008). Different proteome composition of purified mature extracellular viruses has been also characterized by MS-based proteomics technology. The carefully developed workflow used by Loret et al. (2008) allowed the identification of 8 viral capsid proteins, 23 potential tegument proteins, and 13 viral glycoproteins. In this workflow, a multiple reaction monitoring (MRM) approach was used to detect specific viral glycoproteins in mature virion preparations. Interestingly, 49 different host proteins mainly involved in transport, cytoskeleton, and nucleotide binding were also accurately identified. Although it is necessary to functionally validate the presence of these host proteins in the extracellular virion structure,

these data clearly demonstrate that HSV-1 tegumentation may be considered as a highly dynamic process.

PROTEOMIC PROFILING OF HSV-1-INFECTED CELLS

Comparative proteomic strategies have been also used in HSV-1 research to elucidate host proteome modifications during the early stages of HSV-1 infection (**Figure 1**). One of the most popular methods for protein separation is 2D-electrophoresis (2-DE). Based on two independent biochemical characteristics of proteins, it combines isoelectric focusing, which separates proteins according to their isoelectric point (pI), and SDS-PAGE, which separates them further according to their molecular mass (Westermeier and Gorg, 2011). Using ^{35}S labeling and 2-DE, Greco et al. (2000) demonstrated that although a strong shutoff in protein synthesis is induced in HSV-1 infection, the synthesis of some acidic ribosomal proteins is sustained or even induced early in infection. On the other hand, Antrobus et al. identified more than 100 protein species differentially expressed between non-infected and infected Hep-2 cells at 6 hpi. They used conventional 2-DE for protein separation and MS for protein identification. The host proteins identified in this study participate in a plethora of biological process and some of them were validated by western-blot analysis also in human diploid fibroblast (HF) cells (Antrobus et al., 2009).

Advanced prefractionation strategies in combination with MS, have provided powerful means to enrich and analyze organelle-specific subproteomes, obtaining valuable information that greatly expand our knowledge of the molecular mechanisms altered during HSV-1 infection. With the aim of detecting non-ribosomal proteins associated to the ribosome that may contribute to the HSV-1-induced translational control, Greco et al. extracted basic proteins from the ribosomal fraction from mock-infected and HSV-1-HeLa-infected cells. Using ^{35}S, 2-DE, N-terminal sequencing, and MS, viral proteins such as VP19C and VP26, and host poly(A) binding protein 1 were identified associated to ribosomes with different kinetics upon HSV-1 infection (Greco et al., 2001). More recently, we have used complementary protein and peptide labeling strategies to understand the dynamics of the human hepatoma cell proteome behavior upon HSV-1 infection. To increase the efficiency of proteomic analysis, Santamaría et al. fractionated mock-infected and HuH7-infected cells to obtain cytosolic and microsomal proteomes independently, at different early time points of HSV-1 infection. After validating the efficiency of the enrichment procedure, proteome dynamics was analyzed in both subcellular fractions by two-dimensional fluorescence difference gel electrophoresis (2D-DIGE). This approach is based on direct labeling of lysine groups on proteins with cyanine CyDye DIGE Fluor minimal dyes before isoelectric focusing, enabling the labeling of two to three samples with different dyes and electrophoresis of all the samples on the same 2D gel, minimizing spot pattern variability and the number of gels in an experiment (Tannu and Hemby, 2006). Using this approach, 16 unique deregulated host protein species mainly involved in apoptosis, signal transduction, and endoplasmic reticulum associated degradation pathway were identified in HuH7-infected cells by LC–MS/MS analyses (Santamaria et al., 2009). Interestingly, three of these proteins (FK506-binding protein 4, hnRNPK and eukaryotic translation initiation factor 3 subunit 2) were also deregulated early upon infection in Hep-2 cells (Antrobus et al., 2009). These coincident proteins suggest that cellular mechanisms involved in microtubule dynamics and mRNA processing are common in infected cells with different origin indicating the importance of these targets for HSV-1 infection. Santamaria et al. (2009) demonstrated the activation of mitochondrial apoptotic and different canonical signaling pathways identifying PP2A as a pivotal target that may mediate the transduction of cell death signals and promote cell survival pathway arrest in HuH7 cells. In the near future, it would be interesting to study the specific role of PP2A in different kind of cells infected with other HSV-1 strains to obtain robust conclusions. Moreover, deciphering the potential interactome of PP2A together with phosphoproteome-wide analysis of infected cells would increase our knowledge about the specific role of phosphorylation in HSV-1-infected cells.

Taking into account that HSV-1 replicates in the nucleus of the host cells, Sanchez-Quiles et al. (2011) have combined 2D-DIGE and tandem mass tag isobaric labeling (TMT) techniques to analyze nuclear proteome alterations in HuH7-infected cells. TMT is a liquid-based method that labels samples at the peptide level (Dayon et al., 2008). While DIGE separates only soluble proteins included in a pH range of 3–11 and a determined molecular weight, TMT can identify proteins outside these ranges. Moreover, DIGE is able to detect differential post-translationally modified proteins as well as different isoforms by resolving spots at different pI and molecular weight. However, these isoforms may not be distinguished with TMT approach, since labeling is completed at the peptide level and most peptide sequences are identical among a group of isoforms. In addition, proteins with extreme isoelectric points, large molecular weights, low solubility (hydrophobic proteins) and low copy numbers are poorly represented in 2D-DIGE experiments. The application of two different proteomic strategies was particularly useful in obtaining complementary information, identifying 62 differential components of the nuclear proteome of Huh7 hepatoma cells that may regulate host–virus interaction, cell cycle regulation, and RNA homeostasis upon infection (Sanchez-Quiles et al., 2011). In particular, Lamin A–C, also differentially expressed in Hep-2 infected cells (Antrobus et al., 2009), showed a complex differential isoform pattern upon HSV-1 infection, suggesting regulatory mechanisms based on post-translational modification events. Interestingly, 32 host proteins were enriched in infected nuclei. One of these early up-regulated proteins was protein quaking (QKI), involved in the regulation of mRNA stability, nuclear retention, and RNA transport (Galarneau and Richard, 2005). Using immunofluorescence assays, Sánchez-Quiles et al. have demonstrated that QKI-5 suffers a time-dependent redistribution in infected cells, shuttling from the nucleus to the cytosol upon HSV-1 infection. Interestingly, QKI depletion by knockdown strategy induces a clear delay in viral-protein synthesis, reducing the viral yield in infected cells (Sanchez-Quiles et al., 2011). Although the viral necessity of maintaining high expression levels of QKI during the infection should be demonstrated as a possible global mechanism of HSV-1 interference with host cells, these data suggest that QKI may be a potential target in the development of antiviral therapy.

All differential proteins provided by proteomic studies have undoubtedly extended our knowledge about HSV-1 infection at the molecular level. However, the protein repertoires reported are barely coincident. This variability is likely associated with specific biological properties of the samples analyzed (different cell lines, HSV-1 strains, and time point of infection used) and the heterogeneity of the analytical procedures used (fractionation methods to isolate specific organelles, and the use of gel-based or gel free proteomic workflows). Although differential proteomics has contributed to a better understanding about the specific proteome changes that occur early in infection, additional research is needed to elucidate whether these differentially expressed proteins are cellular targets used for HSV-1 to modulate the host proteome or are part of molecular events orchestrated by the cell to limit viral replication and propagation.

FUTURE DIRECTIONS

Although 2D-electrophoresis has been the technique of choice to monitor changes at protein level in HSV-1-infected cells, this approach presents some inherent disadvantages such as many protein spots are likely comprised of multiple proteins, poor spot resolution at higher pI values, and the difficulty in electrophoresing large and hydrophobic proteins in the first dimension separation. However, the rapid advances in high-resolution MS-based proteomics strategies may facilitate the global analysis of protein interacting partners of HSV-1 virion proteomes (Bailer and Haas, 2009), host protein components in HSV-1-infected secretome (Higa et al., 2008; Deng et al., 2010; Lietzen et al., 2011), and also the detection, identification, and quantitation of thousands of novel HSV-1 targets in host cells to finally obtain an integrative view of proteome modifications during the viral cycle. In the near future, alternative proteomics methods such as SILAC (Ong and Mann, 2006; Harsha et al., 2008) or stable isotope dimethyl labeling (Boersema et al., 2009) will lead to more comprehensive and time-dependent analysis of HSV-1-induced changes in host proteomes. Nowadays, these high-throughput approaches have been established and constantly optimized in order to improve our understanding of phosphorylation events. Large-scale proteomic studies based on SILAC in combination with strong cation exchange (SCX) and titanium dioxide (TiO_2) for phosphopeptide enrichment (Macek et al., 2009) would greatly contribute to the study of phosphorylation dynamics in HSV-1-infected cells. Using this shotgun approach, unexpected novel phosphorylation sites could be discovered in HSV-1 proteome, increasing our biological knowledge about the activation/deactivation status of multiple host signaling pathways during the infection. Moreover, the combination of immunoaffinity chromatography and MS-based quantitative MS (Pan et al., 2011), will be a valuable approach to characterize the glycoproteome of HSV-1-infected cells and also to map the specific changes in glycosylation patterns of HSV-1 surface proteins during the viral cycle. Finally, the application of native and ion-mobility MS in the near future (Uetrecht et al., 2011) will provide useful information about viral-protein and protein-complex structure, conformation, stoichiometry of an assembly, binding affinities, and the topology of a viral-protein complex (Uetrecht and Heck, 2011) increasing our knowledge on structural HSV-1 biology.

REFERENCES

Al-Dujaili, L. J., Clerkin, P. P., Clement, C., Mcferrin, H. E., Bhattacharjee, P. S., Varnell, E. D., Kaufman, H. E., and Hill, J. M. (2011) Ocular herpes simplex virus: how are latency, reactivation, recurrent disease and therapy interrelated? *Future Microbiol.* 6, 877–907.

Antrobus, R., Grant, K., Gangadharan, B., Chittenden, D., Everett, R. D., Zitzmann, N., and Boutell, C. (2009). Proteomic analysis of cells in the early stages of herpes simplex virus type-1 infection reveals widespread changes in the host cell proteome. *Proteomics* 9, 3913–3927.

Argnani, R., Marconi, P., Volpi, I., Bolanos, E., Carro, E., Ried, C., Santamaria, E., Pourchet, A., Epstein, A. L., Brocker, T., Corrales, F. J., Manservigi, R., Goicoechea, I., Foschini, M., and Hernandez-Alcoceba, R. (2011). Characterization of herpes simplex virus 1 strains as platforms for the development of oncolytic viruses against liver cancer. *Liver Int.* 31, 1542–1553.

Bailer, S. M., and Haas, J. (2009). Connecting viral with cellular interactomes. *Curr. Opin. Microbiol.* 12, 453–459.

Bernhard, O. K., Diefenbach, R. J., and Cunningham, A. L. (2005). New insights into viral structure and virus-cell interactions through proteomics. *Expert Rev. Proteomics* 2, 577–588.

Boersema, P. J., Raijmakers, R., Lemeer, S., Mohammed, S., and Heck, A. J. (2009). Multiplex peptide stable isotope dimethyl labeling for quantitative proteomics. *Nat. Protoc.* 4, 484–494.

Chisholm, C., and Lopez, L. (2011). Cutaneous infections caused by Herpesviridae: a review. *Arch. Pathol. Lab. Med.* 135, 1357–1362.

Clement, C., Bhattacharjee, P. S., Kaufman, H. E., and Hill, J. M. (2009). Heat-induced reactivation of HSV-1 in latent mice: upregulation in the TG of CD83 and other immune response genes and their LAT-ICP0 locus. *Invest. Ophthalmol. Vis. Sci.* 50, 2855–2861.

Clement, C., Popp, M. P., Bloom, D. C., Schultz, G., Liu, L., Neumann, D. M., Bhattacharjee, P. S., and Hill, J. M. (2008). Microarray analysis of host gene expression for comparison between naive and HSV-1 latent rabbit trigeminal ganglia. *Mol. Vis.* 14, 1209–1221.

Clements, J. B., Watson, R. J., and Wilkie, N. M. (1977). Temporal regulation of herpes simplex virus type 1 transcription: location of transcripts on the viral genome. *Cell* 12, 275–285.

Dayon, L., Hainard, A., Licker, V., Turck, N., Kuhn, K., Hochstrasser, D. F., Burkhard, P. R., and Sanchez, J. C. (2008). Relative quantification of proteins in human cerebrospinal fluids by MS/MS using 6-plex isobaric tags. *Anal. Chem.* 80, 2921–2931.

Deng, W., De Hoog, C. L., Yu, H. B., Li, Y., Croxen, M. A., Thomas, N. A., Puente, J. L., Foster, L. J., and Finlay, B. B. A. (2010). Comprehensive proteomic analysis of the type III secretome of *Citrobacter rodentium*. *J. Biol. Chem.* 285, 6790–6800.

Dohner, K., Radtke, K., Schmidt, S., and Sodeik, B. (2006). Eclipse phase of herpes simplex virus type 1 infection: efficient dynein-mediated capsid transport without the small capsid protein VP26. *J. Virol.* 80, 8211–8224.

Fontaine-Rodriguez, E. C., Taylor, T. J., Olesky, M., and Knipe, D. M. (2004). Proteomics of herpes simplex virus infected cell protein 27: association with translation initiation factors. *Virology* 330, 487–492.

Galarneau, A., and Richard, S. (2005). Target RNA motif and target mRNAs of the quaking STAR protein. *Nat. Struct. Mol. Biol.* 12, 691–698.

Greco, A., Bausch, N., Coute, Y., and Diaz, J. J. (2000). Characterization by two-dimensional gel electrophoresis of host proteins whose synthesis is sustained or stimulated during the course of herpes simplex virus type 1 infection. *Electrophoresis* 21, 2522–2530.

Greco, A., Bienvenut, W., Sanchez, J. C., Kindbeiter, K., Hochstrasser, D., Madjar, J. J., and Diaz, J. J. (2001). Identification of ribosome-associated viral and cellular basic proteins during the course of infection with herpes simplex virus type 1. *Proteomics* 1, 545–549.

Harsha, H. C., Molina, H., and Pandey, A. (2008). Quantitative proteomics using stable isotope labeling with amino acids in cell culture. *Nat. Protoc.* 3, 505–516.

Higa, L. M., Caruso, M. B., Canellas, F., Soares, M. R., Oliveira-Carvalho, A. L., Chapeaurouge, D. A., Almeida, P. M., Perales, J., Zingali, R. B., and Da Poian, A. T. (2008). Secretome of HepG2 cells infected with dengue virus: implications for pathogenesis. *Biochim. Biophys. Acta* 1784, 1607–1616.

Higaki, S., Gebhardt, B. M., Lukiw, W. J., Thompson, H. W., and Hill, J. M. (2002). Effect of immunosuppression on gene expression in the HSV-1 latently infected mouse trigeminal ganglion. *Invest. Ophthalmol. Vis. Sci.* 43, 1862–1869.

Lee, J. H., Vittone, V., Diefenbach, E., Cunningham, A. L., and Diefenbach, R. J. (2008). Identification of structural protein-protein interactions of herpes simplex virus type 1. *Virology* 378, 347–354.

Lester, J. T., and Deluca, N. A. (2011). Herpes simplex virus 1 ICP4 forms complexes with TFIID and mediator in virus-infected cells. *J. Virol.* 85, 5733–5744.

Lietzen, N., Ohman, T., Rintahaka, J., Julkunen, I., Aittokallio, T., Matikainen, S., and Nyman, T. A. (2011). Quantitative subcellular proteome and secretome profiling of influenza A virus-infected human primary macrophages. *PLoS Pathog.* 7, e1001340. doi:10.1371/journal.ppat.1001340

Loret, S., Guay, G., and Lippe, R. (2008). Comprehensive characterization of extracellular herpes simplex virus type 1 virions. *J. Virol.* 82, 8605–8618.

Macek, B., Mann, M., and Olsen, J. V. (2009). Global and site-specific quantitative phosphoproteomics: principles and applications. *Annu. Rev. Pharmacol. Toxicol.* 49, 199–221.

Mossman, K. L., Macgregor, P. F., Rozmus, J. J., Goryachev, A. B., Edwards, A. M., and Smiley, J. R. (2001). Herpes simplex virus triggers and then disarms a host antiviral response. *J. Virol.* 75, 750–758.

Nguyen, M. L., and Blaho, J. A. (2007). Apoptosis during herpes simplex virus infection. *Adv. Virus Res.* 69, 67–97.

Ong, S. E., and Mann, M. (2006). A practical recipe for stable isotope labeling by amino acids in cell culture (SILAC). *Nat. Protoc.* 1, 2650–2660.

Paludan, S. R., Melchjorsen, J., Malmgaard, L., and Mogensen, S. C. (2002). Expression of genes for cytokines and cytokine-related functions in leukocytes infected with herpes simplex virus: comparison between resistant and susceptible mouse strains. *Eur. Cytokine Netw.* 13, 306–316.

Pan, S., Chen, R., Aebersold, R., and Brentnall, T. A. (2011). Mass spectrometry based glycoproteomics – from a proteomics perspective. *Mol. Cell Proteomics* 10, R110.003251.

Phelan, A., and Barklie Clements, J. (1997). Functional domains within the nucleus of a cell infected with HSV-1. *Rev. Med. Virol.* 7, 229–237.

Ray, N., and Enquist, L. W. (2004). Transcriptional response of a common permissive cell type to infection by two diverse alphaherpesviruses. *J. Virol.* 78, 3489–3501.

Rozenberg, F., Deback, C., and Agut, H. (2011). Herpes simplex encephalitis: from virus to therapy. *Infect. Disord. Drug Targets* 11, 235–250.

Sanchez-Quiles, V., Mora, M. I., Segura, V., Greco, A., Epstein, A. L., Foschini, M. G., Dayon, L., Sanchez, J. C., Prieto, J., Corrales, F. J., and Santamaria, E. (2011). HSV-1 Cgal+ infection promotes quaking RNA binding protein production and induces nuclear-cytoplasmic shuttling of quaking I-5 isoform in human hepatoma cells. *Mol. Cell Proteomics* 10, M111.009126.

Santamaria, E., Mora, M. I., Potel, C., Fernandez-Irigoyen, J., Carro-Roldan, E., Hernandez-Alcoceba, R., Prieto, J., Epstein, A. L., and Corrales, F. J. (2009). Identification of replication-competent HSV-1 Cgal+ strain signaling targets in human hepatoma cells by functional organelle proteomics. *Mol. Cell Proteomics* 8, 805–815.

Shen, Y., and Nemunaitis, J. (2006). Herpes simplex virus 1 (HSV-1) for cancer treatment. *Cancer Gene Ther.* 13, 975–992.

Sun, A., Devi-Rao, G. V., Rice, M. K., Gary, L. W., Bloom, D. C., Sandri-Goldin, R. M., Ghazal, P., and Wagner, E. K. (2004). Immediate-early expression of the herpes simplex virus type 1 ICP27 transcript is not critical for efficient replication in vitro or in vivo. *J. Virol.* 78, 10470–10478.

Taddeo, B., Esclatine, A., and Roizman, B. (2002). The patterns of accumulation of cellular RNAs in cells infected with a wild-type and a mutant herpes simplex virus 1 lacking the virion host shutoff gene. *Proc. Natl. Acad. Sci. U.S.A.* 99, 17031–17036.

Tannu, N. S., and Hemby, S. E. (2006). Two-dimensional fluorescence difference gel electrophoresis for comparative proteomics profiling. *Nat. Protoc.* 1, 1732–1742.

Taylor, T. J., Brockman, M. A., Mcnamee, E. E., and Knipe, D. M. (2002). Herpes simplex virus. *Front. Biosci.* 7, d752–d764.

Taylor, T. J., and Knipe, D. M. (2004). Proteomics of herpes simplex virus replication compartments: association of cellular DNA replication, repair, recombination, and chromatin remodeling proteins with ICP8. *J. Virol.* 78, 5856–5866.

Tian, Q., Stepaniants, S. B., Mao, M., Weng, L., Feetham, M. C., Doyle, M. J., Yi, E. C., Dai, H., Thorsson, V., Eng, J., Goodlett, D., Berger, J. P., Gunter, B., Linseley, P. S., Stoughton, R. B., Aebersold, R., Collins, S. J., Hanlon, W. A., and Hood, L. E. (2004). Integrated genomic and proteomic analyses of gene expression in mammalian cells. *Mol. Cell Proteomics* 3, 960–969.

Uetrecht, C., Barbu, I. M., Shoemaker, G. K., Van Duijn, E., and Heck, A. J. (2011). Interrogating viral capsid assembly with ion mobility-mass spectrometry. *Nat. Chem.* 3, 126–132.

Uetrecht, C., and Heck, A. J. (2011). Modern biomolecular mass spectrometry and its role in studying virus structure, dynamics, and assembly. *Angew. Chem. Int. Ed. Engl.* 50, 8248–8262.

Vittone, V., Diefenbach, E., Triffett, D., Douglas, M. W., Cunningham, A. L., and Diefenbach, R. J. (2005). Determination of interactions between tegument proteins of herpes simplex virus type 1. *J. Virol.* 79, 9566–9571.

Westermeier, R., and Gorg, A. (2011). Two-dimensional electrophoresis in proteomics. *Methods Biochem. Anal.* 54, 411–439.

Zeier, Z., Aguilar, J. S., Lopez, C. M., Devi-Rao, G. B., Watson, Z. L., Baker, H. V., Wagner, E. K., and Bloom, D. C. (2009). A limited innate immune response is induced by a replication-defective herpes simplex virus vector following delivery to the murine central nervous system. *J. Neurovirol.* 15, 411–424.

Conflict of Interest Statement: The authors declare that the research was conducted in the absence of any commercial or financial relationships that could be construed as a potential conflict of interest.

Received: 02 February 2012; accepted: 02 March 2012; published online: 20 March 2012.

Citation: Santamaría E, Sánchez-Quiles V, Fernández-Irigoyen J and Corrales F (2012) Contribution of MS-based proteomics to the understanding of herpes simplex virus type 1 interaction with host cells. Front. Microbio. ***3****:107. doi: 10.3389/fmicb.2012.00107*

This article was submitted to Frontiers in Virology, a specialty of Frontiers in Microbiology.

frontiers in
MICROBIOLOGY

MINI REVIEW ARTICLE
published: 28 May 2012
doi: 10.3389/fmicb.2012.00181

Deciphering novel host–herpesvirus interactions by virion proteomics

Roger Lippé*

Department of Pathology and Cell biology, University of Montreal, Montreal, QC, Canada

Edited by:
Kevin Coombs, University of Manitoba, Canada

Reviewed by:
Bruce W. Banfield, Queen's University, Canada
Lori Frappier, University of Toronto, Canada

****Correspondence:***
Roger Lippé, Department of Pathology and Cell Biology, University of Montreal, PO Box 6128, Succursale Centre-Ville, Montreal, QC, Canada H3C 3J7.
e-mail: roger.lippe@umontreal.ca

Over the years, a vast array of information concerning the interactions of viruses with their hosts has been collected. However, recent advances in proteomics and other system biology techniques suggest these interactions are far more complex than anticipated. One particularly interesting and novel aspect is the analysis of cellular proteins incorporated into mature virions. Though sometimes considered purification contaminants in the past, their repeated detection by different laboratories suggests that a number of these proteins are *bona fide* viral components, some of which likely contribute to the viral life cycles. The present mini review focuses on cellular proteins detected in herpesviruses. It highlights the common cellular functions of these proteins, their potential implications for host–pathogen interactions, discusses technical limitations, the need for complementing methods and probes potential future research avenues.

Keywords: herpes, virus, host–pathogen interactions, HSV, PRV, HCMV, EBV γHV68, KSHV

INTRODUCTION

Over the last decades, many host–pathogen interactions have been characterized using genetics, biochemical, and microscopy approaches. These discoveries relied on mutants, pharmacological reagents, immunoprecipitations, immunofluorescence, electron microscopy, cell fractionation, and Western blotting to name a few of the methods employed. These approaches provided much precious information but, given the typical focus of these approaches on individual molecules, likely only revealed a small portion of the proteins involved. Other methods such as high throughput two-hybrid and genetic screens, nucleic acid arrays, RNA interference, and proteomics are now proving essential tools to tackle the complexity of these interactions. The main advantages of mass spectrometry, for instance, are that it is a fast, sensitive and potentially a quantitative approach to identify putative novel players, particularly when coupled to efficient purification schemes. Already, proteomics revealed how viruses modulate the expression of host proteins (Rassmann et al., 2006; Sun et al., 2008; Tong et al., 2008; Antrobus et al., 2009; Pastorino et al., 2009; Thanthrige-Don et al., 2009; Zandi et al., 2009; Zhang et al., 2009, 2010; Coombs et al., 2010; Emmott et al., 2010; Lu et al., 2010, 2012; Munday et al., 2010; Bartel et al., 2011; Lietzen et al., 2011; Ramirez-Boo et al., 2011; Chou et al., 2012). A relatively new and interesting field is the characterization of host–pathogen interactions within mature purified virions. As reviewed on several occasions, several studies reported the presence of individual cellular proteins in viral particles (Bernhard et al., 2005; Maxwell and Frappier, 2007; Viswanathan and Fruh, 2007; Friedel and Haas, 2011; Zheng et al., 2011). This includes vaccinia virus (Krauss et al., 2002), influenza virus (Shaw et al., 2008), HIV (Gurer et al., 2002; Cantin et al., 2005; Ott, 2008), vesicular stomatitis virus (Moerdyk-Schauwecker et al., 2009), and several herpesviruses (see below). Though these cellular components have often been considered purification contaminants, the presence of similar proteins in both related and unrelated viruses suggests that some of them may be biologically relevant. The identification of virion-associated host proteins could thus lead to the discovery of novel therapeutic tools against viruses. The present review focuses on their identification and putative roles with respect to the proteomics of herpesviruses.

PROTEOMICS OF HERPESVIRIONS

Thus far, the protein composition of eight different herpesvirions has been studied by mass spectrometry. These studies include the alphaherpesvirinae herpes simplex virus type 1 (HSV-1) and pseudorabies virus (PRV; Loret et al., 2008; Kramer et al., 2011), the betaherpesvirinae human and murine cytomegaloviruses (HCMV and MCMV, respectively; Kattenhorn et al., 2004; Varnum et al., 2004) and the gammaherpesvirinae Kaposi sarcoma herpesvirus (KSHV), gamma herpesvirus 68 (γHV68), Epstein–Barr virus (EBV), and Alcelaphine (Bortz et al., 2003; Johannsen et al., 2004; Bechtel et al., 2005; Zhu et al., 2005; Dry et al., 2008). Interestingly, host proteins were detected in all herpesvirions analyzed so far, as summarized in **Table 1**. For instance, our laboratory previously reported the protein composition of mature extracellular HSV-1 viral particles and identified as many as 49 cellular proteins (Loret et al., 2008). Similarly, studies focusing on PRV and EBV reported up to 48 and 43 cellular proteins, respectively (Johannsen et al., 2004; Kramer et al., 2011). Meanwhile, Varnum et al. (2004) found as many as 70 different host proteins in extracellular HCMV virions. While fewer cellular proteins were reported for other viral particles, it is clear that herpesviruses can potentially incorporate many proteins from its host. Moreover, of the 173 different proteins detected in herpesvirions, nine protein groups are present in at least four distinct herpesvirions. This includes 14-3-3, actin, annexins, cofilin, translation factors, GAPDH, heat shock proteins, pyruvate kinase M2, and various Rab GTPases. These results indicate that, first of all, it is common for herpesviruses to incorporate cellular proteins into their viral particles and, secondly, that

Table 1 | Proteomics studies of herpesviruses associated host proteins.

Uniprot/ Swissprot	NCBI	Host protein name	Alphaherpes		Betaherpes		Gammaherpes				
			HSV-1*	PRV*[2]	HCMV*[3]	MCMV*[4]	EBV*[5]	KSHV*[6]	KSHV*[7]	Murine γ HV68*[8]	Alcelaphine*[9] (cell-assoc)
P31946	4507949	14-3-3 Protein beta (tyrosine 2-monooxygenase beta)		+	+				+?		
P62258	5803225	14-3-3 Protein epsilon (tyrosine-3-monooxygenase epsilon)	+	+	+		+		+		
P61981		14-3-3 Protein gamma (tyrosine-3-monooxygenase gamma)	+								
P31947		14-3-3 Protein sigma (tyrosine-3-monooxygenase sigma)		+							
P27348	5803227	14-3-3 protein theta (tyrosine-3-monooxygenase theta)		+	+						
P63104	4507953	14-3-3 protein zeta/delta (tyrosine-3-monooxygenase zeta/delta)	+		+		+		+		
P68133	1070613	Actin (alpha)	+?		+	+?					+?
P60709	4501885	Actin (beta)	+?		+	+?	+	+	+	+	+?
P63261		Actin (gamma)	+?			+?					+?
P12814	112959	Actin (alpha)		+	+		+				
P04075	49168540	Aldolase A					+				
P15144	113743	Aminopeptidase N (CD13)			+						
P08195.3	21361344	Amino acid transporter					+				
P80385	2507205	AMP-activated protein kinase subunit gamma-1							+		
P04083	4502101	Annexin A1	+		+	+?				+	+
P07355	4757756	Annexin A2	+		+				+	+	+
P08758	3212603	Annexin A5	+	+	+	+?					
P08133.3	113962	Annexin A6			+		+		+		
P13928		Annexin A8		+							
	1065361	Adp-ribosylation factor 1 chain A			+						
P84077		Arf1	+	+	+						
P61204	1351907	Arf3	+	+							
P18085		Arf4	+								
P84085		Arf5	+								
P00966.2	4557337	Arginosuccinate synthetase					+				
P61158.3	5031573	ARP3 (actin-related protein)					+				
P08243.4	19718772	Asparagine synthetase					+				
P11021.2	121567	BIP (GRP78)			+						
P27797.1	4757900	Calreticulin			+						

(Continued)

Table 1 | Continued

Uniprot/ Swissprot	NCBI	Host protein name	Alphaherpes		Betaherpes		Gammaherpes				
			HSV-1*	PRV*[2]	HCMV*[3]	MCMV*[4]	EBV*[5]	KSHV*[6]	KSHV*[7]	Murine γ HV68*[8]	Alcelaphine*[9] (cell-assoc)
P62158		Calmodulin		+							
P68400	4503095	Casein kinase 2	+	+	+						
P08195.2	112803	CD98 (lymphocyte activation antigen 4F2 large subunit)			+						
O00299		Chloride intracellular channel protein 1		+							
Q00610.5	4758012	Clathrin heavy chain			+		+				
P23528	5031635	Cofilin 1	+		+	+	+				
Q5G6V9		Cofilin 2		+							
P12277.1	21536286	Creatine kinase					+				
P62937	118102	Cyclophilin A	+		+				+		
P21291		Cystein-glycine rich protein 1	+								
Q92499.2	4826686	Dead box protein 1			+						
O00571	4503295	DDX3X (dead box protein 3; ATP dependant RNA helicase)	+	+	+						
P60981		Destrin		+							
	219588	DnaJ human homolog			+						
Q9H4M9.2	30240932	EH-domain containing protein(s)					+				
P58021.1		Endomembrane protein 70 (transmembrane 9 superfamily member 2 precursor)								+	
P14625.1	4507677	Endoplasmin precursor (tumor rejection antigen; gp96)			+						
	2135068	Enhancer protein			+						
P06733.2	4503571	Enolase 1 (alpha)			+		+	+	+		
P68104.1	4503471	Eukaryotic translation elongation factor 1			+		+				
	1169475	EF-1α (EF-Tu)				+					
P13639.4	4503483	Eukaryotic translation elongation factor 2			+		+	+	+		
P60842	4503529	Eukaryotic initiation factor 4A-I		+	+						
Q15056		Eukaryotic translation initiation factor 4H (eIF4H=WBSCR1)	+	+	+? (eIF4A)						
P63241		Eukaryotic initiation factor 5A-I		+							
P21333.4	4503745	Filamin 1 (actin binding protein 280)			+		+				
P04899.3	4504041	G protein alpha-I					+				

(Continued)

Table 1 | Continued

Uniprot/ Swissprot	NCBI	Host protein name	Alphaherpes		Betaherpes		Gammaherpes				
			HSV-1*	PRV*[2]	HCMV*[3]	MCMV*[4]	EBV*[5]	KSHV*[6]	KSHV*[7]	Murine γ HV68*[8]	Alcelaphine*[9] (cell-assoc)
P17931		Galectin 3		+							
P50395.2	13638228	Rab GDP Dissociation Inhibitor Beta (Rab GDI)			+						
P80031		Glutathione *S*-transferase		+							
P04406	7669492	Glyceraldehyde-3-phosphate dehydrogenase (GAPDH)	+		+	+	+		+		
P62993	4504111	Growth factor receptor bound protein 2	+	+	+						
P62879		Guanine nucleotide-binding protein subunit alpha-2		+							
P08107.5	2119712	HSPa1L (DNAK-type molecular chaperone; Heat shock 70 kDa protein 1A/1B or 1/2; HSP70.1/HSP70.2)			+						
Q5S1U1		HSP27		+	+						
Q27965.1	2495339	Heat shock protein 70 (HSP70.2)							+		
P54652.1	1708307	Heat shock 70 protein 2			+						
P11021.2	16507237	Heat Shock 70 protein 5 (78 kDa glucose-regulated protein precursor; BIP?)					+				
P48741.2	1346317	Heat shock 70 protein 7 (heat shock 70 kDa protein B)			+						
P11142	5729877	Heat shock 70 protein 8 (HspA8; LAP1)	+				+				
P19120	5729877	Heat Shock 70 protein 10 (Hsc71)			+			+			
P07900.5	123678	Heat shock 90 protein 1 alpha (HSP 86)					+				
P08238.4	6680307	Heat shock 90 protein 1 beta			+		+				
P07900	6016267	Heat shock protein HSP90			+			+	+		
P22752.3	121961	Histone 2A				+?					
		Histone 2B				+?					+
		Histone 4									+
P22626		HNRNPA2B1		+							
P22626		HNRNPF		+							
P22626		HNRNPK		+							
P22626		HNRNPH3		+							
Q9GLP0		Integrin beta-1		+							
P04264		Keratin 1	+		+						
	1082558	Keratin 9			+						

(Continued)

Table 1 | Continued

Uniprot/ Swissprot	NCBI	Host protein name	Alphaherpes		Betaherpes		Gammaherpes				
			HSV-1*	PRV*[2]	HCMV*[3]	MCMV*[4]	EBV*[5]	KSHV*[6]	KSHV*[7]	Murine γ HV68*[8]	Alcelaphine*[9] (cell-assoc)
P13645		Keratin 10	+		+						
Q08431.2	422992	Lactadherin (milk fat globule protein)			+						
Q08431.2	5174557	Lactadherin isoform a preproprotein (Milk Fat Globule-EGF Factor 8 Protein)			+						
P00338.2	5031857	Lactate dehydrogenase A			+						
P07195.2	4557032	Lactate dehydrogenase B			+						
P28838.3	7705688	Leucine aminopeptidase (cytosol aminopeptidase)					+				
Q9GKE8		Leukocyte surface antigen CD47		+							
O60488		Long chain fatty acid CoA ligase 4		+							
P13796.6	4504965	L plastin (lymphocyte cytosolic protein 1; plastin-2)					+		+		
Q53EU6		Lung cancer metastasis-associated protein (1-acylglycerol-3-phosphate *O*-acyltransferase 9)	+								
P14174		Macrophage migration inhibitory factor (glycosylation-inhibiting factor; phenylpyruvate tautomerase)	+								
P28482		MAPK1		+							
P13987		Membrane attack complex inhibition factor (CD59)	+								
P30515.1	231348	MHC_I (Class I histocompatibility antigen, A alpha chain)					+				
AAH01112	4505257	Myosin			+		+	+			
P35579.4	6166599	Myosin heavy chain (myosin-9; non-muscle myosin heavy chain A)			+				+		
P60660		Myosin light polypeptide 6		+							
O00159		Myosin Ic		+							
P30101.4	1085373	PDI ER60 precursor (protein disulfide-isomerase A3; endoplasmic reticulum resident protein 57)			+						
Q06830		Peroxiredoxin-1 (thioredoxin-dependent peroxide reductase 2; natural killer cell-enhancing factor A)	+								
P32119		Peroxiredoxin-2	+								

(Continued)

Table 1 | Continued

Uniprot/ Swissprot	NCBI	Host protein name	Alphaherpes		Betaherpes		Gammaherpes				
			HSV-1*	PRV*[2]	HCMV*[3]	MCMV*[4]	EBV*[5]	KSHV*[6]	KSHV*[7]	Murine γ HV68*[8]	Alcelaphine*[9] (cell-assoc)
P00558.3	129902	Phosphoglycerate kinase 1 (primer recognition protein 2; PRP 2; cell migration-inducing gene 10 protein)			+		+		+		
P15531		NM23A (nucleoside diphosphate kinase A; granzyme A-activated Dnase; metastasis inhibition factor nm23)	+								
P22392		NM23B	+								
	1362872	Nuclear protein import factor			+						
Q15365		Poly(rC)-binding protein 1		+							
P07737		Profilin-1	+		+						
P13861.2	4758958	Protein kinase A (cAMP-dependent protein kinase type II-alpha regulatory subunit)					+				
P62136	4506003	Protein phosphatase 1 (catalytic subunit, alpha isoform)		+	+						
P61292		Protein phosphatase 1 (catalytic subunit, beta isoform)		+							
P30153.4	107300	Protein phosphatase 2 (alpha regulatory chain; PP2A subunit A isoform R1-alpha)			+						
O75340		Programmed cell death protein 6	+								
P14618		Pyruvate kinase			+		+	+	+		+
	107554	Pyruvate kinase M2							+		
P62820		Rab1a	?	+			+				
P61019		Rab2a	+	+							
Q8WUD1		Rab2b	+								
P61018		Rab4b	+?								
P51148		Rab5c	+								
P20339		Rab5a	+								
P61020		Rab5b	+								
P20340		Rab6a	+	+							
P20340		Rab6b	+								
Q9H0N0		Rab6c	+								
P51149		Rab7A	+	+					+		
P61026		Rab10	+								
P62491		Rab11a	+								
Q15907		Rab11b	+								
P61106		Rab14		+							

(Continued)

Table 1 | Continued

Uniprot/ Swissprot	NCBI	Host protein name	Alphaherpes		Betaherpes		Gammaherpes				
			HSV-1*	PRV*[2]	HCMV*[3]	MCMV*[4]	EBV*[5]	KSHV*[6]	KSHV*[7]	Murine γ HV68*[8]	Alcelaphine*[9] (cell-assoc)
P59190		Rab15	+								
Q9H082		Rab33B	+								
Q15286		Rab35 (Rab1c)	+								
Q5HYI8		Rab-like protein 3	+								
P26044		Radixin		+							
P46940.1	4506787	Ras GAP			+						
P61586		RhoA		+							
Q99PT1.3	21759130	Rho GDI				+					
P31949		S100 calcium protein binding A11 (calgizzarin)	+								
Q9UDX3		Sec14-like protein 4 (TAP3)	+								
P05023.1	114374	Sodium/potassium transporting ATPase subunit alpha 1			+		+		+		
Q86Y82		Syntaxin12		+							
P17987.1	13540473	T-complex (T-complex protein 1 subunit alpha isoform a)					+				
P49368.4	31542292	TCP1 subunit 3 [T-complex protein 1 subunit gamma isoform a; chaperonin containing TCP1, subunit 3 (gamma)]					+				
P48643.1	24307939	TCP1 subunit 5 (T-complex protein 1 subunit epsilon)					+				
Q99832.2	5453607	TCP1 subunit 7 (T-complex protein 1 subunit eta isoform a)					+				
P50990.4		TCP1 subunit 8 [T-complex protein 1, theta subunit; chaperonin containing TCP1, subunit 8 (theta)]					+				
P60174		Triosephosphate isomerase	+		+						
P68363.1		Tubulin, alpha, ubiquitous (tubulin alpha-1B chain)			+						
Q71U36.1		Tubulin alpha (tubulin alpha-1A chain)			+		+	+			
P07437.2		Tubulin beta-1 chain (tubulin beta-5 chain)			+		+				
P62987		Ubiquitin C (60S ribosomal protein L40)	+								
P62987		Polyubiquitin 3 (ubiquitin C; 60S ribosomal protein L40)			+						
P68036		Ubiquitin-conjugating enzyme E2 L3 (UBCH7)	+								

(Continued)

Table 1 | Continued

Uniprot/ Swissprot	NCBI	Host protein name	Alphaherpes		Betaherpes		Gammaherpes				
			HSV-1*	PRV*[2]	HCMV*[3]	MCMV*[4]	EBV*[5]	KSHV*[6]	KSHV*[7]	Murine γ HV68*[8]	Alcelaphine*[9] (cell-assoc)
P55072.4		Valocin containing protein (transitional endoplasmic reticulum ATPase)					+				
Q15836		VAMP3/cellubrevin		+							
O95857		Tetraspanin 13	+								
P82460		Thioredoxin (=peroxiredoxin?)		+	+						
P07996.2		Thrombospondin 1							+		
Q15654.3		Thyroid receptor interacting protein 6 (Zyxin-related protein 1; ZRP-1; Opa-interacting protein 1)			+						
P02786		Transferrin receptor protein 1 (CD71)	+								
P37802		Transgelin 2	+	+	+						
P29401.3		Transketolase			+						
Q3ZCQ8		Translocase of inner mitochondrial membrane 50 (TIMM50)	+								
P15311.4		Villin 2 (Ezrin)					+	+			
P08670.4		Vimentin			+						
	4507877	Vinculin			+						
O75083		WD repeat containing protein 1		+							
	1065111	Chain A, mixed disulfide intermediate between mutant human thioredoxin and A 13 residue peptide of NF-kB			+						
		Up to:	**49 proteins**	**48 proteins**	**70 proteins**	**11 proteins**	**43 proteins**	**9 proteins**	**20 proteins**	**4 proteins**	**6 proteins**

The table shows a compilation of the various host proteins identified in these mature herpesvirions enriched from the extracellular milieu. One notable exception is Alcelaphine, where cell-associated viral particles were analyzed. The study by Padula and colleagues, which found that annexin A2 is present in HSV-1 perinuclear virions, was omitted from the table since preliminary for the moment (Padula et al., 2009).

+: Detected in that study.

+?: Indicates an uncertainty as to the subtype (e.g., alpha, beta, gamma, a, b, c, ...).

All extracellular virions except the study by Dry (cell associated).

NB: The uniprot/swissprot numbers are not available for all proteins due to the constant evolving of protein and gene databases.

NB: Multiple accession numbers are sometimes possible and may therefore differ among the above studies.

**[1]: Loret et al. (2008)*

**[2]: Kramer et al. (2011)*

**[3]: Varnum et al. (2004)*

**[4]: Kattenhorn et al. (2004)*

**[5]: Johannsen et al. (2004)*

**[6]: Bechtel et al. (2005)*

**[7]: Zhu et al. (2005)*

**[8]: Bortz et al. (2003)*

**[9]: Dry et al. (2008).*

different viruses share similar host proteins. Most excitingly, it also suggests that these host proteins may play common roles throughout the herpesviral family. This defines an interesting and novel set of host–pathogen interactions taking place within the virus itself, rather than the cell.

It is tempting to speculate that some viruses might have a higher capacity to steal cellular proteins because of their size and symmetry. Herpesviruses are indeed large viruses containing a layer called the tegument between their capsids and envelopes that could accommodate non-viral proteins. Though some host proteins may randomly be incorporated into virions, others may rather be selected to insure the optimal replication of the viruses that carry them.

PUTATIVE FUNCTIONS OF HOST PROTEINS ASSOCIATED WITH HERPESVIRIONS

Bioinformatics databases such as the KEGG, Gene Ontology, or DAVID are useful tools to get an overview of the functional interplay of proteins (Ashburner et al., 2000; Huang Da et al., 2009; Kanehisa et al., 2010). As pointed out by Friedel and Haas (2011), complex statistical tools are available to quantitatively evaluate the implication of proteins in various processes but these are beyond the scope of the present review. Here an analysis of the proteins identified in herpesvirions was instead performed with the Ingenuity Pathways Analysis database (Ingenuity® Systems), which contains all the known physical and functional links among cellular proteins and defines their most significant functions. That analysis indicates that many of the cellular proteins found in herpesvirions normally modulate trafficking, cell proliferation, cell death, cell migration, cell metabolism, or the cytoskeleton (**Figure 1**, upper pie chart). Though subtle differences between family members are noticeable when looking at individual viruses, similar functions are found (**Figure 1**, other charts). Immune-related molecules are also important constituents for several viruses, including HSV-1, KSHV, γHV68, Alcelaphine, and MCMV. Altogether, this provides an overall picture whereby herpesviruses, not surprisingly, modulate all of the important aspects of the cell but where each virus might deploy its energies slightly differently. The main surprise is that so many cellular proteins are detected within assembled viral particles, which raises an important question as to their biological significance and mode of action.

IMPLICATIONS OF VIRION-ASSOCIATED HOST PROTEINS FOR HERPESVIRUSES

The overall picture that several important cellular functions might be modulated by the host proteins incorporated into viral particles is intriguing. This clever strategy is consistent with the parasitic nature of all viruses, including herpesviruses, which would presumably gain some replication advantage from stealing cellular modulators rather than coding for them in their own genomes. The most critical question is the benefit for the viruses to incorporate these cellular proteins in their assembled particles, particularly since these proteins also exist in the cells. While this is open to discussion, one possibility is that some of the incorporated cellular proteins may be remnants of the final capsid envelopment process. Alternatively, this may allow the prompt action of some of these proteins immediately upon viral entry. This could jumpstart the expression and/or duplication of the viral genome, as it is the case for the herpesviral VHS, VP16, ICP0, and ICP4 proteins that are present in virions (Lam et al., 1996; Everett, 2000; Halford and Schaffer, 2001; Ellison et al., 2005; Hancock et al., 2006; Loret et al., 2008; Sarma et al., 2008; Loret and Lippe, 2012). Other early potential sites of action are the process of viral entry itself, intracellular capsid transport, import of the viral genome through the nuclear pore or immune modulation, all common steps among herpesviruses. Whatever the case might be, the question remains as to why the cellular pool of these proteins would not suffice. Several options may be considered. First, it may be that the virions incorporate specific isoforms, splice variants or post-translationally modified proteins that could have properties or functions distinct than their cellular counterparts. Second, the incorporation of a host protein from one cell type might permit the infection of a different cell type that does not express such protein. For example, alpha herpesviruses initially infect mucosal cells and could acquire host proteins that are beneficial to infect dormant neuronal cells. Finally, the host proteins might be in complex with viral proteins and it is those complexes that are active to promote the infection. These possibilities are of course speculative at this point and need to be explored.

One aspect where the incorporation of host proteins in mature virions might be beneficial is molecules involved in intracellular trafficking. Work by numerous laboratories demonstrated that the transport machinery used to move cellular proteins is also employed by viruses (Simons and Warren, 1984; Lodish et al., 2000; Sollner, 2004; Greber and Way, 2006; Mercer et al., 2010). This is essential for their proteins and particles to reach their final destination, for example, the site of viral replication, assembly, and/or envelopment. Along with SNARES proteins, Rab and Arf GTPases are master regulators of molecular trafficking throughout the cell (Sollner and Rothman, 1996; Zerial and McBride, 2001; Mizuno-Yamasaki et al., 2012). So far, VAMP3, a SNARE, was identified in PRV virions (Kramer et al., 2011) but it may only be a matter of time until other SNARES are discovered in other members of the herpes family. This is relevant as another SNARE was reported to facilitate the envelopment of MCMV capsids (Cepeda and Fraile-Ramos, 2011). In contrast, a great number of Rab proteins have been identified in herpesvirions, particularly HSV-1 and PRV (**Table 1**). One stimulating option is that these proteins regulate the displacement of viral capsids in the cell, which could justify their incorporation in the viral particles. As Rab and Arf proteins collectively modulate several intracellular transport steps within the cell, it is anticipated they may be involved in various stages of the infection. For instance, Rab1, which is present in HSV-1 extracellular virions (Loret et al., 2008), and Rab43 were recently demonstrated to modulate the final envelopment of the virus (Zenner et al., 2011). Similarly, Rab6, found in HSV-1 and PRV (Loret et al., 2008; Kramer et al., 2011), is also necessary for the efficient assembly of the related HCMV (Indran and Britt, 2011). It will now be of interest to determine if the virion-associated pool of these GTPases actively participates in the viral life cycle. Interestingly, several Rab proteins have been implicated in autophagosome formation and maturation (Chua et al., 2011). While it is difficult to consider how virion-incorporated Rab proteins play a role at that stage, they might rather be incorporated into the virions as

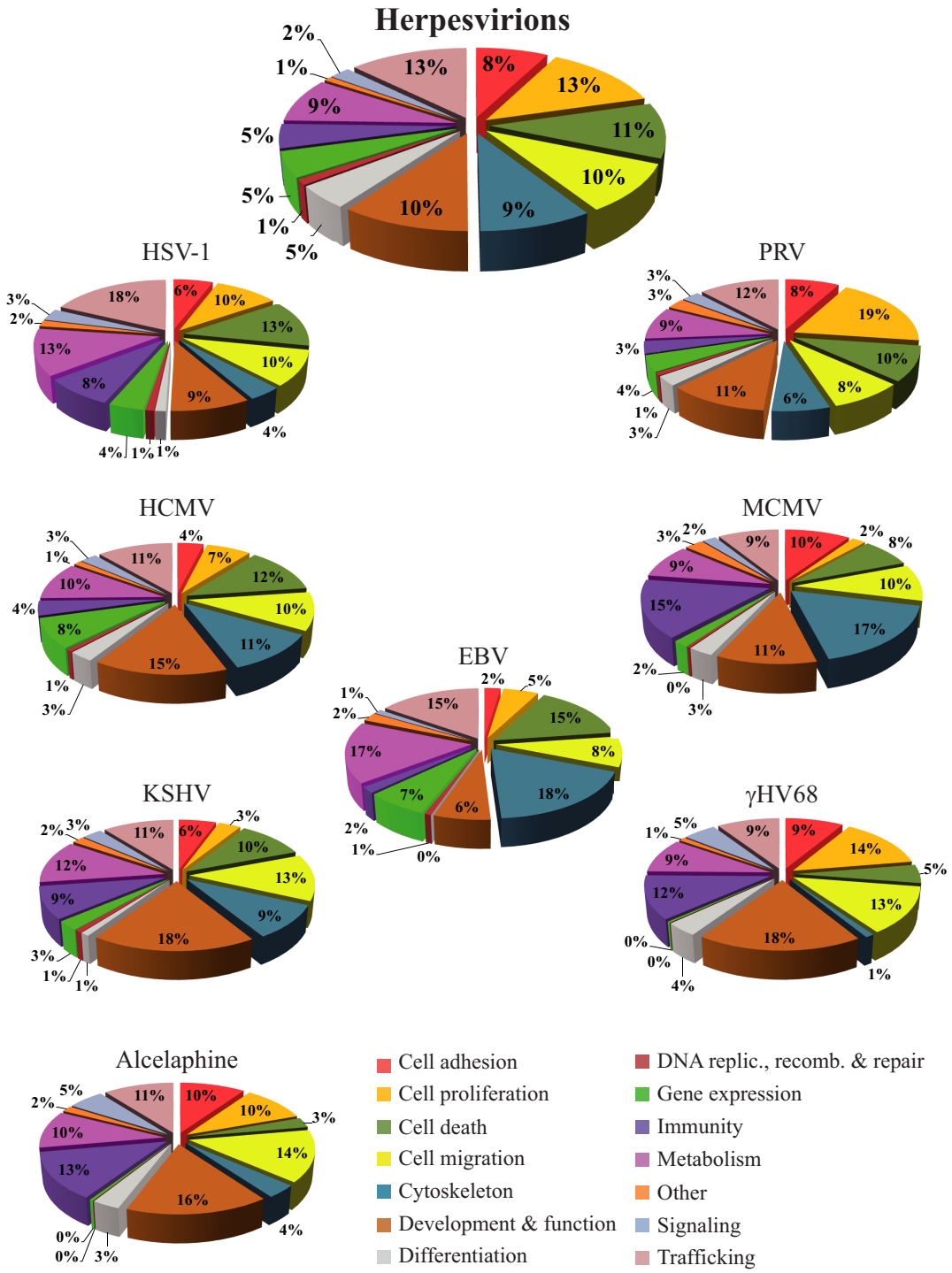

FIGURE 1 | The proteins from Table 1 were analyzed with the Ingenuity database to define their putative functions in the context of an infection. To this end, the protein accession numbers (or GI numbers) were queried from the Ingenuity database. For the purpose of this figure, all known functions associated with these proteins were exported to Microsoft Excel and regrouped. In the top pie chart, the cellular proteins found in all the herpesvirions were analyzed collectively, while the other pie charts depict the host proteins incorporated into each virus. Since each protein can be associated with multiples functions in the database, the results of those analyses are expressed as relative values instead of raw numbers, which consequently exceeds the original number of proteins analyzed. The percentages therefore represent the number of proteins falling into a given category with the total of each pie chart being 100%. A graphical legend of the categories is provided at the bottom right corner of the figure.

a consequence of their involvement in autophagosome formation and concomitant viral envelopment. Given the vast impact of Rab proteins on the cell, it will be a major challenge to decipher all their roles in the life cycle of herpesviruses, particularly for the pool present in mature virions.

Molecular trafficking is not only dependent on SNARES, Rab, and Arf proteins, it is also intimately linked to the cytoskeleton. It is thus not surprising that herpesviruses devote some of their resources toward regulating this central cellular machinery. For instance, herpesviruses significantly reorganize both cellular and nuclear actin as well as microtubules (Norrild et al., 1986; Avitabile et al., 1995; Sharma-Walia et al., 2004; Simpson-Holley et al., 2005; De Regge et al., 2006; Saksena et al., 2006). They also travel along microtubules during both entry and egress and interact with several cellular molecular motors (Sodeik et al., 1997; Smith et al., 2001; Dohner et al., 2002; Marozin et al., 2004; Lee et al., 2006; Wolfstein et al., 2006; Radtke et al., 2010) as well as cortical and nuclear actin filaments (Forest et al., 2005; Feierbach et al., 2006; Roberts and Baines, 2011). Furthermore, some members incorporate in their viral particles tubulin or actin-related components (**Table 1**; Wong and Chen, 1998; Grunewald et al., 2003). Actin has been reported to compensate the loss of various viral tegument proteins in PRV (del Rio et al., 2005; Michael et al., 2006) and may thus act as an abundant filling agent, so its significance in herpesviral particles remains enigmatic. Similarly, the relevance of intermediate filament components vimentin and keratins in some herpes virions (**Table 1**) is difficult to assess given these filaments are not as well characterized as other cytoskeletal elements. It may nevertheless be important for herpesviruses, particularly since they are not all associated with the common skin or hair contaminants often detected in mass spectrometry (Hertel, 2011).

Viruses tend to monopolize for their own purpose their host expression apparatus, including protein translation (Bushell and Sarnow, 2002). For example, the prototypic HSV-1 ICP27 viral protein regulates all aspect of mRNAs including transcription, splicing, nuclear export, and translation for the benefit of the virus (Rice and Knipe, 1988; Sekulovich et al., 1988; Sandri-Goldin and Mendoza, 1992; Smith et al., 1992; Hardwicke and Sandri-Goldin, 1994; Hardy and Sandri-Goldin, 1994; Brown et al., 1995; Soliman et al., 1997; Chen et al., 2002; Lindberg and Kreivi, 2002; Ellison et al., 2005; Larralde et al., 2006; Fontaine-Rodriguez and Knipe, 2008). As these cellular functions are highly regulated, the inclusion of DDX3X, a multifunctional RNA helicase that also regulates transcription, nuclear export, and translation that is used by several viruses (Schroder, 2010, 2011) may be relevant. Its incorporation into mature virions could thus accelerate viral gene expression in the early stages of the infection. Similarly, the presence of translation initiation or elongation factors in virions (**Table 1**) may also jumpstart gene expression in favor of the viruses.

Interestingly, HSV-1 does not require cells to be in the S-phase and even arrests the cell cycle at the G1/S transition step (Shadan et al., 1994; Song et al., 2000), which partly explains why it can grow in non-dividing neurons. While the precise mechanism of this arrest is unclear, it is known that the viral ICP0 protein and the VP16 cellular partner HCF modulate the cell cycle (Hobbs and DeLuca, 1999; Lomonte and Everett, 1999; Piluso et al., 2002). Moreover, ICP0 interacts with the host cyclin D3 (Kawaguchi et al., 1997). However, it was recently reported that stress, rather than the cell cycle *per se*, may be a critical feature (Bringhurst and Schaffer, 2006). Clearly, the interaction of herpesviruses with the cell proliferation apparatus is complex and likely involves several host and viral proteins. Identifying novel players that might be incorporated into mature virions may thus be very useful to clarify this process.

An interesting scenario is the possible regulation of apoptosis by host proteins loaded onto viral particles. Apoptosis is regulated both negatively and positively by several viruses (Teodoro and Branton, 1997; Goodkin et al., 2004), presumably to insure their survival at the early stages of the infection but their efficient release later on. Conceptually, the presence of anti-apoptotic proteins in herpes particles might thus provide a mean to quickly evade death upon entry, while the presence of pro-apoptotic proteins on newly assembled/enveloped viral particles may trigger or stimulate their extracellular release. Only further work will resolve this open question.

TECHNICAL LIMITATIONS

Several factors generally contribute to variation among proteomic studies. Hence, the preparation of the samples (e.g., in-gel trypsin digestion versus liquid digestion and chromatography) may lead to the detection of different populations of tryptic peptides. Moreover, the sensitivity of the mass spectrometers and the abundance of the proteins in the samples also impact peptide detection. The relative abundance of a peptide is itself influenced by the complexity of the samples, where some proteins may evade identification. Finally, each protein differs in its properties (ionization, resolution in SDS-PAGE gels), which will be reflected in their detection. This includes SNARES, which are transmembrane proteins resistant to SDS extraction (Yang et al., 1999; Kubista et al., 2004). It is thus likely that some of the proteins in **Table 1** are present in more viral particles than reported and that additional proteins are indeed incorporated in herpesvirions. More specific aspects regarding herpesviruses includes the purification schemes employed to enrich the viral particles, which will directly influence the purity of the samples and hence the potential detection of contaminants. One important caveat is that some host proteins may simply stick to the large viral particles. Another one is common contaminants such as some hair/skin associated keratins or as mentioned above actin, which may simply fill the virions. However, even potential contaminants cannot simply be discarded since actin and even some keratins may indeed participate in viral life cycles. Moreover, the relative abundance of all the cellular proteins within the cell is unknown, so it is not possible to rule out potential contaminants on the sole basis of abundance. It is thus critical to orthogonally validate all proteomics hits.

Various tools are available to define the biological relevance of host proteins identified in viral particles, including Western blotting, immuno-electron microscopy or functional screens. One powerful method is RNA interference. However, given the dual presence of the host proteins within the viral particles and the cell itself, this becomes a challenging task. RNA interference also has its own caveats (false positives and negatives). Another common step is the expression of dominant positive or negative mutants.

In all cases, one major difficulty is that the host proteins may be essential for the cells and their depletion may lead to cytotoxicity, thus proper controls are needed. In addition, the host proteins might be essential for the virus within the cells but only accessory within the virions. Consequently, depletion of a protein may have limited impact on the virus since complemented by the other pool of that protein in the virus or the cell. Small reduction or stimulation in viral yields may thus result. It such cases, it may be necessary to produce the virus on cells that lack these proteins to see if this makes a difference. One should also consider animal models since tissue culture based screens may miss important players, for instance modulators of the immune system or virulence factors. Clearly, multiple experimental strategies are needed to ultimately insure the biological significance of the host proteins found in viral particles.

CONCLUDING REMARKS AND FUTURE DIRECTIONS

The identification and functions of host proteins in viral particles is an important step toward the elucidation of novel host-pathogen interactions. In the case of herpesvirions, this is well under way with eight different family members analyzed so far. One main aspect is to sort biologically relevant cellular proteins from sticky contaminants. The orthogonal validation of the host proteins found in herpesvirions using biologically relevant assays is thus critical. As pointed out above, it will necessary to analyze all these proteins in the background of two pools, one cellular and one virion-associated, which are likely to complement one another. An interesting possibility is that some isoforms or specific post-translationally modified host proteins may be loaded into the capsids. Thus a detailed analysis of the host proteins present in viral particles will be important and a potential way to distinguish them from their cell-associated counterparts. Another issue is the expected variation among cell types. In that respect, it would be most interesting to examine the cellular protein content of HSV-1 produced in neurons in opposition to the virions produced on other cell types. Finally, the mechanisms by which all these host proteins are recruited to the viral particles will also need to be explored. Thus the proteomics of viral particles is only the beginning of the adventure, which should prove most exciting yet challenging.

ACKNOWLEDGMENTS

I am indebted to the Canadian Institutes of Health Research (grant # MOP82921) for funding our proteomics research. I also wish to thank Kerstin Radtke for excellent suggestions and Daniel Henaff for critical reading of the manuscript.

REFERENCES

Antrobus, R., Grant, K., Gangadharan, B., Chittenden, D., Everett, R. D., Zitzmann, N., and Boutell, C. (2009). Proteomic analysis of cells in the early stages of herpes simplex virus type-1 infection reveals widespread changes in the host cell proteome. *Proteomics* 9, 3913–3927.

Ashburner, M., Ball, C. A., Blake, J. A., Botstein, D., Butler, H., Cherry, J. M., Davis, A. P., Dolinski, K., Dwight, S. S., Eppig, J. T., Harris, M. A., Hill, D. P., Issel-Tarver, L., Kasarskis, A., Lewis, S., Matese, J. C., Richardson, J. E., Ringwald, M., Rubin, G. M., and Sherlock, G. (2000). Gene ontology: tool for the unification of biology. The Gene Ontology Consortium. *Nat. Genet.* 25, 25–29.

Avitabile, E., Di Gaeta, S., Torrisi, M. R., Ward, P. L., Roizman, B., and Campadelli-Fiume, G. (1995). Redistribution of microtubules and Golgi apparatus in herpes simplex virus-infected cells and their role in viral exocytosis. *J. Virol.* 69, 7472–7482.

Bartel, S., Doellinger, J., Darsow, K., Bourquain, D., Buchholz, R., Nitsche, A., and Lange, H. A. (2011). Proteome analysis of vaccinia virus IHD-W-infected HEK 293 cells with 2-dimensional gel electrophoresis and MALDI-PSD-TOF MS of on solid phase support N-terminally sulfonated peptides. *Virol. J.* 8, 380.

Bechtel, J. T., Winant, R. C., and Ganem, D. (2005). Host and viral proteins in the virion of Kaposi's sarcoma-associated herpesvirus. *J. Virol.* 79, 4952–4964.

Bernhard, O. K., Diefenbach, R. J., and Cunningham, A. L. (2005). New insights into viral structure and virus-cell interactions through proteomics. *Expert Rev. Proteomics* 2, 577–588.

Bortz, E., Whitelegge, J. P., Jia, Q., Zhou, Z. H., Stewart, J. P., Wu, T. T., and Sun, R. (2003). Identification of proteins associated with murine gammaherpesvirus 68 virions. *J. Virol.* 77, 13425–13432.

Bringhurst, R. M., and Schaffer, P. A. (2006). Cellular stress rather than stage of the cell cycle enhances the replication and plating efficiencies of herpes simplex virus type 1 ICP0- viruses. *J. Virol.* 80, 4528–4537.

Brown, C. R., Nakamura, M. S., Mosca, J. D., Hayward, G. S., Straus, S. E., and Perera, L. P. (1995). Herpes simplex virus trans-regulatory protein ICP27 stabilizes and binds to 3′ ends of labile mRNA. *J. Virol.* 69, 7187–7195.

Bushell, M., and Sarnow, P. (2002). Hijacking the translation apparatus by RNA viruses. *J. Cell Biol.* 158, 395–399.

Cantin, R., Methot, S., and Tremblay, M. J. (2005). Plunder and stowaways: incorporation of cellular proteins by enveloped viruses. *J. Virol.* 79, 6577–6587.

Cepeda, V., and Fraile-Ramos, A. (2011). A role for the SNARE protein syntaxin 3 in human cytomegalovirus morphogenesis. *Cell. Microbiol.* 13, 846–858.

Chen, I. H., Sciabica, K. S., and Sandri-Goldin, R. M. (2002). ICP27 interacts with the RNA export factor Aly/REF to direct herpes simplex virus type 1 intronless mRNAs to the TAP export pathway. *J. Virol.* 76, 12877–12889.

Chou, W., Ngo, T., and Gershon, P. D. (2012). An overview of the vaccinia virus infectome: a survey of the proteins of the poxvirus-infected cell. *J. Virol.* 86, 1487–1499.

Chua, C. E., Gan, B. Q., and Tang, B. L. (2011). Involvement of members of the Rab family and related small GTPases in autophagosome formation and maturation. *Cell. Mol. Life Sci.* 68, 3349–3358.

Coombs, K. M., Berard, A., Xu, W., Krokhin, O., Meng, X., Cortens, J. P., Kobasa, D., Wilkins, J., and Brown, E. G. (2010). Quantitative proteomic analyses of influenza virus-infected cultured human lung cells. *J. Virol.* 84, 10888–10906.

De Regge, N., Nauwynck, H. J., Geenen, K., Krummenacher, C., Cohen, G. H., Eisenberg, R. J., Mettenleiter, T. C., and Favoreel, H. W. (2006). Alpha-herpesvirus glycoprotein D interaction with sensory neurons triggers formation of varicosities that serve as virus exit sites. *J. Cell Biol.* 174, 267–275.

del Rio, T., Decoste, C. J., and Enquist, L. W. (2005). Actin is a component of the compensation mechanism in pseudorabies virus virions lacking the major tegument protein VP22. *J. Virol.* 79, 8614–8619.

Dohner, K., Wolfstein, A., Prank, U., Echeverri, C., Dujardin, D., Vallee, R., and Sodeik, B. (2002). Function of dynein and dynactin in herpes simplex virus capsid transport. *Mol. Biol. Cell* 13, 2795–2809.

Dry, I., Haig, D. M., Inglis, N. F., Imrie, L., Stewart, J. P., and Russell, G. C. (2008). Proteomic analysis of pathogenic and attenuated alcelaphine herpesvirus 1. *J. Virol.* 82, 5390–5397.

Ellison, K. S., Maranchuk, R. A., Mottet, K. L., and Smiley, J. R. (2005). Control of VP16 translation by the herpes simplex virus type 1 immediate-early protein ICP27. *J. Virol.* 79, 4120–4131.

Emmott, E., Rodgers, M. A., Macdonald, A., Mccrory, S., Ajuh, P., and Hiscox, J. A. (2010). Quantitative proteomics using stable isotope labeling with amino acids in cell culture reveals changes in the cytoplasmic, nuclear, and nucleolar proteomes in Vero cells infected with the coronavirus infectious bronchitis virus. *Mol. Cell Proteomics* 9, 1920–1936.

Everett, R. D. (2000). ICP0, a regulator of herpes simplex virus during lytic and latent infection. *Bioessays* 22, 761–770.

Feierbach, B., Piccinotti, S., Bisher, M., Denk, W., and Enquist, L. W. (2006). Alpha-herpesvirus infection induces the formation of nuclear actin filaments. *PLoS Pathog.* 2, e85. doi:10.1371/journal.ppat.0020085

Fontaine-Rodriguez, E. C., and Knipe, D. M. (2008). Herpes simplex virus ICP27 increases translation of a subset of viral late mRNAs. *J. Virol.* 82, 3538–3545.

Forest, T., Barnard, S., and Baines, J. D. (2005). Active intranuclear movement of herpesvirus capsids. *Nat. Cell Biol.* 7, 429–431.

Friedel, C. C., and Haas, J. (2011). Virus-host interactomes and global models of virus-infected cells. *Trends Microbiol.* 19, 501–508.

Goodkin, M. L., Morton, E. R., and Blaho, J. A. (2004). Herpes simplex virus infection and apoptosis. *Int. Rev. Immunol.* 23, 141–172.

Greber, U. F., and Way, M. (2006). A superhighway to virus infection. *Cell* 124, 741–754.

Grunewald, K., Desai, P., Winkler, D., Heymann, J., Belnap, D., Baumeister, W., and Steven, A. (2003). Three-dimensional structure of herpes simplex virus from cryo-electron tomography. *Science* 302, 1396–1398.

Gurer, C., Cimarelli, A., and Luban, J. (2002). specific incorporation of heat shock protein 70 family members into primate lentiviral virions. *J. Virol.* 76, 4666–4670.

Halford, W. P., and Schaffer, P. A. (2001). ICP0 is required for efficient reactivation of herpes simplex virus type 1 from neuronal latency. *J. Virol.* 75, 3240–3249.

Hancock, M. H., Corcoran, J. A., and Smiley, J. R. (2006). Herpes simplex virus regulatory proteins VP16 and ICP0 counteract an innate intranuclear barrier to viral gene expression. *Virology* 352, 237–252.

Hardwicke, M. A., and Sandri-Goldin, R. M. (1994). The herpes simplex virus regulatory protein ICP27 contributes to the decrease in cellular mRNA levels during infection. *J. Virol.* 68, 4797–4810.

Hardy, W. R., and Sandri-Goldin, R. M. (1994). Herpes simplex virus inhibits host cell splicing, and regulatory protein ICP27 is required for this effect. *J. Virol.* 68, 7790–7799.

Hertel, L. (2011). Herpesviruses and intermediate filaments: close encounters with the third type. *Viruses* 3, 1015–1040.

Hobbs, W. E. II, and DeLuca, N. A. (1999). Perturbation of cell cycle progression and cellular gene expression as a function of herpes simplex virus ICP0. *J. Virol.* 73, 8245–8255.

Huang Da, W., Sherman, B. T., and Lempicki, R. A. (2009). Systematic and integrative analysis of large gene lists using DAVID bioinformatics resources. *Nat. Protoc.* 4, 44–57.

Indran, S. V., and Britt, W. J. (2011). A role for the small GTPase Rab6 in assembly of human cytomegalovirus. *J. Virol.* 85, 5213–5219.

Johannsen, E., Luftig, M., Chase, M. R., Weicksel, S., Cahir-Mcfarland, E., Illanes, D., Sarracino, D., and Kieff, E. (2004). Proteins of purified Epstein-Barr virus. *Proc. Natl. Acad. Sci. U.S.A.* 101, 16286–16291.

Kanehisa, M., Goto, S., Furumichi, M., Tanabe, M., and Hirakawa, M. (2010). KEGG for representation and analysis of molecular networks involving diseases and drugs. *Nucleic Acids Res.* 38, D355–D360.

Kattenhorn, L. M., Mills, R., Wagner, M., Lomsadze, A., Makeev, V., Borodovsky, M., Ploegh, H. L., and Kessler, B. M. (2004). Identification of proteins associated with murine cytomegalovirus virions. *J. Virol.* 78, 11187–11197.

Kawaguchi, Y., Van Sant, C., and Roizman, B. (1997). Herpes simplex virus 1 alpha regulatory protein ICP0 interacts with and stabilizes the cell cycle regulator cyclin D3. *J. Virol.* 71, 7328–7336.

Kramer, T., Greco, T. M., Enquist, L. W., and Cristea, I. M. (2011). Proteomic characterization of pseudorabies virus extracellular virions. *J. Virol.* 85, 6427–6441.

Krauss, O., Hollinshead, R., Hollinshead, M., and Smith, G. L. (2002). An investigation of incorporation of cellular antigens into vaccinia virus particles. *J. Gen. Virol.* 83, 2347–2359.

Kubista, H., Edelbauer, H., and Boehm, S. (2004). Evidence for structural and functional diversity among SDS-resistant SNARE complexes in neuroendocrine cells. *J. Cell. Sci.* 117, 955–966.

Lam, Q., Smibert, C. A., Koop, K. E., Lavery, C., Capone, J. P., Weinheimer, S. P., and Smiley, J. R. (1996). Herpes simplex virus VP16 rescues viral mRNA from destruction by the virion host shutoff function. *EMBO J.* 15, 2575–2581.

Larralde, O., Smith, R. W., Wilkie, G. S., Malik, P., Gray, N. K., and Clements, J. B. (2006). Direct stimulation of translation by the multifunctional herpesvirus ICP27 protein. *J. Virol.* 80, 1588–1591.

Lee, G. E., Murray, J. W., Wolkoff, A. W., and Wilson, D. W. (2006). Reconstitution of herpes simplex virus microtubule-dependent trafficking in vitro. *J. Virol.* 80, 4264–4275.

Lietzen, N., Ohman, T., Rintahaka, J., Julkunen, I., Aittokallio, T., Matikainen, S., and Nyman, T. A. (2011). Quantitative subcellular proteome and secretome profiling of influenza A virus-infected human primary macrophages. *PLoS Pathog.* 7, e1001340. doi:10.1371/journal.ppat.1001340

Lindberg, A., and Kreivi, J. P. (2002). Splicing inhibition at the level of spliceosome assembly in the presence of herpes simplex virus protein ICP27. *Virology* 294, 189–198.

Lodish, H., Berk, A., Zipursky, S. L., Matsudaira, P., Baltimore, D., and Darnell, J. (2000). *Viruses: Structure, Function, and Uses. Molecular Cell Biology*, 4th Edn. (New York: W.H. Freeman and Company), 191–207.

Lomonte, P., and Everett, R. D. (1999). Herpes simplex virus type 1 immediate-early protein Vmw110 inhibits progression of cells through mitosis and from G(1) into S phase of the cell cycle. *J. Virol.* 73, 9456–9467.

Loret, S., Guay, G., and Lippe, R. (2008). Comprehensive characterization of extracellular herpes simplex virus type 1 virions. *J. Virol.* 82, 8605–8618.

Loret, S., and Lippe, R. (2012). Biochemical analysis of ICP0, ICP4, UL7 and UL23 incorporated into extracellular herpes simplex type 1 virions. *J. Gen. Virol.* 93, 624–634.

Lu, Q., Bai, J., Zhang, L., Liu, J., Jiang, Z., Michal, J. J., He, Q., and Jiang, P. (2012). Two-dimensional liquid chromatography-tandem mass spectrometry coupled with isobaric tags for relative and absolute quantification (iTRAQ) labeling approach revealed first proteome profiles of pulmonary alveolar macrophages infected with porcine reproductive and respiratory syndrome virus. *J. Proteome Res.* 11, 2890–2903.

Lu, Z., Qin, A., Qian, K., Chen, X., Jin, W., Zhu, Y., and Eltahir, Y. M. (2010). Proteomic analysis of the host response in the bursa of Fabricius of chickens infected with Marek's disease virus. *Virus Res.* 153, 250–257.

Marozin, S., Prank, U., and Sodeik, B. (2004). Herpes simplex virus type 1 infection of polarized epithelial cells requires microtubules and access to receptors present at cell-cell contact sites. *J. Gen. Virol.* 85, 775–786.

Maxwell, K. L., and Frappier, L. (2007). Viral proteomics. *Microbiol. Mol. Biol. Rev.* 71, 398–411.

Mercer, J., Schelhaas, M., and Helenius, A. (2010). Virus entry by endocytosis. *Annu. Rev. Biochem.* 79, 803–833.

Michael, K., Klupp, B. G., Mettenleiter, T. C., and Karger, A. (2006). Composition of pseudorabies virus particles lacking tegument protein US3, UL47, or UL49 or envelope glycoprotein E. *J. Virol.* 80, 1332–1339.

Mizuno-Yamasaki, E., Rivera-Molina, F., and Novick, P. (2012). GTPase networks in membrane traffic. *Annu. Rev. Biochem.* PMID: 22463690. [Epub ahead of print].

Moerdyk-Schauwecker, M., Hwang, S. I., and Grdzelishvili, V. Z. (2009). Analysis of virion associated host proteins in vesicular stomatitis virus using a proteomics approach. *Virol. J.* 6, 166.

Munday, D. C., Hiscox, J. A., and Barr, J. N. (2010). Quantitative proteomic analysis of A549 cells infected with human respiratory syncytial virus subgroup B using SILAC coupled to LC-MS/MS. *Proteomics* 10, 4320–4334.

Norrild, B., Lehto, V. P., and Virtanen, I. (1986). Organization of cytoskeleton elements during herpes simplex virus type 1 infection of human fibroblasts: an immunofluorescence study. *J. Gen. Virol.* 67(Pt 1), 97–105.

Ott, D. E. (2008). Cellular proteins detected in HIV-1. *Rev. Med. Virol.* 18, 159–175.

Padula, M. E., Sydnor, M. L., and Wilson, D. W. (2009). Isolation and preliminary characterization of herpes simplex virus 1 primary enveloped virions from the perinuclear space. *J. Virol.* 83, 4757–4765.

Pastorino, B., Boucomont-Chapeaublanc, E., Peyrefitte, C. N., Belghazi, M., Fusai, T., Rogier, C., Tolou, H. J., and Almeras, L. (2009). Identification of cellular proteome modifications in response to West Nile virus infection. *Mol. Cell Proteomics* 8, 1623–1637.

Piluso, D., Bilan, P., and Capone, J. P. (2002). Host cell factor-1 interacts with and antagonizes transactivation by the cell cycle regulatory factor Miz-1. *J. Biol. Chem.* 277, 46799–46808.

Radtke, K., Kieneke, D., Wolfstein, A., Michael, K., Steffen, W., Scholz, T., Karger, A., and Sodeik, B. (2010). Plus- and minus-end directed microtubule motors bind simultaneously to herpes simplex virus capsids using different inner tegument

structures. *PLoS Pathog.* 6, e1000991. doi:10.1371/journal.ppat.1000991

Ramirez-Boo, M., Nunez, E., Jorge, I., Navarro, P., Fernandes, L. T., Segales, J., Garrido, J. J., Vazquez, J., and Moreno, A. (2011). Quantitative proteomics by 2-DE, 16O/18O labelling and linear ion trap mass spectrometry analysis of lymph nodes from piglets inoculated by porcine circovirus type 2. *Proteomics* 11, 3452–3469.

Rassmann, A., Henke, A., Zobawa, M., Carlsohn, M., Saluz, H. P., Grabley, S., Lottspeich, F., and Munder, T. (2006). Proteome alterations in human host cells infected with coxsackievirus B3. *J. Gen. Virol.* 87, 2631–2638.

Rice, S. A., and Knipe, D. M. (1988). Gene-specific transactivation by herpes simplex virus type 1 alpha protein ICP27. *J. Virol.* 62, 3814–3823.

Roberts, K. L., and Baines, J. D. (2011). Actin in herpesvirus infection. *Viruses* 3, 336–346.

Saksena, M. M., Wakisaka, H., Tijono, B., Boadle, R. A., Rixon, F., Takahashi, H., and Cunningham, A. L. (2006). Herpes simplex virus type 1 accumulation, envelopment, and exit in growth cones and varicosities in mid-distal regions of axons. *J. Virol.* 80, 3592–3606.

Sandri-Goldin, R. M., and Mendoza, G. E. (1992). A herpesvirus regulatory protein appears to act post-transcriptionally by affecting mRNA processing. *Genes Dev.* 6, 848–863.

Sarma, N., Agarwal, D., Shiflett, L. A., and Read, G. S. (2008). Small interfering RNAs that deplete the cellular translation factor eIF4H impede mRNA degradation by the virion host shutoff protein of herpes simplex virus. *J. Virol.* 82, 6600–6609.

Schroder, M. (2010). Human DEAD-box protein 3 has multiple functions in gene regulation and cell cycle control and is a prime target for viral manipulation. *Biochem. Pharmacol.* 79, 297–306.

Schroder, M. (2011). Viruses and the human DEAD-box helicase DDX3: inhibition or exploitation? *Biochem. Soc. Trans.* 39, 679–683.

Sekulovich, R. E., Leary, K., and Sandri-Goldin, R. M. (1988). The herpes simplex virus type 1 alpha protein ICP27 can act as a trans-repressor or a trans-activator in combination with ICP4 and ICP0. *J. Virol.* 62, 4510–4522.

Shadan, F. F., Cowsert, L. M., and Villarreal, L. P. (1994). n-Butyrate, a cell cycle blocker, inhibits the replication of polyomaviruses and papillomaviruses but not that of adenoviruses and herpesviruses. *J. Virol.* 68, 4785–4796.

Sharma-Walia, N., Naranatt, P. P., Krishnan, H. H., Zeng, L., and Chandran, B. (2004). Kaposi's sarcoma-associated herpesvirus/human herpesvirus 8 envelope glycoprotein gB induces the integrin-dependent focal adhesion kinase-Src-phosphatidylinositol 3-kinase-rho GTPase signal pathways and cytoskeletal rearrangements. *J. Virol.* 78, 4207–4223.

Shaw, M. L., Stone, K. L., Colangelo, C. M., Gulcicek, E. E., and Palese, P. (2008). Cellular proteins in influenza virus particles. *PLoS Pathog.* 4, e1000085. doi:10.1371/journal.ppat.1000085

Simons, K., and Warren, G. (1984). Semliki forest virus: a probe for membrane traffic in the animal cell. *Adv. Protein Chem.* 36, 79–132.

Simpson-Holley, M., Colgrove, R. C., Nalepa, G., Harper, J. W., and Knipe, D. M. (2005). Identification and functional evaluation of cellular and viral factors involved in the alteration of nuclear architecture during herpes simplex virus 1 infection. *J. Virol.* 79, 12840–12851.

Smith, G. A., Gross, S. P., and Enquist, L. W. (2001). Herpesviruses use bidirectional fast-axonal transport to spread in sensory neurons. *Proc. Natl. Acad. Sci. U.S.A.* 98, 3466–3470.

Smith, I. L., Hardwicke, M. A., and Sandri-Goldin, R. M. (1992). Evidence that the herpes simplex virus immediate early protein ICP27 acts post-transcriptionally during infection to regulate gene expression. *Virology* 186, 74–86.

Sodeik, B., Ebersold, M. W., and Helenius, A. (1997). Microtubule-mediated transport of incoming herpes simplex virus 1 capsids to the nucleus. *J. Cell Biol.* 136, 1007–1021.

Soliman, T. M., Sandri-Goldin, R. M., and Silverstein, S. J. (1997). Shuttling of the herpes simplex virus type 1 regulatory protein ICP27 between the nucleus and cytoplasm mediates the expression of late proteins. *J. Virol.* 71, 9188–9197.

Sollner, T. H. (2004). Intracellular and viral membrane fusion: a uniting mechanism. *Curr. Opin. Cell Biol.* 16, 429–435.

Sollner, T. H., and Rothman, J. E. (1996). Molecular machinery mediating vesicle budding, docking and fusion. *Experientia* 52, 1021–1025.

Song, B., Liu, J. J., Yeh, K. C., and Knipe, D. M. (2000). Herpes simplex virus infection blocks events in the G1 phase of the cell cycle. *Virology* 267, 326–334.

Sun, J., Jiang, Y., Shi, Z., Yan, Y., Guo, H., He, F., and Tu, C. (2008). Proteomic alteration of PK-15 cells after infection by classical swine fever virus. *J. Proteome Res.* 7, 5263–5269.

Teodoro, J. G., and Branton, P. E. (1997). Regulation of apoptosis by viral gene products. *J. Virol.* 71, 1739–1746.

Thanthrige-Don, N., Abdul-Careem, M. F., Shack, L. A., Burgess, S. C., and Sharif, S. (2009). Analyses of the spleen proteome of chickens infected with Marek's disease virus. *Virology* 390, 356–367.

Tong, A., Wu, L., Lin, Q., Lau, Q. C., Zhao, X., Li, J., Chen, P., Chen, L., Tang, H., Huang, C., and Wei, Y. Q. (2008). Proteomic analysis of cellular protein alterations using a hepatitis B virus-producing cellular model. *Proteomics* 8, 2012–2023.

Varnum, S. M., Streblow, D. N., Monroe, M. E., Smith, P., Auberry, K. J., Pasa-Tolic, L., Wang, D., Camp, D. G. II, Rodland, K., Wiley, S., Britt, W., Shenk, T., Smith, R. D., and Nelson, J. A. (2004). Identification of proteins in human cytomegalovirus (HCMV) particles: the HCMV proteome. *J. Virol.* 78, 10960–10966.

Viswanathan, K., and Fruh, K. (2007). Viral proteomics: global evaluation of viruses and their interaction with the host. *Expert Rev. Proteomics* 4, 815–829.

Wolfstein, A., Nagel, C. H., Radtke, K., Dohner, K., Allan, V. J., and Sodeik, B. (2006). The inner tegument promotes herpes simplex virus capsid motility along microtubules in vitro. *Traffic* 7, 227–237.

Wong, M. L., and Chen, C. H. (1998). Evidence for the internal location of actin in the pseudorabies virion. *Virus Res.* 56, 191–197.

Yang, B., Gonzalez, L. Jr., Prekeris, R., Steegmaier, M., Advani, R. J., and Scheller, R. H. (1999). SNARE interactions are not selective. Implications for membrane fusion specificity. *J. Biol. Chem.* 274, 5649–5653.

Zandi, F., Eslami, N., Soheili, M., Fayaz, A., Gholami, A., and Vaziri, B. (2009). Proteomics analysis of BHK-21 cells infected with a fixed strain of rabies virus. *Proteomics* 9, 2399–2407.

Zenner, H. L., Yoshimura, S., Barr, F. A., and Crump, C. M. (2011). Analysis of Rab GTPase-activating proteins indicates that Rab1a/b and Rab43 are important for herpes simplex virus 1 secondary envelopment. *J. Virol.* 85, 8012–8021.

Zerial, M., and McBride, H. (2001). Rab proteins as membrane organizers. *Nat. Rev. Mol. Cell Biol.* 2, 107–117.

Zhang, L., Jia, X., Zhang, X., Sun, J., Peng, X., Qi, T., Ma, F., Yin, L., Yao, Y., Qiu, C., and Lu, H. (2010). Proteomic analysis of PBMCs: characterization of potential HIV-associated proteins. *Proteome Sci.* 8, 12.

Zhang, X., Zhou, J., Wu, Y., Zheng, X., Ma, G., Wang, Z., Jin, Y., He, J., and Yan, Y. (2009). Differential proteome analysis of host cells infected with porcine circovirus type 2. *J. Proteome Res.* 8, 5111–5119.

Zheng, J., Sugrue, R. J., and Tang, K. (2011). Mass spectrometry based proteomic studies on viruses and hosts – a review. *Anal. Chim. Acta* 702, 149–159.

Zhu, F. X., Chong, J. M., Wu, L., and Yuan, Y. (2005). Virion proteins of Kaposi's sarcoma-associated herpesvirus. *J. Virol.* 79, 800–811.

Conflict of Interest Statement: The author declares that the research was conducted in the absence of any commercial or financial relationships that could be construed as a potential conflict of interest.

Received: 11 April 2012; accepted: 27 April 2012; published online: 28 May 2012.

*Citation: Lippé R (2012) Deciphering novel host–herpesvirus interactions by virion proteomics. Front. Microbio. **3**:181. doi: 10.3389/fmicb.2012.00181*

This article was submitted to Frontiers in Virology, a specialty of Frontiers in Microbiology.

frontiers in
MICROBIOLOGY

MINI REVIEW ARTICLE
published: 04 July 2012
doi: 10.3389/fmicb.2012.00240

Proteomic analysis of HIV–T cell interaction: an update

Gertjan Kramer[1], Perry D. Moerland[2,3], Rienk E. Jeeninga[4], Wytze J. Vlietstra[2], Jeffrey H. Ringrose[3,4†], Carsten Byrman[2,3], Ben Berkhout[4] and Dave Speijer[1]*

[1] Department of Medical Biochemistry, Academic Medical Center, University of Amsterdam, Amsterdam, Netherlands

[2] Bioinformatics Laboratory, Department of Clinical Epidemiology, Biostatistics and Bioinformatics, Academic Medical Center, University of Amsterdam, Amsterdam, Netherlands

[3] Netherlands Proteomics Center, H.R. Kruytgebouw, Utrecht, Netherlands

[4] Laboratory of Experimental Virology, Department of Medical Microbiology, Center for Infection and Immunity Amsterdam, Amsterdam, Netherlands

Edited by:
Kevin Coombs, University of Manitoba, Canada

Reviewed by:
Wataru Nomura, Tokyo Medical and Dental University, Japan
Kevin Coombs, University of Manitoba, Canada

***Correspondence:**
Dave Speijer, K1–262, Medical Biochemistry, Academic Medical Center, University of Amsterdam, Meibergdreef 15, 1105 AZ Amsterdam, Netherlands.
e-mail: d.speijer@amc.uva.nl

†Present address:
Biomolecular Mass Spectrometry and Proteomics, Bijvoet Center for Biomolecular Research, Utrecht Institute for Pharmaceutical Sciences, Utrecht University, Utrecht, Netherlands

This mini-review summarizes techniques applied in, and results obtained with, proteomic studies of human immunodeficiency virus type 1 (HIV-1)–T cell interaction. Our group previously reported on the use of two-dimensional differential gel electrophoresis (2D-DIGE) coupled to matrix assisted laser-desorption time of flight peptide mass fingerprint analysis, to study T cell responses upon HIV-1 infection. Only one in three differentially expressed proteins could be identified using this experimental setup. Here we report on our latest efforts to test models generated by this data set and extend its analysis by using novel bioinformatic algorithms. The 2D-DIGE results are compared with other studies including a pilot study using one-dimensional peptide separation coupled to MS^E, a novel mass spectrometric approach. It can be concluded that although the latter method detects fewer proteins, it is much faster and less labor intensive. Last but not least, recent developments and remaining challenges in the field of proteomic studies of HIV-1 infection and proteomics in general are discussed.

Keywords: DIGE, HIV-1, host–virus interaction, proteomics, LC–MS/MS^E

INTRODUCTION

Human immunodeficiency virus type 1 (HIV-1), the causative agent of AIDS, uses $CD4^+$ T cells as a host. In order to do so efficiently the virus adapts the host cell's intracellular metabolism. The host cell, in turn, initiates intracellular antiviral responses and signals to the host's immune system (Lever and Jeang, 2011). Thus, HIV-1 infection and the host response trigger many physiological changes in the infected cell (Gomez and Hope, 2005). HIV-1 survives and persists in infected cells preparing them for production and release of new viral particles. Intracellular changes due to HIV-1 infection have been studied extensively, focusing on the contribution of HIV-1's accessory proteins to these processes, using microarrays or serial analysis of gene expression (SAGE) to detect mRNA changes in the cell (Van't Wout et al., 2003; Giri et al., 2006; Roeth and Collins, 2006; Lefebvre et al., 2011; Wu et al., 2011). Gene expression profiling with microarrays is of course easy to perform, generating large datasets quickly (Heller, 2002), but sequences must be known in advance, which SAGE does not require. SAGE, based on direct sequencing of mRNA tags, also does not use hybridization as microarrays do, leading to more reliable probing of mRNA levels. SAGE is currently being replaced by high-throughput sequencing technologies (RNA-Seq; Baginsky et al., 2010). Proteome changes upon HIV infection have also been studied in detail with mass spectrometry (Coiras et al., 2006; Chan et al., 2007; Ringrose et al., 2008; Navare et al., 2012), lately focusing on studies specifically monitoring direct interactions between viral and cellular proteins (Jager et al., 2012a,b).

Changes in gene expression patterns characterize the cellular response to HIV-1 infection. However, changes in mRNA levels are only part of the story. Often stringent correlation between mRNA and protein levels is lacking (Pradet-Balade et al., 2001). In human cells, transcription seems to explain only 30% of variation in protein levels, with translation and protein degradation contributing up to 40% (Vogel et al., 2010; Schwanhausser et al., 2011). In *E. coli*, relative contributions to regulation of protein levels via transcriptional and/or translational control have even been shown to vary greatly with the kind of signal the cell responds to (Kramer et al., 2010). Direct cellular responses are also strongly accompanied by coordinated protein modifications. A protein can exist in many different isoforms, each with its own specific function, with a relatively limited number of genes giving rise to vast amounts of (functionally) distinct proteins (Jensen, 2006). This is mostly accomplished by post-translational protein modification (PTM). PTMs constitute highly versatile systems allowing cells to respond very quickly to both external and internal signals, as illustrated by protein phosphorylation in signal transduction or metabolic regulation. Of course, such PTM responses cannot be detected using DNA/RNA sequencing technologies. Thus, proteomic studies using mass spectrometry

to detect and quantify differences in protein expression, protein isoforms and complexes, as well as PTMs, are essential for understanding the complete set of intracellular responses to HIV-1 infection. In this way new insights and intervention strategies can be developed.

In a previous study, we used the fluorescence two-dimensional differential gel electrophoresis (2D-DIGE) technique for a comparison of uninfected and HIV-1 infected T cells (Ringrose et al., 2008). This technique starts out with minimal protein labeling using cyanine based fluorescent probes recognizing lysine. A subsequent two-dimensional gel electrophoresis allows the quantification of changes in protein expression by mixing cell extracts labeled either with Cy3 or Cy5 and running them on a single gel (Unlu et al., 1997; Alban et al., 2003). Next, differentially expressed proteins can be identified by peptide mass fingerprinting (PMF) using a matrix assisted laser-desorption time of flight (MALDI-TOF) mass spectrometer. PMF uses lists of masses of peptides ("fingerprints") generated by tryptic digestion of proteins for their identification. NB: In this approach quantification is based on amount of fluorescence and not on ion detection level in a mass spectrometer. The study confirmed several HIV-1 effects on pathways and cellular processes previously described using stable isotope labeling combined with liquid chromatography–mass spectrometry (LC–MS; Chan et al., 2007). But there were novel findings as well, most importantly the downregulation of proteins involved in glycolysis upon full-blown HIV-1 infection, presumably part of a complete metabolic rerouting to preserve glucose for the pentose phosphate pathway, the source of riboses for subsequent viral nucleic acid synthesis (Ringrose et al., 2008). However, despite the success of this 2D-DIGE PMF approach it also comes with some limitations: the technique is very labor intensive and about two-thirds of all the differentially expressed proteins detected could not be identified using PMF because they were not present in sufficient abundance. As we are planning to extend our proteomic analysis of HIV-1 T cell interaction to subcellular fractions, a faster method would be preferable. To that end we compared the 2D-DIGE PMF with one-dimensional separation of peptides using reversed phase LC coupled to MS^E (Geromanos et al., 2009) analysis, again using T cells infected with HIV-1. In this approach target proteins are digested with trypsin (as in the PMF method mentioned above), and resulting peptides (parent ions in **Figure 1**) are now identified as coming from certain proteins by the mass analysis of their fragments (daughter ions in **Figure 1**), which allows peptide sequencing [in both data-dependent modes of acquisition (DDA) and MS^E applications described below] as well as protein quantitation by peptide signal abundance.

A PILOT STUDY USING LC–MS^E

One of the most exciting new developments in proteomic analyses is the possibility to perform quantitative protein comparisons without having to introduce quantifiable labels: label-free proteomics. Here we report on the use of label-free proteomics in a pilot study of T cells (PM1 T cell line) infected with HIV-1 (LAI isolate). In this setup a novel data-independent alternate scanning technique (MS^E) on a quadrupole time of flight (QTOF) instrument is used. In contrast to DDA, making up the standard method on various types of instruments used in peptide based proteomics, MS^E does not select a single precursor ion for fragmentation but rather fragments "all" ions present at any given time during chromatographic separation. As such, mass spectrometric data are collected (in principle) on fragments of "all" ions instead of a subset that is selected for fragmentation during DDA analysis. This decreases bias toward selecting only highly abundant peptides and eliminates the need to measure samples multiple times in order to collect tandem-MS data for "all" ions present (**Figure 1**). In this manner, MS^E greatly expands the number of peptides detected using limited LC-separation compared to DDA on QTOF type instruments (Geromanos et al., 2009).

A drawback of MS^E is its incompatibility with quantitation schemes that make use of an amine reactive isotopic-label and specific reporter fragment ions to ascertain protein quantity such as iTRAQ (isobaric tag for relative and absolute quantification; Wiese et al., 2007). This approach was used very recently for quantitation of early effects of HIV infection (Navare et al., 2012) using multi-dimensional separation and an Orbitrap mass spectrometer (Makarov and Scigelova, 2010) in which 1448 proteins were reliably quantified. However, LC–MS^E is well suited for *label-free* quantitation and pilot studies applying it to our model system (uninfected PM1 T cells vs. cells at the peak of HIV-1 infection) are promising. So far we could quantify 358 proteins, with at least 16 proteins clearly up- or downregulated (more than twofold). Six enzymes involved in glycolysis were identified. Consistent with our previous observations these were found either to be hardly changed or downregulated. Several other proteins found to be changed in abundance previously (Ringrose et al., 2008) were again detected, but whereas, e.g. Stathmin (Q96CE4) is downregulated as before, several 14-3-3 proteins are now upregulated instead of downregulated (see Discussion). Total numbers of identified proteins are obviously lower than in the 2D-DIGE approach, but the technique is much faster, and less labor intensive (days vs. months). Also, as lower amounts of protein are needed for analysis, smaller and more reproducible cell culture samples can be used. In the future we plan to combine this approach with in-line enrichment of phosphopeptides using titanium dioxide chromatography (Pinkse et al., 2004, 2011) to look at changes in the cellular phosphoproteome upon HIV-1 infection. In addition, LC–MS^E will be used with cell lines containing an inducible HIV-1 provirus (Jeeninga et al., 2008). This allows a more synchronous induction of virus production compared to viral infection, increasing the sensitivity of the assay such that small biological changes can be detected. This will also make it feasible to discriminate between changes induced by the initial virus infection and the subsequent stage of new virus production.

FOLLOW-UP RESEARCH USING RNAi-MEDIATED KNOCKDOWN OF CELL FACTORS

Follow-up study on some of the proteins identified in the 2D-DIGE study was performed with an RNA interference (RNAi) knockdown screen. Protein induction may reflect host defensive mechanisms to prevent or restrict virus infection or replication. Alternatively, such changes may represent a viral strategy to induce

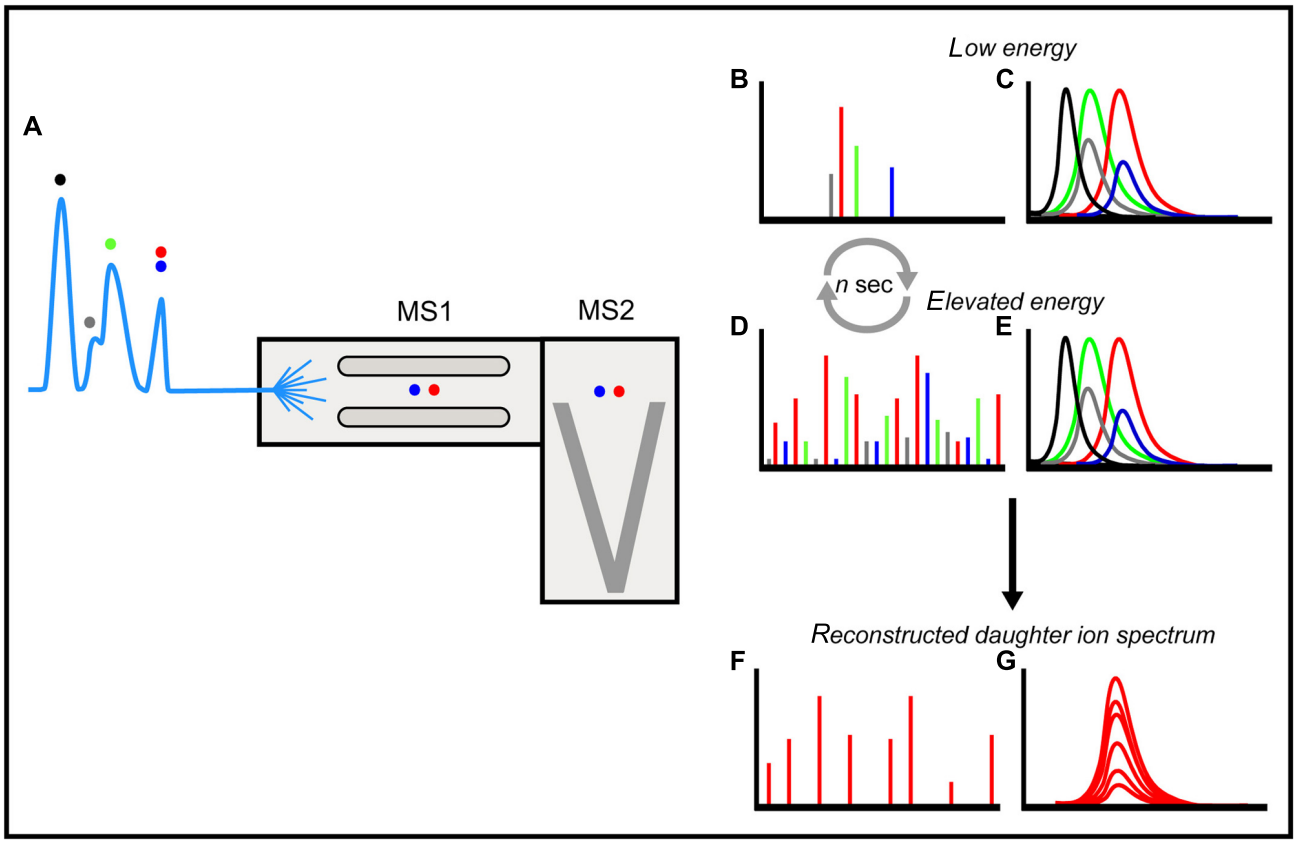

FIGURE 1 | An overview of LC–MS^E. Separation of peptides (colored dots) on an LC coupled to a QTOF instrument in a data-independent mode of acquisition using electrospray ionization **(A)**. In a data-independent mode of acquisition the quadrupole (MS1) continuously allows passage of all ions, in contrast to DDA where the quadrupole selects ions for fragmentation based on their intensity. Energy in the collision cell is continuously cycled between a low and an elevated profile. This generates spectra of all parent **(B)** and daughter ions **(D)** throughout the LC–MS run in the time of flight analyzer (MS2) without bias with respect to their relative intensities. In order to reconstruct fragment ion spectra with daughter ions from a single parent only, an ion-accounting algorithm compares the retention time profiles of all individual parent ions **(C)** to all individual daughter ions **(E)** matching them on the basis of retention time profile and intensity **(G)**. In this manner the algorithm creates a reconstructed daughter ion spectrum matched to a single precursor **(F)** that can be used by proteome search engines to identify peptides and link these to proteins. The unbiased data-independent scanning mode greatly expands the number of peptides – and thus of proteins – detected, compared to the DDA mode of acquisition on QTOF type instruments, especially using limited LC separations on complex mixtures to increase throughput. Adapted from (Plumb et al., 2006).

cellular factors facilitating specific steps of the replication cycle (cofactors). For 76 cellular targets the impact on HIV-1 replication was studied upon mRNA knockdown, using short hairpin RNA (shRNA) inhibitors from the Mission^{TM} library (Moffat et al., 2006). For each target gene four to five shRNAs to generate stably transduced T cells were used, thus reducing the chance of scoring off-target effects. Knockdown of 38 individual mRNA targets resulted in decreased virus replication, possibly because of suppression of a viral cofactor. Of these, 27 proteins were upregulated during HIV-1 infection in our previous 2D-DIGE proteomic screen, fitting the cofactor role. For three targets an increase in viral replication was observed, raising the possibility that a viral restriction factor was hit (unpublished results).

BIOINFORMATIC ANALYSIS OF 2D-DIGE DATA

As mentioned above, one of the most severe limitations of the 2D-DIGE PMF approach lies in the fact that about two-thirds of all the differentially expressed proteins detected cannot be identified using PMF, as they are not sufficiently abundant. This reflects the major challenge in all proteomic studies: identification and (relative) quantification of proteins with lower abundancies. We detected 1920 spots, of which 15% (288) were differentially expressed at 7–10 days post-infection (p.i.; Ringrose et al., 2008). Of these 288 differentially expressed protein spots, 182 remain to be identified. However, we have some additional information regarding these unidentified protein spots: we know the p*I* and Mw of the protein, i.e. of the specific isoform(s) detected, which in most cases represent the most abundant, mature protein form(s). We can also surmise what pathways the proteins most likely are involved in, based on the results obtained for the ∼100 identified spots. Using this information we are developing bioinformatic algorithms to come up with accurate lists of candidate differentially expressed proteins upon virus infection. Obviously, such candidates have to be confirmed experimentally, checked for instance with highly sensitive antibody-based methods such as western blotting. We developed a prioritization approach

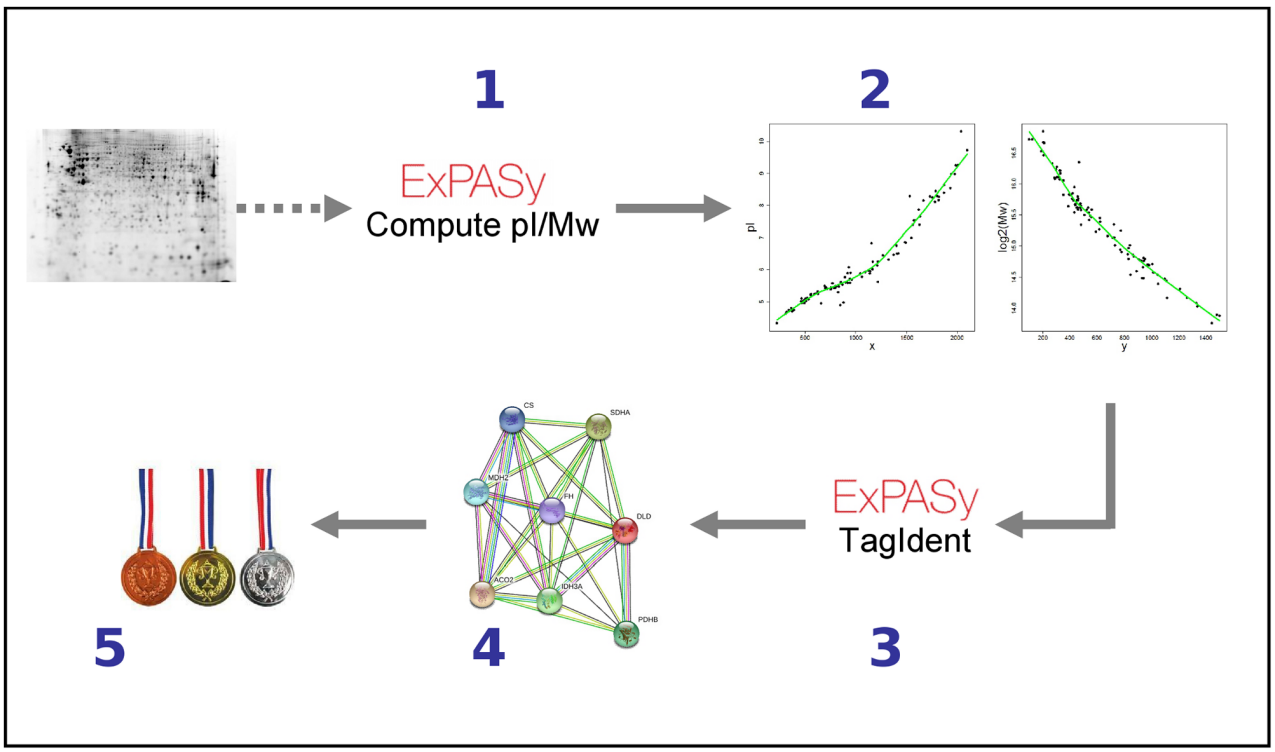

FIGURE 2 | How to identify candidate proteins based on p*I* and Mw. For details see text.

consisting of five steps (**Figure 2**). First, for the PMF-identified proteins the theoretical p*I* and Mw are computed for the mature form using "Compute pI/Mw"[1]. Second, two non-linear models are fitted to predict p*I* and Mw, respectively. Parameters of the model are estimated from the *x*/*y*-coordinates of the identified spots and the p*I* and Mw determined in the previous step. Next, we use these models to predict p*I* and Mw for unidentified spots. Third, for each unidentified spot a list of candidate proteins is determined using the estimated p*I* and Mw as input for TagIdent[2]. TagIdent requires specifying a window size for the estimated p*I* and Mw. Because of uncertainty in the p*I* and Mw values, we choose relatively large windows so that the candidate list is likely to include the correct protein. However, candidate lists thus often contain hundreds of proteins. This is addressed in the last two steps, using the principle of "guilt by association": more likely candidate proteins share more features with already identified proteins, e.g., being present in the same pathway. In the fourth step of our algorithm the physical and/or functional interactions of the ∼100 identified proteins are extracted from the Search Tool for the Retrieval of Interacting Genes (STRING) database (Szklarczyk et al., 2011). STRING covers co-occurrence in pathways, physical protein–protein interactions, co-occurrence in the abstracts of scientific reports, etc., and provides confidence scores for strengths of the associations. In step 5, candidate proteins are ranked using confidence scores by summing weighted interactions with our "identified protein" STRING set. By combining 2D-DIGE with this kind of bioinformatic algorithm it would become one of the first techniques able to identify differential proteins in the lower regions of the dynamic range.

DISCUSSION

Comparing proteomic studies that address HIV–T cell interaction, it is observed that the various approaches yield a wide range in reported numbers of quantifiable proteins, ranging from 3255 (Chan et al., 2007) and 1448 (Navare et al., 2012) in total quantifiable proteins for techniques using multi-dimensional separation of peptides to 92 differentially expressed proteins (out of 1,920 spots) in a 2D-DIGE approach (Ringrose et al., 2008). In contrast, the numbers of differentially expressed proteins are somewhat comparable at various times p.i. Ringrose et al. (2008) reported 9 (42 h p.i.) and 92 (7–10 days p.i.) regulated proteins upon infection, while the group of Katze detected 687 (36 h p.i.) changed proteins (Chan et al., 2007) and found 266 (4 h p.i.), 60 (8 h p.i.), and 22 (20 h p.i.) proteins differentially expressed earlier on in infection (Navare et al., 2012). Although numbers can of course vary according to statistical significance settings, only a small subset of proteins is usually identified by all methods (Fahey et al., 2011). Each experimental setup yields a considerable group of proteins that are not scored by the other methods. This complementarity can be explained not only by differences in detection and quantification methods, but frequently by differences in the experimental biological systems as well. Variations include: host cell type and virus isolate (e.g., with a different receptor use and cell tropism),

[1]http://web.expasy.org/compute_pi/
[2]http://web.expasy.org/tagident/

and timepoint of sampling. Especially the impact of this latter variable should not be underestimated. It can even determine whether differentially expressed protein(form)s are found to be up- *or* downregulated in the interaction between HIV-1 and its host. 14-3-3 protein epsilon (P62258) is a case in point: it is upregulated after 4 h p.i. and downregulated later on at 7–10 days p.i. (Ringrose et al., 2008). Three other 14-3-3 proteins now seem to follow suit: tau/theta (P27348), gamma (P61981), and zeta/delta (P63104) are found to be upregulated in our latest MS^E experiments, but were clearly found to be downregulated in (Ringrose et al., 2008). These proteins can be phosphorylated on serine as well as threonine, e.g., influencing their migration on 2D, and consequently pattern and abundance changes can be difficult to interpret. As mentioned, an interesting recent study to look at the earliest events in HIV infection characterizing the host response at the protein level in $CD4^+$ SUP-T1 cells 4, 8, and 20 h p.i. using HIV-1 strain LAI, was performed by Navare et al. (2012). Comparison of this study to Ringrose et al. (2008), again shows the virus–cell interaction being highly dynamic. Just a few examples: high-mobility group box 1 (P09429) and cofilin (P23528) are strongly upregulated 4 h p.i., return to "normal" 4 and 16 h later, while at 7–10 days p.i. both are downregulated; glucose-6-phosphate isomerase (P06744) is upregulated at 8 h p.i., but at 7–10 days p.i. is found to be downregulated.

Given all this complexity, it is safe to say that proteomic studies on HIV-1 in general, and on HIV–T cell interaction in particular, will continue to generate new insights. But it will not be easy to translate these snapshot datasets into a comprehensive mechanistic understanding of all interactions involved (Haarburger and Pillay, 2010; Zhang et al., 2010). As mentioned, another problem of proteomic studies is identification and quantification of proteins with lower abundancies. One of the possible solutions to do this in a relatively unbiased fashion is sampling a proteome via interaction with random hexameric peptides using Arg, Lys, His, Phe, Tyr, Trp, Leu, and Val only: proteominer beads (Boschetti and Righetti, 2008). Samples still seem to be dominated by the most abundant proteins, however. "Looking at less to see more" might be the better way ahead. Such focusing could be on the analysis of specific cellular fractions (e.g. mitochondrial preparations), or on the selective study of specific classes of protein or PTMs, such as the phosphoproteome mentioned above.

Another example of zooming in on specific protein subsets is the use of methods to enrich for cellular factors that directly interact with HIV-1 proteins. Exciting results have been obtained with such "interactome proteomics" methods. The most general approach was performed with tagged versions of all 18 HIV-1 (poly)proteins. The accessory factors Vif, Vpu, Vpr, and Nef, Tat and Rev, as well as the polyproteins Gag, Pol, and Gp160, and their processed products (MA, CA, NC, and p6; PR, RT, and IN; Gp120 and Gp41, respectively) were used as bait. Interacting proteins were subjected to proteomic analysis by tryptic digestion followed by LC–MS/MS, again using an Orbitrap (Jager et al., 2012a). Interactomics for individual HIV-1 proteins have also been reported. Vif interactomics revealed how Vif targets the antiviral APOBEC3G protein for degradation via CBF-β, using the method just described (Jager et al., 2012a,b). The Rev protein was used as bait to fish for partners in HeLa cell extracts, which were then analyzed by MudPIT (Multidimensional Protein Identification Technology) LC–MS/MS (Naji et al., 2012). "Indirect" interactomics has also been performed by expressing either wild-type Vpu or Vpu that is unable to associate with F-box protein β-TrCP in HeLa cells. Without this interaction Vpu cannot target certain cellular proteins for degradation by the proteasome. Potential targets of Vpu were then identified by quantitative proteomics using SILAC (stable isotope labeling by amino acids in cell culture) followed by LC–MS/MS (Douglas et al., 2009). Much attention has been focused on the multiple roles of the CA (capsid) protein (Mascarenhas and Musier-Forsyth, 2009) and the Tat protein (Sobhian et al., 2010).

In many cases results of proteomic studies were compared with the results of stable RNAi-knockdown experiments. Global approaches to identify host cofactors usually consist of screening for reduced viral replication upon RNAi knockdown, or enhanced replication in case a cellular restriction factor is hit (Zhou et al., 2008; An and Winkler, 2010). Such genome wide RNAi screens can easily lead to both false positives (by off-target effects) and false negatives (by inefficient knockdown). These considerations emphasize the importance of performing a concerted multi-disciplinary experimental approach, including gene expression (transcriptome analysis), RNAi and proteomic studies using different detection and labeling techniques. At the same time, such a wider survey will generate more and larger datasets in formats which are not at all easily compared: an enormous future challenge for bioinformaticians. In light of this we also stress the importance of specific, non "omic," hypothesis driven follow-up research: not generating large new datasets but asking highly specific questions. The answers might just make integrating these large datasets a lot easier.

REFERENCES

Alban, A., David, S. O., Bjorkesten, L., Andersson, C., Sloge, E., Lewis, S., and Currie, I. (2003). A novel experimental design for comparative two-dimensional gel analysis: two-dimensional difference gel electrophoresis incorporating a pooled internal standard. *Proteomics* 3, 36–44.

An, P., and Winkler, C. A. (2010). Host genes associated with HIV/AIDS: advances in gene discovery. *Trends Genet.* 26, 119–131.

Baginsky, S., Hennig, L., Zimmermann, P., and Gruissem, W. (2010). Gene expression analysis, proteomics, and network discovery. *Plant Physiol.* 152, 402–410.

Boschetti, E., and Righetti, P. G. (2008). The ProteoMiner in the proteomic arena: a non-depleting tool for discovering low-abundance species. *J. Proteomics* 71, 255–264.

Chan, E. Y., Qian, W. J., Diamond, D. L., Liu, T., Gritsenko, M. A., Monroe, M. E., Camp, D. G., Smith, R. D., and Katze, M. G. (2007). Quantitative analysis of human immunodeficiency virus type 1-infected CD4+ cell proteome: dysregulated cell cycle progression and nuclear transport coincide with robust virus production. *J. Virol.* 81, 7571–7583.

Coiras, M., Camafeita, E., Urena, T., Lopez, J. A., Caballero, F., Fernandez, B., Lopez-Huertas, M. R., Perez-Olmeda, M., and Alcami, J. (2006). Modifications in the human T cell proteome induced by intracellular HIV-1 Tat protein expression. *Proteomics* 6(Suppl. 1), S63–S73.

Douglas, J. L., Viswanathan, K., McCarroll, M. N., Gustin, J. K., Fruh, K., and Moses, A. V. (2009). Vpu directs the degradation of the human immunodeficiency virus restriction factor BST-2/tetherin via a {beta}TrCP-dependent mechanism. *J. Virol.* 83, 7931–7947.

Fahey, M. E., Bennett, M. J., Mahon, C., Jager, S., Pache, L., Kumar, D., Shapiro, A., Rao, K., Chanda, S. K., Craik, C. S., Frankel, A. D., and Krogan, N. J. (2011). GPS-Prot: a web-based visualization platform

for integrating host–pathogen interaction data. *BMC Bioinformatics* 12, 298. doi: 10.1186/1471-2105-12-298

Geromanos, S. J., Vissers, J. P., Silva, J. C., Dorschel, C. A., Li, G. Z., Gorenstein, M. V., Bateman, R. H., and Langridge, J. I. (2009). The detection, correlation, and comparison of peptide precursor and product ions from data independent LC–MS with data dependant LC–MS/MS. *Proteomics* 9, 1683–1695.

Giri, M. S., Nebozhyn, M., Showe, L., and Montaner, L. J. (2006). Microarray data on gene modulation by HIV-1 in immune cells: 2000–2006. *J. Leukoc. Biol.* 80, 1031–1043.

Gomez, C., and Hope, T. J. (2005). The ins and outs of HIV replication. *Cell. Microbiol.* 7, 621–626.

Haarburger, D., and Pillay, T. S. (2010). Discovery proteomics: application to HIV infection. *J. Clin. Pathol.* 63, 285–287.

Heller, M. J. (2002). DNA microarray technology: devices, systems, and applications. *Annu. Rev. Biomed. Eng.* 4, 129–153.

Jager, S., Cimermancic, P., Gulbahce, N., Johnson, J. R., McGovern, K. E., Clarke, S. C., Shales, M., Mercenne, G., Pache, L., Li, K., Hernandez, H., Jang, G. M., Roth, S. L., Akiva, E., Marlett, J., Stephens, M., D'Orso, I., Fernandes, J., Fahey, M., Mahon, C., O'Donoghue, A. J., Todorovic, A., Morris, J. H., Maltby, D. A., Alber, T., Cagney, G., Bushman, F. D., Young, J. A., Chanda, S. K., Sundquist, W. I., Kortemme, T., Hernandez, R. D., Craik, C. S., Burlingame, A., Sali, A., Frankel, A. D., and Krogan, N. J. (2012a). Global landscape of HIV–human protein complexes. *Nature* 481, 365–370.

Jager, S., Kim, D. Y., Hultquist, J. F., Shindo, K., LaRue, R. S., Kwon, E., Li, M., Anderson, B. D., Yen, L., Stanley, D., Mahon, C., Kane, J., Franks-Skiba, K., Cimermancic, P., Burlingame, A., Sali, A., Craik, C. S., Harris, R. S., Gross, J. D., and Krogan, N. J. (2012b). Vif hijacks CBF-beta to degrade APOBEC3G and promote HIV-1 infection. *Nature* 481, 371–375.

Jeeninga, R. E., Westerhout, E. M., van Gerven, M. L., and Berkhout, B. (2008). HIV-1 latency in actively dividing human T cell lines. *Retrovirology* 5, 37.

Jensen, O. N. (2006). Interpreting the protein language using proteomics. *Nat. Rev. Mol. Cell Biol.* 7, 391–403.

Kramer, G., Sprenger, R. R., Nessen, M. A., Roseboom, W., Speijer, D., de Jong, L., de Mattos, M. J., Back, J., and de Koster, C. G. (2010). Proteome-wide alterations in *Escherichia coli* translation rates upon anaerobiosis. *Mol. Cell. Proteomics* 9, 2508–2516.

Lefebvre, G., Desfarges, S., Uyttebroeck, F., Munoz, M., Beerenwinkel, N., Rougemont, J., Telenti, A., and Ciuffi, A. (2011). Analysis of HIV-1 expression level and sense of transcription by high-throughput sequencing of the infected cell. *J. Virol.* 85, 6205–6211.

Lever, A. M., and Jeang, K. T. (2011). Insights into cellular factors that regulate HIV-1 replication in human cells. *Biochemistry* 50, 920–931.

Makarov, A., and Scigelova, M. (2010). Coupling liquid chromatography to Orbitrap mass spectrometry. *J. Chromatogr. A* 25, 2938–2945.

Mascarenhas, A. P., and Musier-Forsyth, K. (2009). The capsid protein of human immunodeficiency virus: interactions of HIV-1 capsid with host protein factors. *FEBS J.* 276, 6118–6127.

Moffat, J., Grueneberg, D. A., Yang, X., Kim, S. Y., Kloepfer, A. M., Hinkle, G., Piqani, B., Eisenhaure, T. M., Luo, B., Grenier, J. K., Carpenter, A. E., Foo, S. Y., Stewart, S. A., Stockwell, B. R., Hacohen, N., Hahn, W. C., Lander, E. S., Sabatini, D. M., and Root, D. E. (2006). A lentiviral RNAi library for human and mouse genes applied to an arrayed viral high-content screen. *Cell* 124, 1283–1298.

Naji, S., Ambrus, G., Cimermancic, P., Reyes, J. R., Johnson, J. R., Filbrandt, R., Huber, M. D., Vesely, P., Krogan, N. J., Yates, J. R. III, Saphire, A. C., and Gerace, L. (2012). Host cell interactome of HIV-1 Rev includes RNA helicases involved in multiple facets of virus production. *Mol. Cell. Proteomics* 4, M111.

Navare, A. T., Sova, P., Purdy, D. E., Weiss, J. M., Wolf-Yadlin, A., Korth, M. J., Chang, S. T., Proll, S. C., Jahan, T. A., Krasnoselsky, A. L., Palermo, R. E., and Katze, M. G. (2012). Quantitative proteomic analysis of HIV-1 infected CD4+ T cells reveals an early host response in important biological pathways: protein synthesis, cell proliferation, and T-cell activation. *Virology* 429, 37–46.

Pinkse, M. W., Lemeer, S., and Heck, A. J. (2011). A protocol on the use of titanium dioxide chromatography for phosphoproteomics. *Methods Mol. Biol.* 753, 215–228.

Pinkse, M. W., Uitto, P. M., Hilhorst, M. J., Ooms, B., and Heck, A. J. (2004). Selective isolation at the femtomole level of phosphopeptides from proteolytic digests using 2D-NanoLC-ESI-MS/MS and titanium oxide precolumns. *Anal. Chem.* 76, 3935–3943.

Plumb, R. S., Johnson, K. A., Rainville, P., Smith, B. W., Wilson, I. D., Castro-Perez, J. M., and Nicholson, J. K. (2006). UPLC/MS(E); a new approach for generating molecular fragment information for biomarker structure elucidation. *Rapid Commun. Mass Spectrom.* 20, 1989–1994.

Pradet-Balade, B., Boulme, F., Beug, H., Mullner, E. W., and Garcia-Sanz, J. A. (2001). Translation control: bridging the gap between genomics and proteomics? *Trends Biochem. Sci.* 26, 225–229.

Ringrose, J., Jeeninga, R. E., Berkhout, B., and Speijer, D. (2008). Proteomic studies reveal coordinated changes in T cell expression patterns upon HIV-1 infection. *J. Virol.* 82, 4320–4330.

Roeth, J. F., and Collins, K. L. (2006). Human immunodeficiency virus type 1 Nef: adapting to intracellular trafficking pathways. *Microbiol. Mol. Biol. Rev.* 70, 548–563.

Schwanhausser, B., Busse, D., Li, N., Dittmar, G., Schuchhardt, J., Wolf, J., Chen, W., and Selbach, M. (2011). Global quantification of mammalian gene expression control. *Nature* 473, 337–342.

Sobhian, B., Laguette, N., Yatim, A., Nakamura, M., Levy, Y., Kiernan, R., and Benkirane, M. (2010). HIV-1 Tat assembles a multifunctional transcription elongation complex and stably associates with the 7SK snRNP. *Mol. Cell* 38, 439–451.

Szklarczyk, D., Franceschini, A., Kuhn, M., Simonovic, M., Roth, A., Minguez, P., Doerks, T., Stark, M., Muller, J., Bork, P., Jensen, L. J., and von Mering C. (2011). The STRING database in 2011: functional interaction networks of proteins, globally integrated and scored. *Nucleic Acids Res.* 39, D561–D568.

Unlu, M., Morgan, M. E., and Minden, J. S. (1997). Difference gel electrophoresis: a single gel method for detecting changes in protein extracts. *Electrophoresis* 18, 2071–2077.

Van't Wout, A., Lehrman, G. K., Mikheeva, S. A., O'Keeffe, G. C., Katze, M. G., Bumgarner, R. E., Geiss, G. K., and Mullins, J. I. (2003). Cellular gene expression upon human immunodeficiency virus type 1 infection of CD4(+)-T-cell lines. *J. Virol.* 77, 1392–1402.

Vogel, C., Abreu, R. S., Ko, D., Le, S. Y., Shapiro, B. A., Burns, S. C., Sandhu, D., Boutz, D. R., Marcotte, E. M., and Penalva, L. O. (2010). Sequence signatures and mRNA concentration can explain two-thirds of protein abundance variation in a human cell line. *Mol. Syst. Biol.* 6, 400.

Wiese, S., Reidegeld, K. A., Meyer, H. E., and Warscheid, B. (2007). Protein labeling by iTRAQ: a new tool for quantitative mass spectrometry in proteome research. *Proteomics* 7, 340–350.

Wu, J. Q., Dwyer, D. E., Dyer, W. B., Yang, Y. H., Wang, B., and Saksena, N. K. (2011). Genome-wide analysis of primary CD4+ and CD8+ T cell transcriptomes shows evidence for a network of enriched pathways associated with HIV disease. *Retrovirology* 8, 18.

Zhang, L., Zhang, X., Ma, Q., and Zhou, H. (2010). Host proteome research in HIV infection. *Genomics Proteomics Bioinformatics* 8, 1–9.

Zhou, H., Xu, M., Huang, Q., Gates, A. T., Zhang, X. D., Castle, J. C., Stec, E., Ferrer, M., Strulovici, B., Hazuda, D. J., and Espeseth, A. S. (2008). Genome-scale RNAi screen for host factors required for HIV replication. *Cell Host Microbe* 4, 495–504.

Conflict of Interest Statement: The authors declare that the research was conducted in the absence of any commercial or financial relationships that could be construed as a potential conflict of interest.

Received: 05 April 2012; accepted: 15 June 2012; published online: 04 July 2012.

Citation: Kramer G, Moerland PD, Jeeninga RE, Vlietstra WJ, Ringrose JH, Byrman C, Berkhout B and Speijer D (2012) Proteomic analysis of HIV–T cell interaction: an update. Front. Microbio. ***3****:240. doi: 10.3389/fmicb.2012.00240*

This article was submitted to Frontiers in Virology, a specialty of Frontiers in Microbiology.

frontiers in
MICROBIOLOGY

MINI REVIEW ARTICLE
published: 22 August 2012
doi: 10.3389/fmicb.2012.00308

Activity based protein profiling to detect serine hydrolase alterations in virus infected cells

Md. Shahiduzzaman[1,2,4]* and Kevin M. Coombs[1,2,3]

[1] *Department of Medical Microbiology, Faculty of Medicine, University of Manitoba, Winnipeg, MB, Canada*
[2] *Manitoba Centre for Proteomics & Systems Biology, Winnipeg, MB, Canada*
[3] *Manitoba Institute of Child Health, Winnipeg, MB, Canada*
[4] *Department of Parasitology, Bangladesh Agricultural University, Mymensingh, Bangladesh*

Edited by:
Ben Berkhout, University of Amsterdam, Netherlands

Reviewed by:
Masa Shuda, University of Pittsburgh, USA
Dave Speijer, University of Amsterdam, Netherlands

****Correspondence:***
Md. Shahiduzzaman, Department of Parasitology, Bangladesh Agricultural University, Mymensingh 2202, Bangladesh.
e-mail: szamanpara@yahoo.com

Activity-based protein profiling (ABPP) is a newly emerging technique that uses active site-directed probes to monitor the functional status of enzymes. Serine hydrolases are one of the largest families of enzymes in mammals. More than 200 serine hydrolases have been identified, but little is known about their specific roles. Serine hydrolases are involved in a variety of physiological functions, including digestion, immune response, blood coagulation, and reproduction. ABPP has been used recently to investigate host–virus interactions and to understand the molecular pathogenesis of virus infections. Monitoring the altered serine hydrolases during viral infection gives insight into the catalytic activity of these enzymes that will help to identify novel targets for diagnostic and therapeutic application. This review presents the usefulness of ABPP in detecting and analyzing functional annotation of host cell serine hydrolases as a result of host–virus interaction.

Keywords: Activity based protein profiling, serine hydrolase, cellular proteomes, viral infection antiviral development

ACTIVITY-BASED PROTEIN PROFILING

Most enzymes are tightly regulated post-translationally. Many enzymes are synthesized as zymogens, which are functionally inactive. Moreover, enzyme functions can be changed by alterations in pH and binding to inhibitors. Thus, methods that allow direct quantification of protein activities rather than simply protein abundance are required to delineate distinct protein functions in physiological and pathological events. Activity-based protein profiling (ABPP) is a chemoproteomic platform for monitoring active proteins or enzymes. ABPP utilizes chemical probes to interrogate the functional state of large numbers of enzymes in complex proteomes *in vitro* or *in vivo* biological systems. ABPP probes consist of two key elements: (1) a reactive group/warhead (e.g., small molecule inhibitors, substrate-based scaffolds, or protein-reactive molecules) for binding and covalently labeling the active sites of many members of a given enzyme class (or classes), and (2) a reporter tag for the detection, enrichment, and/or identification of labeled enzymes from proteomes. A variety of reporter tags are used in ABPP, such as fluorophores (e.g., rhodamine) for visualization, biotin for enrichment as well as "clickable" handles, such as azides and acetylenes for *in vivo* or *in situ* labeling of proteins. The linker region is a flexible chain of varying length and hydrophobicity that connects and acts as a spacer between the warhead and the reporter tag.

Serine hydrolases represent one of the largest and most diverse classes of enzymes in higher eukaryotes, collectively composing about 3% of the predicted *Drosophila* proteome (Rubin et al., 2000) and about 1% of all predicted expressed human genes (Lander et al., 2001). Serine hydrolases are involved in a variety of physiological and pathological processes including blood coagulation (Kalafatis et al., 1997), T cell cytotoxicity (Smyth et al., 1996), inflammation (Bonventre et al., 1997), neural plasticity (Yoshida and Shiosaka, 1999), neurotransmitter catabolism (Taylor, 1991; Cravatt et al., 1996), peptide/protein processing (Steiner, 1998), protein/lipid digestion (Lowe, 1997), angiogenesis (Mignatti and Rifkin, 1996), emphysema (Kato, 1999), and cancer (DeClerck et al., 1997). Serine hydrolases also perform crucial functions in bacteria and viruses, where they contribute to pathogen life cycle (Steuber and Hilgenfeld, 2010), virulence (White et al., 2011), and drug resistance (Damblon et al., 1996). Most enzymes hydrolyze metabolites, peptides or post-translational ester and thioester modifications on proteins. Because of the biological importance of serine hydrolases, clinically approved drugs target members of this enzyme class to treat diseases such as obesity (Henness and Perry, 2006), diabetes (Thornberry and Weber, 2007), microbial infections (Kluge and Petter, 2010), and Alzheimer's disease (Racchi et al., 2004).

Proteolytic cleavages of viral proteins by cellular or viral proteases are necessary for host cell attachment, invasion, and reproduction of viral progeny. Host serine proteases are essential for the influenza virus life cycle because the viral hemagglutinin is synthesized as a precursor which requires proteolytic maturation (Garten and Klenk, 2008). Recently, the non-structural 3 protease (NS3 – is a chymotrypsin-like serine protease which requires a polypeptide cofactor NS2B for activation) has been shown to be responsible for cleavage of the viral polyprotein precursor and to play a pivotal role in the replication of flaviviruses (Falgout et al., 1991; Mukhopadhyay et al., 2005; Chappell et al., 2006) including Hepatitis C (HCV), West Nile virus, and Dengue virus. NS3 also facilitates viral pathogenicity by cleaving host proteins and down-regulating the innate immune response of the cell (Failla et al., 1994; Meylan et al., 2005). In fact, site-directed mutagenesis

that focused on the NS3 cleavage sites in the polyprotein precursor abolishes viral infectivity (Chappell et al., 2006). Cell culture models provided important clues about potential inhibition of several protease inhibitors against NS3 for Dengue virus and West Nile virus (Cregar-Hernandez et al., 2011; Steuer et al., 2011). Clinical trials of NS3 serine protease inhibitors showed good success rates (Lee et al., 2012) as anti-HCV. Therefore, NS3 is one of the most promising targets for drug development against Flaviviridae infections (Kolykhalov et al., 2000; Chappell et al., 2008). Other serine proteases involved in the pathogenesis and virus life cycles are being considered as targets for chemotherapy. The catalytic activity of the herpes simplex virus type 1 serine protease is essential for viral nucleocapsid formation and for viral replication (Gao et al., 1994). A trypsin-like serine protease is involved in pseudorabies viral penetration of the basement membrane during mucosal invasion (Glorieux et al., 2011). Serine protease inhibitors inhibit pseudorabies virus invasion in basal membranes. A vaccinia virus serine protease inhibitor prevents virus induced cell fusion (Law and Smith, 1992). Serine protease inhibitor AEBSF and pAB significantly reduce influenza A virus replication in mouse models (Bahgat et al., 2011). However, identification of active SHS and their functional characterization are necessary for better understanding the molecular pathogenesis and development of antiviral strategies.

All serine hydrolases possess a common catalytic mechanism that involves activation of a conserved serine nucleophile for attack on a substrate ester/thioester/amide bond to form an acyl-enzyme intermediate, followed by water-catalyzed hydrolysis of this intermediate to liberate the product. The greatly enhanced nucleophilicity of the catalytic serine renders it susceptible to covalent modification by many types of electrophiles, including fluorophosphonates (FPs) and aryl phosphonates, sulfonyl fluorides, and carbamates (Alexander and Cravatt, 2005; Jessani et al., 2005; Okerberg et al., 2005). FPs are highly reactive and provide broad coverage, with the capacity to react with nearly all essential serine hydrolases (Bachovchin et al., 2010). Therefore, they are ideal reagents to use for ABPP of serine hydrolases (Liu et al., 1999; Patricelli et al., 2001). However, certain serine proteases displayed restricted substrate selectivities that reduce their labeling with FPs. To address this limitation of FPs, selective inhibitors (e.g., carbamates, triazole ureas) have been introduced to probe the function of individual serine hydrolase in biological systems (Bachovchin et al., 2010; Adibekian et al., 2011).

ABPP IN HOST VIRUS INTERACTION

Microarray technologies in the field of genomics (transcriptomics), and mass spectrometry and bioinformatics technologies in proteomics, have facilitated the specific and global analyses of genes and their expression, and this has accelerated understanding the molecular basis of disease. These technologies, coupled with two-dimensional gel electrophoresis, mass spectrometry enhanced with chromatographic separations such as MudPIT (Shaw et al., 2008), or isotope coding-ICAT (Yan et al., 2004), iTRAQ (Lu et al., 2012), and SILAC (Coombs et al., 2010), have provided valuable insight into the quantitative differences in protein abundance during virus infections. However, these methods lack the inherent ability to profile and distinguish proteins according to their actual biological activities or functional state, which has more important bearings on understanding the implications of these macromolecules *in vivo* (Barglow and Cravatt, 2007). The lack of functional assessment of these other omic methods has prompted the development of alternative strategies such as ABPP, for the discovery and characterization of enzyme activities within highly complex biological samples.

COMPARATIVE ABPP FOR TARGET DISCOVERY

A typical target discovery experiment would comparatively analyze two or more proteomes by ABPP to identify enzymes with differing levels of activity (**Figure 1**). The differentially expressed serine hydrolases in healthy and diseased samples can be hypothesized to regulate the host–virus interaction. The testing of such hypotheses, of course, requires further experimentation for validation (e.g., functional interference of the target enzyme). ABPP has been used to profile a number of enzyme classes including proteases, hydrolases, oxidoreductases, and isomerases in the process of host–virus interaction (Kattenhorn et al., 2005; Schlieker et al., 2005; Wang et al., 2006; Gredmark et al., 2007; Jarosinski et al., 2007; Shah et al., 2010). Profiling of hydrolases in Huh7 cells replicating HCV identified CES1 (carboxylesterase 1) as a differentially active enzyme which has an important role in HCV propagation (Blais et al., 2010). We have examined the activity of serine hydrolases during reovirus, Influenza A, and Sindbis virus replication in cell culture in different cell lines. Differential serine hydrolase activities were induced by different viruses and alterations of serine hydrolases were dependent on the time course of viral infection. Several of these differentially active serine hydrolases represent possible virus–host interactions that could be targeted for development of antivirals.

COMPETITIVE ABPP FOR INHIBITOR DISCOVERY

ABPP can also be used as a competitive screen to identify both reversible and irreversible enzyme inhibitors and also to confirm target inhibition because inhibitors have the ability to block probe labeling of enzymes (Kidd et al., 2001; Greenbaum et al., 2002; Leung et al., 2003; Adibekian et al., 2011). Competitive ABPP has already led to the discovery of selective serine inhibitors (e.g., carbamates, trizole ureas) for several enzymes (e.g., peptidase, lipases), which have in turn been used to test the function of these proteins in living systems (Bachovchin et al., 2010; Adibekian et al., 2011). An alternative omic strategy would be to examine libraries of commercially available protease inhibitors for their ability to inhibit a virus' pathological process; this would potentially lead to development of novel therapeutic options.

QUANTITATIVE ABPP

Quantification of differentially expressed active proteins after virus infection is essential for better analysis of results, particularly when examining enzymes. It is difficult to compare the altered serine hydrolases between healthy and infected samples by simply visualizing gel images or merely by mass spectrometry. To address this problem an advanced quantitative mass spectrometry-based method called ABPP-SILAC (stable isotope labeling with amino acid in cell culture) has been used to identify alterations in the levels of active enzyme targets (Everley

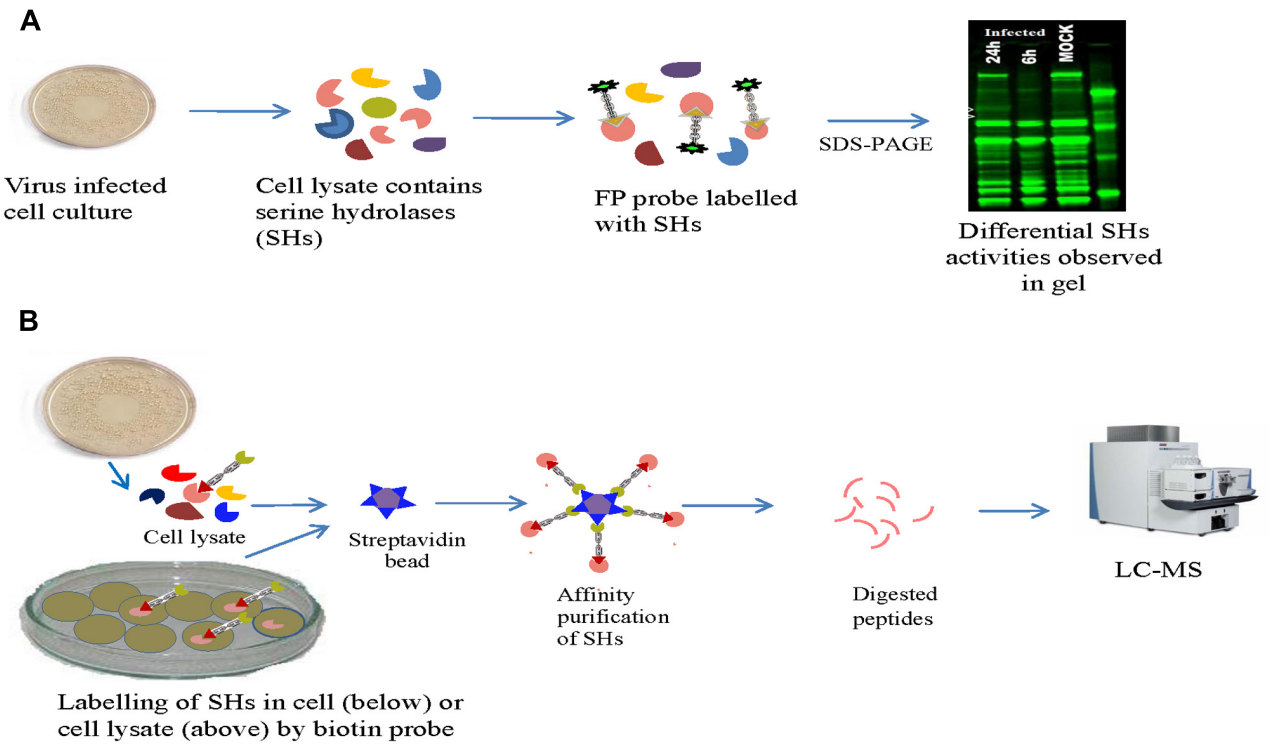

FIGURE 1 | When probe is incubated with crude cell lysates **(A)** or, if the probe is cell permeable **(B)**, with whole cells the reactive group specifically interacts with active site of serine hydrolase (SHs) and forms a covalent linkage. The labeled proteome can be directly analyzed by gel image **(A)**, or analyzed by Mass spectrometry following enrichment of SHs **(B)**.

et al., 2007) and in small molecule-binding proteins in cell lysates (Ong et al., 2009). Comparative ABPP -SILAC can be used to quantify more accurately the intricate changes in host proteins caused by viral infection. Similarly, competitive ABPP-SILAC is valuable to identify inhibited enzymes during global screening of inhibitors.

PERSPECTIVE OF VIRUS ABPP FOR SERINE HYDROLASE

Many enzymes and metabolites display difficult physicochemical properties that complicate their analysis in biological samples, and many metabolic pathways that enzymes regulate in a disease-specific context are not understood. These challenges can be addressed by applying innovative metabolomics and ABPP approaches to mapping biochemical pathways that support disease. Using selective inhibitors developed through competitive ABPP efforts or RNA interference technology, the function of an enzyme of interest can be specifically blocked, and then the metabolites that the enzyme regulates can be profiled. In this manner, not only can the substrates and products of an enzyme in specific (patho)physiological contexts be examined, but also the metabolic networks that the enzyme regulates can be identified and annotated. Collectively, this platform will allow identification of novel biochemical roles of already characterized enzymes, or may allow the identification of metabolic roles of completely uncharacterized enzymes.

Understanding the mechanisms by which viruses develop resistance is a vital component of the fight against viral diseases, and can lengthen the lifespan of existing antivirals. Potentially any antivirus molecule could be transformed into an activity-based or affinity-based probe, allowing isolation and characterization of enzymes that detoxify the antiviral drug.

ABPP with live cell imaging may provide additional insight into understanding the pathogenesis due to viral infection (Furman et al., 2009). Identification and functional characterization of serine hydrolases involved in pathogenesis and virulence of viruses would be a novel approach to uncover molecular processes at the basis of viral diseases.

Natural products represent an important treasure box of biologically active molecules, from which many drug candidates have been developed (Newman and Cragg, 2007). Since a large number of the proteome remains functionally uncharacterized and is therefore difficult to assemble into larger biochemical networks, competitive ABPP will inevitably accelerate the development of novel inhibitors from natural products.

CONCLUSION

This mini review describes briefly a limited number of approaches involved in profiling serine hydrolases during viral infection and assigning catalytic functions to previously uncharacterized serine hydrolases. Visualization of the altered active serine hydrolase *in situ* during viral disease progression, trying to fully understand mechanisms of resistance and developing new antiviral therapeutics and viral diagnostics will make the ABPP application more worthwhile for the field of virology.

REFERENCES

Adibekian, A., Martin, B. R., Wang, C., Hsu, K. L., Bachovchin, D. A., Niessen, S., Hoover, H., and Cravatt, B. F. (2011). Click-generated triazole ureas as ultrapotent in vivo-active serine hydrolase inhibitors. *Nat. Chem. Biol.* 15, 469–478.

Alexander, J. P., and Cravatt, B. F. (2005). Mechanism of carbamate inactivation of FAAH: implications for the design of covalent inhibitors and in vivo functional probes for enzymes. *Chem. Biol.* 12, 1179–1187.

Bachovchin, D. A., Ji, T., Li, W., Simon, G. M., Blankman, J. L., Adibekian, A., Hoover, H., Niessen, S., and Cravatt, B. F. (2010). A superfamily-wide portrait of serine hydrolase inhibition achieved by library-versus-library screening. *Proc. Natl. Acad. Sci. U.S.A.* 107, 20941–20946.

Bahgat, M. M., Blazejewska, P., and Schughart, K. (2011). Inhibition of lung serine proteases in mice: a potentially new approach to control influenza infection. *Virol. J.* 20, 27.

Barglow, K. T., and Cravatt, B. F. (2007). Activity-based protein profiling for the functional annotation of enzymes. *Nat. Methods* 4, 822–827.

Blais, D. R., Lyn, R. K., Joyce, M. A., Rouleau, Y., Steenbergen, R., Barsby, N., Zhu, L. F., Pegoraro, A. F., Stolow, A., Tyrrell, D. L., and Pezacki, J. P. (2010). Activity-based protein profiling identifies a host enzyme, carboxylesterase 1, which is differentially active during hepatitis C virus replication. *J. Biol. Chem.* 285, 25602–25612.

Bonventre, J. V., Huang, Z., Taheri, M. R., O'Leary, E., Li, E., Moskowitz, M. A., and Sapirstein, A. (1997). Reduced fertility and postischaemic brain injury in mice deficient in cytosolic phospholipase A2. *Nature* 390, 622–625.

Chappell, K. J., Stoermer, M. J., Fairlie, D. P., and Young, P. R. (2006). Insights to substrate binding and processing by West Nile Virus NS3 protease through combined modeling, protease mutagenesis, and kinetic studies. *J. Biol. Chem.* 281, 38448–38458.

Chappell, K. J., Stoermer, M. J., Fairlie, D. P., and Young, P. R. (2008). West Nile Virus NS2B/NS3 protease as an antiviral target. *Curr. Med. Chem.* 15, 2771–2784.

Coombs, K. M., Berard, A., Xu, W., Krokhin, O., Meng, X., Cortens, J. P., Kobasa, D., Wilkins, J., and Brown, E. G. (2010). Quantitative proteomic analyses of influenza virus-infected cultured human lung cells. *J. Virol.* 84, 10888–10906.

Cravatt, B. F., Giang, D. K., Mayfield, S. P., Boger, D. L., Lerner, R. A., and Gilula, N. B. (1996). Molecular characterization of an enzyme that degrades neuromodulatory fatty-acid amides. *Nature* 384, 83–87.

Cregar-Hernandez, L., Jiao, G. S., Johnson, A. T., Lehrer, A. T., Wong, T. A., and Margosiak, S. A. (2011). Small molecule pan-dengue and West Nile virus NS3 protease inhibitors. *Antivir. Cheem. Chemother.* 21, 209–217.

Damblon, C., Raquet, X., Lian, L. Y., Lamotte-Brasseur, J., Fonze, E., Charlier, P., Roberts, G. C., and Frère, J. M. (1996). The catalytic mechanism of β-lactamases: NMR titration of an active-site lysine residue of the TEM-1 enzyme. *Proc. Natl. Acad. Sci. U.S.A.* 93, 1747–1752.

DeClerck, Y. A., Imren, S., Montgomery, A. M. P., Mueller, B. M., Reisfeld, R. A., and Laug, W. E. (1997). Proteases and protease inhibitors in tumor progression. *Adv. Exp. Med. Biol.* 425, 89–97.

Everley, P. A., Gartner, C. A., Haas, W., Saghatelian, A., Elias, J. E., Cravatt, B. F., Zetter, B. R., and Gygi, S. P. (2007). Assessing enzyme activities using stable isotope labeling and mass spectrometry. *Mol. Cell. Proteomics* 6, 1771–1777.

Failla, C., Tomei, L., and De Francesco, R. (1994). Both NS3 and NS4A are required for proteolytic processing of hepatitis C virus nonstructural proteins. *J. Virol.* 68, 3753–3760.

Falgout, B., Pethel, M., Zhang, Y. M., and Lai, C. J. (1991). Both nonstructural proteins NS2B and NS3 are required for the proteolytic processing of dengue virus nonstructural proteins *J. Virol.* 65, 2467–2475.

Furman, L. M., Maaty, W. S., Petersen, L. K., Ettayebi, K., Hardy, M. E., and Bothner, B. (2009). Cysteine protease activation and apoptosis in murine norovirus infection. *Virol. J.* 6, 139.

Gao, M., Matusick-Kumar, L., Hurlburt, W., DiTusa, S. F., Newcomb, W. W., Brown, J. C., McCann, P. J., Deckman, I., and Colonno, R. J. (1994). The protease of herpes simplex virus type 1 is essential for functional capsid formation and viral growth. *J. Virol.* 68, 3702–3712.

Garten, W., and Klenk, H. D. (2008). "Cleavage activation of the influenza virus hemagglutinin and its role in pathogenesis," in *Avian Influenza: Monographs in Virology,* Vol. 27, eds H. D. Klenk, M. N. Matrosovich, and J. Stech (Karger: Basel), 156–167.

Glorieux, S., Favoreel, H. W., Steukers, L., Vandekerckhove, A. P., and Nauwynck, H. J. (2011). A trypsin-like serine protease is involved in pseudorabies virus invasion through the basement membrane barrier of porcine nasal respiratory mucosa. *Vet. Res.* 42, 58.

Gredmark, S., Schlieker, C., Quesada, V., Spooner, E., and Ploegh, H. L. (2007). A functional ubiquitin-specific protease embedded in the large tegument protein (ORF64) of murine gammaherpesvirus 68 is active during the course of infection. *J. Virol.* 81, 10300–10309.

Greenbaum, D. C., Arnold, W. D., Lu, F., Hayrapetian, L., Baruch, A., Krumrine, J., Toba, S., Chehade, K., Brömme, D., Kuntz, I. D., and Bogyo, M. (2002). Small molecule affinity fingerprinting. A tool for enzyme family subclassification, target identification, and inhibitor design. *Chem. Biol.* 9, 1085–1094.

Henness, S., and Perry, C. M. (2006). Orlistat: a review of its use in the management of obesity. *Drugs* 66, 1625–1656.

Jarosinski, K., Kattenhorn, L., Kaufer, B., Ploegh, H., and Osterrieder, N. (2007). A herpesvirus ubiquitin-specific protease is critical for efficient T cell lymphoma formation. *Proc. Natl. Acad. Sci. U.S.A.* 104, 20025–20030.

Jessani, N., Niessen, S., Wei, B. Q., Nicolau, M., Humphrey, M., Ji, Y., Han, W., Noh, D. Y., Yates, J. R. III, Jeffrey, S. S., and Cravatt, B. F. (2005). A streamlined platform for high-content functional proteomics of primary human specimens. *Nat. Methods* 2, 691–697.

Kalafatis, M., Egan, J. O., van't Veer, C., Cawthern, K. M., and Mann, K. G. (1997). The regulation of clotting factors. *Crit. Rev. Eukaryot. Gene Expr.* 7, 241–280.

Kato, G. J. (1999). Human genetic diseases of proteolysis. *Hum. Mutat.* 13, 87–98.

Kattenhorn, L. M., Korbel, G. A., Kessler, B. M., Spooner, E., and Ploegh, H. L. (2005). A deubiquitinating enzyme encoded by HSV-1 belongs to a family of cysteine proteases that is conserved across the family Herpesviridae. *Mol. Cell* 19, 547–557.

Kidd, D., Liu, Y., and Cravatt, B. F. (2001). Profiling serine hydrolase activities in complex proteomes. *Biochemistry* 40, 4005–4015.

Kluge, A. F., and Petter, R. C. (2010). Acylating drugs: redesigning natural covalent inhibitors. *Curr. Opin. Chem. Biol.* 14, 421–427.

Kolykhalov, A. A., Mihalik, K., Feinstone, S. M., and Rice, C. M. (2000). Hepatitis C virus-encoded enzymatic activities and conserved RNA elements in the 3′ nontranslated region are essential for virus replication *in vivo*. *J. Virol.* 74, 2046–2051.

Lander, E. S., Linton, L. M., Birren, B., Nusbaum, C., Zody, M. C., Baldwin, J., Devon, K., Dewar, K., Doyle, M., FitzHugh, W., Funke, R., Gage, D., Harris, K., Heaford, A., Howland, J., Kann, L., Lehoczky, J., LeVine, R., McEwan, P., McKernan, K., Meldrim, J., Mesirov, J. P., Miranda, C., Morris, W., Naylor, J., Raymond, C., Rosetti, M., Santos, R., Sheridan, A., Sougnez, C., Stange-Thomann, N., Stojanovic, N., Subramanian, A., Wyman, D., Rogers, J., Sulston, J., Ainscough, R., Beck, S., Bentley, D., Burton, J., Clee, C., Carter, N., Coulson, A., Deadman, R., Deloukas, P., Dunham, A., Dunham, I., Durbin, R., French, L., Grafham, D., Gregory, S., Hubbard, T., Humphray, S., Hunt, A., Jones, M., Lloyd, C., McMurray, A., Matthews, L., Mercer, S., Milne, S., Mullikin, J. C., Mungall, A., Plumb, R., Ross, M., Shownkeen, R., Sims, S., Waterston, R. H., Wilson, R. K., Hillier, L. W., McPherson, J. D., Marra, M. A., Mardis, E. R., Fulton, L. A., Chinwalla, A. T., Pepin, K. H., Gish, W. R., Chissoe, S. L., Wendl, M. C., Delehaunty, K. D., Miner, T. L., Delehaunty, A., Kramer, J. B., Cook, L. L., Fulton, R. S., Johnson, D. L., Minx, P. J., Clifton, S. W., Hawkins, T., Branscomb, E., Predki, P., Richardson, P., Wenning, S., Slezak, T., Doggett, N., Cheng, J. F., Olsen, A., Lucas, S., Elkin, C., Uberbacher, E., Frazier, M., Gibbs, R. A., Muzny, D. M., Scherer, S. E., Bouck, J. B., Sodergren, E. J., Worley, K. C., Rives, C. M., Gorrell, J. H., Metzker, M. L., Naylor, S. L., Kucherlapati, R. S., Nelson, D. L., Weinstock, G. M., Sakaki, Y., Fujiyama, A., Hattori, M., Yada, T., Toyoda, A., Itoh, T., Kawagoe, C., Watanabe, H., Totoki, Y., Taylor, T., Weissenbach, J., Heilig, R., Saurin, W., Artiguenave, F., Brottier, P., Bruls, T., Pelletier, E., Robert, C., Wincker, P., Smith, D. R., Doucette-Stamm, L., Rubenfield, M., Weinstock, K., Lee, H. M., Dubois, J., Rosenthal, A., Platzer, M., Nyakatura, G., Taudien, S., Rump, A., Yang, H., Yu, J., Wang, J., Huang, G., Gu, J., Hood, L., Rowen, L., Madan, A., Qin, S., Davis, R. W., Federspiel, N. A., Abola, A. P., Proctor, M. J., Myers, R. M., Schmutz, J., Dickson, M., Grimwood, J., Cox, D. R., Olson, M. V., Kaul, R., Raymond, C., Shimizu, N., Kawasaki, K., Minoshima, S., Evans, G. A.,

Athanasiou, M., Schultz, R., Roe, B. A., Chen, F., Pan, H., Ramser, J., Lehrach, H., Reinhardt, R., McCombie, W. R., de la Bastide, M., Dedhia, N., Blöcker, H., Hornischer, K., Nordsiek, G., Agarwala, R., Aravind, L., Bailey, J. A., Bateman, A., Batzoglou, S., Birney, E., Bork, P., Brown, D. G., Burge, C. B., Cerutti, L., Chen, H. C., Church, D., Clamp, M., Copley, R. R., Doerks, T., Eddy, S. R., Eichler, E. E., Furey, T. S., Galagan, J., Gilbert, J. G., Harmon, C., Hayashizaki, Y., Haussler, D., Hermjakob, H., Hokamp, K., Jang, W., Johnson, L. S., Jones, T. A., Kasif, S., Kaspryzk, A., Kennedy, S., Kent, W. J., Kitts, P., Koonin, E. V., Korf, I., Kulp, D., Lancet, D., Lowe, T. M., McLysaght, A., Mikkelsen, T., Moran, J. V., Mulder, N., Pollara, V. J., Ponting, C. P., Schuler, G., Schultz, J., Slater, G., Smit, A. F., Stupka, E., Szustakowski, J., Thierry-Mieg, D., Thierry-Mieg, J., Wagner, L., Wallis, J., Wheeler, R., Williams, A., Wolf, Y. I., Wolfe, K. H., Yang, S. P., Yeh, R. F., Collins, F., Guyer, M. S., Peterson, J., Felsenfeld, A., Wetterstrand, K. A., Patrinos, A., Morgan, M. J., de Jong, P., Catanese, J. J., Osoegawa, K., Shizuya, H., Choi, S., Chen, Y. J.; International Human Genome Sequencing Consortium. (2001). Initial sequencing and analysis of the human genome. *Nature* 409, 860–921.

Law, K. M., and Smith, G. L. (1992). A vaccinia serine protease inhibitor which prevents virus-induced cell fusion. *J. Gen. Virol.* 73, 549–557.

Lee, L. Y., Tong, C. Y., Wong, T., and Wilkinson, M. (2012). New therapies for chronic hepatitis C infection: a systematic review of evidence from clinical trials. *Int. J. Clin. Pract.* 66, 342–355.

Leung, D., Hardouin, C., Boger, D. L., and Cravatt, B. F. (2003). Discovering potent and selective reversible inhibitors of enzymes in complex proteomes. *Nat. Biotechnol.* 21, 687–691.

Liu, Y., Patricelli, M. P., and Cravatt, B. F. (1999). Activity-based protein profiling: the serine hydrolases. *Proc. Natl. Acad. Sci. U.S.A.* 96, 14694–14699.

Lowe, M. E. (1997). Molecular mechanisms of rat and human pancreatic triglyceride lipases. *J. Nutr.* 127, 549–557.

Lu, Q., Bai, J., Zhang, L., Liu, J., Jiang, Z., Michal, J. J., He, Q., and Jiang, P. (2012). Two-dimensional liquid chromatography-tandem mass spectrometry coupled with isobaric tags for relative and absolute quantification (iTRAQ) labeling approach revealed first proteome profiles of pulmonary alveolar macrophages infected with porcine reproductive and respiratory syndrome virus. *J. Proteome Res.* 11, 2890–2903.

Meylan, E., Curran, J., Hofmann, K., Moradpour, D., Binder, M., Bartenschlager, R., and Tschopp, J. (2005). Cardif is an adaptor protein in the RIG-I antiviral pathway and is targeted by hepatitis C virus. *Nature* 437, 1167–1172.

Mignatti, P., and Rifkin, D. B. (1996). Plasminogen activators and matrix metalloproteinases in angiogenesis. *Enz. Protein* 49, 117–137.

Mukhopadhyay, S., Kuhn, R. J., and Rossmann, M. G. (2005). A structural perspective of the flavivirus life cycle. *Nat. Rev. Microbiol.* 3, 13–22.

Newman, D. J., and Cragg, G. M. (2007). Natural products as sources of new drugs over the last 25 years. *J. Nat. Prod.* 70, 461–477.

Okerberg, E. S., Wu, J., Zhang, B., Samii, B., Blackford, K., Winn, D. T., Shreder, K.R., Burbaum, J. J., and Patricelli, M. P. (2005). High-resolution functional proteomics by active-site peptide profiling. *Proc. Natl. Acad. Sci. U.S.A.* 102, 4996–5001.

Ong, S. E., Schenone, M., Margolin, A. A., Li, X., Do, K., Doud, M. K., Mani, D. R., Kuai, L., Wang, X., Wood, J. L., Tolliday, N. J., Koehler, A. N., Marcaurelle, L. A., Golub, T. R., Gould, R. J., Schreiber, S. L., and Carr, S. A. (2009). Identifying the proteins to which small-molecule probes and drugs bind in cells. *Proc. Natl. Acad. Sci. U.S.A.* 106, 4617–4622.

Patricelli, M. P., Giang, D. K., Stamp, L. M., and Burbaum, J. J. (2001). Direct visualization of serine hydrolase activities in complex proteome using fluorescent active site-directed probes. *Proteomics* 1, 1067–1071.

Racchi, M., Mazzucchelli, M., Porrello, E., Lanni, C., and Govoni, S. (2004). Acetylcholinesterase inhibitors: novel activities of old molecules. *Pharmacol. Res.* 50, 441–451.

Rubin, G. M., Yandell, M. D., Wortman, J. R., Gabor, Miklos, G. L., Nelson, C. R., Hariharan, I. K., Fortini, M. E., Li, P. W., Apweiler, R., Fleischmann, W., Cherry, J. M., Henikoff, S., Skupski, M. P., Misra, S., Ashburner, M., Birney, E., Boguski, M. S., Brody, T., Brokstein, P., Celniker, S. E., Chervitz, S. A., Coates, D., Cravchik, A., Gabrielian, A., Galle, R. F., Gelbart, W. M., George, R. A., Goldstein, L. S., Gong, F., Guan, P., Harris, N. L., Hay, B. A., Hoskins, R. A., Li, J., Li, Z., Hynes, R. O., Jones, S. J., Kuehl, P. M., Lemaitre, B., Littleton, J. T., Morrison, D. K., Mungall, C., O'Farrell, P. H., Pickeral, O. K., Shue, C., Vosshall, L. B., Zhang, J., Zhao, Q., Zheng, X. H., and Lewis, S. (2000). Comparative genomics of the eukaryotes. *Science* 287, 2204–2215.

Schlieker, C., Korbel, G. A., Kattenhorn, L. M., and Ploegh, H. L. (2005). A deubiquitinating activity is conserved in the large tegument protein of the herpesviridae. *J. Virol.* 79, 15582–15585.

Shah, P. P., Wang, T., Kaletsky, R. L., Myers, M. C., Purvis, J. E., Jing, H., Huryn, D. M., Greenbaum, D. C., Smith, A. B. III, Bates, P., and Diamond, S. L. (2010). A small-molecule oxocarbazate inhibitor of human cathepsin L blocks severe acute respiratory syndrome and ebola pseudotype virus infection into human embryonic kidney 293T cells. *Mol. Pharmacol.* 78, 319–324.

Shaw, M. L., Stone, K. L., Colangelo, C. M., Gulcicek, E. E., and Palese, P. (2008). Cellular proteins in influenza virus particles. *PLoS Pathog.* 4, e1000085. doi: 10.1371/journal.ppat.1000085

Smyth, M. J., O'Conner, M. D., and Trapani, J. A. (1996). Granzymes: a variety of serine protease specificities encoded by genetically distinct subfamilies. *J. Leukocyte Biol.* 60, 555–562.

Steiner, D. F. (1998). The proprotein convertases. *Curr. Opin. Chem. Biol.* 2, 31–39.

Steuber, H., and Hilgenfeld, R. (2010). Recent advances in targeting viral proteases for the discovery of novel antivirals. *Curr. Top. Med. Chem.* 10, 323–345.

Steuer, C., Gege, C., Fischl, W., Heinonen, K. H., Bartenschlager, R., and Klein, C. D. (2011). Synthesis and biological evaluation of α-ketoamides as inhibitors of the Dengue virus protease with antiviral activity in cell-culture. *Bioorg. Med. Chem.* 19, 4067–4074.

Taylor, P. (1991). The cholinesterases. *J. Biol. Chem.* 266, 4025–4028.

Thornberry, N. A., and Weber, A. E. (2007). Discovery of JANUVIA (Sitagliptin), a selective dipeptidyl peptidase IV inhibitor for the treatment of type 2 diabetes. *Curr. Top. Med. Chem.* **7**, 557–568.

Wang, J., Loveland, A. N., Kattenhorn, L. M., Ploegh, H. L., and Gibson, W. (2006). High-molecular-weight protein (pUL48) of human cytomegalovirus is a competent deubiquitinating protease: mutant viruses altered in its active-site cysteine or histidine are viable. *J. Virol.* 80, 6003–6012.

White, M. J., Savaryn, J. P., Bretl, D. J., He, H., Penoske, R. M., Terhune, S. S., and Zahrt, T. C. (2011). The HtrA-like serine protease PepD interacts with and modulates the *Mycobacterium tuberculosis* 35-kDa antigen outer envelope protein. *PLoS ONE* 6, e18175. doi: 10.1371/journal.pone.0018175

Yan, W., Lee, H., Yi, E. C., Reiss, D., Shannon, P., Kwieciszewski, B. K., Coito, C., Li, X. J., Keller, A., Eng, J., Galitski, T., Goodlett, D. R., Aebersold, R., and Katze, M. G. (2004). System-based proteomic analysis of the interferon response in human liver cells. *Genome Biol.* 5, R54.

Yoshida, S., and Shiosaka, S. (1999). Plasticity-related serine proteases in the brain (review). *Int. J. Mol. Med.* 3, 405–409.

Conflict of Interest Statement: The authors declare that the research was conducted in the absence of any commercial or financial relationships that could be construed as a potential conflict of interest.

Received: 04 June 2012; accepted: 03 August 2012; published online: 22 August 2012.

Citation: Shahiduzzaman M and Coombs KM. (2012) Activity based protein profiling to detect serine hydrolase alterations in virus infected cells. Front. Microbio. ***3****:308. doi: 10.3389/fmicb.2012.00308*

This article was submitted to Frontiers in Virology, a specialty of Frontiers in Microbiology.

frontiers in
MICROBIOLOGY

REVIEW ARTICLE
published: 09 November 2012
doi: 10.3389/fmicb.2012.00391

Toward system-level understanding of baculovirus–host cell interactions: from molecular fundamental studies to large-scale proteomics approaches

Francisca Monteiro[1,2], Nuno Carinhas[1,2], Manuel J. T. Carrondo[1,2,3], Vicente Bernal[4]* and Paula M. Alves[1,2]*

[1] *Animal Cell Technology Unit, Instituto de Biologia Experimental e Tecnológica, Oeiras, Portugal*
[2] *Animal Cell Technology Unit, Instituto de Tecnologia Quimica e Biológica, Oeiras, Portugal*
[3] *Departamento de Química, Faculdade de Ciências e Tecnologia, Universidade Nova de Lisboa, Caparica, Portugal*
[4] *Departamento de Bioquímica y Biología Molecular B e Inmunología, Facultad de Química, Regional Campus of International Excellence "Campus Mare Nostrum", Universidad de Murcia, Murcia, Spain*

Edited by:
Kevin Coombs, University of Manitoba, Canada

Reviewed by:
Hsei-Wei Wang, National Yang Ming University, Taiwan
Peter Krell, University of Guelph, Canada

****Correspondence:***
Vicente Bernal, Departamento de Bioquímica y Biología Molecular B e Inmunología, Facultad de Química, Regional Campus of International Excellence "Campus Mare Nostrum", Universidad de Murcia, 30100 Murcia, Spain.
e-mail: vbernal@um.es;
Paula M. Alves, Animal Cell Technology Unit, Instituto de Biologia Experimental e Tecnológica and Instituto de Tecnologia Quimica e Biológica, Apartado 12, 27801-901 Oeiras, Portugal.
e-mail: marques@itqb.unl.pt

Baculoviruses are insect viruses extensively exploited as eukaryotic protein expression vectors. Molecular biology studies have provided exciting discoveries on virus–host interactions, but the application of omic high-throughput techniques on the baculovirus–insect cell system has been hampered by the lack of host genome sequencing. While a broader, systems-level analysis of biological responses to infection is urgently needed, recent advances on proteomic studies have yielded new insights on the impact of infection on the host cell. These works are reviewed and critically assessed in the light of current biological knowledge of the molecular biology of baculoviruses and insect cells.

Keywords: baculovirus, virus–host interactions, cytoskeleton, apoptosis, stress response, proteomics

BRIEF INTRODUCTION TO THE BACULOVIRUS–INSECT CELL SYSTEM

Baculoviruses are rod-shaped viruses with double-stranded DNA genomes. They infect arthropods, mainly insects, a feature that encouraged their usage as ecologically friendly biopesticides (Miller, 1997). Later on, baculoviruses started to be exploited as viral vectors for eukaryotic protein expression, which quickened the pace of their characterization at the cellular and molecular levels (Possee, 1993). The best-studied member of this family, *Autographa californica* multicapsid nucleopolyhedrovirus (*Ac*MNPV), encodes for 150 genes and has its own genome completely sequenced. The cell lines used for *Ac*MNPV propagation are derived from the pupal ovarian tissue of the fall armyworm *Spodoptera frugiperda*, being the *Sf*9 clonal isolate the most frequently used. Insect cells possess several advantages as protein expression factories. They grow in suspension without serum supplementation, are able to perform post-translational modifications and the scale-up of cultures is quite straightforward (Ikonomou et al., 2003). However, the production potential of insect cells has been hampered by the so called "cell density effect," i.e., the drop in specific productivity when cells are infected with baculovirus at high cell concentration. As *Sf*9 cells attain high densities, central metabolism suffers a general down-regulation (Bernal et al., 2009). Viral infection induces a multi-level response in the host, during which a vast number of intracellular pathways are activated/deactivated (i.e., regulated) and profound metabolic changes occur. These changes are ultimately responsible for the production performance of the system. A deeper understanding of such phenomena will certainly allow for the rational design of strategies for bioprocess optimization. The genome of *S. frugiperda* remains unsequenced, which limits the extent to which high-throughput (genome-scale) technologies can be applied. To date, only few proteomic-based high-throughput studies concerning the impact of baculovirus infection on their host cells have been pursued. The aim of this review is to summarize the state of the art in the molecular biology of the baculovirus replication and host–virus interaction in this system. The implications of these mechanisms for proper infection and their potential use for the improvement of baculoviruses-based applications such as protein production and use as gene therapy vectors will be highlighted.

BACULOVIRUS LIFE CYCLE: FROM *IN VIVO* TO *IN VITRO* CULTURES

Baculoviruses have a biphasic replication cycle in the insect host, involving the formation of two types of virions which are produced in different phases of the infection process and have different roles: the occlusion-derived virions (ODVs), adapted for stability outside the insect host, and the budded virions (BVs), non-occluded and responsible for the systemic, cell-to-cell dissemination of the virus within the insect. Specific roles, morphology, and functionality of both virion types are described in more detail below. Moreover, the virus life cycle is temporally divided into three consecutive phases (immediate-early/early; late and very late) regarding gene expression programming (Passarelli and Guarino, 2007). Specific constraints and events of each phase are summarized along the text.

Baculovirus infection starts when insect larvae ingest the occlusion bodies (Keddie et al., 1989). These are forms resistant to environmental factors. ODVs are embedded in a proteinaceous matrix mostly composed of the very late expressed protein polyhedrin. When facing the alkaline conditions in the insect midgut, the occlusion body dissolves and releases the ODVs, and the polyhedrin matrix is in turn degraded by proteinases present in the gut or associated with the virions (Wang and Granados, 1997). The replicative cycle begins when ODVs infect the midgut columnar epithelial cells. ODVs possess a set of specific envelope-associated proteins, called *per os* infectivity factors (*pif*), which mediate virion-specific binding to receptors located at the membrane of midgut epithelial cells (Horton and Burand, 1993; Kikhno et al., 2002). To date, six proteins have been identified as members of this family, P74 (PIF-0), PIF-1, PIF-2, PIF-3, PIF-4, and PIF-5 (ODV-E56; Faulkner et al., 1997; Kikhno et al., 2002; Pijlman et al., 2003; Ohkawa et al., 2005; Fang et al., 2009a; Harrison et al., 2010; Sparks et al., 2011). P74, PIF-1, and PIF-2 were shown to co-localize at the ODV envelope (Faulkner et al., 1997; Kikhno et al., 2002; Fang et al., 2006, 2009a; Harrison et al., 2010) and, together with PIF-3, constitute the core PIF complex that mediates viral entry. Afterward, viral entry occurs via a non-endocytic pathway through membrane fusion of the virion envelope with microvilli of epithelial cells, accompanied by the release of nucleocapsids into the cytoplasm. Nucleocapsids then migrate to the nucleus in a process that involves actin polymerization (Ohkawa et al., 2010).

Once having reached the nucleus, the host cell RNA polymerase-dependent transcription of viral immediate-early/early genes initiates (0–6 h post-infection, hpi). This set of genes encodes mainly for transactivators essential for both subsequent viral gene expression and subversion of host cell activity (Passarelli and Miller, 1993). The transition from early to late phase is marked by the onset of viral DNA replication (6–18 hpi) and the activity of a virus-encoded RNA polymerase (Grula et al., 1981). Viral DNA replication occurs together with the expression of viral components necessary for the assembly of new nucleocapsids. The newly assembled nucleocapsids are transported from the nucleus to the plasma membrane for budding through GP64-enriched areas, thus originating the so called budded viruses (BVs; Passarelli, 2012). BVs are non-occluded virions surrounded by a plasma membrane-derived envelope containing GP64 as a major structural protein (Washburn et al., 2003). BVs are required for secondary infection: once released, they are transported throughout the hemolymph to infect new cells, a process which, in contrast to what is described for ODVs, is undertaken by GP64 via clathrin-mediated endocytosis (Blissard and Wenz, 1992; Long et al., 2006). In this regard, BVs are the virus form responsible for viral dissemination throughout the host, culminating in a systemic infection. A secondary infection cycle begins with the entrance of BVs into another cell of the insect. After entering the cell, the infection process is similar to what happens in a primary infection, with the nucleocapsids traveling to the nucleus for DNA replication and subsequent viral protein expression. The very late phase of infection (18 hpi) initiates with the expression of proteins that constitute the crystalline matrix of the ODVs, namely polyhedrin. After nucleocapsid assembly, they are enveloped by the polyhedrin matrix to constitute the ODVs. The secondary cycle ends with the extensive infection of larvae tissues and cell lysis, culminating in insect larvae death, and dissemination of ODVs to the environment, where they can remain viable for several years until being ingested by other larvae (Volkman, 1997). Summarizing, BVs and ODVs are genetically identical but differ in their envelope compositions and tissue tropisms, and are produced at different times during infection.

The *in vitro* life cycle of baculovirus is similar to what happens *in vivo*, with a major difference that cultured cells need to be directly infected with the BVs. Since ODVs are forms resistant to environmental factors, there is no need of an occlusion matrix for *in vitro* virus survival. In fact, polyhedrin can be viewed as non-essential for baculovirus *in vitro* cell culture. Given that, recombinant baculoviruses are constructed by replacing the polyhedrin gene (*polh*) by a gene of interest under the control of the very late *polh* promoter (Merrington et al., 1997). Besides the strong activity of *polh* promoter, that allows high productivities of the recombinant protein, it is only expressed in the very late stage of the infection cycle.

BACULOVIRUS INFECTION: IMPACT ON THE HOST CELL

In the different phases of infection, baculoviruses induce profound changes on host cell properties. For that aim, several virus-encoded proteins interact with host cell factors, altering cellular structures and normal functions, and taking control of cellular gene expression machinery for their own profit (**Table 1**). As a result of such alterations several effects arise: cellular cytoskeleton rearrangement, cell cycle arrest and cytomegaly, apoptosis inhibition, metabolism subversion, and global shut-off of host protein synthesis. Current knowledge on the biology of the proteins involved in the regulation of each of these specific responses are reviewed and detailed below.

VIRUS ENTRY, INTRACELLULAR TRANSPORT, AND EGRESS OF VIRIONS

Viruses exploit cellular structures in order to be actively transported in the cells. Cytoskeleton proteins have been identified as important factors for viral replication and/or transcription (Fowler, 1990; De et al., 1991). In fact, virus entry, transport, and intracellular localization have been correlated with the reorganization of cytoskeleton proteins (Strauss, 1996; Cudmore et al., 1997).

Table 1 | Baculovirus genes affecting host function.

	Baculovirus protein/factors	Host counterparts	Function	Reference
Cellular adhesion/ entry	ODV: *pifs* (P74, PIF-1, and PIF-2)	Receptors on midgut epithelial cells	Viral entry through membrane fusion	Faulkner et al. (1997), Kikhno et al. (2002), Fang et al. (2006, 2009a), Harrison et al. (2010)
	BV: GP-64	Receptors on cells	Viral entry by clathrin-mediated endocytosis	Blissard and Wenz (1992), Long et al. (2006)
Cytoskeleton remodeling	VP39, P78, VP80	F-actin	Actin cables formation for nucleocapsids transport across the cytoplasm	Xu et al. (2007), Ohkawa et al. (2010), Marek et al. (2012)
	Arif-1	F-actin	Actin cables accumulation at cell borders	Roncarati and Knebel-Mörsdorf (1997), Dreschers et al. (2001)
	Ie-1, PE38, HE65, Ac004, Ac102, Ac152	G-actin	Drive G-actin accumulation into the nucleus	Ohkawa et al. (2002)
	P78/83-C42	G-actin	Arp2/3-mediated nuclear actin polymerization	Braunagel et al. (2001), Wang et al. (2008), Li et al. (2010)
	P10	?	Nuclear integrity	Carpentier et al. (2008)
	EXON0	β-Tubulin	Nucleocapsids engagement to microtubular network and further egress	Fang et al. (2007, 2009a)
	Ac93	?	Intranuclear microvesicles formation for virions maturation and egress	Yuan et al. (2011)
	Bm61	?	Egress	Shen and Chen (2012)
Cell cycle arrest	EC27	Cdc2	Cell cycle arrest at G2/M	Belyavskyi et al. (1998)
	EC27	Cdk6	Override cellular checkpoints to allow viral DNA replication	Belyavskyi et al. (1998)
Cellular stress response	*Lefs*	ATM and/or ATR	Viral DNA replication, shut off of host protein synthesis	Kimberly et al. (2009)
	PK1?; others	PI3K–Akt/MAPK–ERK–JNK members	Viral DNA replication/late gene expression and progeny production	Reilly and Guarino (1994), Katsuma et al. (2007), Xiao et al. (2009)
	P35	Effector caspases	Blockage of the apoptotic pathway	Clem et al. (1991), Kamita and Majima (1993), Bump et al. (1995), Bertin et al. (1996), Xu et al. (2001)
	P49	Initiator and effector caspases	Blockage of the apoptotic pathway	Du et al. (1999), Pei et al. (2002), Zoog et al. (2002), Guy and Friesen (2008)
	IAPs	?	Inhibition of apoptosis, activation of ubiquitination pathway	Manji et al. (1997), Salvesen and Duckett (2002)
	?	HSP/HSC70	Viral DNA replication, virions assembly and maturation	Lyupina et al. (2010, 2011)
Metabolism	?	?	Boost in catabolic pathways to fuel infection	Iwanaga et al. (2007), Bernal et al. (2009, 2010)

The extent of cytoskeleton reorganization depends on the type of virus, suggesting that a myriad of strategies have co-evolved as a result of the specific interactions established between the virus and its host. Herpesvirus exploits actin and actin-associated myosin motors for viral entry, intranuclear transport of nucleocapsids, and virion egress (Roberts and Baines, 2011). Measles virus induces actin remodeling and microtubule formation upon cell entry, facilitating virus transport into perinuclear spaces, where viral replication occurs, and budding of the newly formed virions (Avota et al., 2011). HIV-1 remodels host cell cytoskeleton in a complex biphasic mode, promoting both inhibition of actin polymerization with looseness of cytoskeleton rigidity in order to favor virus entry, followed by actin remodeling and microtubule network rearrangement for viral cores delivery into the cytoplasm (Stolp and Fackler, 2011).

The impact of baculovirus infection on host cell cytoskeleton has been studied in detail. Baculoviruses encode several proteins that act in an organized and orchestrated way to remodel the cellular actin network throughout their life cycle (**Figure 1**). Such cytoskeleton rearrangements are of crucial importance for baculovirus infection and proper assembly of newly synthesized virions. In fact, filamentous actin (F-actin) has been shown to be required for viral progeny production of lepidopteran nucleopolyhedroviruses such as *Ac*MNPV, *Spodoptera frugiperda* MNPV (*Sf*MNPV), *Bombyx mori* NPV (*Bm*NPV), *Orgyia pseudotsugata* MNPV (*Op*MNPV), *Lymantria dispar* MNPV (*Ld*MNPV), *Anticarsia gemmatalis* MNPV (*Ag*MNPV), and *Helicoverpa zea* SNPV (*Hz*SNPV; Kasman and Volkman, 2000).

During *Ac*MNPV infection, three major actin cytoskeleton rearrangements occur. First, upon cell entry, F-actin cables can be detected throughout the cytoplasm, often associated with viral nucleocapsids. The formation of these actin cables is independent of viral gene expression, and correlates with the release of nucleocapsids from the endosomes upon internalization of BVs. Fluorescence microscopy studies showed the association of the nucleocapsids with one end of these actin cables, which might indicate the putative role of such structures in the transport of the nucleocapsids to the nucleus (Charlton and Volkman, 1993).

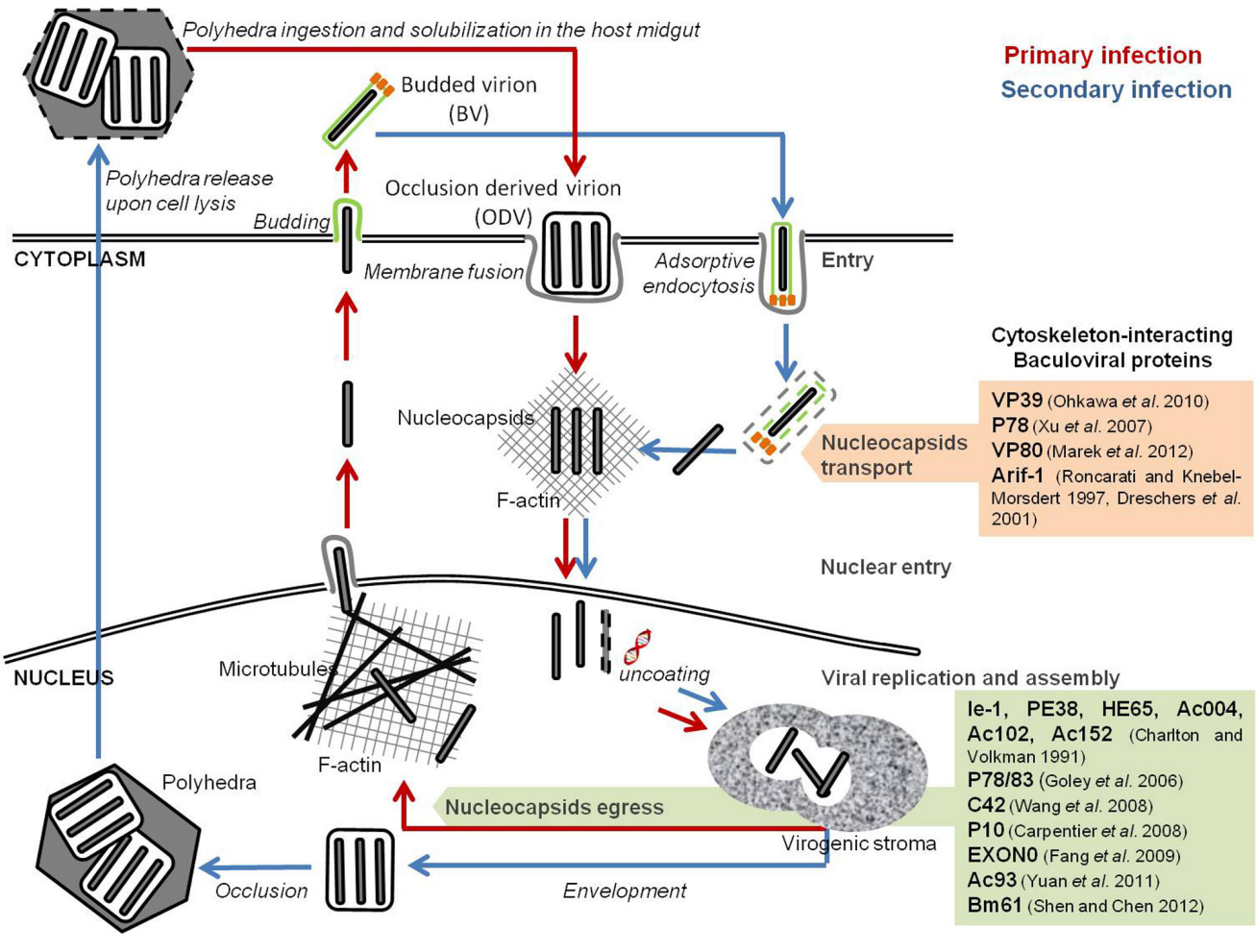

FIGURE 1 | Baculoviral proteins involved in the remodeling of cellular host cytoskeleton. Baculovirus infection induces a reconfiguration of the host cytoskeleton for intracellular traveling of nucleocapsids and virions. Nucleocapsids movement into the nucleus occurs through the F-actin cytoplasmic network. The egress of newly formed virions is dependent on a viral-induced actin polymerization inside the nucleus.

Lu et al. (2004) observed that *Helicoverpa armigera* NPV (*Ha*NPV) VP39 nucleocapsid protein not only binds to actin, but also promotes its complexation to form actin cables structures, *in vitro*. In fact, it has been demonstrated that several *Ac*MNPV nucleocapsid proteins (such as VP39, P78, and VP80) bind to actin directly (Xu et al., 2007; Ohkawa et al., 2010; Marek et al., 2012).

After early gene expression, a second alteration of the cytoskeleton occurs, with the formation of F-actin aggregates at the plasma membrane (Charlton and Volkman, 1991; Roncarati and Knebel-Mörsdorf, 1997). Concomitant with the intracellular release of nucleocapsids, actin cables localize at the cell surface and extend into the cytoplasm. At the onset of early gene expression, a rearrangement of the actin network is observed, during which actin cables become more prominent and accumulate at the cell borders (Roncarati and Knebel-Mörsdorf, 1997). This second change is mediated by the product of a single early viral gene, *arif-1* (actin-rearrangement-inducing factor 1), a 47-kDa phosphoprotein that co-localizes with the F-actin aggregates (Dreschers et al., 2001). Expression of *arif-1* alone leads to actin rearrangements comparable to the changes that happen at the late stage of early gene expression (Roncarati and Knebel-Mörsdorf, 1997). Immunofluorescence studies showed that, following *Ac*MNPV infection, Arif-1 co-localizes with F-actin at the plasma membrane until the onset of late gene expression, when Arif-1-induced actin polymerization is no longer detected. In fact, Arif-1 analysis by SDS-PAGE showed that, between 12 and 48 hpi, multiple bands of higher molecular weight appeared, and that phosphatase treatment could reverse this observation. This suggests that Arif-1 is inactivated by phosphorylation (Dreschers et al., 2001).

A third and more profound reconfiguration takes place during late gene expression, when F-actin appears within the nucleus, a feature almost exclusive to baculoviral infection and essential for nucleocapsids morphogenesis (Volkman, 1988; Ohkawa and Volkman, 1999; Kasman and Volkman, 2000). Monomeric globular actin (G-actin) starts to accumulate in the nucleus upon early gene expression. Six early viral gene products are implicated in this process: *ie-1* and *pe38*, both transcriptional activators of several early, late, and very late genes (Blissard and Rohrmann, 1991; Lu and Carstens, 1993; Passarelli and Miller, 1993; Milks et al., 2003); *he65*, a RNA ligase involved in RNA replication, transcription, and modification (Rohrmann, 2011); and *ac004*, *ac102*, *ac152*, which products have not yet been characterized (Ohkawa et al., 2002; Gandhi et al., 2012). Nuclear actin is then polymerized into filaments (F-actin) by the products of late viral genes (Charlton and Volkman, 1991). Time-lapse microscopy studies showed that nuclear recruitment and actin polymerization is a precisely controlled dynamic process. During *Ac*MNPV infection of TN-368 cells, G-actin accumulates in the nucleus between 10 and 20 hpi, and polymerization started 2 h after nuclear entry (Goley et al., 2006a). Such rapid turnover suggests the presence of a regulatory network that commands nuclear actin assembly during baculovirus infection. One such elemental regulator is the cellular Arp2/3 complex, which is activated to nucleate branched actin filaments by proteins called nucleation-promoting factors (NPFs; Welch and Mullins, 2002; Gandhi et al., 2012). In fact, several nucleopolyhedroviruses encode a capsid-associated protein, called p78/83 in *Ac*MNPV, that contains conserved domains of the Wiskott–Aldrich syndrome protein (WASP) family of NPFs (Machesky et al., 2001). However, both the p78/83 protein and the Arp2/3 complex self-localize in the cytoplasm of uninfected cells (Goley et al., 2006a), which points out that another viral protein must participate to recruit both factors to the nucleus. It has been suggested that *Ac*MNPV encoded nucleocapsid protein, C42, a product of a late gene highly conserved among members of the Baculoviridae family, is responsible for nuclear recruitment of p78/83 and Arp2/3. This protein is present in both BVs and ODVs, possesses a putative nuclear localization signal (NLS) motif and binds to the p78/83 protein in a nucleocapsid-independent manner (Braunagel et al., 2001; Wang et al., 2008; Li et al., 2010). Taken together, the above mentioned cellular and viral factors are believed to act in an orchestrated way to promote actin transport into the nucleus and further polymerization. This step is of paramount importance for proper virion assembly and infectivity, since in the presence of cytochalasin D or latrunculin A, two drugs that interfere with F-actin function, viral progeny production is inhibited, a phenotype observed in several divergent nucleopolyhedroviruses (Kasman and Volkman, 2000).

Also in the late phase of infection, the P10 late viral protein starts to aggregate, forming a thick tubular network surrounding the nucleus that projects into the cytoplasm (Carpentier et al., 2008). During infection the nucleus swells as a result of the accumulation of viral proteins and virions. This P10-associated cage may stabilize the nucleus, preventing its disruption before the ODVs have completely matured and, stabilizing the architecture of cells long enough for the virus to complete its replication process (Carpentier et al., 2008).

Once the virions progeny have properly matured, they need to be transported from the nucleus toward peripheral budding sites. One component that is involved in this egress pathway is EXON0, a conserved structural protein of BV and ODV nucleocapsids found in all lepidopteran alpha-baculoviruses (Fang et al., 2007). Co-immunoprecipitation and confocal immunofluorescence microscopy studies showed that EXON0 interacts with β-tubulin, enabling the "engagement" of BV nucleocapsids with the microtubular network (Fang et al., 2009b). This assists the transport of nucleocapsids in the nucleus from the virogenic stroma to the nuclear envelope and their migration to the plasma membrane. Recently, Yuan et al. (2011) identified a core gene, *ac93*, as an important player in *Ac*MNPV nucleocapsids egress from the nucleus. Mutagenesis assays showed that *ac93* is required for intranuclear microvesicle formation and egress, thus affecting BVs production and ODVs envelopment. Moreover, immunofluorescence microscopy revealed the presence of Ac93 moving toward the cytoplasmic membrane and in the ring zone of the nucleus, late in infection. In fact, this protein was detected in association with the nucleocapsid fraction of both BV and ODV, and the envelope fraction of BV, which further supports its involvement in virion maturation and egress (Yuan et al., 2011). Shen and Chen (2012) identified another core gene, *Bm61*, as a participant in the egress of BVs during *Bm*NPV infection. Deletion of *Bm61* blocked the production of BVs, although DNA replication still occurred. In fact, electron microscopy analysis showed that, despite nucleocapsid assembly still occurred, they remained trapped in the nucleus

by impairment of the egress route to the cytoplasm, leading to loss of BVs production. Furthermore, fluorescence microscopy showed the presence of Bm61 at the intranuclear ring zone and nuclear membrane, which illustrates its role in the transport of nucleocapsids to the cytoplasm (Shen and Chen, 2012).

Summarizing, actin and tubulin networks have important roles throughout baculovirus infection. The virus undertakes a successful and dynamic manipulation of cellular cytoskeleton, and these effects span all the infection process from virus entrance and transport to the nucleus, to nucleocapsid formation and egress, which is at the core of successful infection and replication.

CELL CYCLE ARREST

The cell cycle involves a series of events that take place in a cell leading to its division and duplication. A complete cellular cycle comprises four sequential stages: G1, S, G2, and mitosis. DNA replication and cell division are highly regulated processes that occur at S and M phases, respectively. G1 and G2 are gap phases where the cell prepares itself for the next stage. Progression from one stage to the following is controlled by cyclins and cyclin-dependent kinases (Cdk), which are in turn regulated by a plethora of pathways in response to external stimuli, as well as to the internal conditions of the cell (Morgan, 1995).

A common feature of many viral infections is the subversion of the host cellular cycle to create an intracellular environment suitable for maximized viral DNA replication (Ben-Israel and Kleinberger, 2002; Spink and Fluck, 2003; Chen and Qiu, 2010; Sakai et al., 2011; Li et al., 2012). Very diverse strategies have been developed by viruses, from the stimulation of cell cycle progression in quiescent cells, to blockade of cell cycle progression in proliferating ones (Op De Beeck and Caillet-Fauquet, 1997; Davy and Doorbar, 2007). For instance, HIV Vpr-mediated arrest at G2/M can benefit the early infection stages by increasing the number of integrated proviruses (Groschel and Bushman, 2005). In turn, adenovirus and SV40 polyomavirus infection induces the cell to remain in a pseudo-S phase state, during which normal cellular DNA replication is complete, but the cell still remains competent for viral DNA replication (Lehman et al., 1994, 2000; Ben-Israel and Kleinberger, 2002).

Baculovirus infection of insect cells causes cell cycle arrest in the G2/M phase (**Figure 2**). Braunagel et al. (1998) showed that when *Sf*9 cells were infected with *Ac*MNPV, approximately 84% of the total cellular population was arrested in G2/M phase by 18–24 hpi. Concomitantly, high levels of Cdc2-associated histone H1 kinase and cyclin B were detected, with the kinase activity remaining detectable through the course of infection. Moreover, this arrest was proven to be necessary for optimal ODVs maturation and assembly since arresting *Sf*9 cells at G1/S boundary by chemical treatment led to abnormal intranuclear microvesicle formation and, consequently, impairment of ODV maturation (Braunagel et al., 1998). During regular cell cycle, cyclin B associates with Cdc2 and this complex is responsible for the progression from G2 to M. The complex accumulates in the nucleus, and once activated by Cdc25, induces a cascade of nuclear architecture rearrangements culminating with the breakdown of nuclear lamina with increased envelope fluidity, therefore committing cells to start dividing. Afterward, cellular cyclin B is degraded and the cell progresses to anaphase (Draetta and Beach, 1989; Nurse, 1994). These findings

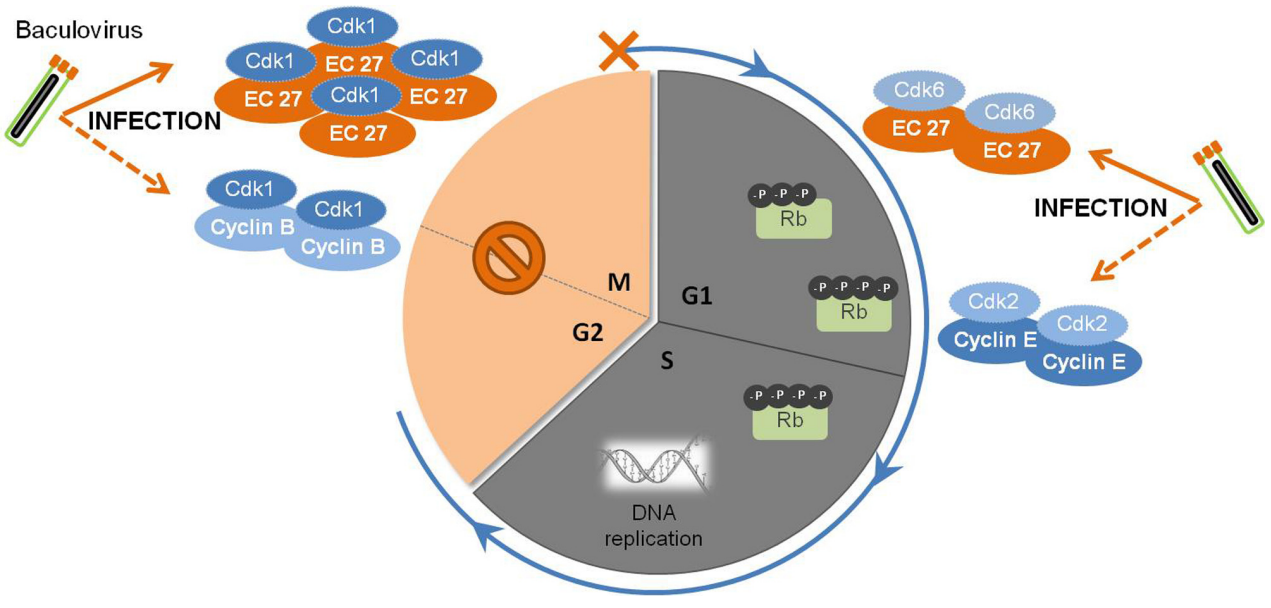

FIGURE 2 | Baculovirus subversion of host cellular cycle. Early in infection, the baculovirus causes the augmentation of cellular levels of Cdk1-cyclin B complexes, which are responsible for the regulation of the transition of G2 to M phase. Later on, a viral homolog of host cyclin B, EC27, starts to be expressed and accumulates in the cell. The complex Cdk1-EC27 blocks the cell cycle, and the cells remain arrested In the G2/M phase during the course of infection. Also, EC27 can act in a cyclin D-dependent manner, forming the complex Cdk6-EC27. As a result, the retinoblastoma protein (Rb) becomes phosphorylated, together with the activation of the complex Cdk2-cyclin E. Such phenomena will trigger the components needed for DNA replication, ensuring an environment favorable for viral DNA synthesis and replication.

suggest that early in infection, the cyclin B-Cdc2 complex may be used to regulate the transition from G2 to M phase. However, since only the kinase activity is detectable throughout infection, the prolonged cell cycle arrest during baculovirus infection may be due to a protein(s) encoded by *Ac*MNPV. In fact, *Ac*MNPV was shown to encode a human cyclin homolog protein, the EC27 protein. This protein was described as having a multifunctional operating mode, being able to act in a cyclin B and cyclin D-dependent manner (Belyavskyi et al., 1998). By encoding a cyclin B-like protein, baculoviruses are able to arrest the cellular cycle at G2/M phase maintaining the nuclear architecture at its best for virions progeny assembly and maturation. Actually, the cellular phenotype alterations manifested throughout baculoviral infection, such as enlarged nucleus, increased envelope fluidity, and induction of microvesicles and membranes in the nucleoplasm (Summers and Arnott, 1969; Braunagel et al., 1998), supports EC27 cyclin B-like functions. However, this baculovirus encoded cyclin B does not lead to the breakdown of the nucleus, which remains intact in infected cells, possibly indicating that there are differences with the host protein.

Baculovirus infection of insect cells induces the shut-off of global host protein synthesis by 18 hpi (Carstens et al., 1979; Du and Thiem, 1997), concomitant with the cell cycle arrest at G2/M (Braunagel et al., 1998; Ikeda and Kobayashi, 1999). In fact, beyond this time frame, cellular DNA replication is no longer detected, in opposition to viral DNA replication and gene expression. The presence of an active Cdk6-EC27 complex with cyclin D-like activity can explain this behavior. In non-infected cells, cyclin D association with Cdk6 promotes G1 to S phase transition by phosphorylation of pRb (retinoblastoma protein), a key regulator of the cell cycle (Dowdy et al., 1993; Ewen et al., 1993). Moreover, Cdk-cyclin complexes can "titrate" Cdk inhibitors resulting in activation of the Cdk2-cyclin E complex (Polyak et al., 1994) which then affects components of the pre-initiation complexes to trigger DNA replication (Stillman, 1996). Such observations clearly show that baculovirus encodes specific mechanisms to override cellular checkpoints, which benefits both viral DNA replication and virion assembly and maturation.

CELLULAR STRESS RESPONSE

Infection is sensed by cells as a stressful situation. Accordingly, viruses trigger diverse cellular responses, including the activation of apoptosis, DNA damage, and heat shock responses (HSR), aimed at fighting the infection by preventing virus replication and dissemination. Consequently, viruses have evolved several strategies in order to circumvent these defense responses. In this section, specific features of baculovirus–host interactions during cellular responses to infection will be discussed. Although these responses are coordinated, for the sake of simplicity, they will be treated separately.

Induction of DNA damage response and pro-survival pathways

Several viruses have evolved mechanisms to manipulate the DNA damage response triggered upon viral infection (Chaurushiya and Weitzman, 2010). The cellular response to the presence of damaged DNA is dependent on the activation of two members of the phosphatidylinositol 3-kinase (PI3K) superfamily, the ataxia telangiectasia mutated (ATM) and rad3-related (ATR) proteins (Seviour and Lin, 2010). These systems respond to double-strand breaks in DNA, and single-strand breaks along with stalled replication forks, respectively (Huang et al., 2011). As discussed later on, the downstream effects of the activation of this system include the phosphorylation of numerous effector proteins which function in cell cycle checkpoints, DNA repair, and stimulation of apoptosis. Interestingly, one important downstream substrate of ATM and ATR is P53, which is actively inhibited by many DNA viruses to avoid the inhibition of cell cycle progression and stimulation of apoptosis in response to DNA damage (Huang et al., 2011).

Several mammalian viruses induce a cellular DNA damage response during replication which, in some cases, is required for optimal virus replication. For instance, SV40 efficient DNA replication and virions assembly is dependent on the activation of ATM (Zhao et al., 2008). HSV and HIV-1 also activate ATM, and that ATM signaling is important for viral replication (Lau et al., 2005; Lilley et al., 2005). This is also the case for baculoviruses. In fact, induced apoptosis and shut-off of host protein synthesis are the result of the activation of cellular DNA damage response, and this activation is triggered by viral DNA replication (Clem and Miller, 1994; LaCount and Friesen, 1997; Kimberly et al., 2009). RNA silencing assays directed to genes essential to *Ac*MNPV replication identified the replicative late expression factors (*lef*) as the source of the critical apoptotic signal in infected cells, which also contribute to the inhibition of host cell protein synthesis (Kimberly et al., 2009). Moreover, the addition of ATM and ATR inhibitors to *Sf*9 cultures infected with *Ac*MNPV decreased viral DNA replication and late gene expression (Huang et al., 2011). In this sense, baculovirus control of the cellular response against infection can be viewed as an equilibrium in which the virus takes advantage of the activation of the DNA damage response for DNA replication, shut-off of host protein synthesis to have the machinery available for viral protein expression, together with inhibition of apoptosis by expressing anti-apoptotic factors (**Figure 3**).

Concomitant with the induction of the stress response, viral infection also activates and modulates pro-survival cellular pathways (Cooray, 2004; Ji and Liu, 2008; Furler and Uittenbogaart, 2010; Qin et al., 2011). The mitogen-activated protein kinases (MAPKs), such as extracellular signal-regulated molecule kinase (ERK) and c-Jun NH_2-terminal kinase (JNK), are involved in the regulation of a plethora of cellular processes, including cell division and control of transcription (Johnson and Lapadat, 2002). The PI3K–Akt pathway controls cell survival and apoptosis, proliferation, migration, and regulates metabolism (Willems et al., 2012). In light of this knowledge, it is not surprising that viruses exploit such cellular pathways to set-up an intracellular environment suitable for efficient replication and progeny production. In fact, hepatitis-B, Epstein–Barr, and vaccinia virus are known to subvert MAPK pathways, a behavior that is behind successful infections (de Magalhães et al., 2001; Zheng et al., 2003; Gao et al., 2004). During influenza A virus infection, the PI3K–Akt signaling pathway is activated, and inhibition of PI3K results in reduced viral RNA synthesis, protein expression, and viral yield (Shin et al., 2007). Also, human cytomegalovirus (Johnson et al.,

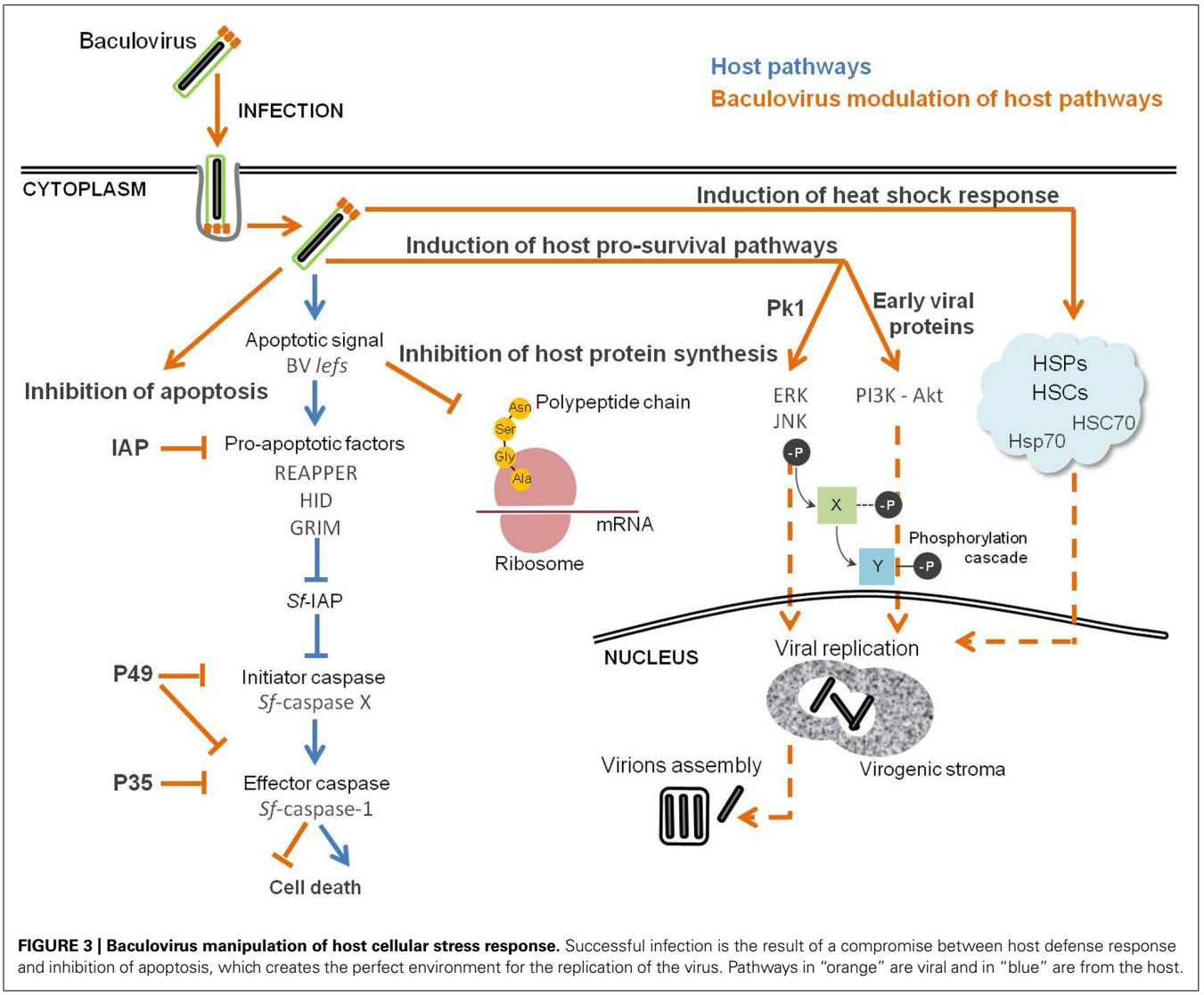

FIGURE 3 | Baculovirus manipulation of host cellular stress response. Successful infection is the result of a compromise between host defense response and inhibition of apoptosis, which creates the perfect environment for the replication of the virus. Pathways in "orange" are viral and in "blue" are from the host.

2001) and coxsackievirus B3 (Luo et al., 2002; Esfandiarei et al., 2004) depend on the activity of PI3K–Akt and/or MAPK–ERK for efficient replication. It has been previously shown that baculovirus efficient infection is dependent on the activation of both MAPK and PI3K signaling (**Figure 3**). Successful infection of *Bm*NPV is dependent on the activation of ERK and JNK signaling pathways (Katsuma et al., 2007). Western blot assays revealed that ERK and JNK were activated at the late stage of *Bm*NPV infection, and inhibition of both kinases after 12 hpi significantly reduced occlusion body formation and BVs production (Katsuma et al., 2007). Also, late and very late gene expression was impaired, suggesting an important role for ERK and JNK in regulating the *Bm*NPV gene expression program. During *Ac*MNPV infection of *Sf*9 cells the levels of phosphorylated Akt became elevated, and inhibition of PI3K–Akt activation significantly reduced viral yield, BV production, and occlusion body formation (Xiao et al., 2009). The activation of the PI3K–Akt signaling pathway occurs at an early stage of *Ac*MNPV infection, and is of major importance for viral DNA replication. Inhibition of PI3K at 12 hpi not only reduces the level of viral DNA synthesis, but also delays late and very late gene expression. This result is not surprising, since the transition from early to late phase is marked by the onset of viral DNA replication, which in turn occurs together with the expression of very late genes coding for viral structural components necessary for the assembly of new virions (Grula et al., 1981). Taken together, these data suggest that the products of early genes prepare the host cell for viral multiplication, shown here by the activation of PI3K–Akt pathway, ensuring an environment suitable for efficient infection. However, it is not clear which viral proteins are involved in the activation of these signaling pathways. Baculoviral PK1 serine/threonine protein kinase is expressed along with *Ac*MNPV infection and it is essential for *Bm*NPV replication in *Bm*N cells (Reilly and Guarino, 1994; Katsuma et al., 2007). These data suggest that phosphorylation of host and/or viral proteins by PK1 is needed for virus replication, indicating PK1 as a viral candidate for the activation of ERK and JNK kinases. Further studies concerning the identification of the viral counterpart(s) responsible(s) for the activation of these signaling pathways are compulsory.

Inhibition of apoptosis

As mentioned before, one of the pathways targeted by the DNA damage response is apoptosis, or programmed cell death, which is a highly regulated process widespread among multicellular organisms. It is characterized by apoptotic body formation, cell shrinkage, membrane blebbing, chromatin condensation and DNA fragmentation, culminating in cellular death (Kerr et al., 1972). Such mechanism is evolutionarily conserved, with the convergence of the apoptotic stimuli to a central pathway that encloses a family of aspartate-specific cysteinyl proteases, i.e., caspases, the main activators and executioners of the apoptotic response. The caspases family is divided in two classes, initiator caspases and effector caspases, which are activated in a sequential manner by auto cleavage in response to apoptotic signaling (Ma and Chang, 2011).

In order to counteract this defense, several viruses have developed mechanisms to block the premature apoptosis of infected cells. These strategies range from mimicking specific cellular regulators, which is the case of the Epstein–Barr virus, African swine fever virus, and herpesvirus, that encode viral homologs for the cellular anti-apoptotic protein Bcl-2, or expressing viral-specific proteins, like the cowpox virus CrmA anti-apoptotic factor (Koyama et al., 2000; Aubert and Blaho, 2001).

Although currently this is observed as a general key strategy, the stimulation of apoptosis by infection was first demonstrated in the baculovirus system (**Figure 3**). Clem et al. (1991) found that baculovirus replication in insect cells triggers apoptosis, and a specific viral gene product, the *Ac*MNPV *p35*, was identified as being responsible for blocking the apoptotic response. In fact, it was later shown that P35 protein is a direct substrate inhibitor of caspases and acts in a stoichiometric manner as a suicide inhibitor (Bump et al., 1995). Caspase-mediated cleavage at the aspartate residue Asp87 within the P35 reactive-site loop leads to the formation of a stable complex covalently bound to the target caspase, subsequently inhibiting apoptosis (Bertin et al., 1996; Xu et al., 2001). In addition to *Ac*MNPV, other baculoviruses have been found to carry *p35* homologs, *Bm*NPV and *Spodoptera litoralis* NPV (*Sl*NPV). The *Bm*NPV *p35* gene has high nucleotide and amino acid sequence identity to the *Ac*MNPV gene, and its presence is needed to inhibit *Bm*NPV induced apoptosis in *B. mori* cells (Kamita and Majima, 1993). The *Sl*NPV *p49* gene encodes a protein with 49% amino acid identity with its *Ac*MNPV homolog *p35* (Du et al., 1999). Computer-assisted modeling and site-directed mutagenesis suggests that the structure of P49 resembles P35, including the presence of a prominent reactive loop that presents Asp94 for cleavage (Pei et al., 2002; Zoog et al., 2002). P49 has the ability to inhibit both initiator and effector caspases, whereas P35 can only inhibit effector caspases. P49 is a substrate inhibitor of the initiator caspase Sf-caspase-X, which is responsible for the proteolysis and activation of Sf-caspase-1 and -2 (Zoog et al., 2002; Guy and Friesen, 2008). This indicates that P49 acts upstream of P35 by inhibiting initiator caspases responsible for the activation of effector caspases.

Another family of baculovirus anti-apoptotic genes is the *iap* (inhibitor of apoptosis) family. These genes are present in genomes from yeasts to humans, and are known to regulate apoptosis and several other cellular functions (Salvesen and Duckett, 2002; Gyrd-Hansen and Meier, 2010). The first *iap* genes described in nature were discovered by complementation assays in *Cydia pomonella* granulovirus (*Cp-iap*) and *Orgyia pseudotsugata* nucleopolyhedrovirus (*Op-iap*; Crook et al., 1993; Birnbaum et al., 1994), in which the *iap* gene compensated for the lack of *p35* in the *annihilator Ac*MNPV mutant. At least one *iap* gene is present in almost all the baculovirus genomes sequenced, whereas *p35* genes are present in only a small subset (Clem, 2005). *Op*-IAP was shown to function upstream of P35 in *Sf*21 cells, since its expression was sufficient to block effector Sf-caspase-1 processing, while P35 was not (Manji et al., 1997; Seshagiri and Miller, 1997). However, besides these two examples many of the *iap* genes tested so far do not seem to have the ability to inhibit apoptosis, or this ability is cell type-specific (Bideshi et al., 1999; Maguire et al., 2000). Moreover, given their ubiquitous distribution, maybe their anti-apoptotic activity is restricted to certain scenarios, or they may possess other functions in different viral processes, such as ubiquitin ligases, as shown for other cellular and viral IAPs (Yang et al., 2000; Imai et al., 2003; Green et al., 2004). Structurally, IAP proteins are metalloproteins with one to three copies of a zinc-binding motif, BIR (Baculovirus IAP Repeat), at the N-terminus, and another zinc-binding motif, RING, at the C-terminus (Hinds et al., 1999). BIR-containing motifs of several IAP proteins bind directly a myriad of pro-apoptotic proteins (Miller, 1999). In fact, BIR2 motif of *Op*-IAP interacts with *Drosophila* pro-apoptotic factors REAPPER, HID, and GRIM, and this binding inhibits apoptosis even during overexpression of such factors in *Sf*21 cells (Vucic et al., 1997, 1998a,b). The RING domain is also important, since its removal completely abolishes *Op*-IAP anti-apoptotic activity and strongly diminishes its ability to protect *Sf*21 cells during HID overexpression (Vucic et al., 1998a; Wright and Clem, 2002). RING motif-containing proteins are involved in many cellular functions, ranging from scaffolding of multi-protein complexes (Borden, 2000) to E3 ubiquitin ligase activity (Tyers and Willems, 1999). Actually, the *Op*-IAP RING domain has been shown to have E3 ubiquitin ligase activity, capable of promoting its own and HID ubiquitination, and this ability is of major importance for *Op*-IAP anti-apoptotic properties (Green et al., 2004). Ubiquitination is a post-translational modification that can have different effects on the targeted substrate, such as targeting to proteasome-dependent proteolysis or the modulation of protein function, structure, assembly, and localization (Deshaies and Joazeiro, 2009). The relevance of this activity for the *in vivo* anti-apoptotic function of *Op*-IAP is still unclear. Direct interaction and subsequent modulation of pro-apoptotic factors by IAP proteins is evident, and further studies are encouraged in order to disclose the peculiarities of such dynamic cross talk.

Induction of the heat shock response

A hallmark of universal cellular defense to various environmental and pharmacological stresses is the activation of the HSR (Gidalevitz et al., 2011). The induction of HSR leads to the rapid and robust expression of members of the chaperone family of heat shock proteins (HSPs) and respective cognates (HSCs), in order to protect the cell from proteotoxic stresses and to maintain protein homeostasis (Fujimoto and Nakai, 2010).

HSP70s and HSP90s, members of the HSPs family, are involved in the replicative cycles of DNA and RNA viruses. Not only have they been identified in the regulation of viral gene expression *via* interaction with specific viral proteins, but they also participate in capsid assembly and disassembly (Mayer, 2005; Xiao et al., 2010; Nagy et al., 2011). Such observations demonstrate that viruses also exploit HSR as an infection strategy. A proteomic study by 2D-GE coupled with mass spectrometry showed that host HSC70 was associated with ODV of *Bm*NPV, suggesting a possible involvement of HSP during the assembly of baculoviral virions (Liu et al., 2008). Nobiron (2003) used a differential display approach to search for host mRNA transcripts that could be up-regulated during *Ac*MNPV infection of *Sf*9 cell line. They found one transiently up-regulated transcript encoded by *hsc70*, for which expression peaked at 6 hpi. Similarly, a microarray approach to analyze the global transcriptional profile of infected *B. mori* cells showed that the *hsc70* ortholog was up-regulated during infection, and this increase was detected only until 24 hpi (Sagisaka et al., 2010). A combined microarray assay complemented with qRT-PCR was applied for *Sf*21 transcriptome analysis during the infection with *Ac*MNPV (Salem et al., 2011). Despite the fact that the majority of cellular genes were down-regulated during the course of infection, the expression of two members of the *hsp70* family were augmented. Lyupina et al. (2010) monitored the induction of HSPs of the 70-kDa family (HSP/HSC70) in *Sf*9 cells after infection with *Ac*MNPV by Western blot analysis. The authors reported that *Ac*MNPV infection induces and stimulates several HSP70s, and that the infection process markedly potentiates HSR by boosting the HSP/HSC70s content (**Figure 3**). The use of chemical inhibitors of HSR decreased the rate of viral DNA synthesis, providing experimental evidence of the importance of such pathway for baculovirus replication. Moreover, HSP70s co-localize with ubiquitinylated proteins in speckles in the cytoplasm of *Ac*MNPV-infected cells, forming aggresome-like structures that can contain proteins for digestion and/or sequestration during infection (Lyupina et al., 2011). In fact, the ubiquitin-proteasome system is required during *Bm*NPV infection, since its inhibition resulted in reduced BV and ODV formation, together with the suppression of polyhedrin expression (Katsuma et al., 2011). Ubiquitin homologs are found in most lepidopteran baculovirus genomes (Katsuma et al., 2008). Although non-essential for viral replication, the baculovirus ubiquitin protein (*v*-UBI) is involved in the formation of *Ac*MNPV viral particles, since its loss resulted in a reduction of BV production (Reilly and Guarino, 1996). Additionally, biochemical experiments suggest a putative role for *v*-UBI in the blocking of the host degradative pathways of short-lived protein(s) during infection (Haas et al., 1996). Taken together, these data suggest a close collaboration of HSPs and ubiquitin-proteasome system during the baculovirus replicative cycle. Studies exploring the interactome profile between viral proteins and factors triggered upon stress induction are strongly encouraged, in order to identify the players and mechanisms responsible for balancing host damage and stress response.

METABOLISM

Viral infection claims an intensification of host cell biosynthetic activity in order to supply building blocks needed for the biogenesis of membrane lipids and for the synthesis of viral nucleic acids and proteins (Munger et al., 2006, 2010). In fact, viruses are considered as "metabolic engineers" (Maynard et al., 2010). In this regard, the success of infection is highly dependent on the metabolic state of the cells at the moment of infection, jointly with the viral manipulation of energy metabolism to fit such needs (Carinhas et al., 2010, 2011a). Despite many recent reports, the characterization of insect cell metabolic response to baculovirus infection is still at its infancy.

Baculovirus infection provokes an important metabolic burden on insect cells, causing an enhancement of the fluxes through the major catabolic pathways, namely glycolysis and tricarboxylic acid cycle (TCA; Bernal et al., 2009) as reflected in the changes in fluxes and enzyme activities after infection (Bernal et al., 2010; **Figure 4**). An increase in the oxygen uptake rate is also observed, which accounts for a higher rate of respiration upon infection (Kamen et al., 1996; Palomares et al., 2004; Bernal et al., 2009). Moreover, there is a drop in systems productivity when insect cells are infected with baculovirus at high cell densities, the so called "cell density effect." Bernal et al. (2009) succeeded in deciphering the metabolic basis of such phenomenon, during which *Sf*9 cells undergo a progressive inhibition of central metabolism (Bernal et al., 2009). Since a successful viral infection strongly correlates with the energetic state of the cell, viral replication is impaired in high cell density cultures. Iwanaga et al. (2007) performed an exploratory analysis using subtractive hybridization in order to identify differentially expressed host genes following *Bm*NPV infection. The authors paid special attention to the response of energy metabolism to infection, and reported the up-regulation of *citrate synthase* and *ATP-dependent proteasome 26S* homologous genes. Citrate synthase is the first enzyme of the TCA cycle, which plays a central role in aerobic energy production and metabolic interconversions in mitochondria (Holloszy et al., 1970). On the other hand, the proteasome-ubiquitin pathway plays an important role during baculovirus infection as mentioned previously (Katsuma et al., 2011). Next-generation sequencing and gene enrichment analysis also showed that gene sets related to mitochondrial function were highly up-regulated during the course of *Bm*NPV infection of *Bm*5 cells (Xue et al., 2012). A recent high-throughput analysis of baculovirus proteomic responses of *Sf*9 cells to infection with *Ac*MNPV identified two up-regulated metabolic enzymes, pyruvate dehydrogenase and aldehyde dehydrogenase (Carinhas et al., 2011b). Therefore, the up-regulation of such cellular proteins indicates that baculoviruses manipulate host energy metabolism to fuel its own replication and further envisages the importance of energy metabolism in supporting infection.

All these alterations described in central metabolism are linked to the host–virus interactions described in the previous sections. Baculovirus replication depends on the activation of PI3K–Akt signaling pathway (Xiao et al., 2009). One of the downstream targets of Akt is the adenosine 5′ monophosphate (AMP)-activated kinase (AMPK), a key sensor which regulates the metabolic status of cells (Cantó et al., 2009). In fact, it is activated by an increase in the AMP:ATP ratio (i.e., a low energy charge) and balances energy homeostasis by up-regulating catabolic processes while inhibits anabolism. A similar regulatory mechanism is activated

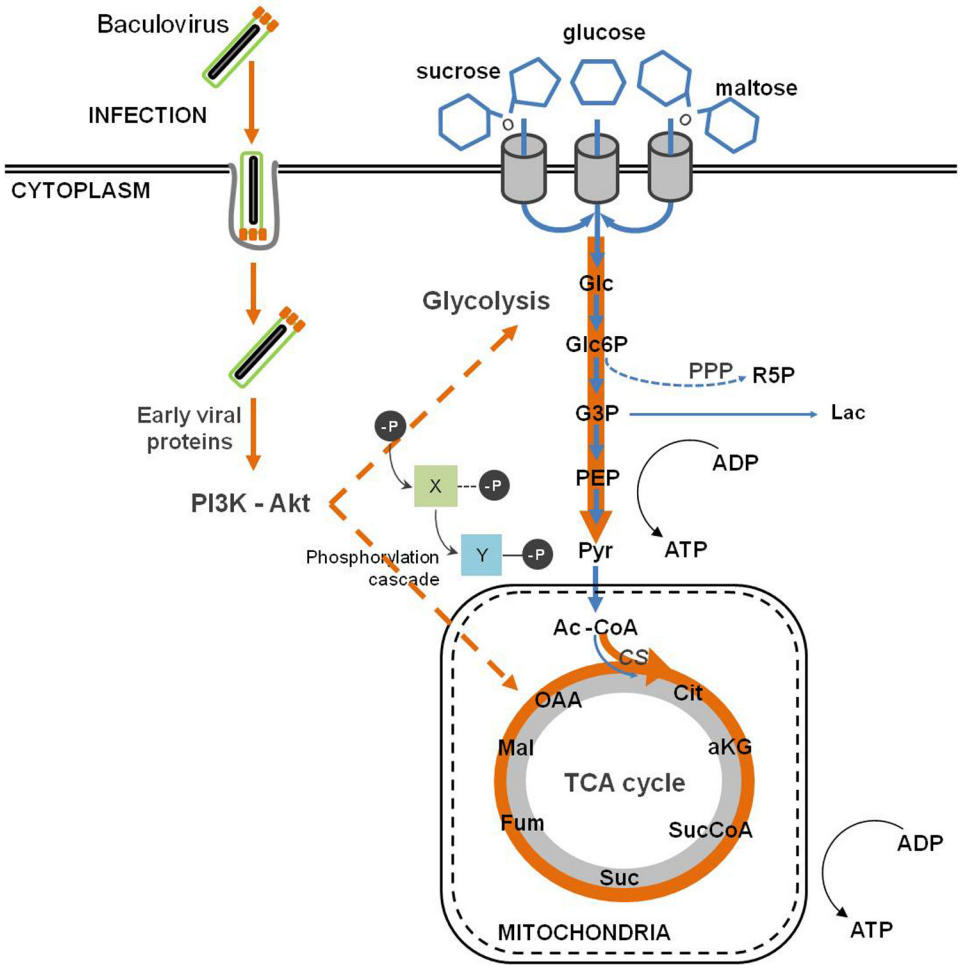

FIGURE 4 | Baculovirus infection impact on host cell metabolism. Baculovirus infection causes an intensification of glycolytic and tricarboxylic acid cycle (TCA) fluxes, which indirectly follows the activation of the PI3K–Akt signaling pathway.

in other viruses (Terry et al., 2012). In addition, both *Ac*MNPV and *Bm*NPV encode nucleotide diphosphate hydrolases belonging to the Nudix family. The corresponding genes are expressed early in infection and are essential for the replication of the virus (Ge et al., 2007; Chen et al., 2010). The essentiality of this activity is intriguing, although several metabolic regulatory roles have been proposed for nucleotides and related metabolites, which might contribute to the observed effects of infection (Tong and Denu, 2010).

PROTEOMIC ANALYSIS OF BACULOVIRUS–HOST CELL INTERACTIONS

As seen along the previous sections, viral infection induces profound alterations on the physiology of the host cells, and the latter respond to such changes by translating a complex network of protein–protein interactions and biochemical signaling events into functional responses. Systems level knowledge about the host effectors involved in the response to virus infection and the functions induced by viruses is crucial to understand the molecular basis of viral pathogenesis at a whole cell/organism level.

In addition to their well proven biotechnological and biomedical potentials, the study of the molecular biology of baculovirus infection has also offered meaningful insights into conserved viral mechanisms of manipulation and subversion of the host cell (Clem, 2001; Goley et al., 2006b).

Despite the advances in the so-called *omic* technologies, their application to the baculovirus–host system has been held back by the lack of sequenced host genomes, and the scarcity of curated databases. While complete genome sequences for more than 53 baculovirus are available (van Oers, 2011), currently, the only fully sequenced insect host is *B. mori* (Xia et al., 2004). Global gene expression profiles of *S. frugiperda* and *B. mori* derived cell lines have been recorded at various time-points, following baculovirus infection (Nobiron, 2003; Iwanaga et al., 2007; Sagisaka et al., 2010; Salem et al., 2011). Also, the temporal gene expression programs of the viral genes of several members of the Baculoviridae family (*Ac*MNPV, *Tn*SNPV, *Bm*NPV) have been elucidated during their respective infection cycles (Yamagishi et al., 2003; Iwanaga et al., 2004, 2007; van Munster et al., 2006). Even scarcer are large scale proteomic studies. Popham et al. (2010) performed a proteomic

analysis based on 2D-GE-MS/MS to examine the protein expression of permissive and non-permissive insect host cells (*H. zea* and *Heliothis virescens* derived cell lines, respectively) for *Ac*MNPV. The authors identified 18 differentially expressed proteins after 24 hpi in the permissive cell line, among which there were members of signal transduction pathways, protein function and homeostasis, and cell survival (Popham et al., 2010). Recently, Carinhas et al. (2011b) applied a SILAC approach for quantitative proteomics of *Sf*9 cells during growth and early baculovirus infection, contributing with the first comparative quantitative proteomic analysis of the response of *S. frugiperda* cells to infection. The lack of an annotated genome sequence was overcome by cross-referencing to a database that included sequences of proteins from *S. frugiperda* and related insect species. The authors found new differentially expressed proteins related to energy metabolism, endoplasmic reticulum and oxidative stress during *Ac*MNPV infection (Carinhas et al., 2011b). In particular, the up-regulation of two metabolic enzymes, PDH-E3 and ALDH, was observed, which account for an increased efficiency of the coupling of glycolysis and the TCA cycle and for the anaplerotic feeding of carboxylic acids, respectively. These observations go along with the increased metabolic fluxes of central carbon metabolism during baculovirus infection (Bernal et al., 2009), emphasizing the importance of energy metabolism during viral infection. Concerning the cellular stress response to infection, the authors observed a decrease in the levels of the chaperone ERp57 and the polypeptide transporter SRP57. Both proteins are effectors of the untranslated-protein response (UPR), and their down-regulation envisages the baculovirus capacity in avoiding the deleterious effects of cellular stress response.

Altogether, these results demonstrate that efficient replication of baculovirus depends on the capacity of viral manipulation of different cellular pathways, the control of which are needed for the success of viral infections.

Systems-level knowledge of baculovirus–host interactions requires an effort from the scientific community in the direction of insect cells/host genome sequencing. Recent efforts by Nguyen et al. (2012) succeeded in the transcriptome sequencing of *H. zea* cell line, providing a microarray platform to investigate baculovirus–insect cell interactions. Also, Xue et al. (2012) used next-generation sequencing to analyze differential gene expression following *Bm*NPV infection of *Bm*5 cell line. A gene enrichment analysis showed that gene sets enclosing cytoskeleton, transcription, translation, energy metabolism, iron metabolism, and ubiquitin-proteasome pathways are altered during the course of baculovirus infection. The information gathered during transcriptional analysis was then used to define the interactome network between *Bm*NPV and host proteins at a systems level, revealing direct interaction of viral proteins with cellular components, such as the proteasome, the cytoskeleton and the spliceosome (Xue et al., 2012).

CONCLUSION

Baculoviruses have developed several strategies to subvert the mechanisms of cellular defense against infection. In this fight, baculoviruses take control of cellular structures, such as the cytoskeleton, and trigger signaling responses leading to cell cycle arrest, induction of the DNA damage response, inhibition of apoptosis and intensification of energy metabolism. Although many of these responses are shared by different viruses, the specific characteristic features of the adaptations evolved by Baculoviruses have been highlighted in this review.

Although many studies concerning baculovirus molecular biology and the infection process have been pursued, there is a lack of a whole-system level integration of cross-platform reported data. Thus far, the application of high-throughput transcriptomic and proteomic approaches has been hampered by the current unavailability of lepidopteran genome sequences.

System-level proteomic studies can provide useful insights on the dynamic host response to infection. Indeed, the direct cross-talk between virus and host occurs mainly at the protein level. Viral proteins are major effectors on the subversion and manipulation of host cell physiology. Mapping such intricate network of interactions and, more importantly, deciphering their outcome at the cellular level, will provide a step-further in our current knowledge on the biological outcome of infection.

ACKNOWLEDGMENTS

This work was supported by the Portuguese *Fundação para a Ciência e Tecnologia* (FCT) through the Project PTDC/EBB-EBI/103359/2008 and by the European Comission FP7, Complex-INC Project. Francisca Monteiro acknowledges FCT for her PhD fellowship grant (SFRH/BD/7013/2010), Nuno Carinhas for his post-doctoral fellowship grant (SFRH/BPD/80514), and Vicente Bernal acknowledges a postdoctoral contract from Universidad de Murcia (Programa Propio).

REFERENCES

Aubert, M., and Blaho, J. A. (2001). Modulation of apoptosis during herpes simplex virus infection in human cells. *Microbes Infect.* 3, 859–866.

Avota, E., Gassert, E., and Schneider-Schaulies, S. (2011). Cytoskeletal dynamics: concepts in measles virus replication and immunomodulation. *Viruses* 3, 102–117.

Belyavskyi, M., Braunagel, S. C., and Summers, M. D. (1998). The structural protein ODV-EC27 of *Autographa californica* nucleopolyhedrovirus is a multifunctional viral cyclin. *Proc. Natl. Acad. Sci. U.S.A.* 95, 11205–11210.

Ben-Israel, H., and Kleinberger, T. (2002). Adenovirus and cell cycle control. *Front. Biosci.* 7, D1369–D1395.

Bernal, V., Carinhas, N., Yokomizo, A. Y., Carrondo, M. J. T., and Alves, P. M. (2009). Cell density effect in the baculovirus–insect cells system: a quantitative analysis of energetic metabolism. *Biotechnol. Bioeng.* 104, 162–180.

Bernal, V., Monteiro, F., Carinhas, N., Ambrósio, R., and Alves, P. M. (2010). An integrated analysis of enzyme activities, cofactor pools and metabolic fluxes in baculovirus-infected *Spodoptera frugiperda* Sf9 cells. *J. Biotechnol.* 150, 332–342.

Bertin, J., Mendrysa, S. M., LaCount, D. J., Gaur, S., Krebs, J. F., Armstrong, R. C., et al. (1996). Apoptotic suppression by baculovirus P35 involves cleavage by and inhibition of a virus-induced CED-3/ICE-like protease. *J. Virol.* 70, 6251–6259.

Bideshi, D. K., Anwar, A. T., and Federici, B. A. (1999). A baculovirus anti-apoptosis gene homolog of the *Trichoplusia ni* granulovirus. *Virus Genes* 19, 95–101.

Birnbaum, M. J., Clem, R. J., and Miller, L. K. (1994). An apoptosis-inhibiting gene from a nuclear polyhedrosis virus encoding a polypeptide with Cys/His sequence motifs. *J. Virol.* 68, 2521–2528.

Blissard, G. W., and Rohrmann, G. F. (1991). Baculovirus gp64 gene expression: analysis of sequences modulating early transcription and transactivation by IE1. *J. Virol.* 65, 5820–5827.

Blissard, G. W., and Wenz, J. R. (1992). Baculovirus gp64 envelope glycoprotein is sufficient to mediate pH-dependent membrane fusion. *J. Virol.* 66, 6829–6835.

Borden, K. L. (2000). RING domains: master builders of molecular scaffolds? *J. Mol. Biol.* 295, 1103–1112.

Braunagel, S. C., Guidry, P. A., Rosas-acosta, G., Engelking, L., and Summers, M. A. X. D. (2001). Identification of BV/ODV-C42, an *Autographa californica* nucleopolyhedrovirus orf101-encoded structural protein detected in infected-cell complexes with ODV-EC27 and p78/83. *J. Virol.* 75, 12331–12338.

Braunagel, S. C., Parr, R., Belyavskyi, M., and Summers, M. D. (1998). *Autographa californica* nucleopolyhedrovirus infection results in Sf9 cell cycle arrest at G2/M phase. *Virology* 244, 195–211.

Bump, N. J., Hackett, M., Hugunin, M., Seshagiri, S., Brady, K., Chen, P., et al. (1995). Inhibition of ICE family proteases by baculovirus antiapoptotic protein p35. *Science* 269, 1885–1888.

Cantó, C., Gerhart-Hines, Z., Feige, J. N., Lagouge, M., Noriega, L., Milne, J. C., et al. (2009). AMPK regulates energy expenditure by modulating NAD+ metabolism and SIRT1 activity. *Nature* 458, 1056–1060.

Carinhas, N., Bernal, V., Monteiro, F., Carrondo, M. J. T., Oliveira, R., and Alves, P. M. (2010). Improving baculovirus production at high cell density through manipulation of energy metabolism. *Metab. Eng.* 12, 39–52.

Carinhas, N., Bernal, V., Teixeira, A. P., Carrondo, M. J., Alves, P. M., and Oliveira, R. (2011a). Hybrid metabolic flux analysis: combining stoichiometric and statistical constraints to model the formation of complex recombinant products. *BMC Syst. Biol.* 5, 34. doi: 10.1186/1752-0509-5-34

Carinhas, N., Robitaille, A. M., Moes, S., Carrondo, M. J. T., Jenoe, P., Oliveira, R., et al. (2011b). Quantitative proteomics of *Spodoptera frugiperda* cells during growth and baculovirus infection. *PLoS ONE* 6, e26444. doi: 10.1371/journal.pone.0026444

Carpentier, D. C. J., Griffiths, C. M., and King, L. A. (2008). The baculovirus P10 protein of *Autographa californica* nucleopolyhedrovirus forms two distinct cytoskeletal-like structures and associates with polyhedral occlusion bodies during infection. *Virology* 371, 278–291.

Carstens, E. B., Tjia, S. T., and Doerfler, W. (1979). Infection of *Spodoptera frugiperda* cells with *Autographa californica* nuclear polyhedrosis virus I. Synthesis of intracellular proteins after virus infection. *Virology* 99, 386–398.

Charlton, C. A., and Volkman, L. E. (1993). Penetration of *Autographa californica* nuclear polyhedrosis virus nucleocapsids into IPLB Sf 21 cells induces actin cable formation. *Virology* 197, 245–254.

Charlton, C. A., and Volkman, L. E. (1991). Sequential rearrangement and nuclear polymerization of actin in baculovirus-infected *Spodoptera frugiperda* cells. *J. Virol.* 65, 1219–1227.

Chaurushiya, M. S., and Weitzman, M. D. (2010). Viral manipulation of DNA repair and cell cycle checkpoints. *DNA Repair* 8, 1166–1176.

Chen, A. Y., and Qiu, J. (2010). Parvovirus infection-induced cell death and cell cycle arrest. *Fut. Virol.* 5, 731–743.

Chen, H., Li, G., Huang, G., Chen, K., and Yao, Q. (2010). Characterization of ORF29 of *Bombyx mori* nucleopolyhedrovirus. *Acta Virol.* 275–280.

Clem, R. J. (2001). Baculoviruses and apoptosis: the good, the bad, and the ugly. *Cell Death Differ.* 8, 137–143.

Clem, R. J. (2005). The role of apoptosis in defense against baculovirus infection in insects. *Curr. Top. Microbiol. Immunol.* 289, 113–129.

Clem, R. J., Fechheimer, M., and Miller, L. K. (1991). Prevention of apoptosis by a baculovirus gene during infection of insect cells. *Science* 254, 1388–1390.

Clem, R. J., and Miller, L. K. (1994). Control of programmed cell death by the baculovirus genes p35 and iap. *Mol. Cell. Biol.* 14, 5212–5222.

Cooray, S. (2004). The pivotal role of phosphatidylinositol 3-kinase-Akt signal transduction in virus survival. *J. Gen. Virol.* 85, 1065–1076.

Crook, N. E., Clem, R. J., and Miller, L. K. (1993). An apoptosis-inhibiting baculovirus gene with a zinc finger-like motif. *J. Virol.* 67, 2168–2174.

Cudmore, S., Reckmann, I., and Way, M. (1997). Viral manipulations of the actin cytoskeleton. *Trends Microbiol.* 5, 142–148.

Davy, C., and Doorbar, J. (2007). G2/M cell cycle arrest in the life cycle of viruses. *Virology* 368, 219–226.

De, B. P., Lesoon, A., and Banerjee, a K. (1991). Human parainfluenza virus type 3 transcription *in vitro*: role of cellular actin in mRNA synthesis. *J. Virol.* 65, 3268–3275.

Deshaies, R. J., and Joazeiro, C. A. P. (2009). RING domain E3 ubiquitin ligases. *Annu. Rev. Biochem.* 78, 399–434.

Dowdy, S. F., Hinds, P. W., Louie, K., Reed, S. I., Arnold, A., and Weinberg, R. A. (1993). Physical interaction of the retinoblastoma protein with human D cyclins. *Cell* 73, 499–511.

Draetta, G., and Beach, D. (1989). The mammalian cdc2 protein kinase: mechanisms of regulation during the cell cycle. *J. Cell Sci. Suppl.* 12, 21–27.

Dreschers, S., Roncarati, R., and Knebel-mo, D. (2001). Actin rearrangement-inducing factor of baculoviruses is tyrosine phosphorylated and colocalizes to F-actin at the plasma membrane. *J. Virol.* 75, 3771–3778.

Du, Q., Lehavi, D., Faktor, O., Qi, Y., and Chejanovsky, N. (1999). Isolation of an apoptosis suppressor gene of the *Spodoptera littoralis* nucleopolyhedrovirus. *J. Virol.* 73, 1278–1285.

Du, X., and Thiem, S. M. (1997). Responses of insect cells to baculovirus infection: protein synthesis shutdown and apoptosis. *J. Virol.* 71, 7866–7872.

Esfandiarei, M., Luo, H., Yanagawa, B., Suarez, A., Dabiri, D., Zhang, J., and McManus, B. M. (2004). Protein kinase B/Akt regulates coxsackievirus B3 replication through a mechanism which is not caspase dependent. *J. Virol.* 78, 4289–4298.

Ewen, M. E., Sluss, H. K., Sherr, C. J., Matsushime, H., Kato, J., and Livingston, D. M. (1993). Functional interactions of the retinoblastoma protein with mammalian D-type cyclins. *Cell* 73, 487–497.

Fang, M., Dai, X., and Theilmann, D. A. (2007). *Autographa californica* multiple nucleopolyhedrovirus EXON0 (ORF141) is required for efficient egress of nucleocapsids from the nucleus. *J. Virol.* 81, 9859–9869.

Fang, M., Nie, Y., Harris, S., Erlandson, M. A., and Theilmann, D. A. (2009a). *Autographa californica* multiple nucleopolyhedrovirus core gene ac96 encodes a per Os infectivity factor (PIF-4). *J. Virol.* 83, 12569–12578.

Fang, M., Nie, Y., and Theilmann, D. A. (2009b). AcMNPV EXON0 (AC141) which is required for the efficient egress of budded virus nucleocapsids interacts with beta-tubulin. *Virology* 385, 496–504.

Fang, M., Nie, Y., Wang, Q., Deng, F., Wang, R., Wang, H., et al. (2006). Open reading frame 132 of *Helicoverpa armigera* nucleopolyhedrovirus encodes a functional per os infectivity factor (PIF-2). *J. Gen. Virol.* 87, 2563–2569.

Faulkner, P., Kuzio, J., Williams, G. V., and Wilson, J. A. (1997). Analysis of p74, a PDV envelope protein of *Autographa californica* nucleopolyhedrovirus required for occlusion body infectivity in vivo. *J. Gen. Virol.* 78(Pt 12), 3091–3100.

Fowler, V. M. (1990). Tropomodulin: a cytoskeletal protein that binds to the end of erythrocyte tropomyosin and inhibits tropomyosin binding to actin. *J. Cell Biol.* 111, 471–481.

Fujimoto, M., and Nakai, A. (2010). The heat shock factor family and adaptation to proteotoxic stress. *FEBS J.* 277, 4112–4125.

Furler, R. L., and Uittenbogaart, C. H. (2010). Signaling through the P38 and ERK pathways: a common link between HIV replication and the immune response. *Immunol. Res.* 48, 99–109.

Gandhi, K. M., Ohkawa, T., Welch, M. D., and Volkman, L. E. (2012). The nuclear localization of actin requires AC102 in *Autographa californica* M nucleopolyhedrovirus-infected cells. *J. Gen. Virol.* 93(Pt 8), 1795–803.

Gao, X., Wang, H., and Sairenji, T. (2004). Inhibition of Epstein-Barr virus (EBV) reactivation by short interfering RNAs targeting p38 mitogen-activated protein kinase or c-myc in EBV-positive epithelial cells. *J. Virol.* 78, 11798–11806.

Ge, J., Wei, Z., Huang, Y., Yin, J., Zhou, Z., and Zhong, J. (2007). AcMNPV ORF38 protein has the activity of ADP-ribose pyrophosphatase and is important for virus replication. *Virology* 361, 204–211.

Gidalevitz, T., Prahlad, V., and Morimoto, R. I. (2011). The stress of protein misfolding: from single cells to multicellular organisms. *Cold Spring Harb. Perspect. Biol.* 3, a009704.

Goley, E. D., Ohkawa, T., Mancuso, J., Woodruff, J. B., D'Alessio, J. A., Cande, W. Z., et al. (2006a). Dynamic nuclear actin assembly by Arp2/3 complex and a baculovirus WASP-like protein. *Science* 314, 464–467.

Goley, E. D., Ohkawa, T., Mancuso, J., Woodruff, J. B., D'Alessio, J. A., Cande, W. Z., et al. (2006b). Dynamic nuclear actin assembly by Arp2/3 complex and a baculovirus WASP-like protein. *Science* 314, 464–467.

Green, M. C., Monser, K. P., and Clem, R. J. (2004). Ubiquitin protein ligase activity of the anti-apoptotic baculovirus protein Op-IAP3. *Virus Res.* 105, 89–96.

Groschel, B., and Bushman, F. (2005). Cell cycle arrest in G2/M promotes early steps of infection by human immunodeficiency virus. *J. Virol.* 79, 5695–5704.

Grula, M. A., Buller, P. L., and Weaver, R. F. (1981). α-Amanitin-resistant viral RNA synthesis in nuclei isolated from

nuclear polyhedrosis virus-infected *Heliothis zea* larvae and *Spodoptera frugiperda* cells. *J. Virol.* 38, 916–921.

Guy, M. P., and Friesen, P. D. (2008). Reactive-site cleavage residues confer target specificity to baculovirus P49, a dimeric member of the P35 family of caspase inhibitors. *J. Virol.* 82, 7504–7514.

Gyrd-Hansen, M., and Meier, P. (2010). IAPs: from caspase inhibitors to modulators of NF-kappaB, inflammation and cancer. *Nat. Rev. Cancer* 10, 561–574.

Haas, A. L., Katzung, D. J., Reback, P. M., and Guarino, L. A. (1996). Functional characterization of the ubiquitin variant encoded by the baculovirus *Autographa californica*. *Biochemistry* 35, 5385–5394.

Harrison, R. L., Sparks, W. O., and Bonning, B. C. (2010). *Autographa californica* multiple nucleopolyhedrovirus ODV-E56 envelope protein is required for oral infectivity and can be substituted functionally by *Rachiplusia ou* multiple nucleopolyhedrovirus ODV-E56. *J. Gen. Virol.* 91, 1173–1182.

Hinds, M. G., Norton, R. S., Vaux, D. L., and Day, C. L. (1999). Solution structure of a baculoviral inhibitor of apoptosis (IAP) repeat. *Nat. Struct. Biol.* 6, 648–651.

Holloszy, J. O., Oscai, L. B., Don, I. J., and Molé, P. A. (1970). Mitochondrial citric acid cycle and related enzymes: adaptive response to exercise. *Biochem. Biophys. Res. Commun.* 40, 1368–1373.

Horton, H. M., and Burand, J. P. (1993). Saturable attachment sites for polyhedron-derived baculovirus on insect cells and evidence for entry via direct membrane fusion. *J. Virol.* 67, 1860–1868.

Huang, N., Wu, W., Yang, K., Passarelli, A. L., Rohrmann, G. F., and Clem, R. J. (2011). Baculovirus infection induces a DNA damage response that is required for efficient viral replication. *J. Virol.* 85, 12547–12556.

Ikeda, M., and Kobayashi, M. (1999). Cell-cycle perturbation in Sf9 cells infected with *Autographa californica* nucleopolyhedrovirus. *Virology* 258, 176–188.

Ikonomou, L., Schneider, Y.-J., and Agathos, S. N. (2003). Insect cell culture for industrial production of recombinant proteins. *Appl. Microbiol. Biotechnol.* 62, 1–20.

Imai, N., Matsuda, N., Tanaka, K., Nakano, A., Matsumoto, S., and Kang, W. (2003). Ubiquitin ligase activities of *Bombyx mori* nucleopolyhedrovirus RING finger proteins. *J. Virol.* 77, 923–930.

Iwanaga, M., Shimada, T., Kobayashi, M., and Kang, W. (2007). Identification of differentially expressed host genes in *Bombyx mori* nucleopolyhedrovirus infected cells by using subtractive hybridization. *Appl. Entomol. Zool.* 42, 151–159.

Iwanaga, M., Takaya, K., Katsuma, S., Ote, M., Tanaka, S., Kamita, S. G., et al. (2004). Expression profiling of baculovirus genes in permissive and nonpermissive cell lines. *Biochem. Biophys. Res. Commun.* 323, 599–614.

Ji, W.-T., and Liu, H. J. (2008). PI3K-Akt signaling and viral infection. *Recent Pat. Biotechnol.* 2, 218–226.

Johnson, G. L., and Lapadat, R. (2002). Mitogen-activated protein kinase pathways mediated by ERK, JNK, and p38 protein kinases. *Science* 298, 1911–1912.

Johnson, R. A., Wang, X., Ma, X. L., Huong, S. M., and Huang, E. S. (2001). Human cytomegalovirus upregulates the phosphatidylinositol 3-kinase (PI3-K) pathway: inhibition of PI3-K activity inhibits viral replication and virus-induced signaling. *J. Virol.* 75, 6022–6032.

Kamen, A. A., Bédard, C., Tom, R., Perret, S., and Jardin, B. (1996). On-line monitoring of respiration in recombinant-baculovirus infected and uninfected insect cell bioreactor cultures. *Biotechnol. Bioeng.* 50, 36–48.

Kamita, S., and Majima, K. (1993). Identification and characterization of the p35 gene of *Bombyx mori* nuclear polyhedrosis virus that prevents virus-induced apoptosis. *J. Virol.* 67, 455–463.

Kasman, L. M., and Volkman, L. E. (2000). Filamentous actin is required for lepidopteran nucleopolyhedrovirus progeny production. *J. Gen. Virol.* 81, 1881–1888.

Katsuma, S., Kawaoka, S., Mita, K., and Shimada, T. (2008). Genome-wide survey for baculoviral host homologs using the *Bombyx* genome sequence. *Insect Biochem. Mol. Biol.* 38, 1080–1086.

Katsuma, S., Mita, K., and Shimada, T. (2007). ERK- and JNK-dependent signaling pathways contribute to *Bombyx mori* nucleopolyhedrovirus infection. *J. Virol.* 81, 13700–13709.

Katsuma, S., Tsuchida, A., Matsuda-Imai, N., Kang, W., and Shimada, T. (2011). Role of the ubiquitin-proteasome system in *Bombyx mori* nucleopolyhedrovirus infection. *J. Gen. Virol.* 92, 699–705.

Keddie, B., Aponte, G., and Volkman, L. (1989). The pathway of infection of *Autographa californica* nuclear polyhedrosis virus in an insect host. *Science* 243, 1728–1730.

Kerr, J. F., Wyllie, A. H., and Currie, A. R. (1972). Apoptosis: a basic biological phenomenon with wide-ranging implications in tissue kinetics. *Br. J. Cancer* 26, 239–257.

Kikhno, I., Gutiérrez, S., Croizier, L., Croizier, G., and Ferber, M. L. (2002). Characterization of pif, a gene required for the *per os* infectivity of *Spodoptera littoralis* nucleopolyhedrovirus. *J. Gen. Virol.* 83, 3013–3022.

Kimberly, L., Schultz, W., and Friesen, P. D. (2009). Baculovirus DNA replication-specific expression factors trigger apoptosis and shutoff of host protein synthesis during infection. *J. Virol.* 83, 11123–11132.

Koyama, A. H., Fukumori, T., Fujita, M., Irie, H., and Adachi, A. (2000). Physiological significance of apoptosis in animal virus infection. *Microbes Infect.* 2, 1111–1117.

LaCount, D. J., and Friesen, P. D. (1997). Role of early and late replication events in induction of apoptosis by baculoviruses. *J. Virol.* 71, 1530–1537.

Lau, A., Swinbank, K. M., Ahmed, P. S., Taylor, D. L., Jackson, S. P., Smith, G. C. M., et al. (2005). Suppression of HIV-1 infection by a small molecule inhibitor of the ATM kinase. *Nat. Cell Biol.* 7, 493–500.

Lehman, J. M., Laffin, J., and Friedrich, T. D. (1994). DNA content distribution of mouse cells following infection with polyoma virus. *Cytometry* 16, 138–143.

Lehman, J. M., Laffin, J., and Friedrich, T. D. (2000). Simian virus 40 induces multiple S phases with the majority of viral DNA replication in the G2 and second S phase in CV-1 cells. *Exp. Cell Res.* 258, 215–222.

Li, K., Wang, Y., Bai, H., Wang, Q., Song, J., Zhou, Y., et al. (2010). The putative pocket protein binding site of *Autographa californica* nucleopolyhedrovirus BV/ODV-C42 is required for virus-induced nuclear actin polymerization. *J. Virol.* 84, 7857–7868.

Li, L., Gu, B., Zhou, F., Chi, J., Wang, F., Liu, G., et al. (2012). Human herpesvirus 6A infects human embryonic fibroblasts and induces G2/M arrest and cell death. *J. Med. Virol.* 84, 657–663.

Lilley, C. E., Carson, C. T., Muotri, A. R., Gage, F. H., and Weitzman, M. D. (2005). DNA repair proteins affect the lifecycle of herpes simplex virus 1. *Proc. Natl. Acad. Sci. U.S.A.* 102, 5844–5849.

Liu, X., Chen, K., Cai, K., and Yao, Q. (2008). Determination of protein composition and host-derived proteins of *Bombyx mori* nucleopolyhedrovirus by 2-dimensional electrophoresis and mass spectrometry. *Intervirology* 51, 369–376.

Long, G., Pan, X., Kormelink, R., and Vlak, J. M. (2006). Functional entry of baculovirus into insect and mammalian cells is dependent on clathrin-mediated endocytosis. *J. Virol.* 80, 8830–8833.

Lu, A., and Carstens, E. B. (1993). Immediate-early baculovirus genes transactivate the p143 gene promoter of *Autographa californica* nuclear polyhedrosis virus. *Virology* 195, 710–718.

Lu, S., Ge, G., and Qi, Y. (2004). Ha-VP39 binding to actin and the influence of F-actin on assembly of progeny virions. *Arch. Virol.* 149, 2187–2198.

Luo, H., Yanagawa, B., Zhang, J., Luo, Z., Zhang, M., Esfandiarei, M., et al. (2002). Coxsackievirus B3 replication is reduced by inhibition of the extracellular signal-regulated kinase (ERK) signaling pathway. *J. Virol.* 76, 3365–3373.

Lyupina, Y. V., Dmitrieva, S. B., Timokhova, A. V., Beljelarskaya, S. N., Zatsepina, O. G., Evgen'ev, M. B., et al. (2010). An important role of the heat shock response in infected cells for replication of baculoviruses. *Virology* 406, 336–341.

Lyupina, Y. V., Zatsepina, O. G., Timokhova, A. V., Orlova, O. V., Kostyuchenko, M. V., Beljelarskaya, S. N., et al. (2011). New insights into the induction of the heat shock proteins in baculovirus infected insect cells. *Virology* 421, 34–41.

Ma, Y.-B., and Chang, H.-Y. (2011). Caspase work model during pathogen infection. *Virol. Sin.* 26, 366–375.

Machesky, L. M., Insall, R. H., and Volkman L. E. (2001). WASP homology sequences in baculoviruses. *Trends Cell Biol.* 11, 286–287.

de Magalhães, J. C., Andrade, A. A., Silva, P. N., Sousa, L. P., Ropert, C., Ferreira, P. C., et al. (2001). A mitogenic signal triggered at an early stage of vaccinia virus infection: implication of MEK/ERK and protein kinase A in virus multiplication. *J. Biol. Chem.* 276, 38353–38360.

Maguire, T., Harrison, P., Hyink, O., Kalmakoff, J., and Ward, V. K. (2000). The inhibitors of apoptosis of *Epiphyas postvittana* nucleopolyhedrovirus. *J. Gen. Virol.* 81, 2803–2811.

Manji, G. A., Hozak, R. R., LaCount, D. J., and Friesen, P. D. (1997). Baculovirus inhibitor of apoptosis functions at or upstream of the

apoptotic suppressor P35 to prevent programmed cell death. *J. Virol.* 71, 4509–4516.

Marek, M., Merten, O.-W., Francis-Devaraj, F., and Oers, M. M. V. (2012). Essential C-terminal region of the baculovirus minor capsid protein VP80 binds DNA. *J. Virol.* 86, 1728–1738.

Mayer, M. P. (2005). Recruitment of Hsp70 chaperones: a crucial part of viral survival strategies. *Rev. Physiol. Biochem. Pharmacol.* 153, 1–46.

Maynard, N. D., Gutschow, M. V., Birch, E. W., and Covert, M. W. (2010). The virus as metabolic engineer. *Biotechnol. J.* 5, 686–694.

Merrington, C. L., Bailey, M. J., and Possee, R. D. (1997). Manipulation of baculovirus vectors. *Mol. Biotechnol.* 8, 283–297.

Milks, M. L., Washburn, J. O., Willis, L. G., Volkman, L. E., and Theilmann, D. A. (2003). Deletion of pe38 attenuates AcMNPV genome replication, budded virus production, and virulence in *Heliothis virescens*. *Virology* 310, 224–234.

Miller, L. K (ed.). (1997). *The Baculoviruses*. New York: Springer.

Miller, L. K. (1999). An exegesis of IAPs: salvation and surprises from BIR motifs. *Trends Cell Biol.* 9, 323–328.

Morgan, D. O. (1995). Principles of CDK regulation. *Nature* 374, 131–134.

Munger, J., Bajad, S. U., Coller, H. a, Shenk, T., and Rabinowitz, J. D. (2006). Dynamics of the cellular metabolome during human cytomegalovirus infection. *PLoS Pathog.* 2, e132. doi: 10.1371/journal.ppat.0020132

Munger, J., Bennett, B. D., Parikh, A., Feng, X.-J., Rabitz, H. A., Shenk, T., et al. (2010). Systems-level metabolic flux profiling identifies fatty acid synthesis as a target for antiviral therapy. *Nat. Biotechnol.* 26, 1179–1186.

van Munster, M., Willis, L. G., Elias, M., Erlandson, M. A., Brousseau, R., Theilmann, D. A., et al. (2006). Analysis of the temporal expression of *Trichoplusia ni* single nucleopolyhedrovirus genes following transfection of BT1-Tn-5B1-4 cells. *Virology* 354, 154–166.

Nagy, P. D., Wang, R. Y., Pogany, J., Hafren, A., and Makinen, K. (2011). Emerging picture of host chaperone and cyclophilin roles in RNA virus replication. *Virology* 411, 374–382.

Nguyen, Q., Palfreyman, R. W., Chan, L. C. L., Reid, S., and Nielsen, L. K. (2012). Transcriptome sequencing of and microarray development for a *Helicoverpa zea* cell line to investigate *in vitro* insect cell-baculovirus interactions. *PLoS ONE* 7, e36324. doi: 10.1371/journal.pone.0036324

Nobiron, I. (2003). *Autographa californica* nucleopolyhedrovirus infection of *Spodoptera frugiperda* cells: a global analysis of host gene regulation during infection, using a differential display approach. *J. Gen. Virol.* 84, 3029–3039.

Nurse, P. (1994). Ordering S phase and M phase in the cell cycle. *Cell* 79, 547–550.

van Oers, M. M. (2011). Opportunities and challenges for the baculovirus expression system. *J. Invertebr. Pathol.* 107(Suppl.) S3–S15.

Ohkawa, T., Rowe, A. R., and Volkman, L. E. (2002). Identification of six *Autographa californica* multicapsid nucleopolyhedrovirus early genes that mediate nuclear localization of G-actin. *J. Virol.* 76, 12281–12289.

Ohkawa, T., and Volkman, L. E. (1999). Nuclear F-actin is required for AcMNPV nucleocapsid morphogenesis. *Virology* 264, 1–4.

Ohkawa, T., Volkman, L. E., and Welch, M. D. (2010). Actin-based motility drives baculovirus transit to the nucleus and cell surface. *J. Cell Biol.* 190, 187–195.

Ohkawa, T., Washburn, J. O., Sitapara, R., Sid, E., and Volkman, L. E. (2005). Specific binding of *Autographa californica* M nucleopolyhedrovirus occlusion-derived virus to midgut cells of *Heliothis virescens* larvae is mediated by products of pif genes Ac119 and Ac022 but not by Ac115. *J. Virol.* 79, 15258–15264.

Op De Beeck, A., and Caillet-Fauquet, P. (1997). Viruses and the cell cycle. *Prog. Cell Cycle Res.* 3, 1–19.

Palomares, L. A., López, S., and Ramírez, O. T. (2004). Utilization of oxygen uptake rate to assess the role of glucose and glutamine in the metabolism of infected insect cell cultures. *Biochem. Eng. J.* 19, 87–93.

Passarelli, A. L., and Guarino, L. A. (2007). Baculovirus late and very late gene regulation. *Curr. Drug Targets* 8, 1103–1115.

Passarelli, A. L., and Miller, L. K. (1993). Three baculovirus genes involved in late and very late gene expression: ie-1, ie-n, and lef-2. *J. Virol.* 67, 2149–2158.

Passarelli, A. L. (2012). Barriers to success: how baculoviruses establish efficient systemic infections. *Virology* 411, 383–392.

Pei, Z., Reske, G., Huang, Q., Hammock, B. D., Qi, Y., and Chejanovsky, N. (2002). Characterization of the apoptosis suppressor protein P49 from the *Spodoptera littoralis* nucleopolyhedrovirus. *J. Biol. Chem.* 277, 48677–48684.

Pijlman, G. P., Pruijssers, A. J., and Vlak, J. M. (2003). Identification of pif-2, a third conserved baculovirus gene required for *per os* infection of insects. *J. Gen. Virol.* 84, 2041–2049.

Polyak, K., Kato, J. Y., Solomon, M. J., Sherr, C. J., Massague, J., Roberts, J. M., et al. (1994). p27Kip1, a cyclin-Cdk inhibitor, links transforming growth factor-beta and contact inhibition to cell cycle arrest. *Genes Dev.* 8, 9–22.

Popham, H. J. R., Grasela, J. J., Goodman, C. L., and McIntosh, A. H. (2010). Baculovirus infection influences host protein expression in two established insect cell lines. *J. Insect Physiol.* 56, 1237–1245.

Possee, R. D. (1993). Baculovirus expression vectors – a laboratory manual. *Trends Biotechnol.* 11, 267–268.

Qin, D., Feng, N., Fan, W., Ma, X., Yan, Q., Lv, Z., et al. (2011). Activation of PI3K/AKT and ERK MAPK signal pathways is required for the induction of lytic cycle replication of Kaposi's sarcoma-associated herpesvirus by herpes simplex virus type 1. *BMC Microbiol.* 11, 240. doi: 10.1186/1471-2180-11-240

Reilly, L. M., and Guarino, L. A. (1994). The pk-1 gene of *Autographa californica* multinucleocapsid nuclear polyhedrosis virus encodes a protein kinase. *J. Gen. Virol.* 75 (Pt 11), 2999–3006.

Reilly, L. M., and Guarino, L. A. (1996). The viral ubiquitin gene of *Autographa californica* nuclear polyhedrosis virus is not essential for viral replication. *Virology* 218, 243–247.

Roberts, K. L., and Baines, J. D. (2011). Actin in herpesvirus infection. *Viruses* 3, 336–346.

Rohrmann, G. F. (2011). "The AcMNPV genome: gene content, conservation, and function," in *Baculovirus Molecular Biology*, 2nd Edn, ed. G. F. Rohrmann (Bethesda, MD: National Center for Biotechnology Information), 2–23.

Roncarati, R., and Knebel-Mörsdorf, D. (1997). Identification of the early actin-rearrangement-inducing factor gene, arif-1, from *Autographa californica* multicapsid nuclear polyhedrosis virus. *J. Virol.* 71, 7933–7941.

Sagisaka, A., Fujita, K., Nakamura, Y., Ishibashi, J., Noda, H., Imanishi, S., et al. (2010). Genome-wide analysis of host gene expression in the silkworm cells infected with *Bombyx mori* nucleopolyhedrovirus. *Virus Res.* 147, 166–175.

Sakai, K., Barnitz, R. A., Chaigne-Delalande, B., Bidère, N., and Lenardo, M. J. (2011). Human immunodeficiency virus type 1 Vif causes dysfunction of Cdk1 and CyclinB1: implications for cell cycle arrest. *Virol. J.* 8, 219.

Salem, T. Z., Zhang, F., Xie, Y., and Thiem, S. M. (2011). Comprehensive analysis of host gene expression in *Autographa californica* nucleopolyhedrovirus-infected *Spodoptera frugiperda* cells. *Virology* 412, 167–178.

Salvesen, G. S., and Duckett, C. S. (2002). IAP proteins: blocking the road to death's door. *Nat Rev. Mol. Cell Biol.* 3, 401–410.

Seshagiri, S., and Miller, L. K. (1997). Baculovirus inhibitors of apoptosis (IAPs) block activation of Sf-caspase-1. *Proc. Natl. Acad. Sci. U.S.A.* 94, 13606–13611.

Seviour, E. G., and Lin, S. -Y. (2010). The DNA damage response: balancing the scale between cancer and ageing. *Aging* 2, 900–907.

Shen, H., and Chen, K. (2012). BM61 of *Bombyx mori* nucleopolyhedrovirus: its involvement in the egress of nucleocapsids from the nucleus. *FEBS Lett.* 586, 990–995.

Shin, Y.-K., Liu, Q., Tikoo, S. K., Babiuk, L. A., and Zhou, Y. (2007). Effect of the phosphatidylinositol 3-kinase/Akt pathway on influenza A virus propagation. *J. Gen. Virol.* 88, 942–950.

Sparks, W. O., Harrison, R. L., and Bonning, B. C. (2011). *Autographa californica* multiple nucleopolyhedrovirus ODV-E56 is a *per os* infectivity factor, but is not essential for binding and fusion of occlusion-derived virus to the host midgut. *Virology* 409, 69–76.

Spink, K. M., and Fluck, M. M. (2003). Polyomavirus hr-t mutant-specific induction of a G2/M cell-cycle arrest that is not overcome by the expression of middle T and/or small T. *Virology* 307, 191–203.

Stillman, B. (1996). Cell cycle control of DNA replication. *Science* 274, 1659–1664.

Stolp, B., and Fackler, O. T. (2011). How HIV takes advantage of the cytoskeleton in entry and replication. *Viruses* 3, 293–311.

Strauss, E. J. (1996). Intracellular pathogens: a virus joins the movement. *Curr. Biol.* 6, 504–507.

Summers, M. D., and Arnott, H. J. (1969). Ultrastructural studies on inclusion formation and virus occlusion in nuclear polyhedrosis and granulosis virus-infected cells of *Trichoplusia ni* (Hübner). *J. Ultrastruct. Res.* 28, 462–480.

Terry, L. J., Vastag, L., Rabinowitz, J. D., and Shenk, T. (2012). Human kinome profiling identifies a requirement for AMP-activated protein kinase during human cytomegalovirus infection. *Proc. Natl. Acad. Sci. U.S.A.* 109, 3071–3076.

Tong, L., and Denu, J. M. (2010). Function and metabolism of sirtuin metabolite *O*-acetyl-ADP-ribose. *Biochim. Biophys. Acta* 1804, 1617–1625.

Tyers, M., and Willems, A. R. (1999). One ring to rule a superfamily of E3 ubiquitin ligases. *Science* 284, 601, 603–604.

Volkman, L. E. (1988). *Autographa californica* MNPV nucleocapsid assembly: inhibition by cytochalasin D. *Virology* 163, 547–553.

Volkman, L. E. (1997). Nucleopolyhedrovirus interactions with their insect hosts. *Adv. Virus Res.* 48, 313–348.

Vucic, D., Kaiser, W. J., Harvey, A. J., and Miller, L. K. (1997). Inhibition of reaper-induced apoptosis by interaction with inhibitor of apoptosis proteins (IAPs). *Proc. Natl. Acad. Sci. U.S.A.* 94, 10183–10188.

Vucic, D., Kaiser, W. J., and Miller, L. K. (1998a). A mutational analysis of the baculovirus inhibitor of apoptosis Op-IAP. *J. Biol. Chem.* 273, 33915–33921.

Vucic, D., Kaiser, W. J., and Miller, L. K. (1998b). Inhibitor of apoptosis proteins physically interact with and block apoptosis induced by *Drosophila* proteins HID and GRIM. *Mol. Cell. Biol.* 18, 3300–3309.

Wang, P., and Granados, R. R. (1997). An intestinal mucin is the target substrate for a baculovirus enhancin. *Proc. Natl. Acad. Sci. U.S.A.* 94, 6977–6982.

Wang, Y., Wang, Q., Liang, C., Song, J., Li, N., Shi, H., et al. (2008). *Autographa californica* multiple nucleopolyhedrovirus nucleocapsid protein BV/ODV-C42 mediates the nuclear entry of P78/83. *J. Virol.* 82, 4554–4561.

Washburn, J. O., Chan, E. Y., Volkman, L. E., Jared, J., Jarvis, D. L., and Aumiller, J. J. (2003). Early synthesis of budded virus envelope fusion protein GP64 enhances *Autographa californica* multicapsid nucleopolyhedrovirus virulence in orally infected *Heliothis virescens. J. Virol.* 77, 280–290.

Welch, M. D., and Mullins, R. D. (2002). Cellular control of actin nucleation. *Annu. Rev. Cell Dev. Biol.* 18, 247–288.

Willems, L., Tamburini, J., Chapuis, N., Lacombe, C., Mayeux, P., and Bouscary, D. (2012). PI3K and mTOR signaling pathways in cancer: new data on targeted therapies. *Curr. Oncol. Rep.* 14, 129–138.

Wright, C. W., and Clem, R. J. (2002). Sequence requirements for Hid binding and apoptosis regulation in the baculovirus inhibitor of apoptosis Op-IAP. Hid binds Op-IAP in a manner similar to Smac binding of XIAP. *J. Biol. Chem.* 277, 2454–2462.

Xia, Q., Zhou, Z., Lu, C., Cheng, D., Dai, F., Li, B., et al. (2004). A draft sequence for the genome of the domesticated silkworm (*Bombyx mori*). *Science* 306, 1937–1940.

Xiao, A., Wong, J., and Luo, H. (2010). Viral interaction with molecular chaperones: role in regulating viral infection. *Arch. Virol.* 155, 1021–1031.

Xiao, W., Yang, Y., Weng, Q., Lin, T., Yuan, M., Yang, K., et al. (2009). The role of the PI3K-Akt signal transduction pathway in *Autographa californica* multiple nucleopolyhedrovirus infection of *Spodoptera frugiperda* cells. *Virology* 391, 83–89.

Xu, G., Cirilli, M., Huang, Y., Rich, R. L., Myszka, D. G., and Wu, H. (2001). Covalent inhibition revealed by the crystal structure of the caspase-8/p35 complex. *Nature* 410, 494–497.

Xu, H., Yao, L., Lu, S., and Qi, Y. (2007). Host filamentous actin is associated with *Heliothis armigera* single nucleopolyhedrosis virus (*Ha*SNPV) nucleocapsid transport to the host nucleus. *Curr. Microbiol.* 54, 199–206.

Xue, J., Qiao, N., Zhang, W., Cheng, R.-L., Zhang, X.-Q., Bao, Y.-Y., et al. (2012). Dynamic interactions between *Bombyx mori* nucleopolyhedrovirus and its host cells revealed by transcriptome analysis. *J. Virol.* 86, 7345–7359.

Yamagishi, J., Isobe, R., Takebuchi, T., and Bando, H. (2003). DNA microarrays of baculovirus genomes: differential expression of viral genes in two susceptible insect cell lines. *Arch. Virol.* 148, 587–597.

Yang, Y., Fang, S., Jensen, J. P., Weissman, A. M., and Ashwell, J. D. (2000). Ubiquitin protein ligase activity of IAPs and their degradation in proteasomes in response to apoptotic stimuli. *Science* 288, 874–877.

Yuan, M., Huang, Z., Wei, D., Hu, Z., Yang, K., and Pang, Y. (2011). Identification of *Autographa californica* nucleopolyhedrovirus ac93 as a core gene and its requirement for intranuclear microvesicle formation and nuclear egress of nucleocapsids. *J. Virol.* 85, 11664–11674.

Zhao, X., Madden-fuentes, R. J., Lou, B. X., Pipas, J. M., Gerhardt, J., Rigell, C. J., et al. (2008). Ataxia telangiectasia-mutated damage-signaling kinase- and proteasome-dependent destruction of Mre11-Rad50-Nbs1 subunits in Simian virus 40-infected primate cells. *J. Virol.* 82, 5316–5328.

Zheng, Y., Li, J., Johnson, D. L., and Ou, J.-H. (2003). Regulation of hepatitis B virus replication by the ras-mitogen-activated protein kinase signaling pathway. *J. Virol.* 77, 7707–7712.

Zoog, S. J., Schiller, J. J., Wetter, J. A., Chejanovsky, N., and Friesen, P. D. (2002). Baculovirus apoptotic suppressor P49 is a substrate inhibitor of initiator caspases resistant to P35 *in vivo. EMBO J.* 21, 5130–5140.

Conflict of Interest Statement: The authors declare that the research was conducted in the absence of any commercial or financial relationships that could be construed as a potential conflict of interest.

Received: 06 July 2012; accepted: 23 October 2012; published online: 09 November 2012.

Citation: Monteiro F, Carinhas N, Carrondo MJT, Bernal V and Alves PM (2012) Toward system-level understanding of baculovirus–host cell interactions: from molecular fundamental studies to large-scale proteomics approaches. Front. Microbio. ***3****:391. doi: 10.3389/fmicb.2012.00391*

This article was submitted to Frontiers in Virology, a specialty of Frontiers in Microbiology.

frontiers in
MICROBIOLOGY

REVIEW ARTICLE
published: 16 November 2012
doi: 10.3389/fmicb.2012.00393

Current approaches on viral infection: proteomics and functional validations

***Jie Zheng*[1], *Boon Huan Tan*[2], *Richard Sugrue*[3] *and Kai Tang*[1]*

[1] Division of Chemical Biology and Biotechnology, School of Biological Sciences, Nanyang Technological University, Singapore
[2] Defence Medical and Environmental Research Institute, DSO National Laboratories, Singapore
[3] Division of Molecular and Cell Biology, School of Biological Science, Nanyang Technological University, Singapore

Edited by:
Kevin Coombs, University of Manitoba, Canada

Reviewed by:
Dale L. Barnard, Utah State University, USA
Aaron T. Irving, Monash Institute of Medical Research, Australia

***Correspondence:**
Kai Tang, Division of Chemical Biology and Biotechnology, School of Biological Sciences, Nanyang Technological University, 60 Nanyang Drive, 637551, Singapore.
e-mail: tkai@ntu.edu.sg

Viruses could manipulate cellular machinery to ensure their continuous survival and thus become parasites of living organisms. Delineation of sophisticated host responses upon virus infection is a challenging task. It lies in identifying the repertoire of host factors actively involved in the viral infectious cycle and characterizing host responses qualitatively and quantitatively during viral pathogenesis. Mass spectrometry based proteomics could be used to efficiently study pathogen-host interactions and virus-hijacked cellular signaling pathways. Moreover, direct host and viral responses upon infection could be further investigated by activity-based functional validation studies. These approaches involve drug inhibition of secretory pathway, immunofluorescence staining, dominant negative mutant of protein target, real-time PCR, small interfering siRNA-mediated knockdown, and molecular cloning studies. In this way, functional validation could gain novel insights into the high-content proteomic dataset in an unbiased and comprehensive way.

Keywords: virus infection, host responses, virus-host interactions, activity-based functional validations, mass spectrometry based proteomics

INTRODUCTION

Invasive viruses are adaptively infectious and pathogenic. Although host cells evolve and occupy a network of multiple defensive measures, microbial pathogens could in turn manipulate cellular machinery to counteract those immune defenses in order to evade or neutralize them (Finlay and McFadden, 2006). This might be in part attributed to the fact that viruses evolve and mutate much more quickly than their hosts, and result in emerging mutants with enhanced viral attacks. For instance, viral genomes of RNA viruses, e.g., influenza A virus, intrinsically exhibit hypervariations and continued mutations due to a lack of proofreading RNA dependent RNA polymerases (Holland et al., 1982). This may also be derived from the diversity of virus families and a vast number of formidable viruses threatening mankind; for examples, the representatives are human immunodeficiency virus, influenza virus, respiratory syncytial virus (RSV), severe acute respiratory syndrome (SARS), dengue virus, and so on. Epidemic or even pandemic diseases occurred in recent years upon breakout of those infectious viruses.

In recent decades, the field of virology is rapidly expanding with the advances of high throughput genome sequencing and proteome screening technologies. To date, the numbers of complete viral genomes and proteomes that cover 118 taxonomy groups have reached to 2853 and 1932 in the NCBI and Uniprot databases, respectively[1,2]. As these databases expand, the daunting challenge still lies in illustrative delineation of sophisticated pathogen-host interactions or virus-hijacked signaling pathways. Advancements in mass spectrometry (MS) based proteomics have tremendously facilitated the investigations of viral proteomes as well as host responses associated with viral infections. Several popular MS based approaches have been applied to study viruses and their hosts (**Table 1**). These include 2D gel, tandem affinity purification (TAP), co-immunoprecipitation (Co-IP), and quantitative stable isotope labeling strategies, such as isotope coded affinity tag (ICAT), isobaric tag for relative and absolute quantitation (iTRAQ), and stable isotope labeling of amino acids in cell culture (SILAC). Others developed novel approaches such as HLA peptidome scanning chips to study host responses upon virus infection (Zheng et al., 2011). These MS based proteomic approaches are capable to explore from individual binding partners to quantitatively altered proteomes upon virus infections. Moreover, two other MS based approaches developed to study protein–protein interactions (PPIs) and protein conformational changes have also contributed to virology studies. These are chemical cross-linking and hydrogen/deuterium exchange (HDX) based MS methodologies.

CROSS-LINKING BASED MS METHODOLOGY

Formaldehyde cross-linking could be applied to study the binding between nucleotides, e.g., DNA and RNA, and proteins (Petrotchenko and Borchers, 2010). Formaldehyde is a reactive cross-linking agent that could bind nucleic acids, peptides, or proteins. Its carbon atom center is nucleophilic to bind cytosine and it could also react with side chains of lysine, arginine, histidine, and cysteine to form methylol groups, schiff-bases, or methylene

[1]http://www.ncbi.nlm.nih.gov/genomes/GenomesGroup.cgi?taxid=10239&opt=Virus
[2]http://www.uniprot.org/taxonomy/?query=virus+AND+reviewed%3ayes&offset=250

Table 1 | A summary of proteomic techniques and their applications in virology.

Mass spectrometry based proteomic approaches	Main applications in virology	Relevant reference
Tandem affinity purification based MS approach	Protein–protein interactions	Jorba et al. (2008), Mayer et al. (2005), Mayer et al. (2007)
Co-immunoprecipitation based MS approach	Binding partners of target protein	Moresco et al. (2010), Noisakran et al. (2008)
HLA peptidome scanning chip based MS approach	Searching for disease related peptides or differently expressed proteins after virus infection	Herberts et al. (2003), Wahl et al. (2010)
Isotope coded affinity tag (ICAT) Isobaric tag for relative and absolute quantitation (iTRAQ) Stable isotope labeling of amino acids in cell culture (SILAC) Difference gel electrophoresis (DIGE)	Mapping differently expressed proteins in host proteome upon virus infection	Yan et al. (2004), Booy et al. (2005) Zhang et al. (2009), Chen et al. (2008) Dreger et al. (2009), Hammond et al. (2010) Pastorino et al. (2009), Sun et al. (2011a)
Cross-linking based MS approach	Investigating protein-nucleotides binding sites	Deval et al. (2007), Bhardwaj et al. (2008)
Hydrogen/deuterium exchange (HDX) based MS approach etc.	Conformational dynamics of host or viral proteins	Lisal et al. (2005), Monroe et al. (2010)

bridges. These cross-links could be reversed by heating and the eluted peptides are further submitted to MS for sequence identifications (Orlando et al., 1997; Metz et al., 2004). For its applications, the helicase-like regions within the viral polymerase involved in RNA binding were characterized by reversible formaldehyde cross-linking and MS (Kim et al., 2005; Deval et al., 2007; Han et al., 2009).

HYDROGEN/DEUTERIUM EXCHANGE BASED MS METHODOLOGY

Hydrogen/deuterium exchange combined with MS is able to investigate the protein structures and dynamics by studying their conformational alternations. Some amide hydrogens at the backbone could be readily exchanged when incubated in a deuterated environment while some amide hydrogens hidden in the interior of the protein or involved in hydrogen bonding have restricted access to deuterium. A quench condition (0°C, pH 2.5) is used to stop the exchange reaction followed by pepsin digestion of proteins prior to MS analysis. Therefore, the deuterium labeling induced mass shift and H/D exchange rate could reflect the protein conformational information and hydrogen bond interactions (Hamuro et al., 2003; Engen, 2009). HDX combined with high resolution MS was capable of studying structural information such as protein-nucleic acid bindings, protein–protein interplays, and protein maturation rearrangements. Viral molecular motors, e.g., helicases or packaging factors, are associated with nucleic acid binding and hydrolysis functions. The hexameric packaging motor (P4) of cystovirus enabled to bind viral RNAs through its RNA binding channel coupled with ATPase activities. The conformational dynamics of P4 in the presence and absence of RNA were examined by HDX coupled with MS. The HDX kinetics revealed distinctive states for different domains of P4 in response to nucleotide-binding, RNA loading, and translocation as well as ATPase activities, and thus provided a comprehensive understanding to P4 molecular architecture in different biological states (Lisal et al., 2005). Assembly of MS2 viral coat protein is initiated by binding with a RNA stem-loop, resulting in a conformational switch from a symmetric dimer to an asymmetric structure. In this circumstance, detailed structural information was characterized by HDX and MS that some known RNA binding regions showed a more fluctuated HDX kinetics (Morton et al., 2010). PPI dynamics could also be studied by HDX and MS. For instance, Kong et al. (2010) comparatively studied the local conformational rearrangements within HIV-1 gp120 in the presence or absence of CD4. Monroe et al. (2010) also applied HDX combined with LTQ-FT MS to study the immature, mature, and mutant Gag polyprotein to further unravel the capsid assembly.

COMPUTATIONAL VALIDATIONS BY PROTEOMIC SOFTWARE

With the advent of high throughput short-gun proteomics, liquid chromatography coupled with tandem MS (LC-MS/MS) could characterize numerous fragment ion spectra and thus is able to identify large number of peptide sequences. In addition, accessing highlighted post translational modifications (PTMs) and protein quantifications by stable isotope labeling or label-free analysis have incorporated into the multi-functional search engines, enriching the mass spectrometric data. Presently, several proteomic search engines are available from distinctive searching algorithms and compatible with mass spectrometric data, including some traditional ones, e.g., Mascot, SEQUEST, X!TANDEM, as well as some new search engine, e.g., ProluCID, etc. Mascot incorporates peptide mass fingerprint, sequence query, and MS/MS ions search. It is a possibility-based scoring engine by calculating the observed match between experimental data and theoretical sequence data (Perkins et al., 1999). For instance, Lai et al. (2007) employed Mascot to analyzed the nano LC-MS/MS data and identified up-regulated proteins in human promonocyte cells stably expressing SARS CoV 3C-like protease. Although Mascot provides high throughput protein identification dependent on possibility rankings, there exist some limitations associated with searching

non-independent dataset, and non-statistical validation of atypical sequence entries. SEQUEST could correlate ion fragmentations in the processed tandem mass spectrometric data with their corresponding amino acid sequences in the FASTA database files. There are generally four steps of this search algorithm, including tandem mass spectra reduction, matching spectra with amino acids, generating high-ranked sequences, and correlating with protein identification (Eng et al., 1994; Yates, 1998). SEQUEST also is able to search several covalent modification-bearing peptides by matching the nascent tandem mass spectra (Yates et al., 1995). It had been applied to identify secretome of human monocyte-derived macrophages after HIV-1-infection (Ciborowski et al., 2007). X!TANDEM is an open-source platform for proteomic researchers to efficiently process MS/MS data (Craig and Beavis, 2004). Its analysis on a mixture of peptides is based on one axiom: for each detectable protein in the original protein mixture, there will be at least one good tryptic peptide match within a designed scope. In the first step of the analysis, a smaller set of protein sequences is generated from the original protein database by thoroughly filtering with the designed scope that set as small as possible. From this step onward, the subsequent searches are within this refined protein sequences, thus improving the efficiency and saving the overall search time. In the second step of analysis, a bigger scope is set to perform multiple comparisons of the spectra with those refined protein sequences in respect to the different peptide modifications, number of missed cleavages, and non-specific hydrolysis, etc (Craig and Beavis, 2003). Trans-Proteomic Pipeline (TPP) was utilized to statistically analyze the viral and host proteins in purified RSV (Radhakrishnan et al., 2010). And global proteome machine (gpm) is a well-established open-source search engine based on TANDEM[3]. Recently, Xu et al. developed a new search engine ProluCID, which is based on binomial probability preliminary scoring scheme to filter candidate peptides for further isotopic distribution analysis (Xu et al., 2006). And high sensitivity and specificity of ProLuCID could be achieved compared to SEQUEST.

In addition to these searching algorithms, there emerge several multi-functional proteomic pipelines which could incorporate statistical analysis and guarantee high confident searching results. Since different search engines have distinctive algorithms and sensitivities, some important low-abundant hits may be identified by only few software. To cope with this problem, one advantage of Scaffold proteomic pipeline is that peptides simultaneously identified by several different searching engines, e.g., Mascot, SEQUEST, TANDEM, etc, could be integrated into "a folder" by Peptide Prophet Algorithm, resulting in a list of combined peptide sequences. And a further statistical calculation and validation by Protein Prophet algorithm is processed with MS/MS data to generate protein identifications (Searle, 2010). Similarly, TPP also supports the original data generated by Mascot, SEQUEST, TANDEM, etc. Peptide or protein identification is performed by peptide prophet or protein prophet algorithm, respectively. It also combines the advantages of statistical validations by iProphet tool and quantitative analysis by XPRESS, ASAPRatio, or Libra algorithm (Deutsch et al., 2010). Moreover, the Scripps Research Institute developed an integrated Proteomics Pipeline (IP2), which provides a simple and efficient platform for rapid identifications and quantifications to proteomic researchers[4]. It is compatible with both SEQUEST and ProluCID search engines for high resolution MS spectra analysis (Xu et al., 2006). Subsequently, DTASelect set spectrum filtering parameters to ensure low false-positive rate and refine the confidence of protein output (Tabb et al., 2002; Cociorva and Yates, 2007). Census is further incorporated into IP2 to enable large-scale quantitative analysis on isotope-labeled, e.g., N15, SILAC, and iTRAQ, or label-free samples (Park et al., 2008). Some well-established PTMs, especially phosphopeptides, could also be specifically searched during the IP2 ProluCID analysis step, yielding potential highlights for further functional validations.

ACTIVITY-BASED FUNCTIONAL VALIDATIONS

LIMITATIONS OF PROTEOMIC DATA

Although the introduction of software is a significant advance to a variety of proteomic studies by performing statistical analysis and filtering out low confident protein candidates, the development of bioinformatics is still hampered by computational limitations. For tandem mass spectra, only a small number of most abundant precursors are generally selected for subsequent MS/MS analysis due to limited sampling rate of MS. It therefore results in missed identification of some lower abundant proteins could escape identification. The method may also identify some non-specific proteins or contaminants, for instance, HSC70 was identified associated with purified RSV by proteomic approach, yet validation by fluorescence microscopy showed that the proteomic observation of HSC70 in RSV was false-positive (Radhakrishnan et al., 2010). Also, for large-scale quantitative proteomic analysis, such as 2D gel and 2D LC-MS/MS, it is hard to validate the functional activity of each protein due to the large quantity of protein IDs and shortages of antibodies. More importantly, mass spectrometric data may also contain proteins from indirect secondary cellular responses that are not directly related to virus infections. For instance, some indirect cellular processes during the late stages of HIV or RSV infection, such as syncytium formation that causes severe secondary host countermeasures could also be detected in proteomic analysis.

To overcome such limitations, more accurate assessments are required to functionally validate the active state of viral or host proteins identified by MS. In this way, functional validations, which highlight proteins involved in direct cellular responses upon virus infections, would provide novel insights to proteomic datasets. These approaches involve drug inhibition of secretory pathway, immunofluorescence staining, dominant negative mutant of protein target, microarrays, small interfering siRNA-mediated knockdown, molecular cloning studies, or activity-based protein profiling (ABPP) (**Figure 1**). In parallel to our previous review stressing global proteomic studies on virus and host interaction (Zheng et al., 2011), this review mainly focuses on the diverse activity-based applications to validate distinctive proteomic datasets concerning pathogen-host interactions.

[3] http://www.thegpm.org/

[4] http://integratedproteomics.com/

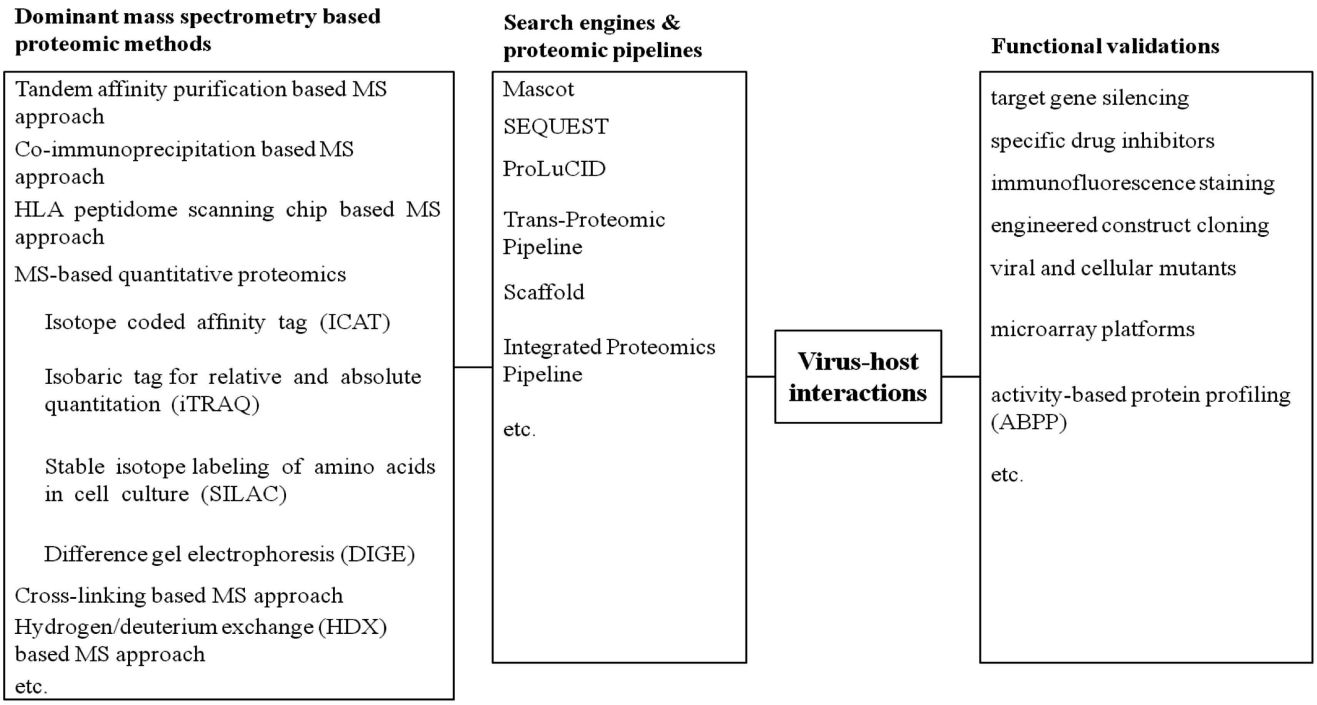

FIGURE 1 | A summary of current approaches on virus-host interactions.

FUNCTIONAL VALIDATIONS BY GENE SILENCING

Nucleic acid-based antisense agents have been widely used to inhibit or knockdown targeted gene expression. These antisense technologies constitute antisense oligonucleotides (ODNs), ribozymes, DNAzymes, and RNA interference (RNAi). Each approach has its own strengths and weaknesses. For instance, although there are some off-target effects, RNAi is regarded as a potent and efficient tool for gene silencing even that its sequence target is in low concentration. Also, it could implement *in vivo* and *in vitro* systems, escape the immune responses, and involve in network pathways (Scherer and Rossi, 2003). RNAi is based on the posttranscriptional gene silencing mechanism, which is induced and mediated by small interfering 21–23 nucleotide dsRNA (siRNA; Novina and Sharp, 2004). It targets specific sequence and results in degradation and knockdown of this gene expression. Specifically, natural dsRNAs from the cytoplasm are recognized by RNAi DEfective family member-4 (RDE-4), resulting in dicer-mediated cleavage into 21–23 nucleotide siRNA. These cleaved siRNAs are then recruited into a RNA-inducing silencing complex (RISC), which consists of helicase, exonuclease, endonuclease, and homology searching domains. On one hand, the duplex siRNAs are unwound by helicase. On the other hand, one antisense single strand associated with RISC directs its binding with complementary mRNA. And this binding induces and stimulates the ATP-dependent activities of exonuclease and endonuclease, which could cleave the targeted homologous transcript mRNA (Lee and Sinko, 2006; Pushparaj et al., 2008). Besides natural siRNA, chemically synthesized siRNAs, short hairpin RNA (shRNA), and microRNA (miRNA) could also induce gene silencing in similar mechanisms (Dykxhoorn et al., 2003). A pioneering trial of siRNA was applied to tomato cell lines and antisense 25 nucleotides specific to 1-aminocyclopro-pane-1-carboxylate oxidase (ACO) mRNA were detected (Hamilton and Baulcombe, 1999). In the following 2 years, Elbashir et al. (2001) firstly utilized duplexes of 21-nucleotide siRNAs to mediate the degradation of corresponding mRNAs in mammalian cells. It was also regarded as a breakthrough approach in the year 2002 by *Science* (Couzin, 2002).

In the recent decade, this breakthrough technique has been playing an indispensable role in the realm of virology (Tan and Yin, 2004). In addition, it could integrate and highlight proteomic data by shedding a light at the protein function level. And numerous researches have implemented gene silencing, especially siRNA knockdown, in validating the proteomic data in respect to virus infection. To explore the cellular interacting partners of NS5A of hepatitis C virus, a proteomic technique, Co-IP, was employed (Gonzalez et al., 2009). Heat shock proteins, hsc40 and hsc70, were identified for interacting with NS5A and validated by western blot analysis. NS5A was known to be able to affect the internal ribosome entry site (IRES) mediated translation of HCV. To further determine the roles of these two proteins related to IRES mediated translation, sihsc70 and sihsc40 knockdown combined with a cell culture-based bicistronic luciferase reporter system were designed. The ratio of Firefly to Renilla luciferase expression could reflect the effectiveness of IRES mediated translation. And this ratio is significantly decreased by the knockdown of hsc70, suggesting the importance of hsc70's role involved in the NS5A alternation of IRES mediated translation. Similarly, Katoh

et al. (2011) also used Co-IP purification technique followed by MS to identify the binding partner of flavivirus core protein. Heterogeneous nuclear ribonucleoprotein (hnRNP) A2 was found to interact with flavivirus core protein. By applying siRNA knockdown of this protein, a 90% reduction of viral replication was discovered and vRNA synthesis was delayed, indicating its significant role in regulating virus replications. In another study, TAP based proteomic approach was utilized to explore the interacting complexes associated with viral polymerases of influenza A virus (Jorba et al., 2008). KIAA0136 (NXP2), SFPQ/PSF protein, DEAD/H box polypeptide 3 (DDX3), HNRNP-M protein, coactivator activator, growth regulated nuclear 68 protein (DDX5), beta 5-tubulin, HNRP-H1 protein, ribosomal protein-small subunit S3, and similar to zinc finger protein 71 were specifically identified. Immunofluorescence imaging further confirmed the co-localizations of those host proteins with viral RNPs. And among those identified host factors, a series of functional studies was performed *in vivo* and *in vitro* for characterizing the nuclear associated protein SFPQ/PSF (Landeras-Bueno et al., 2011). siRNA silencing of SFPQ/PSF was found to reduce virus propagations. In particular, the accumulations of vRNA and mRNA were interrupted and reduced; polyadenylation step in viral mRNA assembly was also disturbed when siRNA silencing of SFPQ/PSF was implemented.

To functionally study host proteins associated with virions, siRNA-mediated transcript knockdown is utilized to validate the roles of host proteins involved in virus infection. In one study, highly purified RSV particles were analyzed by proteomic approach, and a total of 25 host proteins were identified to be associated with virions (Radhakrishnan et al., 2010). Among those cellular components, two heat shock proteins, e.g., hsc70 and hsp90, were further selected to examine their effects on virus infection. RSV-infected cells were transfected with either sihsc70 or sihsc90 at 20 hpi. The transfected cells were then fixed and stained with anti-hsc70, anti-hsc90, and antiviral fusion protein (anti-F). In both the sihsc70 and sihsc90 treated groups, obvious reductions in hsc70 and hsp90 staining signals visualized by immunofluorescence imaging were observed, accompanying with decreased viral fusion protein expression. In another study, Spurgers et al. (2010) applied LC-MS/MS and siRNA screening to identify and validate the host proteins associated with Filoviruses (ebola viruses and marburgvirus). The specific knockdown of HSPA5 and ribosomal protein L18 (RPL18) greatly affected ebola virus and marburgvirus infection. qRT-PCR was also applied to confirm the reduced host gene expressions at the transcript level.

For most viruses, the detailed mechanism of virus and host signaling pathways associated with virus survival remains elusive. Since lipid raft plays important roles in virus assembly, signaling, and sorting pathways, delineation of those host proteins associated with lipid rafts could assist to understand the key regulators and mediators involved in viral maturation. Mannova and Beretta (2005) used 2D gel coupled with LC-ESI/Q-TOF/MS-MS to characterize the protein contents of lipid rafts of hepatitis C virus infected cell membranes. N-Ras was identified as a key activator of PI3K-Akt-mTOR pathway and it was important for cellular signaling behaviors. siRNA silencing of N-Ras was observed to inhibit the host PI3K-Akt-mTOR pathway and thus enhanced the HCV replications. A similar effect was observed when cells were treated with PI3K inhibitor LY294002 or transfected with mTOR siRNA. In another study, Gaither et al. (2010) utilized drug inhibition assays, iTRAQ coupled with LC-MS/MS, and RNAi screening to identify key factors involved in HCV replication pathways. Cyclophilins A, H, 40, and E were identified and validated to associate with multiple signaling pathways of HCV replication. One cyclophilin inhibitor NIM811 could strongly suppress these multiple pathways and result in reduced virus release. In another study by Hwang et al. (2007) annexin 1 was discovered to be a key effector to apoptosis pathways associated with infectious pancreatic necrosis virus (IPNV) infected cells. They employed 2D gel electrophoresis and MALDI TOF/TOF MS and identified annexin 1 as an up-regulated protein upon virus infection. SiRNA-mediated knockdown of annexin 1 not only increased the apoptotic effects of cell death, but also suppressed viral protein synthesis until 10 h post infection.

Compared with siRNA knockdown, shRNA and miRNA mediated gene silencing were less reported as functional validation strategies to examine proteomic data. In one study, cellular c-Cbl was known to play a key role in macropinocytosis for entry of kaposi's sarcoma-associated herpesvirus (KSHV). Valiya Veettil et al. (2010) utilized MS to analyze the immunoprecipitation (IP) of c-Cbl and identified a novel interacting protein, myosin IIA. shRNA mediated knockdown of c-Cbl was then performed and the binding between c-Cbl and myosin IIA was abolished. Overall, these gene silencing studies showed that effective silencing of gene expression has a profound influence to functional virology studies in conjunction with proteomic techniques. What is more, it could provide a more rigorously demonstrated result at the functional level when siRNA-mediated knockdown is comprehensively combined with other approaches, such as immunofluorescence imaging, molecular cloning, RT-PCR, drug inhibition of secretory pathways.

FUNCTIONAL VALIDATIONS BY DRUG INHIBITIONS

Quantitative proteomic approaches have been frequently utilized to study the relative expression level of viral and cellular proteomes upon virus infection. Precise measurement of expression shift could highlight the groups of significantly up-regulated and down-regulated proteins, which may serve as key mediators or regulators involved in virus-hijacked secretory pathways. Therefore, these significantly regulated proteins characterized by quantitative proteomics could be considered as potential biomarkers or drug targets for diagnostic or therapeutic purposes. In one study, a proteomic approach, 2D gel combined with quantitative analysis was performed to unravel the changes in the cellular proteome before and after dengue virus serotype 2 (DEN-2) infection (Kanlaya et al., 2010a). Sixteen host proteins were found to be up-regulated and twenty two proteins down-regulated. Ubiquitin-activating enzyme E1 (UBE1) was identified as a greatly up-regulated protein and its specific inhibitor, UBE1-41, was selected to explore the effect of UBE1 inhibition on virus propagation and infectivity. The treatment resulted in reduced viral protein synthesis and fivefold decrease in virus release. Therefore the importance of ubiquitin-proteasome pathway to DEN-2 infection could be revealed by specifically counteracting UBE1. Another quantitative

proteomic study was designed to illustrate sub-cellular changes upon expression of measles virus nucleoprotein (NP), which is a key mediator involved in cellular apoptosis pathway via triggering reactive oxygen species (ROS) and caspase 3 (Bhaskar et al., 2011). The inhibition of caspase 3 by ascorbic acid could partially reverse and counteract the NP-induced apoptosis. Furthermore, in order to highlight the essential components responsible for antiviral and cell death signaling pathways of influenza A virus infected macrophages, 2D gel coupled with LC-MS/MS was used to quantitatively analyze the up-regulated or down-regulated host proteins in the cytosolic and mitochondrial proteomes (Ohman et al., 2009). As a result, cytoskeleton proteins, e.g., actin and tubulin, were significantly up-regulated in the mitochondrial fraction; and deliveries of certain proteins involved in the antiviral machinery from cytosolic to mitochondrial region were clearly observed. Also, drug inhibition of actin networks by cytochalasin D could impair the expression of certain major antiviral proteins, such as interferon (IFN)-β and TNF-α. These indicate that actin could regulate the antiviral and cell death signaling pathways involved in mitochondrial responses. In another study, as Epstein–Barr virus (EBV) plays a role in gastric carcinogenesis, Fukagawa et al. (2008) used 2D gel followed by LC-MS/MS to quantitatively study the differentially expressed proteins in EBV infected carcinoma cells. Heat shock protein 27 was identified as a significantly up-regulated phosphorylated protein upon virus infection. Drug inhibition studies demonstrated that PI3K/Akt pathway was closely related to Hsp27/phosphorylation, as phosphorylation level was reduced upon treatment with PI3K inhibitors (LY294002 and wortmannin). As a result, suppression of PI3K signaling pathway could inhibit hsp27 function in EBV-induced gastric carcinomas.

Besides Heat shock protein 27, other heat shock proteins are also known to be closely involved in the dynamics of virus and host interactions. Heat shock proteins 40 and 70 were identified by proteomics as binding partners of hepatitis C viral protein NS5A. Gonzalez et al. (2009) used quercetin to inhibit the activities of host factor HSPs upon HCV infection. Both viral replication and release were found to be greatly reduced in a dose-dependent manner compared to a mock group. In another study, heat shock protein 90 (hsp90) was identified to be associated with RSV particles by LC-MS/MS (Radhakrishnan et al., 2010). Immunofluorescence imaging revealed the co-localization of hsp90 with viral filaments and two drug inhibitors, geldanamycin and 17-allylaminogeldanamycin, were used to examine hsp90's role during virus infection. Viral filamentous staining patterns were greatly impaired while treated with these two inhibitors. Also, the efficiency of virus infectivity and transmission, indicated by estimating numbers of virus infected cells, were reduced by fivefold when treated with these drugs. Although most cellular heat shock proteins function at transcription or replication levels, the low-abundant hsp90 present inside the RSV plays a major role in the formation of virus filaments and virus transmission.

Inhibition of PTM signaling pathways could display therapeutic effects to virus infection, since distinctive PTMs could play different roles in virus infectious cycle. For instance, PB1-F2 is encoded by an alternative open reading frame of the PB1 gene. It is a phosphorylated protein predominantly localized in the mitochondria of some virus infected cells to initiate the apoptosis pathway. Also, PB1-F2 is a virulent factor that it could aggravate virus infection by enhancing the secondary bacterial inflammations (Krumbholz et al., 2011). To explore the innate mechanism of PB1-F2 associated with cellular apoptosis, Mitzner et al. (2009) explored protein kinase C (PKC) mediated-phosphorylation of PB1-F2 by LC-MS/MS and demonstrated the importance of phosphorylation signaling pathways to facilitate apoptosis. Phosphorylation level of PB1-F2 was measured in the presence of inhibitor and activator of PKC, and it is reduced or increased *in vitro*, respectively. When a mutant virus strain with abrogated PB1-F2 phosphorylation sites was produced to infect primary human monocytes, initiation of cellular apoptosis was impaired and virus propagation was reduced. As another example, the spike protein (S) of SARS is a glycosylation-bearing protein, which is important to viral attachment and subsequent fusion steps. Ritchie et al. (2010) utilized the combination of MALDI TOF MS, negative mode Q-TOF MS, and HPLC to comprehensively study the various types of N-linked carbohydrates associated with the viral spike protein. Major complex glycans were clearly characterized. And treatment of SARS infected Vero E6 cell with α-glucosidase inhibitor *N*-butyl-deoxynojirimycin (NB-DNJ) revealed that the suppression of glycosylation process could inhibit the virus infection by blocking the initial stage.

Drug inhibitions specifically targeting viral proteins have been increasingly in demand to block virus infections. However, some viral proteins, e.g., hemagglutinin (HA) and neuraminidase of the influenza A virus, could exhibit their remarkable potentials to mutate to new subtypes. Thus it is necessary to require an updated drug discovery strategy to cope with prophylaxis upon virus infection. Clinically, there are two available drugs against neuraminidase: zanamivir and oseltamivir (Shahrour, 2001). Oseltamivir, also known as tamiflu, was the first orally active neuraminidase inhibitor able to defend the H5N1 avian flu and H1N1 swine flu in early infection (Agrawal et al., 2010). And zanamivir is effective to prevent symptomatic laboratory-confirmed influenza virus and its transmission in healthy adults (Jackson et al., 2011). In addition, adamantine is widely used to block the Matrix 2 (M2) ion channel in vaccine and antiviral drug designs. Nevertheless, both adamantine-resist and tamiflu-resist circulating influenza A virus strains were emerged in the last century (Deyde et al., 2007; Hayden and de Jong, 2011; Sheu et al., 2011). Therefore, a strategy for updated drugs or vaccines targeting new viral mutants should be urgently established in preparation for the next pandemics or epidemics. The utility of proteomics has been efficiently employed to facilitate the vaccine design and antiviral drug discovery. For example, the binding between influenza HA and α-2, 6-sialylated glycoprotein receptor is the initial step to induce human infection. Also, the HA precursor is further cleaved by proteases on the virus surface to generate the C-terminal fragment HA1 and the N-terminal fragment HA2, triggering the potential ability of membrane fusion process (Wiley and Skehel, 1987). Thus, HA or its binding with sialic acid receptors could be regarded as potential drug targets to block the initial stage of virus infection. To characterize the innate immunity antiviral components from salivary, Chen et al. purified the binding partners of α-2, 6-sialylated glycoprotein receptor. And

α-2-macroglobulin (A2M) was identified by proteomic approach for specifically inhibiting hemagglutination (Chen et al., 2010).

FUNCTIONAL VALIDATIONS BY IMMUNOFLUORESCENCE STAINING

Immunofluorescence staining assay is a powerful tool which combines the utility of specific fluorescent probes, advanced confocal microscopy, and digital image analysis. It has been frequently used for analyzing distinctive biological samples, such as neurons (Zinchuk and Grossenbacher-Zinchuk, 2009), plant cells (French et al., 2008), virus infections, and so on. Co-localization refers to the co-existence of multiple fluorescent probes generated through different fluorochromes, resulting in overlapped images. For instance, in a same specimen, two antigens are visualized by their respective fluorescence-labeled secondary antibodies in microscopy (one is red while the other is green), and a third yellow staining image emerges when these two antigens co-localize, suggesting the interactions of these two macromolecules or particular sub-cellular localizations where this co-existence belongs. However, there also exist some limitations of this technique (Smallcombe, 2001). For example, fluorescence bleed-through and tissue autofluorescence could take place between two fluorochromes, thus resulting in increased non-specific background noises. These obstacles could be overcome by careful sample preparation and appropriate optimization of image acquisition (Smallcombe, 2001; Zinchuk et al., 2007). In addition, the bimolecular fluorescence complementation (BiFC) assay could investigate PPIs in live cells and organisms (Kerppola, 2006, 2008). Two fluorescent protein fragments are fused to target proteins that interact, and these fragments would refold to produce fluorescence upon target protein association. BiFC has been utilized to study the virus-host interaction between HSV-1 regulatory protein ICP27 and one cellular protein, TAP/NXF1 (Hernandez and Sandri-Goldin, 2010). Yet few works were present as a subsequent method to validate proteomics data related to virus infections.

Co-localization has been widely applied to virology studies in order to visualize the co-existence of target proteins in different sub-cellular distributions. In proteomic studies, the confocal imaging technique could further visualize virus-host interactions at the protein level and thus enhance proteomic data from another aspect. In one research, Lee et al. (2011) employed TAP based pull-down assay combined with 1D LC-MS/MS to investigate the essential interaction partners of hepatitis C virus core (HCVc) protein. Huh7 cells were transiently transfected with a plasmid construct bearing exogenous HCVc and TAP components, which were designed to express the biotinylated (B-tag) bait protein with calmodulin-binding peptide (CBP)/protein A tags. This TAP based proteomic approach enabled the authors to identify 36 candidates. Three highest-ranking proteins, hnRNPH1, NF45, and C14orf166, were selected for further validations. These three proteins were also specifically identified and validated as binding partners of HCVc in another affinity pull-down system, which is based on streptavidin-Dynabeads instead of IgG-Dynabeads. Confocal imaging analysis was performed to visualize these interacting partners. In a mock group, hnRNPH1 was found to be localized in the nucleus whereas NF45 and C14orf166 were evenly distributed in both the cytoplasm and the nucleus. In HCVc expressed Huh7 cells, co-staining of HCVc with these three proteins were predominantly localized in the nuclear region, suggesting that HCVc was transferred to nucleus from cytoplasm to interact with its binding partners. In another example, an EBV-encoded protein, latent membrane protein 1 (LMP1), was known to be able to interact with cellular prenylated Rab acceptor 1 (PRA1). This association mainly occurred in Golgi apparatus visualized by immunofluorescence imaging and it was highly involved in LMP1 mediated intracellular trafficking and NF-kB signaling pathways in nasopharyngeal carcinoma (NPC) cells (Liu et al., 2006). To further clarify the role of PRA1 in EBV infected NPC cells, siRNA knockdown of PRA1 was performed to generate PRA1-knockdown NPC clones, which were analyzed by the isobaric mass tags (iTRAQ) labeling approach coupled with 2D LC-MS/MS (Liu et al., 2011). Seventy proteins were found to be significantly up-regulated whereas 20 were down-regulated. The significantly up-regulated proteins (e.g., LAMC2, ITGA6, ITGB4, FABP5, CAV1, and TIP47) responsible for lipid homeostasis and cell migration were selected and analyzed by immunofluorescence imaging in PRA1-knockdown NPC cells. In consistent with the proteomic data, spatial distributions of ITGA6, ITGB4, and CAV1 to perinuclear regions were observed with their elevated fluorescence staining patterns.

In another study associated with dengue virus infected human endothelial cells, Alix (apoptosis-linked gene-2-interacting protein X) was identified as an up-regulated protein by 2D gel coupled with Q-TOF MS/MS (Pattanakitsakul et al., 2010). Alix was known to play an important role in viral protein transport from endosome to cytosol for viral replication purpose. And double immunofluorescence staining assay confirmed the co-localization of Alix with the late endosome marker, lysobisphosphatidic acid (LBPA), suggesting that interaction of Alix with late endosome could assist the viral nucleocapsid export to the cytoplasm. Also, cells with and without anti-LBPA pretreatment were infected with dengue virus and then measured in different time post infection; immunofluorescence staining by targeting DENV envelop protein revealed delayed virus replication when pre-treated with anti-LBPA, suggesting that the inhibition of endosomal protein could impair functions of Alix to assist viral replication. To explore the possible mechanism underlying vascular leakage upon dengue infection, a similar proteomic approach was utilized to quantitatively analyze significantly regulated proteins (Kanlaya et al., 2009). β-actin was identified to be greatly up-regulated. However, subsequent western blot analysis revealed that the expression level of β-actin was decreased. Furthermore, by applying immunofluorescence imaging, dengue infected cells showed remarkably decreased expression of actin networks and proteins associated with adherens junction, intercellular adhesion, and transendothelial migration. These observed alternations of actin networks and endothelial integrity could shed a light on vascular leakage upon virus infection. Although β-actin was noted as an up-regulated protein in one particular spot by 2D Gel proteomic approach, it was possible that the overall expression level of this abundant protein was decreased, which was consistent with the western blot and immunofluorescence imaging assays. This observation also reflects the necessity of functional validations to proteomic data, which may include false-positive identification or biased quantification results. Meanwhile, due to the limitations of the 2D gel based proteomic approach (Bunai and Yamane, 2005), its accuracy needs to be improved. Besides

β-actin, hnRNPs were also found to be up-regulated upon virus infection, and IP based proteomics identified vimentin as the binding partner of hnRNPs (Kanlaya et al., 2010b). The subsequent co-localization study confirmed the co-existence of vimentin, hnRNPs, and dengue NS1 in perinuclear regions, suggesting their roles associated with assembling in perinucleus upon dengue virus infection. The advances of immunofluorescence staining in visualizing the sub-cellular localizations of specific proteins and their interactions ensure that it remains a vital technique for functional proteomic studies.

FUNCTIONAL VALIDATIONS BY CONSTRUCT CLONING

Construction of plasmid cloning vector encoding gene targets and its subsequent transfection into cells, or bacteria, could lead to the co-expression of endogenous and exogenous proteins. Therefore, this target-based cloning enables us to additionally induce the over-expression of one protein or heterogeneously express proteins encoded by genes of an alternative microorganism, respectively. In recent years, numerous pull-down based proteomic techniques have been widely applied to study PPIs. Specifically, TAP based proteomic approaches facilitate the characterization of interacting partners of the highlighted viral protein, which could be exogenously expressed in host cells by cloning specific construct. And Most TAP based or pull-down proteomics were initial designs followed by proteomics rather than functional validation studies to proteomic data. In one study, in order to discover the binding partners of HCVc fusion protein, Lee et al. (2011) designed a vector construct by inserting the HCVc gene fragment into the pMSCV-BCP vector, this enabled them to express a biotinylated (B-tag) bait protein with CBP/protein A tags. The interacting protein complex of the exogenous intact HCVc protein could be identified by LC-MS/MS and confirmed by confocal imaging microscopy. In another study, Jorba et al. (2008) constructed plasmids encoding influenza A viral polymerase genes fused with the TAP tag, and used MALDI TOF MS to find the binding partners of this heterotrimeric polymerase complex. Human HEK293T cells were transfected with these plasmids expressing viral polymerase proteins fused with the TAP tag. Most successfully identified host proteins were nuclear proteins involved in cellular RNA synthesis, modification, and nuclear trafficking. To further validate the proteomic data, one abundant host factor, KIAA0136 (NXP2), was designed to be over-expressed from the plasmid pcDNA3HA-NXP2 by fusing the gene with the HA tag. And subsequent immunofluorescence imaging assay supported mass spectrometric data and confirmed the co-localization of this tagged-NXP2 with viral RNPs.

What is more, pull-down based proteomic method could also be applied to investigate interacting partners of viral genomes, e.g., HIV tat/rev exon (Marchand et al., 2011), and thus illustrate virus replication mechanisms. The 5′ and 3′ ends of transmissible gastroenteritis virus (TGEV) genome were known to harbor *cis-acting* signals and have affinity preference for host binding partners. Galan et al. (2009) synthesized two respective TGEV genome ends containing first the 504 nucleotides or the last 493 nucleotides by PCR and labeled them with biotin prior to *in vitro* transcription. The biotin labeled RNA were then immobilized on a streptavidin sepharose resin as baits for affinity protein purification, followed by MALDI TOF/TOF MS identification. Nine proteins displayed preferential binding to the C-terminal of the viral genome whereas one protein was found to interact with the N-terminal. And siRNA knockdown of these C-terminal interacting proteins, e.g., PABP, hnRNP Q, and EPRS, resulted in significant reduction in viral RNA synthesis, suggesting their roles associated with viral transcription and replication. In a similar study, KSHV is a DNA virus and its terminal repeat (TR) genome elements could potentially interact with cellular components during virus infection (Si et al., 2006). A triple copy of the 801 bp TR was inserted into a plasmid vector, pBSpuroA3, which could be transfected and amplified in a KSHV-negative cell line and a KSHV-positive cell line. The TR elements associated with cellular factors were digested with corresponding restriction enzymes and purified with affinity column prior to proteomic analysis. Some candidate proteins identified by proteomics (PARP-1, ATR, NPM1, and BRG1) were further corroborated by western blot and co-localization studies. Analogously, Lin et al. (2008) also utilized RNA affinity poll down and proteomics to study protein interacting partner of the 5′ untranslated region of enterovirus 71, and identified hnRNP K. Plasmids encoding different truncated forms of hnRNP K were further designed to specifically locate interaction domains. KH2 and the proline-rich domains were affirmed by western blots and siRNA knockdown of these domains resulted in decreased viral yields and viral RNA synthesis. In addition to RNA precipitation coupled with MS, another proteomic technique, reversible formaldehyde cross-linking coupled MS is able to map the specific peptides that bound to viral RNA (Kim et al., 2005). Viral replicase of potexviruses has a helicase domain, the cDNA of which was cloned into pET32 fused with thioredoxin, a His tag, and an S tag at its N-terminal. This enzymatic protein was expressed in *E. coli*, and purified by immobilized metal affinity chromatography. Subsequently, this purified protein was incubated with a 3′-biotinylated 15-nt RNA in the presence of formaldehyde, a cross-linking agent. After trypsin digestion, peptides bound to RNA were purified by IP, followed by LC-MS/MS analysis. A total of six peptides were identified by proteomics. Their RNA binding affinities were validated by functional mutation analysis.

In addition, quantitative proteomics could reveal virus-host interactions with distinctive profiles after plasmid transfections. The X protein of chronic hepatitis B virus (HBx) was known to induce hepatocellular carcinoma (HCC). In one study, HBx of genotype A, B, C were amplified by PCR and inserted into pXJ40 vector, followed by transfection HepG2 cells (Feng et al., 2010). Cells transfected with those different genotypes of HBx and empty pXJ40 plasmid were labeled with iTRAQ and further submitted to 2D LC-MS/MS. Comprehensive protein profiling displayed some up-regulated cytoskeleton proteins responsible for cytoskeleton movement and migration. For instance, microtubule-actin cross-linking factor 1 (MACF1), annexin A2, high mobility group box 1 (HMGB1), were over-expressed after HBx transfection. To further functionally validate the proteomic data in respect to cellular motility, the HepG2 cells were co-transfected by those HBx genotypes and green fluorescent protein (GFP) to visualize the tracks of cell movement by real-time fluorescence microscopy. And HBx genotype A infected cells revealed more vigorous movement than cells infected with other HBx genotypes. Similarly, Mota et al.

(2008) utilized quantitative proteomics to characterize the differently expressed protein profiles upon the presence of differentially viral components of hepatitis delta virus (HDV). Huh7 cells were transiently transfected with plasmids coding S-HDAg, L-HDAg, gRNA, and agRNA, respectively, and changes in the Huh7 cell proteome were measured by 2D gel and MALDI TOF/TOF MS. Among those differentially expressed proteins, hnRNP D, HSP105, and triosephosphate isomerase were down-regulated and confirmed by RT-PCR. This work was the first to present the overall host alternations upon expression of HDV proteins and genes, thus providing clues to unravel detailed HDV replication mechanisms. Similar approaches have been used to quantify the proteome changes upon expression of exogenous small hepatitis B surface antigen (SHBs) in HepG2 cells (Zhao et al., 2010), recombinant influenza viral protein fused with HIV-1 p17 protein in CD8+ T cells (de Goede et al., 2009).

FUNCTIONAL VALIDATIONS BY MUTANTS

Viruses associated with carcinomas and tumors have presented high risks and occupied an important branch of cancer diagnostics. Deciphering virus and host interplays by Co-IP based proteomics could gain tremendous insights into malignant transformations of carcinomas as well as cellular differentiation and proliferations encountered. In addition, studying the effects of those negative mutants could greatly enhance the validity of proteomic data. Adenovirus (Adv) was a DNA virus model suitable for studying tumor oncogenesis, Komorek et al. (2010) successfully utilized TAP based proteomics to identify multiple cellular proteins interacting with the Adv oncoprotein E1A C-terminal region. The forkhead transcription factors, FOXK1/K2, were identified as novel factors specifically bound to E1A. Numerous recombinant adenoviruses carrying distinctive E1A exon 1 and exon 2 mutants were generated in order to map the specific E1A domain interacting with FOXK1/K2 by western blot analysis. One mutant lacking amino acids 224–238 in exon 2 was found to have significantly reduced staining with FOXKI/K2. Functionally, virus bearing this E1A exon 2 mutant was deficient in association with FOXK1/K2, resulting in enhanced cell proliferation and oncogenic transformation. Thus this indicated that the interaction between FOXK1/K2 with exon 2 of E1A could reversely suppress cell proliferation and oncogenic transformation. Human Papillomavirus (HPV) is another DNA virus causing anogenital carcinomas and oropharyngeal squamous cell carcinomas. The viral gene E7 is retained and integrated into the cancer cell chromosomes. Therefore its E7 oncoprotein plays important role in mediating malignant transformation. In one study, in order to find the novel binding partners of the E7 protein, a recombinant E7 from HPV-16 was constructed by tagging *S. japonicum* GST to its N-terminal, which could be recognized by immobilized glutathione. Human glutathione *S*-transferase P1-1 (GSTP1) was uniquely identified by MS. The interaction between E7 and GSTP1 was structurally characterized by three-dimensional docking program, which assisted to design a E7 mutant deficient in affinity binding with GSTP1 by subtracting residues Val 55, Phe 57, and Met 84. Although real-time PCR showed similar translation levels of GSTP1 in E7 and mutant group, GSTP1 in HPV E7 expressing cells apparently enhanced cell pro-survival abilities by suppressing Jun N-terminal kinase (JNK) mediated-phosphorylation signaling pathway to induce apoptosis. And siRNA knockdown of GSTP1 in HPV E7 expressing cells could reversely counteract this effect (Mileo et al., 2009).

Viral proteins important for manipulating viral gene expressions could be post-translationally modified, playing essential role as intrinsic functional proteins and cofactors assisting or inhibiting virus infection. Validations with viral PTM-deficient proteins by substituting PTM sites enable us to make a comparative study with the control group, uncovering the impact of these modified proteins at the functional level. For instance, ICP27 is one viral regulatory protein of herpes simplex virus type 1 (HSV-1). It is known to be post-translationally modified by kinases and arginine methyltransferases, and closely involved in viral protein export (Sandri-Goldin and Hibbard, 1996). ICP27 bears a glycine- and arginine-rich (GAR) region within an RGG box, which is characterized as an RNA binding domain mediating viral protein export. Souki et al. employed Co-IP approach to purify ICP27 in virus infected cells and performed independent trypsin, pepsin, and thermolysin digestion to comprehensively map the sequence of ICP27 by MALDI TOF/TOF MS (Souki et al., 2009). As a result, this combined protease digestion method was able to detect peptides covering of 90% of the ICP27 sequence, including the major arginine methylation sites, e.g., arginines 138, 148, and 150 within the RGG box. To functionally study the arginine methylation associated with virus infection, site-directed mutagenesis was used to construct point mutation (arginine to lysine) in ICP27, which was inserted in a plasmid and co-transfected with viral DNA into cells. The R150K mutant exhibited the most delayed virus maturations as well as smallest plaque size. Also, microarray assay revealed that both viral gene expression and replication were reduced in the mutants compared to the wild type, suggesting that the role of arginine methylation of ICP27 is closely associated with virus trafficking, assembly, as well as virus genome transcriptions. Similarly, phosphoprotein (P) of parainfluenza virus 5 (PIV5) was heavily phosphorylated and it was responsible for viral RNA synthesis upon infection (Sun et al., 2011b). IP was carried out to bait the viral P protein by using immobilized anti-V5-conjugated agarose, followed by SDS-PAGE gel and LC-MS/MS analysis. T286 of the P protein was found to be phosphorylated and it was further substituted by alanine, aspartic acid, or glutamic acid to study the effects of P mutants to viral infection. Compared to the wide type, the virus carrying the mutant P protein T286A was observed to have a slower growth rate as well as delayed viral mRNA synthesis at the transcription level. This work demonstrated that phosphorylation of the PIV5 P protein is important for virus replication and formation; however the detailed mechanism of key kinases involved in signaling pathways remains elusive. In another study, Duellman et al. (2009) used immobilized metal-affinity chromatography (IMAC) to enrich the phosphorylated peptides of EBV nuclear antigen 1 (EBNA1) followed by nano LC-MS/MS analysis, which resulted in identification of 10 phosphosites on EBNA1. In the subsequent validation works, all the 10 phosphosites were mutated to alanine by PCR mutagenesis and constructs were amplified in stable 293T cells after transfection. The phosphorylation of EBNA1 was essential to virus transcriptions as its phosphorylation-deficient mutant revealed a reduction on transcription activities.

What is more, some host proteins could also balance their distinctive PTM sites, and therefore manipulate cellular immune responses upon virus infections. Retinoic acid-inducible gene I (RIG-I) protein is one cytosolic receptor sensitive to viral RNAs. And this recognition could further undergo ubiquitination at Lys72, which enables to induce the innate immune responses, e.g., type-I IFNs, to inhibit the viral replication. Whereas under the normal condition, some kinases could phosphorylate RIG-I and thereby inhibit ubiquitination and downstream antiviral signal transduction. To map the phosphorylation sites on RIG-I, Gack et al. constructed the GST fusion vector inserted with the RIG-I PCR product, which was expressed in HEK293T cells (Gack et al., 2010). By employing GST pull-down and LC-MS/MS analysis, three phosphorylation sites in the N-terminal caspase recruitment domains (CARDs) of RIG-I were identified. It was hypothesized that phosphorylation at T170 suppresses ubiquitination at Lys172. The T170E mutant was generated to explore this hypothesis under normal circumstances, the phosphorylation level of RIG-I was markedly reduced after virus infection whereas its ubiquitination level was increased in a time-dependent manner. However, the T170E mutant lacked binding ability with tripartite motif protein 25 (TRIM25), which could induce ubiquitination and IFN signal transduction. Furthermore, Maharaj et al. (2012) successfully identified two upstream kinases, PKC -α and C-β that are responsible for phosphorylation of the RIG-I protein. Double knockdown of PKC- α/β by shRNA or siRNA revealed remarkably decreased phosphorylation levels, resulting in increased susceptibility of cells to virus infection.

FUNCTIONAL VALIDATIONS BY MICROARRAY PLATFORMS

In addition to MS based proteomics, protein microarrays have also been considered as a set of rapidly evolving technologies capable of identifying PPI networks, quantitatively profiling protein expression levels, and complementing the high throughput proteomic data (Sobek et al., 2006; Pollard et al., 2007). In the recent decade, much effort has been devoted to systematically study biochemical activities of proteins in a high throughput manner. Yet the major difficulties are screening an entire proteome by expressing clones, accommodating low volume proteins, and meanwhile retaining biochemical activities. Zhu et al. (2001) cloned 5800 open reading frames and purified corresponding proteins in order to construct a yeast proteome chip. GST-labeled proteins were immobilized onto the glass microscope slides through covalent attachment by using aldehyde-amine or nickel-HisX6 tags. In a parallel study, microarrays containing thousands of Cy3 or Cy5 labeled proteins were fabricated by a high-precision contact-printing robot to generate nanoliter protein spots on glass slide. Its applications, such as protein-small molecule and kinase-substrate interactions were successfully verified (MacBeath and Schreiber, 2000). In recent years, both proteomics and protein microarrays are predominantly used as reliable tools in glycomic profiling with a screening effect (Mahal, 2008). Characterization of protein-glycan interaction related to virus infection is another important task in the field of glycoproteomics and glycan microarrays. For instance, the binding specificity of influenza A virus with sialic acids is the main determinant for virus entry and species-dependent infection. To discover the detailed glycan-binding preference for the pandemic "triple reassortant" influenza A virus and a low infectious influenza A virus, Bateman et al. (2010) utilized MALDI TOF MS and GC-MS/MS to extensively map the linear or branched, N- or O-linked glycans expressed on the surface of primary swine respiratory epithelial cells (SRECs). Different sialic acid linkages, such as α-2, 3 or α-2, 6 linkage, were also determined by MS after corresponding sialidase digestions. Both NeuAc and NeuGc were identified on the SRECs surface with NeuAc occupying a much higher abundance. By applying glycomic microarray analysis, it revealed that both virus strains were ready to bind to NeuAcα2-6 glycans, sialylated polylactosamine and sialylated *N*-glycans. Therefore, the structural characterization of a wide variety of glycans by proteomics and functional microarray based on HA-sialic acid interactions could expand our knowledge on the molecular basis of virus-host interactions. In a similar study, Song et al. (2011) generated a total of 77 α-2, 3 or α-2, 6-sialylated structures incorporating different types of modified or nature sialic acids. All these sialylated glycans were examined by MALDI TOF MS and fabricated on a NHS-activated microarray glass slide. Several human influenza viruses, such as H1N1, H3N2 were tested on this glycan microarray, and both viruses were able to bind specifically to α-2, 6 linked sialic acid derivatives, α-2, 6 linked Neu5Ac, and α-2, 6 linked Neu5Ac9Lt. H1N1 displayed a broader range of binding specificities than H3N2 with an additional binding to α-2, 6-sialylatedNA2 structures. In this way integrated with proteomics, microarray screening of glycan-pathogen interactions with a wide variety of sialic acids provides an efficient way to explore glycan recognition at the molecular level.

What is more, these emerging large-scale screening technologies have tremendous impact on deciphering pathogen-host interplays. For instance, antiviral immune responses by production of type-I IFNs upon virus infection are regulated by TANK-binding kinase 1 (TBK1) and I-kB kinase ε (IKKi). TBK1 was observed to play a more profound role than IKKi (Hemmi et al., 2004). To understand the molecular interacting network of TBK1/IKKi involved in regulating IFNs upon virus infections, Goncalves et al. employed TAP based MS to study interacting partners of TBK1, IKKi, and their corresponding adaptor proteins, TANK, Sintbad, and NAP1. Consequently, MS identified 30 binding partners of these five proteins, representing a small interaction network of TBK1 and IKKi. Using RNA based microarray assay, overall changes at the transcription level were illustrated by intensity in response to virus infection or poly (I:C) simulation, and it was found that TBK1-TANK binding contributed greatly to the TBK1 activation (Goncalves et al., 2011). Clinically, high throughput proteome microarray bearing antigens of HPVs was able to examine immune responses and antigenicity of HPV proteins in a vast number of patients' serum samples (Luevano et al., 2010).

FUNCTIONAL VALIDATIONS BY ACTIVITY-BASED PROTEIN PROFILING

Although MS based proteomics has high throughput for identification of the altered proteome upon virus infections, it is unable to characterize the dynamic changes of enzymes, which could be induced by distinctive modifications, proteolytic processing, and alternative regulatory proteins. ABPP is a common functional technique designed to measure the dynamic changes of enzyme activities during virus infections (Cravatt et al., 2008; Blais et al.,

2012). The activity-based probes (ABPs) consist of two essential components: a warhead reactive group and a reporter tag, which are designed to covalently target the active site of enzymes and for purification or visualization, respectively. In addition, different levels of enzyme activity induced by viral or host proteins upon virus infections could be studied by comparative ABPP. A non-directed ABPP probe, PS4, was used to profile different levels of enzyme activity related to HCV replications in Huh7 cells (Singaravelu et al., 2010). Nine host candidates such as HSPA8, protein disulfide isomerase A5, and nuclear distribution gene C homolog were identified by MS based on comparative ABPP analysis. What is more, a FP-rhodamine ABPP probe was used to examine the host serine hydrolases required for HCV replication (Blais et al., 2010). After 2D gel, protein spots recognized by the FP-rhodamine ABPP probes were visualized by fluorescence prior to LC/MS/MS analysis. Carboxyl-esterase 1 (CES1) was identified as a differentially active enzyme involved in regulating triglycerides and cholesterol. siRNA knockdown of CES1 further resulted in reduced HCV replication levels and over-expression of CES1 benefited virus replications. To explore different activities of ubiquitin specific proteases under different pathological conditions, Ovaa et al. used HA-tagged Ub-derived active-site-directed probes to comparatively study the enzyme activities in healthy, virus infected, and tumor-derived cells. The altered USPs were purified and followed by LC/MS/MS analysis, resulting in identification of a list of up-regulated USPs in different stages of cellular differentiation (Ovaa et al., 2004). Furthermore, ABPP could also serve as a novel tool for discovering selective drugs or inhibitors. For instance, tetrahydroquinoline oxocarbazate was characterized as a blocker against SARS coronavirus and Ebola pseudotype virus by inhibiting cathepsin L, a member of human lysosomal cysteine proteases (Shah et al., 2010). Therefore, this breakthrough technology demonstrated its advantages by functionally identifying enzyme activities associated with a wide range of diseases, as well as filling up the gap that are unreachable to MS based proteomics.

CONCLUSION

Currently, challenging problems arise when the ever-expanding repertoire of diverse viral proteomes leaves a large number of viral proteins uninvestigated or even larger numbers of virus-host interactions functionally unverified. It relies heavily on high throughput technologies to elucidate the pathogenic biological networks involved in virus infections. At the interface between the realms of virology and proteomics, the conjunction of MS based proteomics with functional validation approaches exhibits a multidisciplinary effort to enhance our understanding into a wide range of viral diseases. These activity-based validation approaches integrated with proteomics include gene silencing, immunofluorescence staining, molecular cloning, drug inhibition, and microarrays, etc. Thus, it is important to stress that functional validations play an indispensable role to studying protein activities that are inaccessible to proteomic data along, contributing enormously and consistently to our understanding of pathogen-host interactions, vaccine designs, biomarker explorations, and drug discoveries.

ACKNOWLEDGMENTS

Kai Tang is supported by Ministry of Health of Singapore, Boon Huan Tan is supported by Defense Science and Technology Agency, and Richard Sugrue is supported by Ministry of Health of Singapore, National Research Foundation, and Defense Science and Technology Agency.

REFERENCES

Agrawal, R., Rewatkar, P. V., Kokil, G. R., Verma, A., and Kalra, A. (2010). Oseltamivir: a first line defense against swine flu. *Med. Chem.* 6, 247–251.

Bateman, A. C., Karamanska, R., Busch, M. G., Dell, A., Olsen, C. W., and Haslam, S. M. (2010). Glycan analysis and influenza A virus infection of primary swine respiratory epithelial cells: the importance of NeuAc{alpha}2-6 glycans. *J. Biol. Chem.* 285, 34016–34026.

Bhardwaj, K., Palaninathan, S., Alcantara, J. M., Yi, L. L., Guarino, L., Sacchettini, J. C., et al. (2008). Structural and functional analyses of the severe acute respiratory syndrome coronavirus endoribonuclease Nsp15. *J. Biol. Chem.* 283, 3655–3664.

Bhaskar, A., Bala, J., Varshney, A., and Yadava, P. (2011). Expression of measles virus nucleoprotein induces apoptosis and modulates diverse functional proteins in cultured mammalian cells. *PLoS ONE* 6, e18765. doi:10.1371/journal.pone.0018765

Blais, D. R., Lyn, R. K., Joyce, M. A., Rouleau, Y., Steenbergen, R., Barsby, N., et al. (2010). Activity-based protein profiling identifies a host enzyme, carboxylesterase 1, which is differentially active during hepatitis C virus replication. *J. Biol. Chem.* 285, 25602–25612.

Blais, D. R., Nasheri, N., Mckay, C. S., Legault, M. C. B., and Pezacki, J. P. (2012). Activity-based protein profiling of host-virus interactions. *Trends Biotechnol.* 30, 89–99.

Booy, A. T., Haddow, J. D., Ohlund, L. B., Hardie, D. B., and Olafson, R. W. (2005). Application of isotope coded affinity tag (ICAT) analysis for the identification of differentially expressed proteins following infection of atlantic salmon (Salmo salar) with infectious hematopoietic necrosis virus (IHNV) or Renibacterium salmoninarum (BKD). *J. Proteome Res.* 4, 325–334.

Bunai, K., and Yamane, K. (2005). Effectiveness and limitation of two-dimensional gel electrophoresis in bacterial membrane protein proteomics and perspectives. *J. Chromatogr. B Analyt. Technol. Biomed. Life Sci.* 815, 227–236.

Chen, C. H., Zhang, X. Q., Lo, C. W., Liu, P. F., Liu, Y. T., Gallo, R. L., et al. (2010). The essentiality of alpha-2-macroglobulin in human salivary innate immunity against new H1N1 swine origin influenza A virus. *Proteomics* 10, 2396–2401.

Chen, L. M., Tran, B. N., Lin, Q., Lim, T. K., Wang, F., and Hew, C. L. (2008). iTRAQ analysis of Singapore grouper iridovirus infection in a grouper embryonic cell line. *J. Gen. Virol.* 89, 2869–2876.

Ciborowski, P., Kadiu, I., Rozek, W., Smith, L., Bernhardt, K., Fladseth, M., et al. (2007). Investigating the human immunodeficiency virus type 1-infected monocyte-derived macrophage secretome. *Virology* 363, 198–209.

Cociorva, D., and Yates, J. R. (2007). Validation of tandem mass spectrometry database search results using DTASelect. *Curr. Protoc. Bioinformatics* Chap. 13, Unit 13.4.

Couzin, J. (2002). Breakthrough of the year. Small RNAs make big splash. *Science* 298, 2296–2297.

Craig, R., and Beavis, R. C. (2003). A method for reducing the time required to match protein sequences with tandem mass spectra. *Rapid Commun. Mass Spectrom.* 17, 2310–2316.

Craig, R., and Beavis, R. C. (2004). TANDEM: matching proteins with tandem mass spectra. *Bioinformatics* 20, 1466–1467.

Cravatt, B. F., Wright, A. T., and Kozarich, J. W. (2008). Activity-based protein profiling: from enzyme chemistry to proteomic chemistry. *Annu. Rev. Biochem.* 77, 383–414.

de Goede, A. L., Boers, P. H. M., Dekker, L. J. M., Osterhaus, A. D. M. E., Gruters, R. A., and Rimmelzwaan, G. F. (2009). Characterization of recombinant influenza A virus as a vector for HIV-1 p17(Gag). *Vaccine* 27, 5735–5739.

Deutsch, E. W., Mendoza, L., Shteynberg, D., Farrah, T., Lam, H., Tasman, N., et al. (2010). A guided tour of the Trans-Proteomic Pipeline. *Proteomics* 10, 1150–1159.

Deval, J., D'Abramo, C. M., Zhao, Z., McCormick, S., Coutsinos, D., Hess, S., et al. (2007). High resolution footprinting of the hepatitis C virus polymerase NS5B in complex with RNA. *J. Biol. Chem.* 282, 16907–16916.

Deyde, V. M., Xu, X. Y., Bright, R. A., Shaw, M., Smith, C. B., Zhang, Y., et al. (2007). Surveillance of resistance to adamantanes among influenza A(H3N2) and A(H1N1) viruses isolated worldwide. *J. Infect. Dis.* 196, 249–257.

Dreger, M., Leung, B. W., Brownlee, G. G., and Deng, T. (2009). A quantitative strategy to detect changes in accessibility of protein regions to chemical modification on heterodimerization. *Protein Sci.* 18, 1448–1458.

Duellman, S. J., Thompson, K. L., Coon, J. J., and Burgess, R. R. (2009). Phosphorylation sites of Epstein-Barr virus EBNA1 regulate its function. *J. Gen. Virol.* 90, 2251–2259.

Dykxhoorn, D. M., Novina, C. D., and Sharp, P. A. (2003). Killing the messenger: short RNAs that silence gene expression. *Nat. Rev. Mol. Cell Biol.* 4, 457–467.

Elbashir, S. M., Harborth, J., Lendeckel, W., Yalcin, A., Weber, K., and Tuschl, T. (2001). Duplexes of 21-nucleotide RNAs mediate RNA interference in cultured mammalian cells. *Nature* 411, 494–498.

Eng, J. K., Mccormack, A. L., and Yates, J. R. (1994). An approach to correlate tandem mass-spectral data of peptides with amino-acid-sequences in a protein database. *J. Am. Soc. Mass Spectrom.* 5, 976–989.

Engen, J. R. (2009). Analysis of protein conformation and dynamics by hydrogen/deuterium exchange MS. *Anal. Chem.* 81, 7870–7875.

Feng, H., Li, X., Niu, D., and Chen, W. N. (2010). Protein profile in HBx transfected cells: a comparative iTRAQ-coupled 2D LC-MS/MS analysis. *J. Proteomics* 73, 1421–1432.

Finlay, B. B., and McFadden, G. (2006). Anti-immunology: evasion of the host immune system by bacterial and viral pathogens. *Cell* 124, 767–782.

French, A. P., Mills, S., Swarup, R., Bennett, M. J., and Pridmore, T. P. (2008). Colocalization of fluorescent markers in confocal microscope images of plant cells. *Nat. Protoc.* 3, 619–628.

Fukagawa, Y., Nishikawa, J., Kuramitsu, Y., Iwakiri, D., Takada, K., Imai, S., et al. (2008). Epstein-Barr virus upregulates phosphorylated heat shock protein 27 kDa in carcinoma cells using the phosphoinositide 3-kinase/Akt pathway. *Electrophoresis* 29, 3192–3200.

Gack, M. U., Nistal-Villan, E., Inn, K. S., Garcia-Sastre, A., and Jung, J. U. (2010). Phosphorylation-mediated negative regulation of RIG-I antiviral activity. *J. Virol.* 84, 3220–3229.

Gaither, L. A., Borawski, J., Anderson, L. J., Balabanis, K. A., Devay, P., Joberty, G., et al. (2010). Multiple cyclophilins involved in different cellular pathways mediate HCV replication. *Virology* 397, 43–55.

Galan, C., Sola, I., Nogales, A., Thomas, B., Akoulitchev, A., Enjuanes, L., et al. (2009). Host cell proteins interacting with the 3 ' end of TGEV coronavirus genome influence virus replication. *Virology* 391, 304–314.

Goncalves, A., Burckstummer, T., Dixit, E., Scheicher, R., Gorna, M. W., Karayel, E., et al. (2011). Functional dissection of the TBK1 molecular network. *PLoS ONE* 6, e23971. doi:10.1371/journal.pone.0023971

Gonzalez, O., Fontanes, V., Raychaudhuri, S., Loo, R., Loo, J., Arumugaswami, V., et al. (2009). The heat shock protein inhibitor Quercetin attenuates hepatitis C virus production. *Hepatology* 50, 1756–1764.

Hamilton, A. J., and Baulcombe, D. C. (1999). A species of small antisense RNA in posttranscriptional gene silencing in plants. *Science* 286, 950–952.

Hammond, D. E., Hyde, R., Kratchmarova, I., Beynon, R. J., Blagoev, B., and Clague, M. J. (2010). Quantitative analysis of HGF and EGF-dependent phosphotyrosine signaling networks. *J. Proteome Res.* 9, 2734–2742.

Hamuro, Y., Coales, S. J., Southern, M. R., Nemeth-Cawley, J. F., Stranz, D. D., and Griffin, P. R. (2003). Rapid analysis of protein structure and dynamics by hydrogen/deuterium exchange mass spectrometry. *J. Biomol. Tech.* 14, 171–182.

Han, Y. T., Hsu, Y. H., Lo, C. W., and Meng, M. H. (2009). Identification and functional characterization of regions that can be crosslinked to RNA in the helicase-like domain of BaMV replicase. *Virology* 389, 34–44.

Hayden, F. G., and de Jong, M. D. (2011). Emerging influenza antiviral resistance threats. *J. Infect. Dis.* 203, 6–10.

Hemmi, H., Takeuchi, O., Sato, S., Yamamoto, M., Kaisho, T., Sanjo, H., et al. (2004). The roles of two IkappaB kinase-related kinases in lipopolysaccharide and double stranded RNA signaling and viral infection. *J. Exp. Med.* 199, 1641–1650.

Herberts, C. A., Meiring, H. M., van Gaans-van den Brink, J. A. M., van der Heeft, E., Poelen, M. C. M., Boog, C. J. P., et al. (2003). Dynamics of measles virus protein expression are reflected in the MHC class I epitope display. *Mol. Immunol.* 39, 567–575.

Hernandez, F. P., and Sandri-Goldin, R. M. (2010). Head-to-tail intramolecular interaction of herpes simplex virus type 1 regulatory protein ICP27 is important for its interaction with cellular mRNA export receptor TAP/NXF1. *mBio* 1, 1–9.

Holland, J., Spindler, K., Horodyski, F., Grabau, E., Nichol, S., and VandePol, S. (1982). Rapid evolution of RNA genomes. *Science* 215, 1577–1585.

Hwang, H. J., Moon, C. H., Kim, H. G., Kim, J. Y., Lee, J. M., Park, J. W., et al. (2007). Identification and functional analysis of salmon annexin 1 induced by a virus infection in a fish cell line. *J. Virol.* 81, 13816–13824.

Jackson, R. J., Cooper, K. L., Tappenden, P., Rees, A., Simpson, E. L., Read, R. C., et al. (2011). Oseltamivir, zanamivir and amantadine in the prevention of influenza: a systematic review. *J. Infect.* 62, 14–25.

Jorba, N., Juarez, S., Torreira, E., Gastaminza, P., Zamarreno, N., Albar, J. P., et al. (2008). Analysis of the interaction of influenza virus polymerase complex with human cell factors. *Proteomics* 8, 2077–2088.

Kanlaya, R., Pattanakitsakul, S. N., Sinchaikul, S., Chen, S. T., and Thongboonkerd, V. (2009). Alterations in actin cytoskeletal assembly and junctional protein complexes in human endothelial cells induced by dengue virus infection and mimicry of leukocyte transendothelial migration. *J. Proteome Res.* 8, 2551–2562.

Kanlaya, R., Pattanakitsakul, S. N., Sinchaikul, S., Chen, S. T., and Thongboonkerd, V. (2010a). The ubiquitin-proteasome pathway is important for dengue virus infection in primary human endothelial cells. *J. Proteome Res.* 9, 4960–4971.

Kanlaya, R., Pattanakitsakul, S. N., Sinchaikul, S., Chen, S. T., and Thongboonkerd, V. (2010b). Vimentin interacts with heterogeneous nuclear ribonucleoproteins and dengue nonstructural protein 1 and is important for viral replication and release. *Mol. Biosyst.* 6, 795–806.

Katoh, H., Mori, Y., Kambara, H., Abe, T., Fukuhara, T., Morita, E., et al. (2011). Heterogeneous nuclear ribonucleoprotein A2 participates in the replication of Japanese encephalitis virus through an interaction with viral proteins and RNA. *J. Virol.* 85, 10976–10988.

Kerppola, T. K. (2006). Visualization of molecular interactions by fluorescence complementation. *Nat. Rev. Mol. Cell Biol.* 7, 449–456.

Kerppola, T. K. (2008). Bimolecular fluorescence complementation: visualization of molecular interactions in living cells. *Methods Cell Biol.* 85, 431–470.

Kim, Y. C., Russell, W. K., Ranjith-Kumar, C. T., Thomson, M., Russell, D. H., and Kao, C. C. (2005). Functional analysis of RNA binding by the hepatitis C virus RNA-dependent RNA polymerase. *J. Biol. Chem.* 280, 38011–38019.

Komorek, J., Kuppuswamy, M., Subramanian, T., Vijayalingam, S., Lomonosova, E., Zhao, L. J., et al. (2010). Adenovirus type 5 E1A and E6 proteins of low-risk cutaneous beta-human papillomaviruses suppress cell transformation through interaction with FOXK1/K2 transcription factors. *J. Virol.* 84, 2719–2731.

Kong, L., Huang, C. C., Coales, S. J., Molnar, K. S., Skinner, J., Hamuro, Y., et al. (2010). Local conformational stability of HIV-1 gp120 in unliganded and CD4-bound states as defined by amide hydrogen/deuterium exchange. *J. Virol.* 84, 10311–10321.

Krumbholz, A., Philipps, A., Oehring, H., Schwarzer, K., Eitner, A., Wutzler, P., et al. (2011). Current knowledge on PB1-F2 of influenza A viruses. *Med. Microbiol. Immunol.* 200, 69–75.

Lai, C. C., Jou, M. J., Huang, S. Y., Li, S. W., Wan, L., Tsai, F. J., et al. (2007). Proteomic analysis of up-regulated proteins in human promonocyte cells expressing severe acute respiratory syndrome coronavirus 3C-like protease. *Proteomics* 7, 1446–1460.

Landeras-Bueno, S., Jorba, N., Perez-Cidoncha, M., and Ortin, J. (2011). The splicing factor proline-glutamine rich (SFPQ/PSF) is involved in influenza virus transcription. *PLoS Pathog.* 7, e1002397. doi:10.1371/journal.ppat.1002397

Lee, J. W., Liao, P. C., Young, K. C., Chang, C. L., Chen, S. S. L., Chang, T. T., et al. (2011). Identification of hnRNPH1, NF45, and C14orf166 as novel host interacting partners of the mature hepatitis C virus core protein. *J. Proteome Res.* 10, 4522–4534.

Lee, S. H., and Sinko, P. J. (2006). siRNA–getting the message out. *Eur. J. Pharm. Sci.* 27, 401–410.

Lin, J. Y., Li, M. L., Huang, P. N., Chien, K. Y., Horng, J. T., and Shih, S. R. (2008). Heterogeneous nuclear ribonuclear protein K interacts with the enterovirus 71 5' untranslated region and participates in virus replication. *J. Gen. Virol.* 89, 2540–2549.

Lisal, J., Lam, T. T., Kainov, D. E., Emmett, M. R., Marshall, A. G., and Tuma, R. (2005). Functional visualization of viral molecular motor by hydrogen-deuterium exchange reveals transient states. *Nat. Struct. Mol. Biol.* 12, 460–466.

Liu, H. P., Wu, C. C., and Chang, Y. S. (2006). PRA1 promotes the intracellular trafficking and NF-kappaB signaling of EBV latent membrane protein 1. *EMBO J.* 25, 4120–4130.

Liu, H. P., Wu, C. C., Kao, H. Y., Huang, Y. C., Liang, Y., Chen, C. C., et al. (2011). Proteome-wide dysregulation by PRA1 depletion delineates a role of PRA1 in lipid transport and cell migration. *Mol. Cell Proteomics* 10, 1–18.

Luevano, M., Bernard, H. U., Barrera-Saldana, H. A., Trevino, V., Garcia-Carranca, A., Villa, L. L., et al. (2010). High-throughput profiling of the humoral immune responses against thirteen human papillomavirus types by proteome microarrays. *Virology* 405, 31–40.

MacBeath, G., and Schreiber, S. L. (2000). Printing proteins as microarrays for high-throughput function determination. *Science* 289, 1760–1763.

Mahal, L. K. (2008). Glycomics: towards bioinformatic approaches to understanding glycosylation. *Anticancer Agents Med. Chem.* 8, 37–51.

Maharaj, N. P., Wies, E., Stoll, A., and Gack, M. U. (2012). Conventional protein kinase C-alpha (PKC-alpha) and PKC-beta negatively regulate RIG-I antiviral signal transduction. *J. Virol.* 86, 1358–1371.

Mannova, P., and Beretta, L. (2005). Activation of the N-Ras-PI3K-Akt-mTOR pathway by hepatitis C virus: control of cell survival and viral replication. *J. Virol.* 79, 8742–8749.

Marchand, V., Santerre, M., Aigueperse, C., Fouillen, L., Saliou, J. M., Van Dorsselaer, A., et al. (2011). Identification of protein partners of the human immunodeficiency virus 1 tat/rev exon 3 leads to the discovery of a new HIV-1 splicing regulator, protein hnRNP K. *RNA Biol.* 8, 325–342.

Mayer, D., Baginsky, S., and Schwemmle, M. (2005). Isolation of viral ribonucleoprotein complexes from infected cells by tandem affinity purification. *Proteomics* 5, 4483–4487.

Mayer, D., Molawi, K., Martinez-Sobrido, L., Ghanem, A., Thomas, S., Baginsky, S., et al. (2007). Identification of cellular interaction partners of the influenza virus ribonucleoprotein complex and polymerase complex using proteomic-based approaches. *J. Proteome Res.* 6, 672–682.

Metz, B., Kersten, G. F., Hoogerhout, P., Brugghe, H. F., Timmermans, H. A., de Jong, A., et al. (2004). Identification of formaldehyde-induced modifications in proteins: reactions with model peptides. *J. Biol. Chem.* 279, 6235–6243.

Mileo, A. M., Abbruzzese, C., Mattarocci, S., Bellacchio, E., Pisano, P., Federico, A., et al. (2009). Human papillomavirus-16 E7 interacts with glutathione S-transferase P1 and enhances its role in cell survival. *PLoS ONE* 4, e7254. doi:10.1371/journal.pone.0007254.

Mitzner, D., Dudek, S. E., Studtrucker, N., Anhlan, D., Mazur, I., Wissing, J., et al. (2009). Phosphorylation of the influenza A virus protein PB1-F2 by PKC is crucial for apoptosis promoting functions in monocytes. *Cell. Microbiol.* 11, 1502–1516.

Monroe, E. B., Kang, S., Kyere, S. K., Li, R., and Prevelige, P. E. (2010). Hydrogen/deuterium exchange analysis of HIV-1 capsid assembly and maturation. *Structure* 18, 1483–1491.

Moresco, J. J., Carvalho, P. C., and Yates, J. R. (2010). Identifying components of protein complexes in C. elegans using co-immunoprecipitation and mass spectrometry. *J. Proteomics* 73, 2198–2204.

Morton, V. L., Burkitt, W., O'Connor, G., Stonehouse, N. J., Stockley, P. G., and Ashcroft, A. E. (2010). RNA-induced conformational changes in a viral coat protein studied by hydrogen/deuterium exchange mass spectrometry. *Phys. Chem. Chem. Phys.* 12, 13468–13475.

Mota, S., Mendes, M., Penque, D., Coelho, A. V., and Cunha, C. (2008). Changes in the proteome of Huh7 cells induced by transient expression of hepatitis D virus RNA and antigens. *J. Proteomics* 71, 71–79.

Noisakran, S., Sengsai, S., Thongboonkerd, V., Kanlaya, R., Sinchaikul, S., Chen, S. T., et al. (2008). Identification of human hnRNP C1/C2 as a dengue virus NS1-interacting protein. *Biochem. Biophys. Res. Commun.* 372, 67–72.

Novina, C. D., and Sharp, P. A. (2004). The RNAi revolution. *Nature* 430, 161–164.

Ohman, T., Rintahaka, J., Kalkkinen, N., Matikainen, S., and Nyman, T. A. (2009). Actin and RIG-I/MAVS signaling components translocate to mitochondria upon influenza a virus infection of human primary macrophages. *J. Immunol.* 182, 5682–5692.

Orlando, V., Strutt, H., and Paro, R. (1997). Analysis of chromatin structure by in vivo formaldehyde cross-linking. *Methods* 11, 205–214.

Ovaa, H., Kessler, B. M., Rolen, U., Galardy, P. J., Ploegh, H. L., and Masucci, M. G. (2004). Activity-based ubiquitin-specific protease (USP) profiling of virus-infected and malignant human cells. *Proc. Natl. Acad. Sci. U.S.A.* 101, 2253–2258.

Park, S. K., Venable, J. D., Xu, T., and Yates, J. R. III. (2008). A quantitative analysis software tool for mass spectrometry-based proteomics. *Nat. Methods* 5, 319–322.

Pastorino, B., Boucomont-Chapeaublanc, E., Peyrefitte, C. N., Belghazi, M., Fusai, T., Rogier, C., et al. (2009). Identification of cellular proteome modifications in response to West Nile virus infection. *Mol. Cell. Proteomics* 8, 1623–1637.

Pattanakitsakul, S. N., Poungsawai, J., Kanlaya, R., Sinchaikul, S., Chen, S. T., and Thongboonkerd, V. (2010). Association of Alix with late endosomal lysobisphosphatidic acid is important for dengue virus infection in human endothelial cells. *J. Proteome Res.* 9, 4640–4648.

Perkins, D. N., Pappin, D. J., Creasy, D. M., and Cottrell, J. S. (1999). Probability-based protein identification by searching sequence databases using mass spectrometry data. *Electrophoresis* 20, 3551–3567.

Petrotchenko, E. V., and Borchers, C. H. (2010). Crosslinking combined with mass spectrometry for structural proteomics. *Mass Spectrom. Rev.* 29, 862–876.

Pollard, H. B., Srivastava, M., Eidelman, O., Jozwik, C., Rothwell, S. W., Mueller, G. R., et al. (2007). Protein microarray platforms for clinical proteomics. Proteomics Clinical Applications. *Proteomics. Clin. Appl.* 1, 934–952.

Pushparaj, P. N., Aarthi, J. J., Manikandan, J., and Kumar, S. D. (2008). siRNA, miRNA, and shRNA: in vivo applications. *J. Dent. Res.* 87, 992–1003.

Radhakrishnan, A., Yeo, D., Brown, G., Myaing, M. Z., Iyer, L. R., Fleck, R., et al. (2010). Protein analysis of purified respiratory syncytial virus particles reveals an important role for heat shock protein 90 in virus particle assembly. *Mol. Cell. Proteomics* 9, 1829–1848.

Ritchie, G., Harvey, D. J., Feldmann, F., Stroeher, U., Feldmann, H., Royle, L., et al. (2010). Identification of N-linked carbohydrates from severe acute respiratory syndrome (SARS) spike glycoprotein. *Virology* 399, 257–269.

Sandri-Goldin, R. M., and Hibbard, M. K. (1996). The herpes simplex virus type 1 regulatory protein ICP27 coimmunoprecipitates with anti-Sm antiserum, and the C terminus appears to be required for this interaction. *J. Virol.* 70, 108–118.

Scherer, L. J., and Rossi, J. J. (2003). Approaches for the sequence-specific knockdown of mRNA. *Nat. Biotechnol.* 21, 1457–1465.

Searle, B. C. (2010). Scaffold: a bioinformatic tool for validating MS/MS-based proteomic studies. *Proteomics* 10, 1265–1269.

Shah, P. P., Wang, T., Kaletsky, R. L., Myers, M. C., Purvis, J. E., Jing, H., et al. (2010). A small-molecule oxocarbazate inhibitor of human cathepsin L blocks severe acute respiratory syndrome and ebola pseudotype virus infection into human embryonic kidney 293T cells. *Mol. Pharmacol.* 78, 319–324.

Shahrour, N. (2001). The role of neuraminidase inhibitors in the treatment and prevention of influenza. *J. Biomed. Biotechnol.* 1, 89–90.

Sheu, T. G., Fry, A. M., Garten, R. J., Deyde, V. M., Shwe, T., Bullion, L., et al. (2011). Dual resistance to adamantanes and oseltamivir among seasonal influenza A(H1N1) viruses: 2008-2010. *J. Infect. Dis.* 203, 13–17.

Si, H., Verma, S. C., and Robertson, E. S. (2006). Proteomic analysis of the Kaposi's sarcoma-associated herpesvirus terminal repeat element binding proteins. *J. Virol.* 80, 9017–9030.

Singaravelu, R., Blais, D. R., McKay, C. S., and Pezacki, J. P. (2010). Activity-based protein profiling of the hepatitis C virus replication in Huh-7 hepatoma cells using a non-directed active site probe. *Proteome Sci.* 8, 5.

Smallcombe, A. (2001). Multicolor imaging: the important question of co-localization. *BioTechniques* 30, 1240–1246.

Sobek, J., Bartscherer, K., Jacob, A., Hoheisel, J. D., and Angenendt, P.

(2006). Microarray technology as a universal tool for high-throughput analysis of biological systems. *Comb. Chem. High Throughput Screen.* 9, 365–380.

Song, X., Yu, H., Chen, X., Lasanajak, Y., Tappert, M. M., Air, G. M., et al. (2011). A sialylated glycan microarray reveals novel interactions of modified sialic acids with proteins and viruses. *J. Biol. Chem.* 286, 31610–31622.

Souki, S. K., Gershon, P. D., and Sandri-Goldin, R. M. (2009). Arginine methylation of the ICP27 RGG box regulates ICP27 export and is required for efficient herpes simplex virus 1 replication. *J. Virol.* 83, 5309–5320.

Spurgers, K. B., Alefantis, T., Peyser, B. D., Ruthel, G. T., Bergeron, A. A., Costantino, J. A., et al. (2010). Identification of essential filovirion-associated host factors by serial proteomic analysis and RNAi screen. *Mol. Cell. Proteomics* 9, 2690–2703.

Sun, J. F., Shi, Z. X., Guo, H. C., Li, S., and Tu, C. C. (2011a). Proteomic analysis of swine serum following highly virulent classical swine fever virus infection. *Virol. J.* 8, 107.

Sun, D. Y., Luthra, P., Xu, P., Yoon, H., and He, B. A. (2011b). Identification of a phosphorylation site within the P protein important for mRNA transcription and growth of parainfluenza virus 5. *J. Virol.* 85, 8376–8385.

Tabb, D. L., McDonald, W. H., and Yates, J. R. III. (2002). DTASelect and Contrast: tools for assembling and comparing protein identifications from shotgun proteomics. *J. Proteome Res.* 1, 21–26.

Tan, F. L., and Yin, J. Q. (2004). RNAi, a new therapeutic strategy against viral infection. *Cell Res.* 14, 460–466.

Valiya Veettil, M., Sadagopan, S., Kerur, N., Chakraborty, S., and Chandran, B. (2010). Interaction of c-Cbl with myosin IIA regulates Bleb associated macropinocytosis of Kaposi's sarcoma-associated herpesvirus. *PLoS Pathog.* 6, e1001238. doi:10.1371/journal.ppat.1001238

Wahl, A., Schafer, F., Bardet, W., and Hildebrand, W. H. (2010). HLA class I molecules reflect an altered host proteome after influenza virus infection. *Hum. Immunol.* 71, 14–22.

Wiley, D. C., and Skehel, J. J. (1987). The structure and function of the hemagglutinin membrane glycoprotein of influenza virus. *Annu. Rev. Biochem.* 56, 365–394.

Xu, T., Venable, J. D., Park, S. K., Cociorva, D., Lu, B., Liao, L., et al. (2006). ProLuCID, a fast and sensitive tandem mass spectra-based protein identification program. *Mol. Cell Proteomics* 5, S174–S174.

Yan, W., Lee, H., Deutsch, E. W., Lazaro, C. A., Tang, W., Chen, E., et al. (2004). A dataset of human liver proteins identified by protein profiling via isotope-coded affinity tag (ICAT) and tandem mass spectrometry. *Mol. Cell. Proteomics* 3, 1039–1041.

Yates, J. R. (1998). Database searching using mass spectrometry data. *Electrophoresis* 19, 893–900.

Yates, J. R., Eng, J. K., Mccormack, A. L., and Schieltz, D. (1995). Method to correlate tandem mass-spectra of modified peptides to amino-acid-sequences in the protein database. *Anal. Chem.* 67, 1426–1436.

Zhang, J., Niu, D., Sui, J., Ching, C. B., and Chen, W. N. (2009). Protein profile in hepatitis B virus replicating rat primary hepatocytes and HepG2 cells by iTRAQ-coupled 2-D LC-MS/MS analysis: insights on liver angiogenesis. *Proteomics* 9, 2836–2845.

Zhao, C., Zhang, W., Tian, X., Fang, C., Lu, H., Yuan, Z., et al. (2010). Proteomic analysis of cell lines expressing small hepatitis B surface antigen revealed decreased glucose-regulated protein 78 kDa expression in association with higher susceptibility to apoptosis. *J. Med. Virol.* 82, 14–22.

Zheng, J., Sugrue, R. J., and Tang, K. (2011). Mass spectrometry based proteomic studies on viruses and hosts–a review. *Anal. Chim. Acta* 702, 149–159.

Zhu, H., Bilgin, M., Bangham, R., Hall, D., Casamayor, A., Bertone, P., et al. (2001). Global analysis of protein activities using proteome chips. *Science* 293, 2101–2105.

Zinchuk, V., and Grossenbacher-Zinchuk, O. (2009). Recent advances in quantitative colocalization analysis: focus on neuroscience. *Prog. Histochem. Cytochem.* 44, 125–172.

Zinchuk, V., Zinchuk, O., and Okada, T. (2007). Quantitative colocalization analysis of multicolor confocal immunofluorescence microscopy images: pushing pixels to explore biological phenomena. *Acta Histochem. Cytochem.* 40, 101–111.

Conflict of Interest Statement: The authors declare that the research was conducted in the absence of any commercial or financial relationships that could be construed as a potential conflict of interest.

Received: 16 August 2012; accepted: 25 October 2012; published online: 16 November 2012.

Citation: Zheng J, Tan BH, Sugrue R and Tang K (2012) Current approaches on viral infection: proteomics and functional validations. Front. Microbio. ***3****:393. doi: 10.3389/fmicb.2012.00393*

This article was submitted to Frontiers in Virology, a specialty of Frontiers in Microbiology.

frontiers in
MICROBIOLOGY

ORIGINAL RESEARCH ARTICLE
published: 20 September 2012
doi: 10.3389/fmicb.2012.00310

Non-biased enrichment does not improve quantitative proteomic delineation of reovirus T3D-infected HeLa cell protein alterations

Jieyuan Jiang*[1†], *Kolawole J. Opanubi*[1] and *Kevin M. Coombs*[1,2,3]

[1] Department of Medical Microbiology, Faculty of Medicine, University of Manitoba, Winnipeg, MB, Canada
[2] Manitoba Center for Proteomics and Systems Biology, University of Manitoba, Winnipeg, MB, Canada
[3] Manitoba Institute of Child Health, University of Manitoba, Winnipeg, MB, Canada

Edited by:
Ben Berkhout, University of Amsterdam, Netherlands

Reviewed by:
Hendrik Huthoff, King's College London, UK
Dave Speijer, University of Amsterdam, Netherlands

****Correspondence:***
Kevin M. Coombs, Manitoba Centre for Proteomics and Systems Biology, John Buhler Research Centre, Room 799, 715 McDermot Avenue, Winnipeg, MB, Canada R3E 3P4. e-mail: kcoombs@cc.umanitoba.ca

†Present address:
Jieyuan Jiang, Institute of Veterinary Medicine, Jiangsu Academy of Agricultural Sciences, Nanjing 210014, China.

Mass spectrometry-based methods have allowed elucidation of alterations in complex proteomes, such as eukaryotic cells. Such studies have identified and measured relative abundances of thousands of host proteins after cells are infected with a virus. One of the potential limitations in such studies is that generally only the most abundant proteins are identified, leaving the deep richness of the cellular proteome largely unexplored. We differentially labeled HeLa cells with light and heavy stable isotopic forms of lysine and arginine and infected cells with reovirus strain T3D. Cells were harvested at 24 h post-infection. Heavy-labeled infected and light-labeled mock-infected cells were mixed together 1:1. Cells were then divided into cytosol and nuclear fractions and each fraction analyzed, both by standard 2D-HPLC/MS, and also after each fraction had been reacted with a random hexapeptide library (Proteominer® beads) to attempt to enrich for low-abundance cellular proteins. A total of 2,736 proteins were identified by two or more peptides at >99% confidence, of which 66 were significantly up-regulated and 67 were significantly down-regulated. Up-regulated proteins included those involved in antimicrobial and antiviral responses, GTPase activity, nucleotide binding, interferon signaling, and enzymes associated with energy generation. Down-regulated proteins included those involved in cell and biological adhesion, regulation of cell proliferation, structural molecule activity, and numerous molecular binding activities. Comparisons of the r^2 correlations, degree of dataset overlap, and numbers of peptides detected suggest that non-biased enrichment approaches may not provide additional data to allow deeper quantitative and comparative mining of complex proteomes.

Keywords: RNA virus, virus infection, host cell alterations, mass spectrometry, liquid chromatography, bioinformatics

INTRODUCTION

The mammalian reoviruses (MRV) are non-enveloped viruses with genomes consisting of 10 segments of double-stranded RNA. MRV is the prototype member of the *Orthoreovirus* genus in the Reoviridae family and was first isolated in the respiratory and enteric tracts of healthy humans in the early 1950s. MRV infections are generally mild in humans. The Orthoreoviruses include non-fusogenic MRV and fusogenic avian reovirus. MRV consist of three serotypes. Each serotype has prototype strains: strain Lang (T1L) for serotype 1, strain Jones (T2J) for serotype 2, and strain Dearing (T3D) for serotype 3 (Tran and Coombs, 2006; Schiff et al., 2007). One of the most potentially useful characteristics of MRV is its ability to selectively kill certain cancer cells (Coffey et al., 1998; Forsyth et al., 2008; Thirukkumaran et al., 2010). An activated Ras pathway and functional p53 appear to be requirements for this selective oncolytic property (Coffey et al., 1998; Pan et al., 2011). Global analyses of oligonucleotide microarrays have detected activation of numerous cellular genes, including many related to apoptosis (Poggioli et al., 2002; DeBiasi et al., 2003). However, global alterations in proteins (the effector molecules) after MRV infection have not yet been reported.

Except for certain epigenetic events (reviewed in Goldberg et al., 2007), a cell's genome generally remains relatively constant. However, the cell's proteome (the total protein repertoire, including all co-translational and post-translational modifications) varies greatly due to its biochemical interactions with the genome, as well as the cell's interactions with the environment. In the case of viruses, which require the host cell's machinery and metabolism to replicate, the cell's proteome also reflects the specific alterations of the pathways induced by virus infection.

Previous analyses of how cells respond to virus infection have used microarray technologies which measure the cellular "transcriptome" (see for example; Geiss et al., 2002; Kobasa et al., 2007). However, there frequently is little concordance between microarray and protein data (Tian et al., 2004; Baas et al., 2006), partly because mRNA levels cannot provide complete information about levels of protein synthesis or extents of post-translational modifications. Thus, proteomic analyses have also been employed

to better understand host alterations induced by virus infection. These have included two-dimensional difference in gel electrophoresis (2D-DIGE; see for examples; Burgener et al., 2008; Lucitt et al., 2008), isotope coded affinity tags (ICAT; Booy et al., 2005; Stewart et al., 2006), isobaric tags for relative and absolute quantitation (iTRAQ; Dwivedi et al., 2009; Zhang et al., 2009), and stable isotope labeling by amino acids in cell culture (SILAC; Skiba et al., 2008). We have previously used SILAC to measure proteomic alterations in influenza virus-infected A549 cells (Coombs et al., 2010). Cells were labeled with either $^{12}C_6$-Lys and $^{12}C_6{}^{14}N_4$-Arg ("light"; **L**), or $^{13}C_6$-Lys and $^{13}C_6{}^{15}N_4$-Arg ("heavy"; **H**), because virtually every tryptic peptide is expected to contain an **L** or **H** label, thereby providing increased protein coverage. In addition, **L** and **H** samples are mixed together early in this process, thereby reducing sample-to-sample variability.

Most quantitative proteomic analyses succeed in identifying and measuring several 1,000 proteins. Head-to-head comparisons suggest SILAC identifies more proteins than other methods (reviewed in Coombs, 2011); however, the 3,000–5,000 identified in many such studies still represents a small fraction of the estimated entire eukaryotic proteome. It is generally assumed that high-abundance proteins are most easily detected and low-abundance proteins masked by other components (Zolotarjova et al., 2008). Some studies have attempted to deplete high-abundance proteins (for example Dwivedi et al., 2009) or to use methods to enrich for selected proteins (Jiang et al., 2007). Both of these methods potentially suffer from selective bias for specific proteins. We decided to attempt to enrich for low-abundance proteins by using Proteominer™ (PM) beads (Bio-rad), which consist of a "library" of 64 million random hexapeptides to non-selectively bind interacting partners. We succeeded in the current study in identifying and measuring 2,736 host proteins. Sixty six proteins were significantly up-regulated, including those involved in antimicrobial and antiviral responses, GTPase activity, nucleotide binding, interferon signaling, and enzymes associated with energy generation. Sixty seven proteins, including those involved in cell and biological adhesion, regulation of cell proliferation, structural molecule activity, and numerous molecular binding activities were significantly down-regulated. However, comparison of the numbers of proteins identified with or without PM enrichment suggests this type of non-biased enrichment may not contribute substantially to deeper proteomic elucidation.

MATERIALS AND METHODS

CELLS AND VIRUSES

Cell lines

Spinner-adapted mouse fibroblast L929 cells (L929) were grown in Joklik's modified minimal essential medium (J-MEM; Gibco, Grand Island, NY, USA) supplemented with 6% fetal bovine serum (FBS; Hyclone, Rockford, IL, USA), and 2 mM L-glutamine as described (Berard and Coombs, 2009). *Reovirus* was grown according to standard lab practice (Berard and Coombs, 2009).

Human HeLa cells were routinely cultured in Dulbecco's modified MEM (DMEM) supplemented with non-essential amino acids, sodium pyruvate, 0.2% (w/v) glucose, 10% FBS (Hyclone), and 2 mM L-glutamine. Cells were maintained as monolayers in 5% CO_2 and were passaged by trypsinization 2–3 times each week.

For SILAC labeling, cells were grown in DMEM media provided with a SILAC™ Phosphoprotein Identification and Quantification Kit (Invitrogen Canada Inc., Burlington, ON, Canada), supplemented as above (except without non-essential amino acids), and with 10% dialyzed FBS (Invitrogen Canada Inc.), plus 100 mg each of "light" (**L**) or "heavy" (**H**) L-lysine and L-arginine per liter of DMEM.

Viruses

Reovirus strain Type 3 Dearing (T3D) is a laboratory stock. Virus amplifications were routinely performed in L929 cell monolayers grown in the presence of 5% CO_2 at 37°C, supplemented with J-MEM as described above, except with 3% FBS instead of 6% FBS in the cell culture media, 100 U/ml of penicillin, 100 μg/ml streptomycin sulfate, and 100 μg/ml amphotericin-B as previously described (Berard and Coombs, 2009).

Virus purification

Large amounts of reovirus T3D were grown in 1 l suspension L929 cell cultures and purified by routine procedures involving Vertrel-XF™ extraction and cesium chloride (CsCl) ultracentrifugation (Mendez et al., 2000). Purified virions were then dialyzed against D-Buffer (150 mM NaCl, 15 mM $MgCl_2$, 10 mM Tris, pH 7.4). Virus concentration was measured by optical density at 260 nm, using the relationship 1 ODU = 2.1×10^{12} particles per milliliter (Smith et al., 1969) and infectivity was titrated.

Virus titrations

Serial 1:10 dilutions of virus samples were made in gel saline (137 mM NaCl, 0.2 mM $CaCl_2$, 0.8 mM $MgCl_2$, 19 mM HBO_3, 0.1 mM $Na_2B_4O_7$, and 0.3% w/v gelatin). HeLa cell and L929 cell monolayers in six-well plates were infected in duplicate, viruses allowed to attach to cells for 1 h with periodic rocking, and each well overlaid with a 50:50 ratio of 2% agar and 2× Medium 199 (M199) supplemented with a final concentration of 3% FBS, 2 mM L-glutamine, 100 U/ml of penicillin, 100 μg/ml streptomycin sulfate, and 100 μg/ml amphotericin-B. Plates were fed 3 days later with fresh agar/M199 and were stained with a 0.04% neutral red solution on day 6. Viral plaques were counted 15–18 h later and titers calculated (Berard and Coombs, 2009).

SILAC infection

Once HeLa cells had grown through six doublings in appropriate SILAC media, **H** cells were infected with gradient-purified T3D at a multiplicity of infection (MOI) of seven plaque forming units (PFU) per cell. An equivalent number of **L** cells were mock-infected with diluent as control. Cells were overlaid with appropriate media and cultured for 24 h.

CELL FRACTIONATION

At 24hpi, **L** and **H** cells in the T75 flasks were collected and counted. To verify infection status of each culture, aliquots of all cultures were saved for virus titration. For comparative SILAC assays, equivalent numbers of **L** and **H** cells were mixed together, and the mixed cells were washed 3× in >50 volumes of ice-cold Phosphate Buffered Saline (PBS). Washed cells were lysed with 0.5% NP-40, supplemented with 1.1 μM pepstatin A, incubated

on ice for 30 min, and nuclei removed by pelleting at 5,000 × *g* for 10 min. The cytosol and soluble membranes (supernatant) were transferred to a fresh microfuge tube; and the two fractions (nuclear pellet and supernatant) were frozen at −80˚C until further processing took place.

Thawed nuclei were extracted with one volume of High Salt Buffer (620 mM NaCl, 1 mM DTT, 10 mM Tris, pH 8.0), insoluble material pelleted at 15,000 × *g* for 10 min, and the supernatant removed and saved. Insoluble pellets were then extracted with 1/3rd volume of 8 M urea, insoluble material pelleted as above, the two extractions combined, and samples stored at −80˚C until further processing took place.

PROTEOMINER™ PURIFICATION

Approximately 90% of each fraction (cytosol and nucleus) was passed through separate PM Mini columns. The columns were processed according to manufacturer's protocol (Bio-Rad Corp). Briefly, the cytosolic and nuclear protein fractions were measured and each fraction concentrated to ≈20 mg/ml (∼1 ml). PM beads were washed twice with Wash Buffer then incubated with each concentrated protein sample for 2 h with end-to-end shaking. Columns were spun at 1,000 × *g* for 2 min to remove excess fluid, washed 3× with Wash Buffer, and then bound proteins eluted with two sequential applications of 200 µl One-step Elution Buffer.

WESTERN BLOTTING

Western blot analyses of HeLa cells were performed essentially as described previously (Coombs et al., 2010). Briefly, unlabelled cells were harvested essentially as described above and cytosolic proteins were resolved on a 10% SDS-PAGE gel at 120 V for 70 min. Proteins were transferred to polyvinylidenedifluoride (PVDF) membranes at 20 V for 30 min in a semi-dry apparatus, and the transfer confirmed by Ponceau staining. Membranes were blocked with 5% skim milk in TBST and probed with various antibodies in 1% BSA in TBST. Primary antibodies were: in-house rabbit anti-reovirus, α-GAPDH (Cell Signaling, cat#2118), α-IFIT2 (Abcam, cat#ab55837), and α-SAMD9 (Sigma cat#HPA021318), goat α-Mx1 (Santa Cruz cat#sc-34128), and mouse anti-STAT1 (Cell Signaling, cat#9176), α-Actin (Sigma, cat#A5441). The secondary antibodies were the appropriate horseradish peroxidase (HRP)-conjugated rabbit anti-mouse or goat anti-rabbit (Cell Signaling, cat#7076 and cat#7074, respectively). Bands were detected by enhanced chemiluminescence using an Alpha Innotech FluorChem Q Multi Image III instrument.

IMMUNOFLUORESCENT MICROSCOPY

HeLa cells were grown overnight in a 37˚C, 5% CO_2 incubator to 80% confluency on autoclaved 12-spot slides and then infected with MRV T3D at a MOI of seven or mock-infected. Mock, 0, 6, 12, and 24 h infected cells were washed 5× with PBS and fixed with 4% paraformaldehyde for 15 min at 4˚C. Cells were then washed 4× with 1× PBS and kept in 1× PBS at 4˚C until the 24 h time point was collected. Cells from all time points were then permeabilized with 0.1% TritonX-100 in 1× PBS for 5 min at 4˚C followed by five washes with 1× PBS. Cells were blocked with 1% BSA in 1× PBS and then treated with primary antibody (in-house rabbit anti-reovirus). Cells were then washed 5× with 1× PBS and treated with Alexa Fluor® 488 Goat anti-Rabbit (Invitrogen, cat#A11008) secondary antibody (all antibodies were diluted in 1% BSA in 1× PBS). Cells were then washed 5× with 1× PBS and Anti-fade prolong gold reagent with DAPI (Invitrogen, Cat# P36935) was added to each spot before slides were covered with coverslips, dried, and sealed. Slides were examined on a Zeiss Axio Observer Z1 inverted microscope using 10 and 20× objectives and fluorescence illumination using ExfoXcite. Images were acquired using AxioVision 4.8.2 software.

PROTEIN DIGESTION

Protein content in the non-purified ("standard") and PM-purified cytosolic and nuclear fractions collected as described above were determined using a BCA™ Protein Assay Kit (Pierce; Rockford, IL, USA) and BSA standards. After protein concentration determinations, samples were diluted with freshly made 100 mM ammonium bicarbonate to provide concentrations of ∼1 mg/ml and pH ∼ 8. Three hundred microliters of each sample (∼300 µg of protein) were reduced, alkylated, and trypsin digested as previously described (Coombs et al., 2010). Briefly, 30 µl of freshly prepared 100 mM dithiothreitol (DTT) in 100 mM ammonium bicarbonate was added, incubated for 45 min at 60˚C, 30 µl of freshly prepared iodoacetic acid (500 mM solution in 100 mM ammonium bicarbonate) was added, and the tubes were then incubated for 30 min at room temperature, in the dark. Finally, 50 µl of 100 mM DTT solution was added to quench the excess iodoacetic acid. Samples were digested overnight at 37˚C with 6 µg of sequencing grade trypsin (Promega, Madison, WI, USA). The samples were lyophilized and stored at −80˚C.

PEPTIDE FRACTIONATION USING 2D RP HPLC

A newly developed orthogonal procedure (Gilar et al., 2005; Spicer et al., 2007) was employed for 2D RP (reversed-phase) high pH – RP low pH peptide fractionation. Lyophilized tryptic digests were dissolved in 200 µl of 20 mM ammonium formate pH 10 (buffer A for first dimension separation), injected onto a 1 mm × 100 mm XTerra (Waters, Milford, MA, USA) column and fractionated using a 0.67% acetonitrile per minute linear gradient (Agilent 1100 Series HPLC system, Agilent Technologies, Wilmington, DE, USA) at a 150 µl/min flow rate. Sixty one-minute fractions were collected (covering ∼40% acetonitrile concentration range) and concatenated using procedures described elsewhere (Spicer et al., 2007; Dwivedi et al., 2008); the last 30 fractions were combined with the first 30 fractions in sequential order (i.e., #1 with #31; #2 with #32, etc.). Combined fractions were vacuum-dried and re-dissolved in buffer A for the second dimension RP separation (0.1% formic acid in water).

A split less nano-flow Tempo LC system (Eksigent, Dublin, CA, USA) with 20 µl sample injection via a 300 µm × 5 mm PepMap 100 pre-column (Dionex, Sunnyvale, CA, USA) and a 100 µm × 200 mm analytical column packed with 5 µm Luna C18(2; Phenomenex, Torrance, CA, USA) were used in the second dimension separation prior to MS analysis. Both eluents A (water) and B (acetonitrile) contained 0.1% formic acid as an ion-pairing modifier. A 0.33% acetonitrile per minute linear gradient (0–30% B) was used for peptide elution, providing a total 2 h run time per fraction in the second dimension.

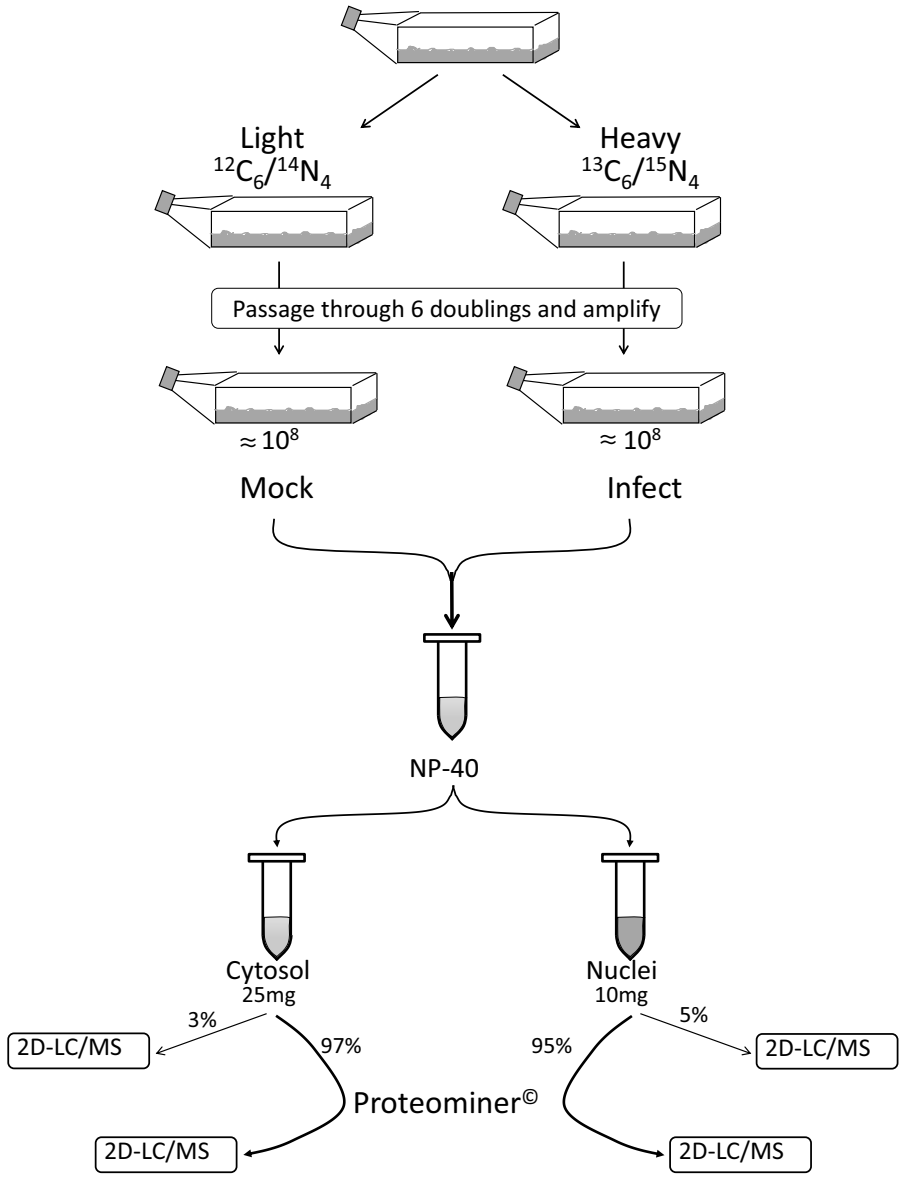

FIGURE 1 | Outline of experimental set-up. Cells were passaged through six doublings in either **L**ight or **H**eavy SILAC medium and the **H** cells infected with reovirus T3D. Infected (**H**) and mock-infected (**L**) cells were mixed together 1:1. After the cells were washed and lysed to separate cytosol from nucleus, 95–95% of each fraction was non-specifically enriched for low-abundance proteins by reaction with Proteominer™(PM) beads. Each of the four fractions (two PM-enriched as well as two residual 3–5% "standard" fractions) were then processed by 2D-HPLC/MS.

MASS SPECTROMETRY, BIOINFORMATICS, AND DATA MINING

A QStar Elite mass spectrometer (Applied Biosystems, Foster City, CA, USA) was used in a data-dependent MS/MS acquisition mode. One-second survey MS spectra were collected (m/z 400–1,500) followed by MS/MS measurements on the three most intense parent ions (80 counts/s threshold, $+2 \pm 4$ charge state, m/z 100–1,500 mass range for MS/MS), using the manufacturer's "smart exit" (spectral quality five) settings. Previously targeted parent ions were excluded from repetitive MS/MS acquisition for 60 s (50 mDa mass tolerance). Raw data files (30 in total for each run) were submitted for simultaneous search using standard SILAC settings for QStar instruments and were analyzed by Protein Pilot®, version 4.0, using the non-redundant human gene database. A decoy database search strategy (NCBInr *Homo sapiens* in which all protein sequences were reversed) was used to estimate the false discovery rate, which for this dataset was <0.8%. Proteins, and their confidences and **H:L** ratios, were returned with GeneInfo Identifier gi accession numbers. Proteins for which at least two fully trypsin digested **L** and **H** peptides were detected at >99% confidence were used for subsequent comparative quantitative analysis.

Differential regulation within each experimental dataset was determined by normalization of each dataset, essentially as

described (Keshamouni et al., 2009). Briefly, every **H:L** ratio was converted into $\log_2$ space to determine geometric means and facilitate normalization. The average $\log_2$ **H:L** ratios and SDs of the $\log_2$ **H:L** ratios were determined for each dataset. Every proteins' $\log_2$ **H:L** ratio was then converted into a z-score, using the formula:

$$\text{Z - score}\,(\sigma)\ \text{ of }\ [b] = \frac{\text{Log}_2\textbf{H:L}\,[b] - \text{average of}\ (\log_2 \text{ of each member},\ a \ldots n)}{\text{standard deviation of}\ (\log_2 \text{ of each member},\ a \ldots n)}$$

where "b" represents an individual protein in a dataset population $a \ldots n$, and z-score is the measure of how many SD units (expressed as "σ") that protein's $\log_2$ **H:L** ratio is away from its population mean. Thus, a protein with a z-score $>1.645\sigma$ indicates that protein's differential expression lies outside the 90% confidence level, $>1.960\sigma$ indicates outside the 95% confidence level, 2.576σ indicates 99% confidence, and 3.291σ indicates 99.9% confidence. z-Scores >1.960 were considered significant. gi numbers of all significantly regulated proteins were converted into HGNC identifiers by Uniprot[1] and HGNC terms were submitted to and analyzed by the DAVID bioinformatic suite at the NIAID, version 6.7 (Dennis et al., 2003; Huang et al., 2009a) and gene ontologies examined with the "FAT" datasets. The gi numbers were also submitted to, and pathways constructed with, Ingenuity Pathway Analysis software (IPA®).

RESULTS AND DISCUSSION

IDENTIFICATION OF ALTERED HOST PROTEINS

We combined $\sim 10^8$ **H**-labeled reovirus-infected HeLa cells with an equivalent amount of **L**-labeled non-infected cells, lysed the cells to generate cytosolic and nuclear fractions, and reacted ∼95% of each fraction with a commercially available random hexapeptide library (PM™) to enrich for low-abundance proteins. This strategy was chosen to attempt to complement the proteomic coverage of high-abundance and medium-abundance proteins expected from standard 2D-HPLC/MS processing (outlined in **Figure 1**). We also confirmed that the majority of HeLa cells demonstrated virus replication under our experimental conditions by 12–24hpi, as measured by immunofluorescent microscopy (**Figure 2**). Our standard 2D-HPLC/MS process identified 2,472 proteins from 21,989 non-redundant **H:L** peptide pairs in the cytosolic fraction. However, exclusion of those proteins whose identification confidence was <99% reduced the number of identified proteins to 1,903 (**Table 1**; **Figure 3A**). Using similar criteria, we found 1,657 proteins at ≥99% confidence in the cytosolic fraction reacted with the PM library and about 1,100 proteins in each of the nuclear fractions. Since crude nuclear fractions were frozen and no attempts were made to remove traces of cytosolic proteins from this fraction, these assays were meant to provide additional cell fractions rather than to allow meaningful distributional characterization and the "nuclear" fractions were expected to be contaminated with some cytosolic proteins.

[1]http://www.uniprot.org/

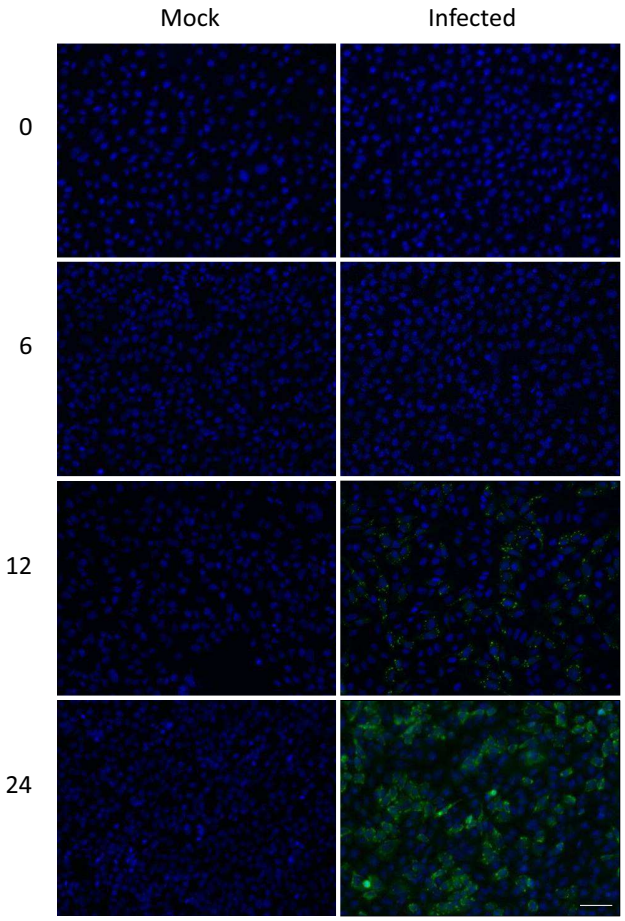

FIGURE 2 | Confirmation of HeLa cell infectivity. HeLa cells were mock-infected (left), or infected with MRV strain T3D at an MOI of 7 (right). Cells were harvested at indicated times post-infection (left) and processed for immunofluorescence microscopy, using in-house rabbit anti-reovirus and Alexa-488-conjugated secondary anti-rabbit antibody (green) and DAPI (blue). Scale bar is 50 μm.

Combination of all fractions, and removal of all proteins identified by only a single peptide, resulted in identification and measurement of 2,759 total unique protein pairs. Each protein's **H:L** ratio was converted to log space and inspection of each dataset indicated variability in each dataset's mean $\log_2$ value and in each dataset's $\log_2$ SD (**Figure 3B**; **Table 1**). Thus, every proteins' **H:L** ratio was converted into a z-score as described in Section "Materials and Methods" (and in Coombs et al., 2010) to facilitate comparisons of each dataset. A number of proteins with significantly high or low $\log_2$ values and corresponding z-scores represented keratins and other proteins identified in other studies as probable contaminants (i.e., S200 binding proteins); thus, these proteins were removed from further calculations.

Stratification of each protein's **H:L** ratio and its corresponding z-score indicated that numerous proteins in each sample could be considered significantly regulated. For example, of the 1,838 proteins identified in the standard cytosolic preparation, 40 were up-regulated at 95% confidence and 14 were also up-regulated

Table 1 | Number of peptides, proteins, log_2 H:L ratio means and SD, and *z*-scores of SILAC-measured HeLa cell proteins.

	Cytosol		Nuclei	
	Standard[1]	**Proteominer[2]**	**Standard**	**Proteominer**
Total number of peptide pairs[3]	24,927	17,484	14,594	13,108
Total number of proteins[4]	1,903	1,657	1,104	1,135
Number of proteins analyzed[5]	1,838	1,570	1,047	1,064
Mean log_2 H:L ratios	0.0124	0.0009	0.0055	0.0156
SD of log_2 H:L ratios	0.2759	0.3526	0.3035	0.3314
Number of proteins at *z*-score cutoff of: $\pm 1.960\sigma$ (95%)	40, 33[6]	34, 27	32, 29	18, 20
$\pm 2.576\sigma$ (99%)	21, 17	19, 20	14, 15	14, 15
$\pm 3.291\sigma$ (99.9%)	14, 5	8, 17	11, 7	8, 11

[1] *Indicated cellular fraction was trypsinized and directly processed by two-dimensional HPLC/MS.*

[2] *Indicated cellular fraction was incubated with Proteominer™ beads, eluted, trypsinized, and processed by 2-D HPLC/MS.*

[3] *Total number of **H:L** peptide pairs for all proteins identified at confidence level ≥99%.*

[4] *Total number of proteins identified at confidence level ≥99%.*

[5] *Number of proteins analyzed after those identified by only a single peptide, as well as possible contaminants, removed.*

[6] *First value is number of up-regulated proteins outside the indicated confidence level; second number is number of down-regulated proteins outside the indicated confidence level.*

at 99.9% confidence (**Table 1**). Thirty three proteins in the same dataset were down-regulated at 95% confidence, and five of these proteins were also down-regulated at 99.9% confidence. Inspection of protein **H:L** ratios and *z*-scores indicated that most proteins differentially regulated at >95% confidence had **H:L** ratios altered by >1.5-fold. Thus, proteins observed more than a single time were considered significantly regulated if at least one of their observations had a *z*-score $\geq 1.960\sigma$, if another observation in the same type of fraction (i.e., standard cytosolic and PM cytosolic) was no more than 0.75σ in the opposite direction, and if the average **H:L** ratio was >1.5-fold. Using the above criteria, we identified and measured 66 proteins that were significantly up-regulated and 67 proteins that were significantly down-regulated (**Table 2**).

Several of the up-regulated and non-regulated proteins that were identified and measured in the SILAC analysis were confirmed by Western blotting (**Figure 4**). Most Western blot results confirmed the SILAC-determined results although some differences in measured ratios probably reflect different levels of sensitivity of the two assays.

PROTEINS UP-REGULATED BY REOVIRUS INFECTION ARE ASSOCIATED WITH ANTIMICROBIAL AND ANTIVIRAL RESPONSES, GTPASE ACTIVITY, NUCLEOTIDE BINDING, INTERFERON SIGNALING, AND ENZYMES ASSOCIATED WITH ENERGY GENERATION

Proteins, and their levels of regulation, were analyzed by a variety of means. Protein gi numbers were imported into Uniprot (see text foot note 1) and converted into HUGO nomenclature committee (HGNC) identifiers. The HGNC IDs that represented significantly up-regulated and down-regulated proteins at the 95% confidence interval were then imported into DAVID (Dennis et al., 2003; Huang et al., 2009b), gene identifications converted to Entrez gene IDs by that suite of programs, and gene ontological biological processes and molecular functions identified at 95% confidence (**Figure 5**).

Up-regulated proteins were assigned to 18 GOTERM biological processes at 95% confidence (**Figure 5**, upper), that included cellular respiration, energy metabolism, and responses to viruses. Up-regulated proteins were also assigned to 11 functional groups (**Figure 5**) including primarily nucleotide binding. Protein gi numbers and levels of regulation were also imported into the Ingenuity Pathways Analysis (IPA®) tool which identified 13 GO categories (**Figure 6A**). Up-regulated proteins were enriched in growth factor, ion channel, kinase, phosphatase, and transmembrane receptor categories, whereas there were proportionally fewer up-regulated peptidase, translation regulators, and "other" (unknown) categories. Interacting pathways were also constructed by IPA. A total of 22 pathways were identified at a confidence level of 95% or greater. Five of these pathways, each with 11 or more "focus" members (significantly up- or down-regulated proteins), shared common members, and it was possible to build a single, merged pathway (**Figure 6B**). One other pathway (RNA post-transcriptional modification) contained only five focus molecules. The other 16 pathways consisted of several proteins, but contained only a single focus protein (data not shown). The five networks that contained 11 or more focus members corresponded to antimicrobial and inflammatory response; gastrointestinal disease; cell cycle, death, growth, proliferation, and movement; and DNA replication pathways (**Figure 6C**). Proteins present in the pathways and identified in our analyses as up-regulated are depicted in shades of red and include FADS3, IFIT1, and SAP130. Proteins present in the pathways and identified as down-regulated are shown in green and include AZGP1, LTF, and WDR5. Proteins present in the pathways and identified in our analyses, but neither up- nor down-regulated, are depicted in gray and include NF-KB complex, MAPK1, and TUBB, and proteins known to participate in the pathways but not identified in our analyses are shown in white and include AGER, IL28A, and MARK1–3. IPA analyses identify interaction nodes. For example, several of the highly up-regulated proteins interact with few other proteins,

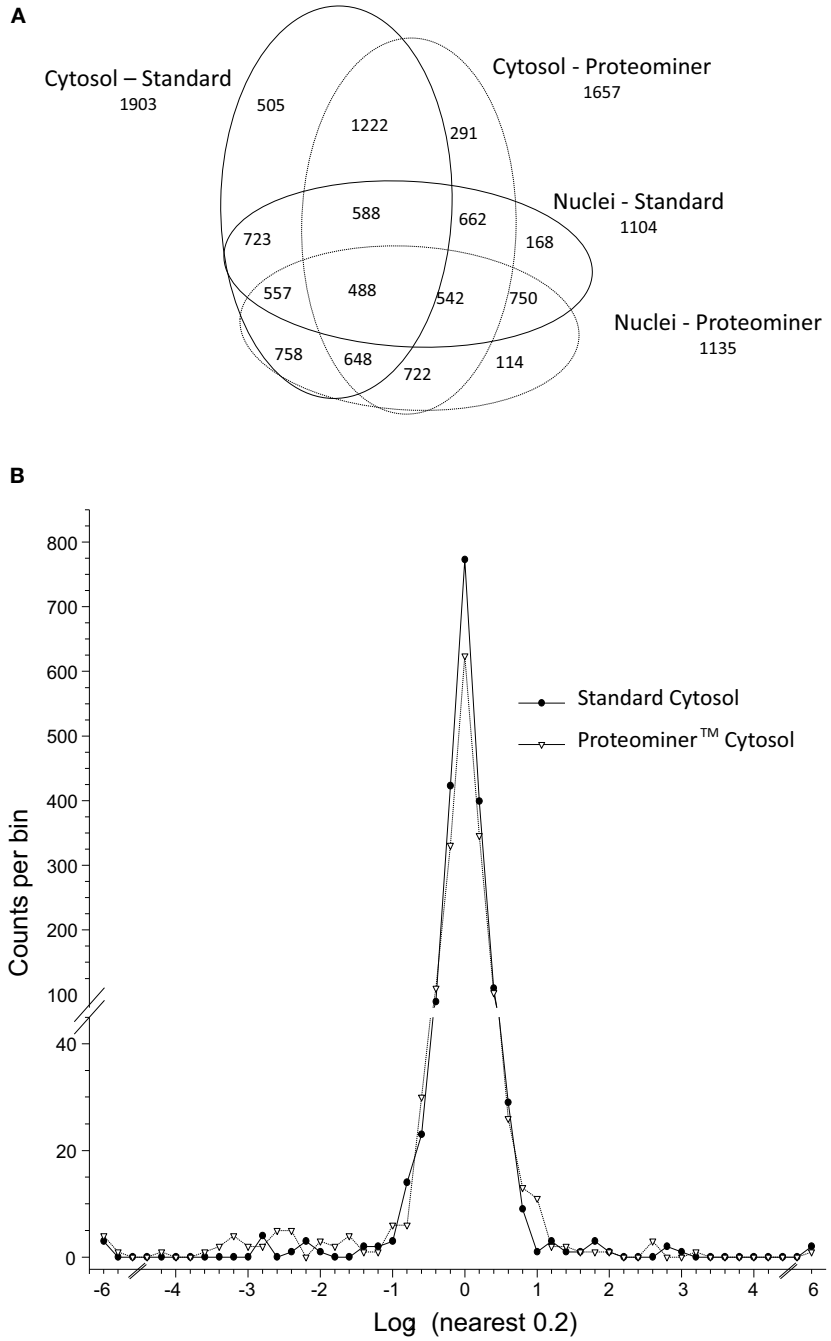

FIGURE 3 | Distributions of proteins identified in various experiments. **(A)** Venn diagram of numbers of identified proteins from various analyses. **(B)** Frequency distributions of identified proteins in two virus-infected sample sets, with **H:L** ratios expressed as $\log_2$ values. Positive values represent up-regulated host proteins in virus-infected cells; negative values represent down-regulated host proteins. Characteristics of all peptide and protein distributions, mean $\log_2$ **H:L** ratios, and SDs of $\log_2$ **H:L** ratios are shown in **Table 1**.

but some, such as STAT, ISG15, and Mx1 interact with four or more. Many of these molecules are involved in innate immunity. In addition, the interferon-induced, large GTPase dynamin-like Mx proteins are important anti viral proteins, particularly against RNA viruses (Haller and Kochs, 2002; Haller et al., 2009) and have been identified in several proteomic studies as up-regulated by influenza virus infection (Baas et al., 2006; Vester et al., 2009; Coombs, 2011). In addition, modulation of interferon response by reoviruses, including through STAT activation, has been demonstrated (Goody et al., 2007; Sherry, 2009; Zurney et al., 2009). Thus, our SILAC observations are validated by, and support, previous findings. Similarly, a few of the down-regulated proteins

Table 2 | Significantly affected HeLa cell proteins after reovirus infection.

Accession	HGNC ID	Name	Cytoplasm					Nucleus				
				Standard		Proteominer			Standard		Proteominer	
			Inf/ Mock[1]	# Peps	*z*-Score	# Peps	*z*-Score	Inf/ Mock[1]	# Peps	*z*-Score	# Peps	*z*-Score
UP-REGULATED PROTEINS												
Proteins detected in multiple similar fractions												
gi|8923450	SDHAF2	Succinate dehydrogenase assembly factor 2, mitochondrial precursor	50.6	4	**24.036**[2]	4	0.526					
gi|222136619	MX1	Myxovirus resistance protein 1	6.12	6	**6.583**	6	**8.839**	42.0	2	**21.873**	3	**5.234**
gi|116534937	IFIT1	Interferon-induced protein with tetratricopeptide repeats 1 isoform 2	6.45	6	**9.877**	4	**7.414**	2.67			2	**4.227**
gi|55741675	K0907	Hypothetical protein LOC22889						4.59	3	−0.368	3	**9.139**
gi|4826649	RM49	Mitochondrial ribosomal protein L49	4.58	2	**10.901**	2	0.178	0.95			8	−0.266
gi|4826774	ISG15	ISG15 ubiquitin-like modifier	3.80	10	**7.170**	5	**5.083**	3.29			4	**5.131**
gi|27881482	DDX58	DEAD/H (Asp-Glu-Ala-Asp/His) box polypeptide RIG-I	3.77	2	**6.322**	2	**5.832**					
gi|6274552	STAT1	Signal transducer and activator of transcription 1 isoform alpha	2.76	19	**5.372**	8	**3.952**	1.81	3	−1.456	6	**3.663**
gi|72534658	IFIT3	Interferon-induced protein with tetratricopeptide repeats 3	2.57	2	0.803	5	4.660	1.02			1	
gi|19743875	FUMH	Fumaratehydratase precursor	1.02	25	0.240	16	−0.136	2.24	4	**5.851**	4	0.098
gi|4507241	SSRP1	Structure specific recognition protein 1	2.12	8	**2.640**	1		0.01	2	**−21.042**		
gi|4506103	E2AK2	Eukaryotic translation initiation factor 2-alpha kinase 2 isoform a	1.95	6	**2.760**	10	**3.010**	1.59			6	**1.972**
gi|4506003	PP1A	Protein phosphatase 1, catalytic subunit, alpha isoform 1	0.94	23	−0.352			1.91	3	**4.587**	3	0.699
gi|112789562	IF16	Interferon, gamma-inducible protein 16	1.70	7	**2.314**	3	**2.858**	1.90	7	**2.219**	4	**3.824**
gi|42516576	GLRX5	Glutaredoxin 5	1.84	3	1.658	4	3.180					
gi|166706903	GBP1	Guanylate binding protein 1, interferon-inducible, 67 kDa	1.81	10	**2.380**	9	**2.933**					
gi|38016914	SAMH1	SAM domain- and HD domain containing protein 1	1.71	2	**4.006**	4	1.599					
gi|50592994	THIO	Thioredoxin	0.98	8	−0.430	11	0.070	1.69	2	−0.620	6	**2.876**
gi|48762920	K6PL	Liver phosphofructokinase	1.69	5	0.603	3	3.920					
gi|52630342	1C07	Major histocompatibility complex, class I, C precursor	1.67	14	0.382	16	3.194	1.27			3	1.007
gi|22035653	APOL2	Apolipoprotein L2	1.64	3	**2.583**	2	1.951					
gi|5031777	IDH3A	Isocitrate dehydrogenase 3 NAD(+) alpha precursor	0.97	18	−0.385	15	0.062	1.57	2	**2.162**	2	1.892
gi|223718097	OXA1L	Oxidase (cytochrome *c*) assembly 1-like	1.57	1		2	2.576					
gi|19923973	KCD12	Potassium channel tetramerization domain containing 12	1.07	7	0.328			1.57	2	**1.969**	3	**1.999**
gi|4758786	NDUS2	NADH dehydrogenase (ubiquinone) Fe-S protein 2	1.55	3	**2.985**	2	0.692	1.56			3	1.880
gi|5031863	LG3BP	Galectin 3 binding protein	1.55	7	1.474	13	**2.083**					
gi|62530384	ECI1	dodecenoyl-Coenzyme A delta isomerase precursor	0.99	12	−0.313	2	0.730	1.55	4	**2.281**	3	1.564
gi|9506689	EXOS4	Exosome component 4	1.08			5	0.297	1.53	2	**4.810**	5	0.132

(Continued)

Table 2 | Continued

Accession	HGNC ID	Name	Cytoplasm					Nucleus				
				Standard		Proteominer			Standard		Proteominer	
			Inf/ Mock[1]	# Peps	z-Score	# Peps	z-Score	Inf/ Mock[1]	# Peps	z-Score	# Peps	z-Score
Proteins detected multiple times/regulated at least once												
gi|33356547	MCM2	Minichromosome maintenance complex component 2	1.13	28	0.439	28	0.584	8.04			3	**9.026**
gi|5453740	ML12A	Myosin, light chain 12A, regulatory, non-sarcomeric	6.89	13	**10.050**			0.84			10	−0.811
gi|24307901	IFI35	Interferon-induced protein 35	3.71	2	**6.811**			3.04	3	**5.269**		
gi|5174513	SMAD3	mothers against decapentaplegic homolog 3 isoform 1	1.23			1		2.03			3	**3.044**
gi|4503049	CRIP2	Cysteine-rich protein 2	1.99			4	**2.809**	1.18			3	0.677
gi|148747351	PACN2	Protein kinase C and casein kinase substrate in neurons 2	1.70	3	**2.742**			1.04			2	0.103
gi|21956645	MTPN	Myotrophin	1.07	3	0.323			1.68			2	**2.211**
gi|33469966	SCFD1	Vesicle transport-related protein isoform a	0.98	3	1.814	8	−0.875	1.68	4	**2.439**		
gi|5902076	SRSF1	Splicing factor, arginine/serine-rich 1 isoform 1	1.63			2	**1.994**	1.07	14	0.109	25	0.336
gi|39780588	TSR1	TSR1, 20S rRNA accumulation	1.00	1				1.58	4	**2.147**		
gi|13540606	CLPB	Caseinolytic peptidase B	1.52	2	**2.158**			0.49	1			
Proteins detected once												
gi|17921993	TBA3C	Tubulin, alpha 3c	100	86	**24.036**							
gi|31543983	ARFG2	ADP-ribosylation factor GTPase activating protein 2						5.73	3	**8.278**		
gi|4758442	GMFB	Glia maturation factor, beta	3.03	2	**5.754**							
gi|19923597	SP130	Sin3A-associated protein, 130 kDa isoform b						2.49	2	**4.318**		
gi|13375616	FADS3	Fatty acid desaturase 3	2.14	2	**3.931**							
gi|74271837	GLNA	Glutamine synthetase	2.01			3	**2.852**					
gi|4502209	ARF5	ADP-ribosylation factor 5						1.90			3	**2.747**
gi|70608211	NT5C3	5(-Nucleotidase, cytosolic III isoform 2	1.88			3	**2.587**					
gi|20631967	BAX	Apoptosis regulator BAX isoform sigma	1.87			2	**2.559**					
gi|4757876	BST2	Bone marrow stromal cell antigen 2						1.87			4	**2.666**
gi|222144328	MYL12B[3]	Myosin regulatory light chain MRCL2 isoform B						1.83	6	**2.847**		
gi|53828918	PGTA	Rabgeranylgeranyltransferase alpha	1.83			2	**2.459**					
gi|190014625	RRP44	DIS3 mitotic control isoform b						1.81	2	**2.810**		
gi|5729820	SYFM	Phenylalanyl-tRNAsynthetase 2 precursor	1.79			2	**2.382**					
gi|4505467	NT5E	5′ Nucleotidase isoform 1 preproprotein						1.74	2	**2.618**		
gi|4505895	PLRG1	Pleiotropic regulator 1 (PRL1 homolog, *Arabidopsis*)						1.71	2	**2.540**		
gi|4505587	PA1B3	Platelet-activating factor acetylhydrolase, isoform Ib, gamma subunit	1.67	2	**2.634**							
gi|28395033	RHOC	Ras homolog gene family, member C precursor	1.62			18	**1.981**					
gi|148536825	CO4A1	Alpha 1 type IV collagen preproprotein	1.59	2	**2.380**							

(Continued)

Table 2 | Continued

Accession	HGNC ID	Name	Cytoplasm					Nucleus				
				Standard		Proteominer			Standard		Proteominer	
			Inf/ Mock[1]	# Peps	z-Score	# Peps	z-Score	Inf/ Mock[1]	# Peps	z-Score	# Peps	z-Score
gi|71044479	DIDO1	Death inducer-obliterator 1 isoform c						1.58	3	**2.153**		
gi|9955963	ABCB6	ATP-binding cassette, sub-family B, member 6	1.56	4	**2.294**							
gi|56676335	RIF1	RAP1 interacting factor 1						1.56	2	**2.083**		
gi|40254978	FIP1	FIP1 like 1 isoform 1						1.54	4	**2.041**		
gi|7706481	CAB39	Calcium binding protein 39	1.54	5	**2.203**							
gi|221316634	LMO7	LIM domain only 7 isoform 2						1.53	6	**1.991**		
gi|194473714	LXN	Latexin	1.52	3	**2.155**							
gi|8923219	TRM1	tRNAmethyltransferase 1 isoform 1	1.50	6	**2.072**							
DOWN-REGULATED PROTEINS												
Proteins detected in multiple similar fractions												
gi|4507241	SSRP1	FACT complex subunit SSRP1	2.12	8	**2.640**	1		0.012	2	**−21.042**		
gi|4506457	RCN2	Reticulocalbin 2 precursor	0.86	14	−0.076	27	−0.993	0.32			2	**−4.994**
gi|4505751	PROF2	Profilin 2 isoform b	0.91	8	−0.215	9	−0.601	0.46			3	**−3.447**
gi|7661832	SSU72	Ssu72 RNA polymerase II CTD phosphatase homolog	0.84	3	−1.873	3	−0.127	0.52			3	**−2.902**
gi|4506929	SH3G1	SH3 domain GRB2-like 1	0.57	5	**−3.424**	3	−1.835	27.85	3	**21.873**	8	−1.062
gi|72534660	SRSF7	Splicing factor, arginine/serine-rich 7	0.57	2	0.155	5	**−3.972**	0.91	6	−1.680	12	0.031
gi|7661672	PDIP2	DNA polymerase delta interacting protein 2	0.88	5	−0.696	3	−0.516	0.58			2	**−2.426**
gi|4758340	SYFA	Phenylalanyl-tRNAsynthetase, alpha subunit	0.96	9	−0.532	13	−0.003	0.58	4	**−2.095**	6	**−2.721**
gi|31543415	G45IP	Growth arrest and DNA-damage-inducible, gamma interacting protein 1						0.60	3	**−21.042**	4	0.149
gi|45359846	G3BP2	Ras-GTPase activating protein SH3 domain-binding protein 2 isoform b						0.60	12	**−3.099**	9	−1.520
gi|4507467	BGH3	Transforming growth factor, beta-induced, 68kDa precursor	0.64	7	**−3.152**	6	−1.196	0.82			5	−0.890
gi|40353740	LARP4	La-related protein 4 isoform b	0.65	1		3	**−2.585**	1.27			2	0.997
gi|4503523	EIF3D	Eukaryotic translation initiation factor 3 subunit D	1.07	8	0.672	3	−0.582	0.66	4	**−2.237**	1	
Proteins detected multiple times/regulated at least once												
gi|16554629	WDR5	WD repeat domain 5	0.011	4	**−23.627**			1.00	2	0.001	2	−0.034
gi|4502337	ZA2G	Alpha-2-glycoprotein 1, zinc	0.11			2	**−8.924**	0.012			2	**−19.301**
gi|60097902	FLG	Filaggrin	0.01			2	**−18.099**	1.99			1	
gi|4557894	LYSC	Lysozyme precursor	0.11			5	**−8.960**	0.17			1	
gi|4505821	PIP	Prolactin-induced protein	0.33			3	**−4.601**	0.29			2	−5.451
gi|58530840	DESP	Desmoplakin isoform I	0.30			11	**−4.902**	0.47			2	−3.371
gi|8922652	ARFG1	ADP-ribosylation factor GTPase activating protein 1 isoform a	1.07			4	0.290	0.46			2	−3.437
gi|116235460	YTHD3	YTH domain family, member 3	0.50			4	**−2.822**	0.88	5	**−3.099**	11	0.145
gi|13129040	SPATA5L1	Spermatogenesis associated 5-like 1	1.12			2	0.454	0.52	2	**−3.090**		
gi|145580575	CTBP2	C-Terminal binding protein 2 isoform 2	1.07			9	0.282	0.53			4	**−2.827**
gi|4826730	MTOR	FK506 binding protein 12-rapamycin associated protein 1	0.99	2	−0.092			0.55	4	**−2.860**		
gi|47271443	SRSF2	Splicing factor, arginine/serine-rich 2	0.56	4	**−3.068**			1.35	5	−1.187	3	**3.590**

(Continued)

Table 2 | Continued

Accession	HGNC ID	Name	Cytoplasm					Nucleus				
				Standard		Proteominer			Standard		Proteominer	
			Inf/ Mock[1]	# Peps	z-Score	# Peps	z-Score	Inf/ Mock[1]	# Peps	z-Score	# Peps	z-Score
gi|4506901	SRSF3	Splicing factor, arginine/serine-rich 3	0.60			5	**−2.120**	0.99	12	0.465	17	−0.448
gi|4885245	FOSL2	FOS-like antigen 2	0.91			2	−0.402	0.60			2	**−2.271**
gi|20127486	PLIN3	Perilipin-3 isoform 1	1.00	24	−0.045			0.61	3	**−2.391**		
gi|7657176	CNPY2	Canopy 2 homolog	0.96	12	−0.242			0.61	2	**−2.337**		
gi|56118310	NUCKS	Nuclear casein kinase and cyclin-dependent kinase substrate 1	1.01	4	0.017			0.66	6	**−2.022**		
gi|89276751	CO5A1	Alpha 1 type V collagen preproprotein	0.86	10	−0.815			0.66	3	**−2.022**		
Proteins detected once												
gi|4885477	MYG	Myoglobin	0.012			2	**−18.099**					
gi|61835172	FXR1	Fragile X mental retardation-related protein 1 isoform c						0.012			2	**−19.301**
gi|119703744	DSG1	Desmoglein 1 preproprotein	0.10			4	**−9.424**					
gi|62122917	FILA2	Filaggrin family member 2	0.11			3	**−9.185**					
gi|54607120	TRFL	Lactotransferrin precursor	0.12			5	**−8.747**					
gi|189458821	TGM3	Transglutaminase 3 precursor	0.18			2	**−6.951**					
gi|38348366	SBSN	Suprabasin						0.21			2	**−6.925**
gi|4885165	CYTA	Cystatin A						0.22			2	**−6.580**
gi|15187164	LACRT	Lacritin precursor	0.24			2	**−5.876**					
gi|170296790	A8CED1	Mesotrypsin isoform 1 preproprotein						0.25	6	**−6.665**		
gi|239755818	LOC100293351[3]	PREDICTED: hypothetical protein isoform 2	0.35			2	**−4.275**					
gi|221316620	CD123	Cell division cycle 12	0.38	3	**−5.063**							
gi|116686122	KIF4A	Kinesin family member 4						0.42	2	**−4.187**		
gi|4501889	ACTH	Actin, gamma 2 propeptide	0.44	85	**−4.302**							
gi|14327896	CCNB1	cyclin B1						0.48	2	**−3.487**		
gi|48762942	HIP1R	Huntingtin interacting protein-1-related						0.50	2	**−3.304**		
gi|155722990	SLC4A1AP	Kanadaptin						0.53	2	**−3.018**		
gi|50658084	BCAT2	Branched chain aminotransferase 2, mitochondrial	0.55	4	**−3.200**							
gi|47825361	NCRP1	Non-specific cytotoxic cell receptor protein 1 homolog	0.56			2	**−2.346**					
gi|4502951	CO3A1	Collagen type III alpha 1 preproprotein	0.57	5	**−2.948**							
gi|114796644	RCC1	Regulator of chromosome condensation 1 isoform a	0.58	3	**−2.920**							
gi|7705999	TMEM9	Transmembrane protein 9	0.58	2	**−2.911**							
gi|19882251	CYTN	Cystatin SN precursor	0.58			3	**−2.238**					
gi|154240704	TM192	Transmembrane protein 192	0.58			2	**−2.210**					
gi|82546824	FOXK1	Forkhead box K1	0.58	3	**−2.866**							
gi|190684694	UBP8	Ubiquitin specific peptidase 8						0.59	2	**−2.567**		
gi|221219053	DNAJC7	DnaJ (Hsp40) homolog, sub-family C, member 7 isoform 1	0.59	3	**−2.795**							
gi|7657655	TRAM1	Translocation associated membrane protein 1						0.63	3	**−2.199**		
gi|4557555	EGLN	Endoglin isoform 2 precursor	0.64	2	**−2.420**							
gi|46909600	ADA15	A disintegrin and metalloproteinase domain 15 isoform 6 preproprotein	0.64	3	**−2.370**							
gi|8393009	FFR	Chromosome 11 open reading frame2	0.64	2	**−2.346**							

(Continued)

Table 2 | Continued

Accession	HGNC ID	Name	Cytoplasm					Nucleus				
				Standard		Proteominer			Standard		Proteominer	
			Inf/ Mock[1]	# Peps	*z*-Score	# Peps	*z*-Score	Inf/ Mock[1]	# Peps	*z*-Score	# Peps	*z*-Score
gi|109255232	CE170	Centrosomal protein 170 kDa isoform gamma	0.65	2	**−2.330**							
gi|63176611	SLTM	SAFB-like transcription modulator isoform a						0.65	5	**−2.051**		
gi|5453958	PPP5	Protein phosphatase 5, catalytic subunit	0.66	3	**−2.249**							
gi|8922331	MGN2	Mago-nashi homolog B						0.66	4	**−1.986**		
gi|30061491	E41L1	Erythrocyte membrane protein band 4.1-like 1 isoform b	0.665	5	**−2.178**							

[1]*Weighted* ***H:L*** *ratios, scaled to number of measured peptides in each sample, if detected in both Standard and Proteominer samples.*

[2]*Bolding indicates a significant z-score (95% confidence), either > 1.960 or <−1.960.*

[3]*Gene removed from NCBI database.*

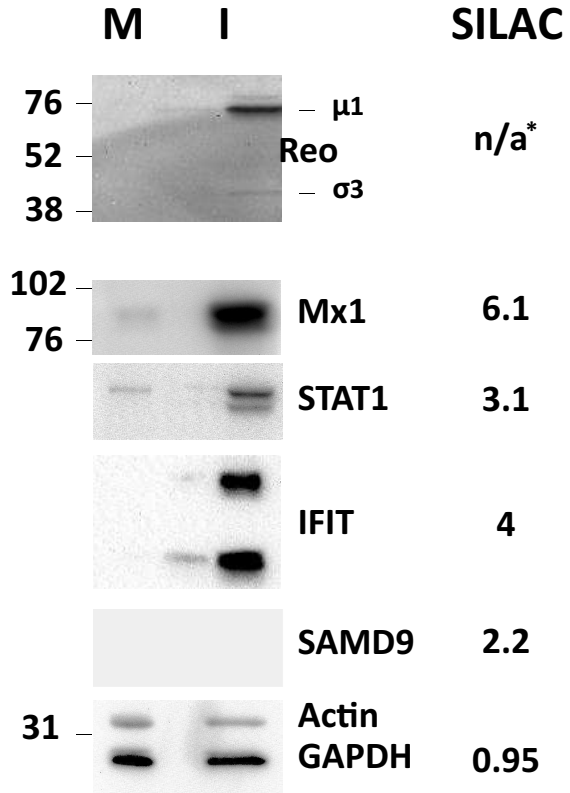

FIGURE 4 | Western blot validation of experimentally determined SILAC ratos. HeLa cells were harvested and lysed with 0.5% NP-40 detergent, nuclei removed, and cytosolic fractions dissolved in SDS electrophoresis sample buffer. Proteins were resolved in 10% mini-SDS-PAGE, transferred to PVDF, and probed with indicated antibodies. Bands were visualized, and intensities measured, with an Alpha Innotech FluorChem®Q Multi Image® III instrument. Molecular weight standards are indicated at left and SILAC-measured ratios are indicated on the right. ∗, No viral proteins measured by SILAC as these are absent from mock-infected samples.

interact with few partners, but several, including WDR5, appear as interaction "hubs." We identified numerous other interaction hubs, such as LGAL53 and NF-KB which were not, themselves, significantly altered, but which interacted with several differentially regulated proteins.

PROTEINS DOWN-REGULATED BY REOVIRUS INFECTION ARE ASSOCIATED WITH CELL DIFFERENTIATION, DERMAL DIFFERENTIATION, AND MOLECULAR BINDING

Down-regulated proteins were assigned to 33 biological processes at 95% confidence (**Figure 5**, lower), that included cell differentiation, peptide cross-linking, and ectoderm and endoderm development. Down-regulated proteins were also assigned to seven functional groups, including structural molecule activity and various factor binding roles (**Figure 5**). IPA-generated GO categories indicated down-regulated proteins were enriched in unknown categories whereas there were proportionally fewer down-regulated enzymatic and transporter categories (**Figure 6A**). Additional IPA pathway analyses indicated numerous components of the "Interferon signaling" and "Role of PKR in interferon induction and antiviral response" canonical pathways were significantly up-regulated, whereas numerous arms of the "Regulation of actin-based motility by rho" canonical pathway were down-regulated (data not shown).

PROTEOMINER ENRICHMENT LED TO IDENTIFICATION OF COMPARABLE NUMBERS OF PROTEINS, BUT PM-ENRICHED PROTEINS WERE IDENTIFIED BY FEWER PEPTIDES

As indicated earlier, 1,903 proteins were identified in the standard cytosolic fraction, compiled from 24,927 **H:L** peptide pairs (**Table 1**). This corresponds to an average of 13.1 peptides/protein (SD ± 20.5; **Figure 7**). In contrast, PM enrichment of the cytosolic fraction led to identification of 17,484 **H:L** peptide pairs and 1,657 proteins (average = 10.3 peptides, ±15.8). Slightly more proteins were identified in the PM-enriched nuclear fraction than in the standard nuclear fraction, but the average numbers of

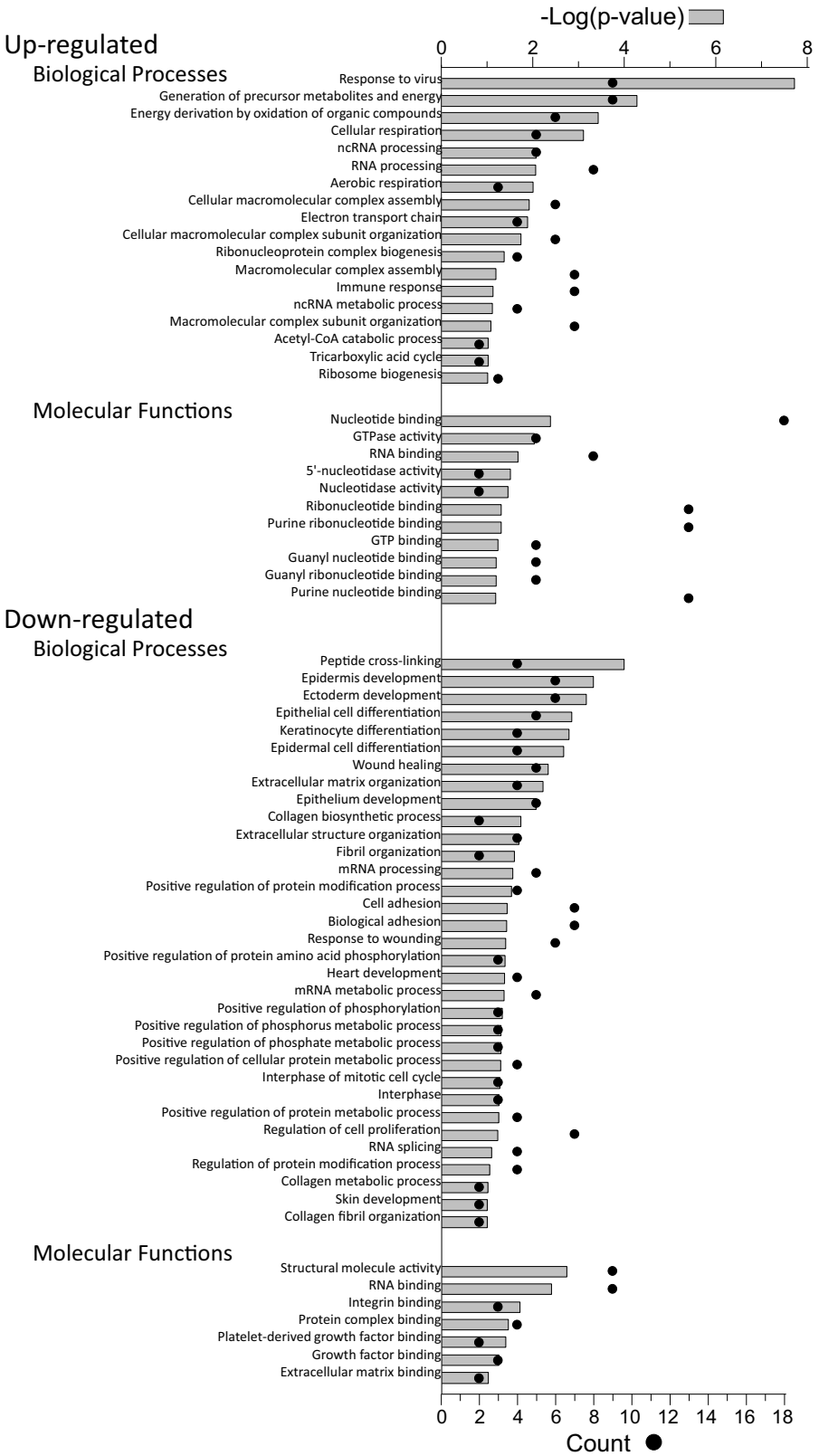

FIGURE 5 | Gene ontology analyses of up-regulated and down-regulated proteins. The proteins identified in **Table 2** were imported into the DAVID gene ontology suite of programs at the NIAID, gene identifications converted by that program, and ontological functions determined by GOTERM.

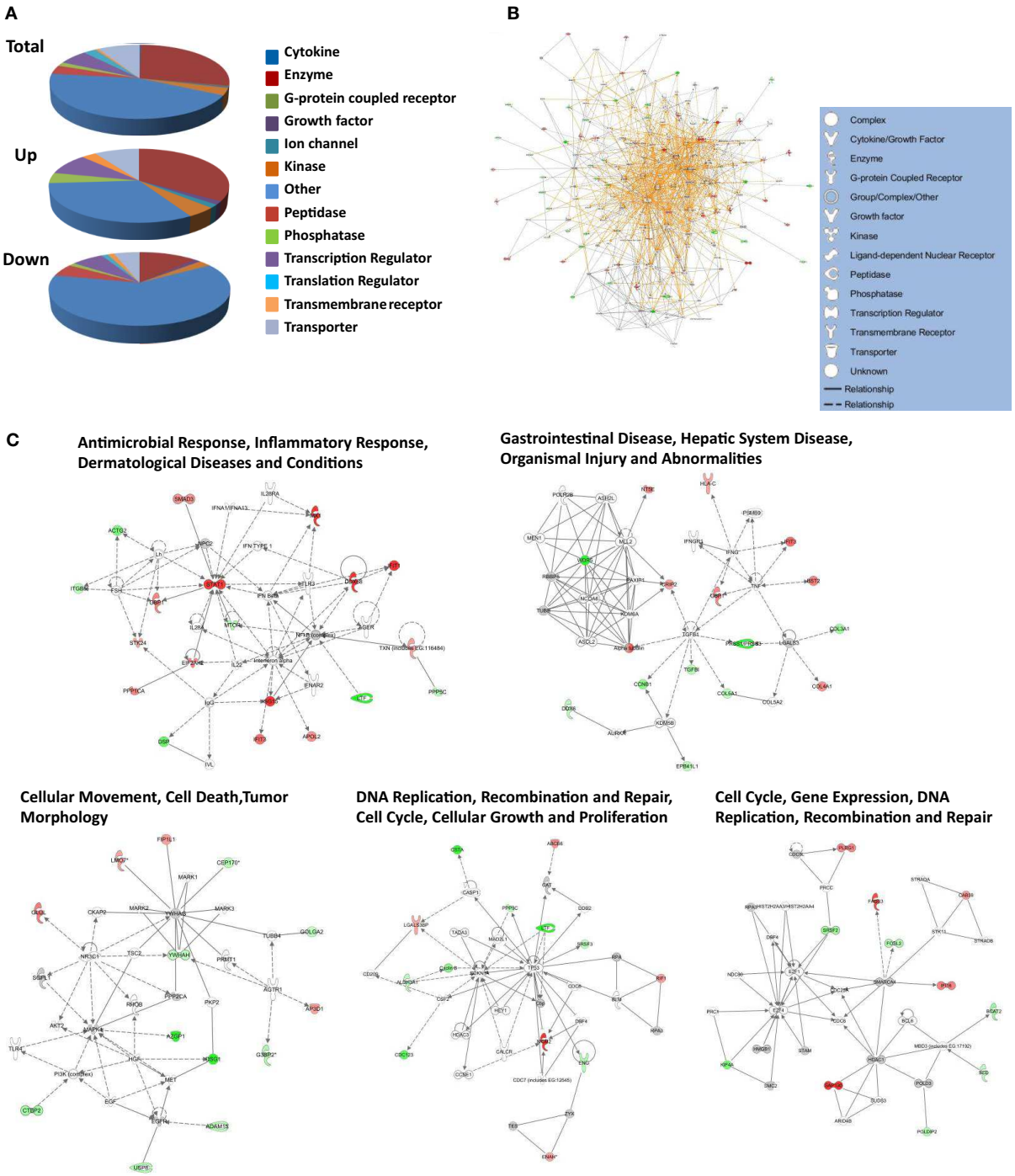

FIGURE 6 | Molecular pathways of regulated proteins. Proteins and their levels of regulation were imported into the Ingenuity Pathways Analysis (IPA®) tool and interacting pathways were constructed. **(A)** Ontological classifications of all measured proteins (Total) as well as those significantly up- and down-regulated. The indicated ontological classifications start at the top of each pie chart and are presented clockwise. **(B)** Merged networks, containing all molecules present in each of the five individual networks. **(C)** The top five networks, identified at 95% confidence and each of which contained 11 or more "focus" molecules (molecules significantly up- or down-regulated), with pathway names indicated. Solid lines: direct known interactions; dashed lines: suspected or indirect interactions; red: significantly up-regulated proteins; pink: moderately up-regulated proteins; gray: proteins identified but not significantly regulated; light green: moderately down-regulated proteins; dark green: significantly down-regulated proteins; white: proteins known to be in network, but not identified in our study.

Table 3 | Correlation and overlap between various sample preparation schemes.

	Cyto St vs. Cyto PM[1]	Nuc St vs. Nuc PM	Cyto St vs. Nuc St	Cyto PM vs. Nuc PM	Biological replicate[2]	Technical replicate[2]
Percentage of overlap	73.7	67.9	65.4	68.0	67.3	81.5
Overall correlation (r^2)	0.444	0.255	0.159	0.606	0.038–0.057	0.660
Correlation (r^2) for up- and down-regulated proteins only	0.236	0.119	0.046	0.448	0.156–0.174	0.414

[1]*Cyto, cytosolic fraction; Nuc, nuclear fraction; St, standard 2D-LC/MS; PM, Proteominer.*

[2]*Biological and technical values observed in another study Coombs et al. (2010); and unpublished.*

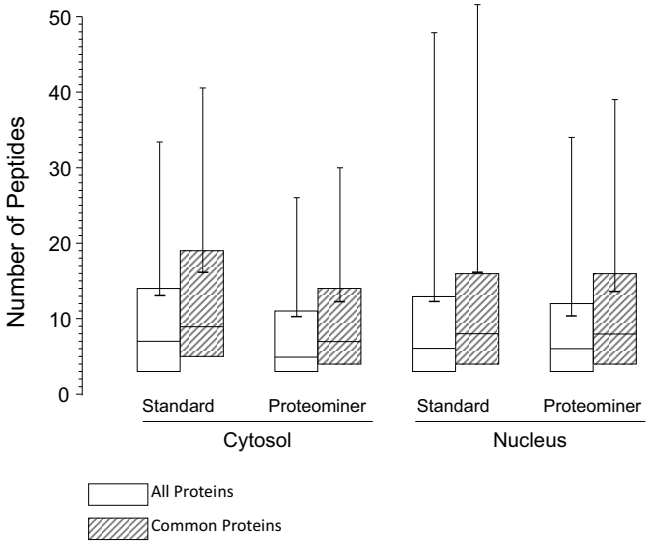

FIGURE 7 | Box plots of number of peptides identified under each experimental condition. The box encompasses the upper and lower quartile. Median values for each condition are indicated by the full horizontal line inside each box, the average is indicated by the shorter thick line, and SDs are indicated by upward error bars □, all identified proteins; ▨, only proteins identified as common to both the standard and PM analyses.

identified peptides, and the corresponding SD, were also lower in the PM-enriched fraction (**Figure 7**). This pattern was seen irrespective of whether all proteins were examined (white boxes), or only proteins common to both the standard and PM enrichment fractions (gray boxes). Previous studies in our lab have shown that biologic replicates have ∼67% overlap and an r^2 degree of correlation of about 0.04, whereas technical replicates of the same biologic replicate have ∼82% overlap and an r^2 value of about 0.66 (Coombs et al., 2010; **Table 3**). Comparisons of the overlap and r^2 values between standard preparations and their cognate PM enrichment preparations showed intermediate values of ∼68–74% overlap and r^2 ranging between 0.25 and 0.44 (**Table 3**), suggesting the PM enrichment strategy did not add substantially to information provided by standard preparations.

NOTE ADDED IN PROOF

The Mann laboratory has recently used label-free approaches to determine the relative quantity of each of thousands of proteins in a variety of human cell lines, including HeLa cells (Geiger et al., 2012). As a more direct analysis to determine whether application of Proteominer beads led to identification of lower abundance proteins, we sorted our datasets and determined there were no significant differences in the average and median quantities of proteins identified by either of the two methods in each of the cytosolic and nuclear fractions, further strengthening the main conclusion of this study, that non-biased enrichment using this particular affinity method does not contribute to deeper proteomic mining.

AUTHOR CONTRIBUTIONS

Jieyuan Jiang and Kolawole J. Opanubi performed experimental work described herein, all co-authors performed database and computational analyses, and all co-authors wrote and edited the manuscript.

ACKNOWLEDGMENTS

This work was supported by grant MT-11630 from the Canadian Institutes of Health Research to Kevin M. Coombs. The authors thank Peyman Ezatti for expert technical assistance, and members of the laboratory for reviewing the manuscript.

REFERENCES

Baas, T., Baskin, C. R., Diamond, D. L., Garcia-Sastre, A., Bielefeldt-Ohmann, H., Tumpey, T. M., Thomas, M. J., Carter, V. S., Teal, T. H., Van Hoeven, N., Proll, S., Jacobs, J. M., Caldwell, Z. R., Gritsenko, M. A., Hukkanen, R. R., Camp, D. G. II, Smith, R. D., and Katze, M. G. (2006). Integrated molecular signature of disease: analysis of influenza virus-infected macaques through functional genomics and proteomics. *J. Virol.* 80, 10813–10828.

Berard, A., and Coombs, K. M. (2009). Mammalian reoviruses: propagation, quantification, and storage. *Curr. Protoc. Microbiol.* Chapter 15, Unit15C.1.

Booy, A. T., Haddow, J. D., Ohlund, L. B., Hardie, D. B., and Olafson, R. W. (2005). Application of isotope coded affinity tag (ICAT) analysis for the identification of differentially expressed proteins following infection of Atlantic salmon (Salmo salar) with infectious hematopoietic necrosis virus (IHNV) or *Renibacterium salmoninarum* (BKD). *J. Proteome Res.* 4, 325–334.

Burgener, A., Boutilier, J., Wachihi, C., Kimani, J., Carpenter, M., Westmacott, G., Cheng, K., Ball, T. B., and Plummer, F. (2008). Identification of differentially expressed proteins in the cervical mucosa of HIV-1-resistant sex workers. *J. Proteome Res.* 7, 4446–4454.

Coffey, M. C., Strong, J. E., Forsyth, P. A., and Lee, P. W. (1998). Reovirus therapy of tumors with activated Ras pathway. *Science* 282, 1332–1334.

Coombs, K. M. (2011). Quantitative proteomics of complex mixtures. *Expert Rev. Proteomics* 8, 659–677.

Coombs, K. M., Berard, A., Xu, W., Krokhin, O., Meng, X., Cortens, J. P.,

Kobasa, D., Wilkins, J., and Brown, E. G. (2010). Quantitative proteomic analyses of influenza virus-infected cultured human lung cells. *J. Virol.* 84, 10888–10906.

DeBiasi, R. L., Clarke, P., Meintzer, S., Jotte, R., Kleinschmidt-Demasters, B. K., Johnson, G. L., and Tyler, K. L. (2003). Reovirus-induced alteration in expression of apoptosis and DNA repair genes with potential roles in viral pathogenesis. *J. Virol.* 77, 8934–8947.

Dennis, G., Sherman, B. T., Hosack, D. A., Yang, J., Gao, W., Lane, H. C., and Lempicki, R. A. (2003). DAVID: Database for annotation, visualization, and integrated discovery. *Genome Biol.* 4. doi: 10.1186/gb-2003-4-9-r60

Dwivedi, R. C., Dhindsa, N., Krokhin, O. V., Cortens, J., Wilkins, J. A., and El-Gabalawy, H. S. (2009). The effects of infliximab therapy on the serum proteome of rheumatoid arthritis patients. *Arthritis Res. Ther.* 11. doi: 10.1186/ar2637

Dwivedi, R. C., Spicer, V., Harder, M., Antonovici, M., Ens, W., Standing, K. G., Wilkins, J. A., and Krokhin, O. V. (2008). Practical implementation of 2D HPLC scheme with accurate peptide retention prediction in both dimensions for high-throughput bottom-up proteomics. *Anal. Chem.* 80, 7036–7042.

Forsyth, P., Roldan, G., George, D., Wallace, C., Palmer, C. A., Morris, D., Cairncross, G., Matthews, M. V., Markert, J., Gillespie, Y., Coffey, M., Thompson, B., and Hamilton, M. (2008). A phase I trial of intratumoral administration of reovirus in patients with histologically confirmed recurrent malignant gliomas. *Mol. Ther.* 16, 627–632.

Geiger, T., Wehner, A., Schaab, C., Cox, J., and Mann M. (2012). Comparative proteomic analysis of eleven common cell lines reveals ubiquitous but varying expression of most proteins. *Mol. Cell. Proteomics.* PMID: 22278370. [Epub ahead of print].

Geiss, G. K., Salvatore, M., Tumpey, T. M., Carter, V. S., Wang, X. Y., Basler, C. F., Taubenberger, J. K., Bumgarner, R. E., Palese, P., Katze, M. G., and Garcia-Sastre, A. (2002). Cellular transcriptional profiling in influenza A virus-infected lung epithelial cells: the role of the nonstructural NS1 protein in the evasion of the host innate defense and its potential contribution to pandemic influenza. *Proc. Natl. Acad. Sci. U.S.A.* 99, 10736–10741.

Gilar, M., Olivova, P., Daly, A. E., and Gebler, J. C. (2005). Orthogonality of separation in two-dimensional liquid chromatography. *Anal. Chem.* 77, 6426–6434.

Goldberg, A. D., Allis, C. D., and Bernstein, E. (2007). Epigenetics: a landscape takes shape. *Cell* 128, 635–638.

Goody, R. J., Beckham, J. D., Rubtsova, K., and Tyler, K. L. (2007). JAK-STAT signaling pathways are activated in the brain following reovirus infection. *J. Neurovirol.* 13, 373–383.

Haller, O., and Kochs, G. (2002). Interferon-induced mx proteins: dynamin-like GTPases with antiviral activity. *Traffic* 3, 710–717.

Haller, O., Staeheli, P., and Kochs, G. (2009). Protective role of interferon-induced Mx GTPases against influenza viruses. *Rev. Sci. Tech.* 28, 219–231.

Huang, D. W., Sherman, B. T., and Lempicki, R. A. (2009a). Systematic and integrative analysis of large gene lists using DAVID bioinformatics resources. *Nat. Protoc.* 4, 44–57.

Huang, Q. L., Wang, L., Bai, S. Y., Lin, W. S., Chen, W. N., Lin, J. Y., and Lin, X. (2009b). Global proteome analysis of hepatitis B virus expressing human hepatoblastoma cell line HepG2. *J. Med. Virol.* 81, 1539–1550.

Jiang, J., Parker, C. E., Fuller, J. R., Kawula, T. H., and Borchers, C. H. (2007). An immunoaffinity tandem mass spectrometry (iMALDI) assay for detection of Francisella tularensis. *Anal. Chim. Acta* 605, 70–79.

Keshamouni, V. G., Jagtap, P., Michailidis, G., Strahler, J. R., Kuick, R., Reka, A. K., Papoulias, P., Krishnapuram, R., Srirangam, A., Standiford, T. J., Andrews, P. C., and Omenn, G. S. (2009). Temporal quantitative proteomics by iTRAQ 2D-LC-MS/MS and corresponding mRNA expression analysis identify post-transcriptional modulation of actin-cytoskeleton regulators during TGF-beta-Induced epithelial-mesenchymal transition. *J. Proteome Res.* 8, 35–47.

Kobasa, D., Jones, S. M., Shinya, K., Kash, J. C., Copps, J., Ebihara, H., Hatta, Y., Kim, J. H., Halfmann, P., Hatta, M., Feldmann, F., Alimonti, J. B., Fernando, L., Li, Y., Katze, M. G., Feldmann, H., and Kawaoka, Y. (2007). Aberrant innate immune response in lethal infection of macaques with the 1918 influenza virus. *Nature* 445, 319–323.

Lucitt, M. B., Price, T. S., Pizarro, A., Wu, W., Yocum, A. K., Seiler, C., Pack, M. A., Blair, I. A., Fitzgerald, G. A., and Grosser, T. (2008). Analysis of the zebrafish proteome during embryonic development. *Mol. Cell Proteomics* 7, 981–994.

Mendez, II, Hermann, L. L., Hazelton, P. R., and Coombs, K. M. (2000). A comparative analysis of freon substitutes in the purification of reovirus and calicivirus. *J. Virol. Methods* 90, 59–67.

Pan, D., Pan, L. Z., Hill, R., Marcato, P., Shmulevitz, M., Vassilev, L. T., and Lee, P. W. K. (2011). Stabilisation of p53 enhances reovirus-induced apoptosis and virus spread through p53-dependent NF-kappa B activation. *Br. J. Cancer* 105, 1012–1022.

Poggioli, G. J., DeBiasi, R. L., Bickel, R., Jotte, R., Spalding, A., Johnson, G. L., and Tyler, K. L. (2002). Reovirus-induced alterations in gene expression related to cell cycle regulation. *J. Virol.* 76, 2585–2594.

Schiff, L. A., Nibert, M. L., and Tyler, K. L. (2007). "Orthoreoviruses and their replication," in *Fields Virology*, Vol. 5, eds D. M. Knipe and P. M. Howley (Philadelphia: Lippincott Williams & Wilkins), 1853–1915.

Sherry, B. (2009). Rotavirus and reovirus modulation of the interferon response. *J. Interferon Cytokine Res.* 29, 559–567.

Skiba, M., Mettenleiter, T. C., and Karger, A. (2008). Quantitative whole-cell proteome analysis of pseudorabies virus-infected cells. *J. Virol.* 82, 9689–9699.

Smith, R. E., Zweerink, H. J., and Joklik, W. K. (1969). Polypeptide components of virions, top component and cores of reovirus type 3. *Virology* 39, 791–810.

Spicer, V., Yamchuk, A., Cortens, J., Sousa, S., Ens, W., Standing, K. G., Wilkins, J. A., and Krokhin, O. (2007). Sequence-specific retention calculator. A family of peptide retention time prediction algorithms in reversed-phase HPLC: applicability to various chromatographic conditions and columns. *Anal. Chem.* 79, 8762–8768.

Stewart, J. J., White, J. T., Yan, X., Collins, S., Drescher, C. W., Urban, N. D., Hood, L., and Lin, B. (2006). Proteins associated with Cisplatin resistance in ovarian cancer cells identified by quantitative proteomic technology and integrated with mRNA expression levels. *Mol. Cell Proteomics* 5, 433–443.

Thirukkumaran, C. M., Nodwell, M. J., Hirasawa, K., Shi, Z. Q., Diaz, R., Luider, J., Johnston, R. N., Forsyth, P. A., Magliocco, A. M., Lee, P., Nishikawa, S., Donnelly, B., Coffey, M., Trpkov, K., Fonseca, K., Spurrell, J., and Morris, D. G. (2010). Oncolytic viral therapy for prostate cancer: efficacy of reovirus as a biological therapeutic. *Cancer Res.* 70, 2435–2444.

Tian, Q., Stepaniants, S. B., Mao, M., Weng, L., Feetham, M. C., Doyle, M. J., Yi, E. C., Dai, H., Thorsson, V., Eng, J., Goodlett, D., Berger, J. P., Gunter, B., Linseley, P. S., Stoughton, R. B., Aebersold, R., Collins, S. J., Hanlon, W. A., and Hood, L. E. (2004). Integrated genomic and proteomic analyses of gene expression in mammalian cells. *Mol. Cell Proteomics* 3, 960–969.

Tran, A. T., and Coombs, K. M. (2006). "Reoviruses," in *Encyclopedia of Life Sciences*, Vol. 2. (Elsevier). doi: 10.1038/npg.els.0004289

Vester, D., Rapp, E., Gade, D., Genzel, Y., and Reichl, U. (2009). Quantitative analysis of cellular proteome alterations in human influenza A virus-infected mammalian cell lines. *Proteomics* 9, 3316–3327.

Zhang, J., Niu, D., Sui, J., Ching, C. B., and Chen, W. N. (2009). Protein profile in hepatitis B virus replicating rat primary hepatocytes and HepG2 cells by iTRAQ-coupled 2-D LC-MS/MS analysis: insights on liver angiogenesis. *Proteomics* 9, 2836–2845.

Zolotarjova, N., Mrozinski, P., Chen, H., and Martosella, J. (2008). Combination of affinity depletion of abundant proteins and reversed-phase fractionation in proteomic analysis of human plasma/serum. *J. Chromatogr. A* 1189, 332–338.

Zurney, J., Kobayashi, T., Holm, G. H., Dermody, T. S., and Sherry, B. (2009). Reovirus mu2 protein inhibits interferon signaling through a novel mechanism involving nuclear accumulation of interferon regulatory factor 9. *J. Virol.* 83, 2178–2187.

Conflict of Interest Statement: The authors declare that the research was conducted in the absence of any commercial or financial relationships that could be construed as a potential conflict of interest.

Received: 17 May 2012; accepted: 06 August 2012; published online: 20 September 2012.

Citation: Jiang J, Opanubi KJ and Coombs KM (2012) Non-biased enrichment does not improve quantitative proteomic delineation of reovirus T3D-infected HeLa cell protein alterations. Front. Microbio. ***3****:310. doi: 10.3389/fmicb.2012.00310*

This article was submitted to Frontiers in Virology, a specialty of Frontiers in Microbiology.

frontiers in
MICROBIOLOGY

GENERAL COMMENTARY
published: 31 October 2012
doi: 10.3389/fmicb.2012.00382

Penetrating insights?

Dave Speijer*

Department of Medical Biochemistry, Academic Medical Center, University of Amsterdam, Amsterdam, Netherlands
**Correspondence: d.speijer@amc.uva.nl*

Edited by:
Ben Berkhout, University of Amsterdam, Netherlands

Reviewed by:
Ben Berkhout, University of Amsterdam, Netherlands

A commentary on

Non-biased enrichment does not improve quantitative proteomic delineation of reovirus T3D-infected HeLa cell protein alterations
by Jiang, J., Opanubi, K. J., and Coombs, K. M. (2012). Front. Microbio. 3:310. doi: 10.3389/fmicb.2012.00310

In this special Frontiers in Microbiology issue focusing on "Global host proteomic responses to virus infection," Coombs and colleagues (Jiang et al., 2012) make a valiant effort to look deeper into (changes in) the proteome of HeLa cells upon reovirus infection. Using some of the latest proteomic techniques, they present a high quality analysis of quantified alterations in the protein content of HeLa cells with, or without, infection by reovirus T3D. The study of the relatively harmless mammalian reoviruses received a boost from their potential to selectively kill certain types of cancer cells (Coffey et al., 1998). Proteomic studies, comparing all proteins and their post translational modifications in a quantitative fashion between control and reovirus infected cells therefore became crucial. However, all proteomic studies are hampered by the large differences in natural protein concentrations. In mass spectrometric (ms) practice, the most conspicuous protein restricts the level of detection to proteins that are, at most, about a thousand fold less abundant. Methods used to overcome this limitation either purge the most abundant, or specifically purify the less abundant proteins. Of course such biased approaches have rather big drawbacks themselves, related to the method of purging and the choice of purification procedure. "Unbiased" approaches, leveling the playing field without prior loss of possibly interesting proteins or enrichment based on known interactions, come in two flavors. One of them is based on the use of antibodies against "every" protein made by a certain organism as illustrated by human tissue profiling (Uhlen and Ponten, 2005). This is a non-ms technique, although immune precipitations can be combined with further ms analysis. The technique would indeed allow sensitive detection of very low abundant proteins, but relies on getting an effective epitope for every gene product and is rather costly. It also has to focus on the most common protein form and will be difficult to use for the detection of less abundant forms, let alone post translational modifications.

The only really unbiased approach available seems to be the use of hexapeptide combinatorial ligand libraries to enrich for all low abundant proteins (Boschetti and Righetti, 2008). The basic idea is simple and rather elegant: generate "random" peptide libraries, coat individual beads with single peptide forms, and allow your protein sample to interact with complex beads mixtures. Highly abundant proteins will saturate the beads they interact with quickly, and the large unbound majority will be washed away. However, proteins that are much less abundant will also find peptide targets to their liking and be retained. To give a somewhat more precise description: the abundance advantage of certain proteins (differences in mol L^{-1}) has to be *more* than compensated for by differing binding affinities (again in mol L^{-1}). Prior work showed hexapeptide libraries (with a combinatorial complexity of 6.4×10^7 peptides) to be optimal in this respect. Of course, not all amino acids in the hexamers contribute to the (strength of) interaction with proteins in the sample equally, three hydrophobic ones (Phe, Trp, and Tyr) and the three basic ones (Arg, His, and Lys) presumably being the most important. This (ProteoMiner) technique is the one that Jiang et al. decided to use. However, in their abstract it is concluded that: "Comparisons of the r^2 correlations, degree of dataset overlap, and numbers of peptides detected suggest that non-biased enrichment approaches may not provide additional data to allow deeper quantitative and comparative mining of complex proteomes." It is refreshing that these authors highlight what could be seen as a "negative" finding. In presenting evidence suggesting that in *this case* non-biased enrichment strategies do not seem to allow us to delve much deeper into the proteome, the authors give us the latest installment in an ongoing saga regarding the effectivity of using a ProteoMiner approach to get a peek at low abundant proteins in an unbiased fashion. The approach has already been used extensively in one of the most important, but at the same time most challenging, areas of clinical research: biomarker discovery in serum (which has tremendous differences in protein abundancies at $\sim 10^{10}$ differences in concentration). Discussions regarding the effectivity of using hexamers seem to have been resolved in favor of the approach, although peptide elution had to be performed at three separate pH values to get full peptide diversity (Bandow, 2010; Di Girolamo et al., 2011). In regards to cellular extracts, an extreme example of protein "imbalance" is found in erythrocytes with 98% hemoglobin. The 2% that remains was much more easily explored upon the use of two different hexamer peptide sets (Roux-Dalvai et al., 2008). Even more striking are the results obtained by Yates and colleagues using "normal" Hela cells: they obtain improvements in silverstained 2D gels as well as statistically significant differences in proteome sets using ms analysis of fractions with or without prior ProteoMiner beads incubation (Fonslow et al., 2011).

So what is going on in the case of these reovirus infected HeLa cells? Actually, the conflicting data can presumably be resolved by highlighting the following two points:

1. As in the case of the earlier discussion, *the elution method seems to be crucial.* The ProteoMiner elution buffer used by the Yates group for the 2D silverstained gels is identical to the one used by Jiang et al., *but they digest their proteins on the beads upon 8 M urea denaturation* for further ms analysis (Fonslow et al., 2011). For the differences in 2D analysis followed by silverstaining, the normal protocol seems to be sufficient, but for efficient mass analysis more harsh conditions are clearly needed. For more important insights regarding the use of ProteoMiner beads as a powerful method of proteome equalization see Righetti et al. (2012).
2. Based on the fact that comparisons of r^2 correlations, dataset overlaps, and numbers of peptides detected were comparable to those found with biological replicates the authors were correct in stating that the enrichment approach did not provide a significant deeper quantitative mining of the proteome under study. However, looking at the Venn diagram of shared and specific proteins found in different experiments (Jiang et al., Figure 3A), I am convinced that future analysis of the "extra" groups of proteins found with the hexameric non-biased enrichment approaches in the nuclear and cytoplasmic fractions will show them to contain more low abundant proteins than the controls.

Indeed, future experiments to check for improvement in detection of low abundant proteins should again be performed with virus infected cells. These systems are especially suited for such an analysis as they contain a specific set of viral proteins that are completely absent from control cells, thus functioning as ideal positive controls. Not only that, many viruses have a pronounced dynamic range of viral protein (form)s of their own, making the challenge of a correct quantitative proteomic description even bigger. Despite not always living up to their full potential yet, random hexapeptide libraries seem to be on track to level the proteomic playing field in the near future.

REFERENCES

Bandow, J. E. (2010). Comparison of protein enrichment strategies for proteome analysis of plasma. *Proteomics* 10, 1416–1425.

Boschetti, E., and Righetti, P. G. (2008). The ProteoMiner in the proteomic arena: a non-depleting tool for discovering low-abundance species. *J. Proteomics* 71, 255–264.

Coffey, M. C., Strong, J. E., Forsyth, P. A., and Lee, P. W. (1998). Reovirus therapy of tumors with activated Ras pathway. *Science* 282, 1332–1334.

Di Girolamo, F., Boschetti, E., Chung, M. C., Guadagni, F., and Righetti, P. G. (2011). "Proteomineering" or not? The debate on biomarker discovery in sera continues. *J. Proteomics* 74, 589–594.

Fonslow, B. R., Carvalho, P. C., Academia, K., Freeby, S., Xu, T., Nakorchevsky, A., et al. (2011). Improvements in proteomic metrics of low abundance proteins through proteome equalization using ProteoMiner prior to MudPIT. *J. Proteome Res.* 10, 3690–3700.

Jiang, J., Opanubi, K. J., and Coombs, K. M. (2012). Non-biased enrichment does not improve quantitative proteomic delineation of reovirus T3D-infected HeLa cell protein alterations. *Front. Microbio.* 3:310. doi: 10.3389/fmicb.2012.00310

Righetti, P. G., Boschetti, E., and Candiano, G. (2012). Mark Twain: how to fathom the depth of your pet proteome. *J. Proteomics* 75, 4783–4791.

Roux-Dalvai, F., Gonzalez de, P. A., Simo, C., Guerrier, L., Bouyssie, D., Zanella, A., et al. (2008). Extensive analysis of the cytoplasmic proteome of human erythrocytes using the peptide ligand library technology and advanced mass spectrometry. *Mol. Cell. Proteomics* 7, 2254–2269.

Uhlen, M., and Ponten, F. (2005). Antibody-based proteomics for human tissue profiling. *Mol. Cell. Proteomics* 4, 384–393.

Received: 02 October 2012; accepted: 13 October 2012; published online: 31 October 2012.

*Citation: Speijer D (2012) Penetrating insights? Front. Microbio. **3**:382. doi: **10.3389/fmicb.2012.00382***

This article was submitted to Frontiers in Virology, a specialty of Frontiers in Microbiology.

frontiers in
MICROBIOLOGY

ORIGINAL RESEARCH ARTICLE
published: 25 October 2012
doi: 10.3389/fmicb.2012.00367

Characterization of Staufen1 ribonucleoproteins by mass spectrometry and biochemical analyses reveal the presence of diverse host proteins associated with human immunodeficiency virus type 1

Miroslav P. Milev [1,2], ***Mukunthan Ravichandran*** [1,2], ***Morgan F. Khan*** [3], ***David C. Schriemer*** [3] ***and Andrew J. Mouland*** [1,2,4]*

[1] *HIV-1 Trafficking Laboratory, Lady Davis Institute at the Jewish General Hospital, Montréal, QC, Canada*
[2] *Division of Experimental Medicine, Department of Medicine, McGill University, Montreal, QC, Canada*
[3] *Department of Biochemistry and Molecular Biology, University of Calgary, Calgary, AB, Canada*
[4] *Department of Microbiology and Immunology, McGill University, Montreal, QC, Canada*

Edited by:
Kevin Coombs, University of Manitoba, Canada

Reviewed by:
Chiaho Shih, Academia Sinica, Taiwan
Mikako Fujita, Kumamoto University, Japan

***Correspondence:**
Andrew J. Mouland, Lady Davis Institute at the Jewish General Hospital and McGill University, 3755 Côte-Ste-Catherine Road, Montréal, QC, Canada H3T 1E2.
e-mail: andrew.mouland@mcgill.ca

The human immunodeficiency virus type 1 (HIV-1) unspliced, 9 kb genomic RNA (vRNA) is exported from the nucleus for the synthesis of viral structural proteins and enzymes (Gag and Gag/Pol) and is then transported to sites of virus assembly where it is packaged into progeny virions. vRNA co-exists in the cytoplasm in the context of the HIV-1 ribonucleoprotein (RNP) that is currently defined by the presence of Gag and several host proteins including the double-stranded RNA-binding protein, Staufen1. In this study we isolated Staufen1 RNP complexes derived from HIV-1-expressing cells using tandem affinity purification and have identified multiple host protein components by mass spectrometry. Four viral proteins, including Gag, Gag/Pol, Env and Nef as well as >200 host proteins were identified in these RNPs. Moreover, HIV-1 induces both qualitative and quantitative differences in host protein content in these RNPs. 22% of Staufen1-associated factors are virion-associated suggesting that the RNP could be a vehicle to achieve this. In addition, we provide evidence on how HIV-1 modulates the composition of cytoplasmic Staufen1 RNPs. Biochemical fractionation by density gradient analyses revealed new facets on the assembly of Staufen1 RNPs. The assembly of dense Staufen1 RNPs that contain Gag and several host proteins were found to be entirely RNA-dependent but their assembly appeared to be independent of Gag expression. Gag-containing complexes fractionated into a lighter and another, more dense pool. Lastly, Staufen1 depletion studies demonstrated that the previously characterized Staufen1 HIV-1-dependent RNPs are most likely aggregates of smaller RNPs that accumulate at juxtanuclear domains. The molecular characterization of Staufen1 HIV-1 RNPs will offer important information on virus-host cell interactions and on the elucidation of the function of these RNPs for the transport of Gag and the fate of the unspliced vRNA in HIV-1-producing cells.

Keywords: Gag, genomic RNA, HIV-1, mass spectrometry, gradient centrifugation, ribonucleoprotein, Staufen1, virus-host interactions

INTRODUCTION

HIV-1 infection is characterized by a progressive depletion of CD4 + T lymphocytes that makes patients susceptible to opportunistic diseases and ultimately leads to the development of acquired immunodeficiency syndrome (AIDS; Ho et al., 1995; Lindwasser et al., 2007). HIV-1 replication is divided into early and late events (Wang et al., 2000; Freed, 2001): the early events include virus entry, uncoating of the viral core that contains the vRNA, reverse transcription of vRNA to cDNA and finally, the integration of the resulting viral double-stranded DNA into host chromosomes. The later events include the transcription of the proviral genome to generate a primary transcript, the vRNA, its processing, maturation and nucleocytoplasmic export and also the synthesis of viral structural proteins, virus assembly and budding. Following transcription, the vRNA either remains unspliced or is spliced to generate more than 30 distinct mRNAs that are grouped into singly spliced, 4 kb mRNAs (encoding the auxiliary proteins Vif, Vpr, Vpu and the glycoprotein, Env) or into multiply spliced, 1.8 kb mRNA species (encoding the early viral regulatory proteins Tat, Rev and Nef; Arrigo et al., 1990; Schwartz et al., 1990; Purcell and Martin, 1993). The 1.8 kb RNAs are constitutively exported from the nucleus early following transcription, while the nuclear export of vRNA and the 4 kb species is dependent on the CRM1/Exportin1 export pathway (Yi et al., 2002). These events are well orchestrated, dynamic and depend on the activities of viral as well as select host cell proteins and machineries that are co-opted by the virus.

The two largest viral mRNA species, which contain intronic sequences, are both exported from the nucleus and translated in the cytoplasm. While usually mRNAs with introns are tagged as aberrant since they are "incompletely spliced" and are degraded by cellular RNA quality control machineries (Doma and Parker, 2007), these viral mRNAs are quite stable (Mouland et al., 2002), and therefore likely evade this surveillance machinery by co-opting host proteins involved in this process (Ajamian et al., 2008; Nathans et al., 2009). Furthermore, vRNA has an additional fate in that it can also be packaged into progeny virions (Butsch and Boris-Lawrie, 2002). This latter step is made possible by a selective interaction between vRNA and its gene product, the precursor Group specific antigen, $pr55^{Gag}$ (termed Gag herein). Gag interacts with a packaging signal in the 5′UTR of vRNA for selection into assembling virions (Lever et al., 1989; Clever et al., 1995). Like other mRNAs, vRNA is likely transported through the cytoplasm in the context of an RNP (Wilhelm and Vale, 1993; Mouland et al., 2001; Lehmann et al., 2009). Indeed, mRNA-binding proteins such as Staufen1 associate closely with Gag to form the HIV-1 RNP that also incorporates vRNA, but none of the spliced HIV-1 RNAs (Chatel-Chaix et al., 2004; Cochrane et al., 2006). Moreover, recent work has demonstrated that HIV-1 RNPs that contain Staufen1 take advantage of endosomal machineries for intracellular trafficking (Lehmann et al., 2009; Molle et al., 2009). Nevertheless, these later events still remain one of the most understudied areas of HIV-1 biology.

Generally, like other cellular RNPs, the composition of cytosolic HIV-1 RNPs is plastic in nature such that proteins may engage in the nucleus, disengage and/or be acquired during transit from the nucleus to the cytoplasm and during the assembly of vRNA into viral particles. The composition of the HIV-1 RNP has not been completely characterized, however. Recent work supports the idea that vRNA interacts with Gag at juxtanuclear and cytoplasmic domains (Poole et al., 2005; Levesque et al., 2006) and considerable efforts are now being made to evaluate how HIV-1 co-opts factors following the nuclear export of the vRNA – a late step in HIV-1 replication that includes RNA transport, utilization (translation) and degradation (Cochrane et al., 2006; Lehmann et al., 2009; Molle et al., 2009; Kemler et al., 2010). The formation of the HIV-1 RNP is initially achieved by the binding of Gag via its nucleocapsid (NC) domain and the RNA packaging signal *psi* in the 5′-end of the vRNA. This early capture may govern the directed movement of vRNA along the cytoskeleton, to the translation apparatus, to sites of viral assembly and finally, into assembling viral particles. A number of host gene products, such as hnRNP A1, PSF/nsr54 and APOBEC3G associate with vRNA (Beriault et al., 2004; Khan et al., 2005). Furthermore, a limited set of host *trans*-acting proteins mediates trafficking by binding to specific *cis*-acting sequence elements in vRNA (Mouland et al., 2001; Levesque et al., 2006). While the stability and functionality of HIV-1 RNP is most probably a result of interactions between a few viral (i.e., Gag) and host cell proteins such as Staufen1 and Upf1 (Up-frameshift protein 1; Chatel-Chaix et al., 2004; Ajamian et al., 2008), the molecular composition of the HIV-1 RNP likely changes and is dictated by HIV-1, either by direct recruitment of, or by binding to host cell factors.

Staufen1 belongs to a growing family of the double-stranded RNA-binding proteins (dsRBPs) that includes protein kinase dsRNA dependent (PKR), the activator of PKR (PACT), TAR-RNA binding protein (TRBP) and RNA Helicase A (RHA, reviewed in (Fierro-Monti and Mathews, 2000; Saunders and Barber, 2003; Tian et al., 2004) and is a principal component of various RNPs that are engaged in the localization and trafficking of cellular mRNAs (Kiebler et al., 1999; Kiebler and DesGroseillers, 2000; Roegiers and Jan, 2000). Staufen1-containing high-molecular weight complexes ranging in size from 10–30 MDa appear as granules dispersed in the cytoplasm of eukaryotic cells. Several components are found in these complexes such as ribosomes, tubulin, actin, dynein, RHA, hnRNP U and nucleolin (Brendel et al., 2004; Villace et al., 2004). RNA-binding by Staufen1 regulates diverse classes of mammalian mRNAs that encode proteins with functions in different metabolic pathways and cellular physiological processes (Kim et al., 2007; Furic et al., 2008).

Our previous work demonstrated that Staufen1 binds to both Gag as well as its vRNA substrate (while excluding all of the spliced HIV-1 RNA species), which likely drives the incorporation of Gag and vRNA into assembling virions through the formation of a HIV-1 RNP (Mouland et al., 2000; Chatel-Chaix et al., 2004). Furthermore, modulating the levels of Staufen1, by siRNAs and overexpression, perturbs HIV-1 assembly, including Gag multimerization and vRNA encapsidation, resulting in negative effects on viral infectivity (Mouland et al., 2000; Chatel-Chaix et al., 2004, 2007, 2008; Abrahamyan et al., 2010). Staufen1 also influences the anterograde trafficking of Gag. Both Staufen1 and Gag were shown to associate in the cytoplasm and also at cholesterol-enriched lipid rafts, which are virus assembly domains (Milev et al., 2010).

Staufen1 potentially may play similar roles in the replication of other retroviruses, such as, HIV-2 and MLV since it was found incorporated within them (Mouland et al., 2000). Importantly it does not associate with any tested DNA virus, including adenovirus, Epstein-Barr virus and human herpesvirus 6, supporting its preferential role in the biology of RNA viruses. In a yeast two-hybrid screen and in co-immunoprecipitation (IP) experiments, Staufen1 was identified as an interactive partner of the influenza A virus non-structural protein, NS1 (Falcon et al., 1999). Recent work demonstrated that Staufen1 also associates to viral RNPs and viral RNAs in influenza virus-infected cells (de Lucas et al., 2010). Staufen1 also associates with the 3′UTR of HCV RNA, the sequence essential for the initiation of (−) strand synthesis (Harris et al., 2006). Together with the numerous other cellular proteins found to interact with this region, Staufen1 most probably also plays a role in HCV replication.

The aim of the work described here was to examine the composition of the Staufen1 RNP proteome and how it is modulated by HIV-1. To do this, Staufen1-binding proteins were purified using tandem affinity purification (TAP) in HIV-1-expressing cells and identified by mass spectrometry. Approximately 200 host proteins were identified using this strategy. The Staufen1 HIV-1 RNP that bound precursor Gag shared many proteins with cytosolic RNA trafficking RNPs. However, notable compositional differences of the Staufen1 RNPs were induced by HIV-1. Furthermore, ∼22% of the identified proteins are found in isolated HIV-1 particles. Biochemical and imaging analyses confirmed many of these

associations. Biochemical fractionation of cellular RNPs revealed further characteristics of the Staufen1 RNPs that are assembled in HIV-1-producing cells. Our results provide a comprehensive view on the composition of Staufen1-containing HIV-1 RNPs and their functional importance that likely resides in the fate of the vRNA.

MATERIALS AND METHODS

CELLS AND CELL LINES

Human embryonic kidney 293T cells HeLa, and Jurkat T cells were maintained at 37°C in Dulbecco's modified Eagle's or RPMI-1640 medium supplemented with 10% decomplemented fetal bovine serum (FBS) and 100 U/ml penicillin, 100 mg/ml streptomycin (Invitrogen). Stable TAP and Staufen1-TAP neomycin-resistant cell lines were generated in 293T and Jurkat T cells. Briefly, 293T cell were plated in 60 mm dishes and Jurkat T cells in 25 cm^2 flasks. The following day these were transfected with 2 and 4 μg plasmid DNA, respectively, using Lipofectamine 2000 according to the protocol provided by the manufacturer (Invitrogen). 24 h post-transfection, 600 μg/ml G418 (Invitrogen) was added to the medium for selection. The cell cultures were maintained at 90% confluence and subsequently, sub-cultured at lower densities. Resistant clones were isolated 14 days following selection. Tissue culture medium was removed from the plates, and cells were washed with sterile PBS. To pick colonies, sterile 3 mm cloning disks were dipped in trypsin solution and placed on colonies for 30 s. The colonies adhered to the cloning disks and were transferred to 24-well dishes. When the cells reached pre-confluence, they were transferred to 6-well plates. For suspension Jurkat T cells, the procedure for isolation of stable clones differed as follows: cells were maintained in RPMI-1640 with 600 μg/ml G418 for 14 days and then were serially diluted and transferred in 24-well dishes for expansion. The surviving stable lines exhibited various expression levels of the TAP tagged Staufen1 as assessed by SDS-PAGE and western blotting. Staufen1-TAP expression levels were constant for each clone and were stable for at least 20 subsequent passages.

TRANSIENT TRANSFECTIONS

For affinity purification experiments, transfection of control TAP and Staufen1-TAP stable cell lines with proviral DNA, pNL4-3, was carried out in 150 cm^2 flasks (Nunc). The cells were plated at 5×10^6 per flask for 24 h before transfection. 20 μg of plasmid and 50 μl Lipofectamine per flask were added, cells were incubated for 20 min and then mixed with tissue culture medium. For IP analyses, HeLa cells were transfected with corresponding amounts of plasmid DNA and cell lysates were prepared as described previously (Mouland et al., 2000; Chatel-Chaix et al., 2004). The overexpression of IMP1 (in the context of IMP1-VenC fusion protein) was performed in both HeLa and 293T cells. Transfection efficiencies were greater than 65% in all experiments (range 65–80%).

Staufen1-HA, pNL4-3 and pNL4-XX and transfection of HeLa cells were described previously (Mouland et al., 2000; Chatel-Chaix et al., 2004; Ajamian et al., 2008). For sucrose gradient fractionation experiments, transfection of proviral DNA, pNL4-3 was carried out in 75 cm^2 flasks (Nunc). The cells were plated at 3×10^6 per flask for 12 h before transfection. Transfection efficiencies were greater than 70% in all experiments (range 65–80%). For RNase A treatments, cell lysates were incubated for 30 min at 4°C with RNase T1 at 1 U/mL. HeLa cells were transfected with either non-silencing siRNA (siNS) or Staufen1 siRNA (siStaufen1) at a final concentration of 10 nM. siRNA transfections were performed with lipofectamine 2000. Thirty-six hours later, the cells were washed with ice cold PBS and lysed in XB buffer for subcellular fractionation in sucrose gradients (see below; Chatel-Chaix et al., 2004).

TANDEM AFFINITY PURIFICATION AND WESTERN BLOTTING

The purification of Staufen1 complexes was adapted using the TAP protocols as described previously (Puig et al., 2001; Villace et al., 2004). Briefly, after transfection, cells were lysed in buffer (50 mM Tris-HCl pH 7.5, 5 mM EDTA, 100 mM NaCl, 1 mM DTT, 0.5% NP-40) and complete protease inhibitor cocktail (Roche). Cell extracts were centrifuged at 4°C for 5 min at 5000 rpm and the recovered supernatants were centrifuged for 15 min at 14,000 × *g*. The lysates were stored at −20°C. In the first affinity purification step, 20–75 mg cell lysates were applied to IgG Sepharose six Fast Flow beads (Amersham Biosciences; at a ratio of 5 μl beads per 1 mg protein). The resin was prepared according to the manufacturer's protocol. After overnight incubation at 4°C, the IgG resin was washed 10 times with 10 volumes of IPP-150 buffer (10 mM Tris-HCl pH 8, 150 mM NaCl, 0.1% NP-40) and five times with 10 volumes of TEV cleavage buffer – TCB (10 mM Tris-HCl pH 8, 150 mM NaCl, 0.1% NP-40, 0.5 mM EDTA). 20 U of ActivTEV – Tobacco Etch Virus protease (Invitrogen, Carlsbad, USA) in TCB (300 μl) was then added to the resin and rotated for 2 h at room temperature in order to release the complexes bound to the resin (100 μl). In the second affinity purification step, the supernatant after TEV cleavage was adjusted with $CaCl_2$ to a 2 mM final concentration and incubated overnight with 60 μl Stratagene Calmodulin-affinity resin (Agilent Technologies, Cedar Creek, USA). The resin was then washed three times with 10 volumes of Calmodulin-binding buffer, CBB (10 mM beta-mercaptoethanol, 10 mM Tris-HCl pH 8, 150 mM NaCl, 0.1% NP-40, 1 mM imidazol, 1 mM MgOAc, 2 mM $CaCl_2$) and two times with 10 volumes of Calmodulin-rinsing buffer, CRB (50 mM ammonium bicarbonate pH 8.0, 75 mM NaCl, 1 mM MgOAc, 1 mM imidazol, 2 mM $CaCl_2$). For the elution of complexes, the beads were resuspended and incubated for several minutes with ∼100 μl of Calmodulin-elution buffer, CEB (50 mM ammonium bicarbonate, 15–25 mM EGTA). Western blotting of input cell lysates and affinity-purified eluates was performed by standard procedures (Abrahamyan et al., 2010) using several of the primary antisera described below. TAP and western blotting results are representative of >5 independent experiments.

COOMASSIE BLUE STAINING AND GEL SLICE EXCISION

For mass spectrometry analysis, the eluates were fractionated on 4–12% SDS-PAGE and the gels were then subjected to three 5 min washes in 300 ml double distillated water (ddH_2O) and stained with 100 ml Bio-Safe Coomassie stain (Bio-Rad) for 60 min followed by destaining. In total, 23 gel slices from each experiment (St-TAP or St-TAP + HIV-1) were excised, placed in a prewashed, low-retention 1.5 ml snap-cap tubes for subsequent in

gel digestion and liquid chromatography and mass spectrometry (LC-MS) analysis.

IN GEL DESTAINING AND DIGESTION

Gel bands were diced into ∼1 mm^2 pieces and rinsed once with 200 µl HPLC-grade water, twice with 200 µl 25 mM ammonium bicarbonate in 50% (v/v) acetonitrile, followed by 100 µl acetonitrile to dehydrate the gel plugs, which were then lyophilized. The dry gel plugs were rehydrated in 5–7 µl of 25 mM ammoniumbicarbonate, pH 8.0, containing 12.5 ng/µl trypsin. After rehydration, an additional 30 µl of 25 mM ammonium bicarbonate was added and the gel plugs were incubated overnight at 37°C. Peptides were extracted from gel plugs by two rounds of incubation with 50 µl of 1% formic acid in 50% acetonitrile. The pooled extracts were reduced to dryness and reconstituted in mobile phase A for reversed phase chromatography.

MASS SPECTROMETRY

Digests were analyzed using an Agilent 1100 LC-Ion-Trap-XCT-Ultra system (Agilent Technologies, Santa Clara, CA, USA) fitted with an integrated fluidics cartridge for peptide capture, separation, and nano-spraying (HPLC Chip). Injected samples were trapped and desalted on a pre-column channel (40 nl volume; Zorbax 300SB-C_{18}) for 5 min with mobile phase A (3% acetonitrile, 0.2% formic acid) delivered by an auxiliary pump at 4 µl/min. The peptides were then reverse-eluted from the trapping column and separated on the analytical column (150 mm length; Zorbax 300SB-C_{18}) at 0.3 µl/min. Peptides were eluted using a 5–70% gradient in mobile phase B (97% acetonitrile, 0.2% formic acid) over 45 min. MS/MS spectra were collected by data-dependent acquisition, with parent ion scans of 8,100 Th/s over m/z 300–2,000 and MS/MS scans at the same rate over m/z 100–2,200. Peak-list data were extracted from these files by DataAnalysis software for the 6300 series ion trap, v3.4 (build 175). Mascot v2.2 (MatrixScience, Boston, MA, USA) was used to search the MS/MS data using the following parameters: 1.6 Da precursor ion mass tolerance, 0.8 Da fragment ion mass tolerance, one potential missed cleavage, and oxidized methionine as a variable modification. NCBI nr 2008.01.03 (5,824,077 sequences) was searched, with a restriction to "other viruses" and humans. Mass spectrometry analyses on isolated TAP eluates were reproduced at least two times in independent experiments.

ANTIBODIES AND REAGENTS

Mouse anti-Staufen1, anti-UPF (1, 2 and 3), anti-RHA and anti-AUF1 antibodies were provided by Luc DesGroseillers (Université de Montréal), Jens-Lykke Andersen (University of California), Juan Ortin (Centro Nacional de Biotecnologia, Madrid, Spain) and William Rigby (Dartmouth University, NH, USA), respectively (Villace et al., 2004; Ajamian et al., 2008; Abrahamyan et al., 2010). Rabbit anti-IMP1 and anti-ABCE1 antibodies were generous gifts from Finn Nielsen (University of Copenhagen) and from Jaisri Lingappa (University of Washington; Zimmerman et al., 2002; Milev et al., 2010), respectively. Mouse anti-Tsg101 and anti-L7 antibodies were purchased from Novus Biologicals (Littleton, USA), anti-eF1α, anti-TDP-43 and anti-CRM1 were purchased from Upstate (Millipore), ProteinTech Group (Chicago, USA) and Santa Cruz (California, USA), respectively; rabbit anti-p17 and sheep anti-gp120 were obtained from the NIH (Abrahamyan et al., 2010). For all immunofluorescence (IF) experiments, secondary AlexaFluor anti-mouse, anti-rabbit or anti-sheep conjugated antibodies were used (Invitrogen) as previously described (Milev et al., 2010).

IMMUNOFLUORESCENCE, FISH AND CONFOCAL MICROSCOPY

At 24–48 h after transfection, cells were washed two times with 1× PBS and fixed in 4% PFA for 20 min, washed two times with 1× PBS and treated with 0.2% Triton X-100 for 10 min. IF and FISH were performed essentially as previously described (Lehmann et al., 2009; Milev et al., 2010; Vyboh et al., 2012). Cells were then incubated for 10 min with 0.1 M glycine, washed and blocked for 30 min in 1× BSA (Roche Applied Science, Germany). The primary antibody was incubated for 1.5 h at room temperature. Cells were washed 2× with PBS and subsequently incubated with secondary antibody for 30 min. After this step the glass coverslips were washed 2× with PBS, mounted on slides and visualized with a Carl Zeiss Pascal LSM5 laser scanning confocal microscope (Carl Zeiss, Germany).

EXPRESSION VECTORS

Plasmids pcDNASt-TAP and pcDNA-TAP were constructed as previously described (Villace et al., 2004). Proviral DNA, pNL4-3 was described in previous work (Adachi et al., 1986; Chatel-Chaix et al., 2004). pNL4-XX, a proviral DNA derived from pNL4-3, harbors two mutations in the *gag* open reading frame to prevent Gag and Gag/Pol synthesis, was described elsewhere (Poon et al., 2002; Abrahamyan et al., 2010). Constructs expressing Staufen1-HA, pGL3-IMP1-VenusC and pGL3-MS2-Venus (full length) were described previously (Milev et al., 2010). pCMV-Gag-RRE was described earlier (Lingappa et al., 2006).

SUBCELLULAR FRACTIONATION

Following transfection, cells were washed with ice cold PBS, homogenized in an equal volume of XB Buffer (20 mM HEPES pH 7.9, 1.5 mM $MgCl_2$, 0.5 mM DTT, protease inhibitor cocktail). The homogenate was centrifuged for 10 min at 5,000 rpm to remove the insoluble material. The supernatant (1 mg total protein) was applied on the top of a 5 ml 5–50% pre-loaded sucrose gradient in XB buffer, as described (Yoon and Mowry, 2004). Lysates were separated by centrifugation at 44,000 rpm for 2 h in SW55i beckman rotor at 17°C. 18–20 250 µl fractions were collected and resolved by SDS-PAGE or processed for slot blot analyses.

RNA SLOT BLOT ANALYSES

In order to evaluate vRNA fractionation in sucrose gradient fractions, an aliquot of each eluate was mixed 1:3 with GTC and FFM solution (10× OPS buffer, 37% Formaldehyde, 99% Formamide) and heated at 65°C for 15 min and transferred to 0.45 µm nylon membrane by intermittent suction for slot blot analyses using a Gibco/BRL slot blot apparatus. A $^{[32]}$P-labeled cDNA probe to the HIV-1 5′ *gag* coding region to recognize the vRNA only was prepared using random prime labeling kit, as described (Yao et al., 1998; Mouland et al., 2000).

RESULTS

GENERATION OF STAUFEN1-TAP AND CONTROL TAP STABLE CELL LINES

Tandem affinity purification is a powerful method for the specific isolation of protein complexes under native conditions. In order to characterize Staufen1 HIV-1 RNP complexes and to determine Staufen1-binding partners, we generated neomycin-resistant human 293T and Jurkat T cell lines expressing Staufen1-TAP (or St-TAP) and TAP control cell lines (**Figures 1A–D**; Puig et al., 2001). Cells were transfected with pcDNA3 in which a TAP tag was cloned at the carboxy-terminus of the Staufen1$^{55\,kDa}$ cDNA (Villace et al., 2004; Ajamian et al., 2008). Previous studies have demonstrated that St-TAP protein has the same properties as the native protein (Villace et al., 2004). Two of the 12 single-cell clones that were expanded in expressed the fusion protein as assessed by western blotting. St-TAP#11 was used for all subsequent experiments (**Figure 1B**; shown in Ajamian et al., 2008), because the expression levels were similar to that of endogenous Staufen1$^{55\,kDa}$. Jurkat St-TAP#13 (**Figure 1C**) was used for subsequent purification and characterization of Staufen1 complexes. A control cell line was also generated expressing only the TAP tag (**Figure 1D**). The subcellular distribution of TAP and St-TAP proteins in these stable 293T cell lines were assessed by IF using a monoclonal anti-Protein A antibody that recognizes the IgG binding domain of Protein A (the carboxy-terminal part of the TAP tag). TAP tag was found to be uniformly distributed throughout the cell (**Figure 1E**, left panel) and St-TAP was found principally in the cytoplasm of stable expressing cells (**Figure 1E**, right panel), corresponding to the localization pattern of endogenous Staufen1 (Wickham et al., 1999; Thomas et al., 2005). These results indicate

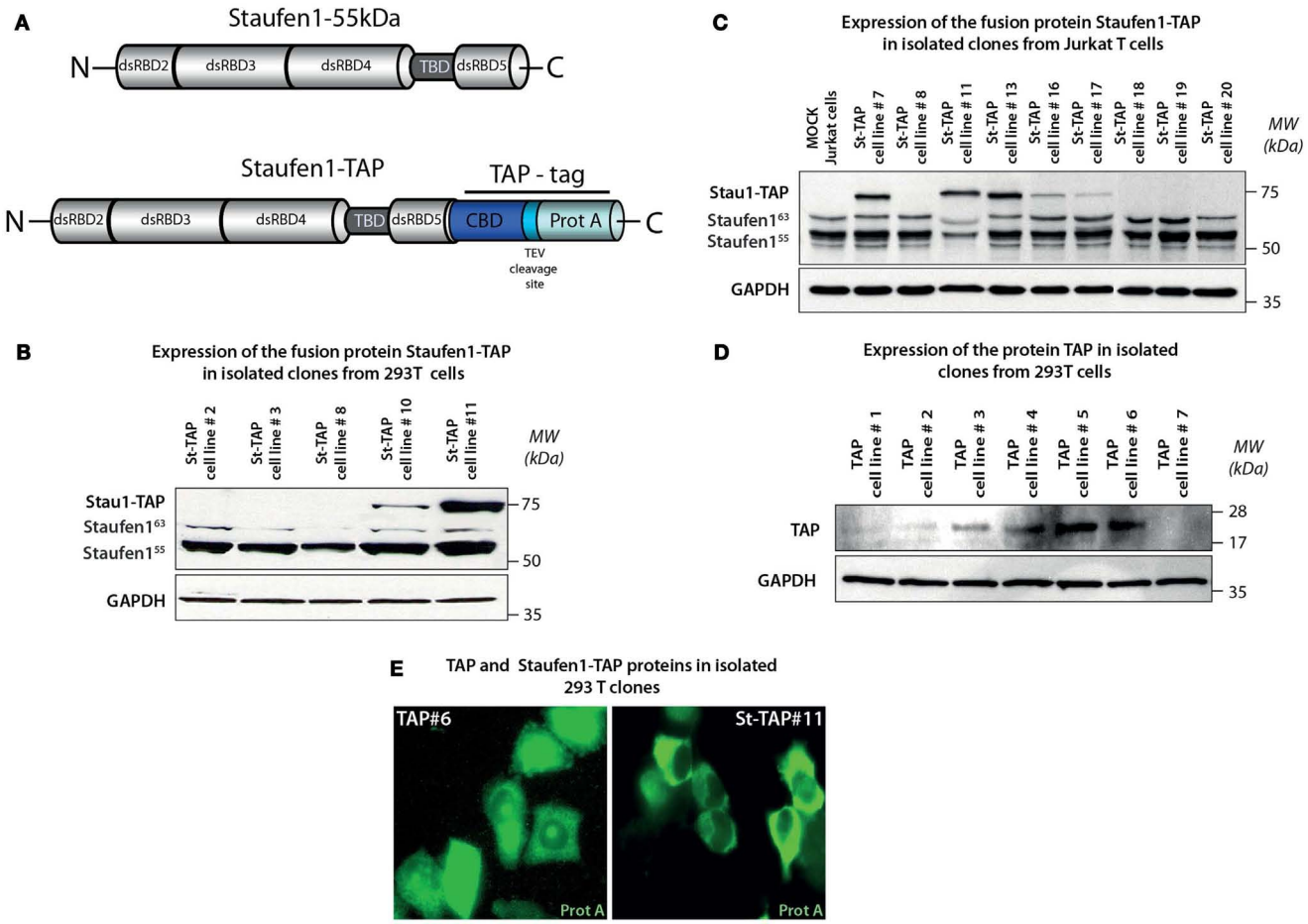

FIGURE 1 | Generation and isolation of stable neomycin-resistant cell lines expressing Staufen1-TAP and TAP proteins. (A) Structures of the Tandem Affinity Purification (TAP) tag cassette and Staufen1-TAP fusion protein. TAP tag consists of two sequences responsible for the affinity purification – IgG binding domain of Protein A and Calmodulin-binding peptide separated by a unique cleavage site for Tobacco Etch Virus (TEV) protease. **(B,C)** Expression levels of St-TAP in stable 293T and Jurkat T cell clones detected by western blotting analysis using a monoclonal mouse anti-Staufen1 antibody that recognizes both Staufen1^{55} (55 kDa), Staufen1^{63} (63 kDa), the endogenous isoforms and exogenous St-TAP (∼75 kDa) fusion protein, respectively. GAPDH is the loading control. 293T cell clone #11 and Jurkat T cell clone #13 were used in experiments. **(D)** Expression levels of TAP protein in 7 (#1–#7) control 293T clones and verified by western blotting. Clone #6 was used in control experiments. **(E)** Stable cell lines TAP#6 and St-TAP#11 were stained with mouse monoclonal anti-protein A antibody. The primary antibody was detected by Alexa Fluor 488 goat anti–mouse IgG antibody and the stained cells were visualized by epifluorescence microscopy.

that the Staufen1 component of the fusion protein, rather than the TAP tag, is responsible for correctly localizing the fusion protein to the cytosol.

PURIFICATION OF STAUFEN1 HIV-1 RIBONUCLEOPROTEIN COMPLEXES

We used the TAP-to-MS protocol to discover compositional changes in Staufen1-containing complexes when HIV-1 is expressed. We performed parallel purifications of extracts obtained from stably expressing St-TAP (Mock) or TAP (control) cell lines transiently transfected with pNL4-3. At 40 h post-transfection cells were harvested and 20 mg total protein was used for TAP purification. We also isolated Staufen1 complexes from both HIV-1 infected or uninfected Jurkat T cells that expressed St-TAP. Staufen1$^{55\,kDa}$ and St-TAP were present in RNPs both before and after affinity purification (**Figures 2A,C**). The TEV protease-mediated cleavage of St-TAP (75 kDa) fusion proteins resulted in the formation of St-CBP protein that migrated at ∼64 kDa (**Figures 2A,C**). Both endogenous 55 and 63 kDa isoforms of Staufen1 were recruited to RNPs likely due to their ability to form homo- and heterodimers and to accumulate in RNPs (Martel et al., 2010). When HIV-1 was expressed, higher amounts of endogenous Staufen1 were found in the eluates.

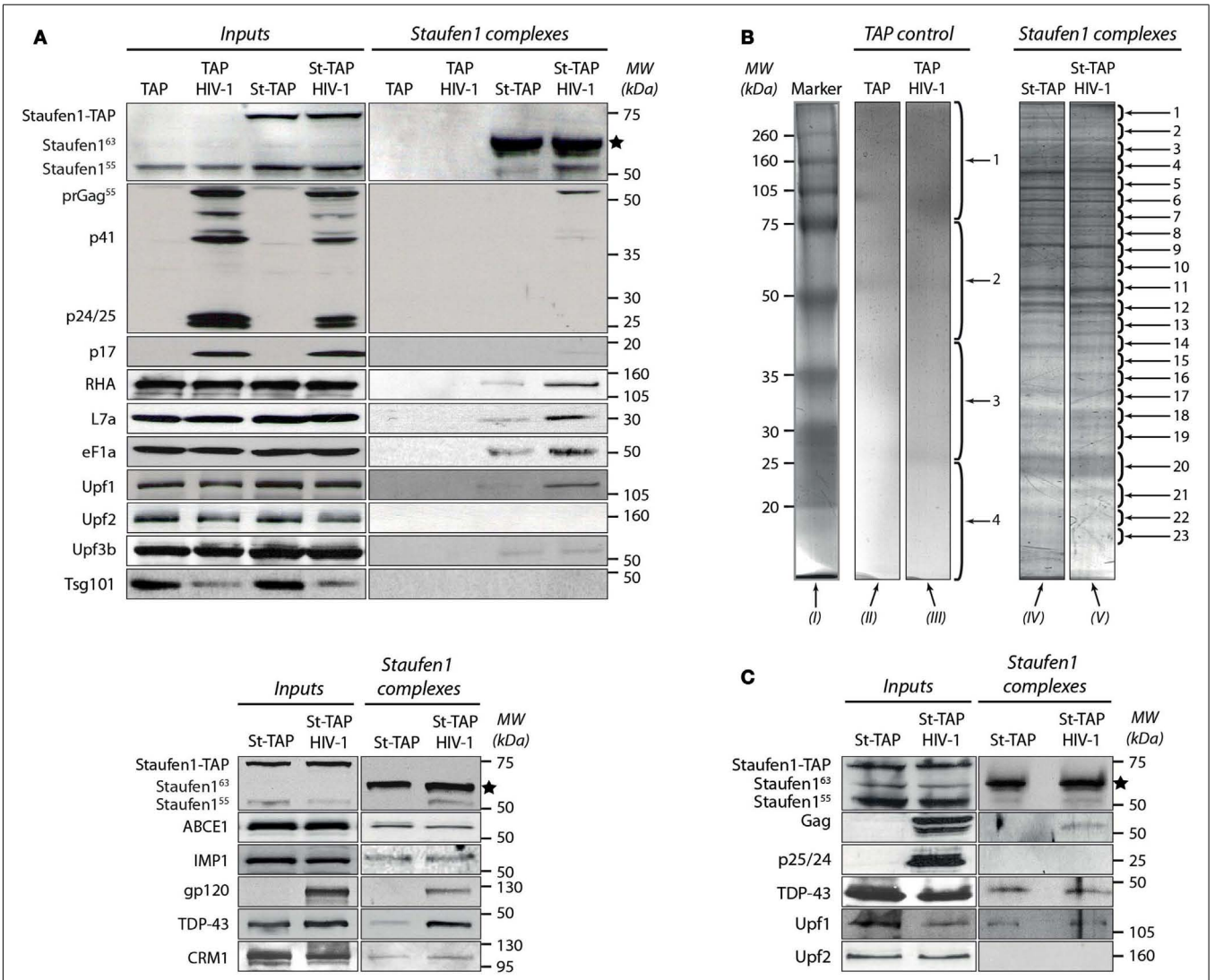

FIGURE 2 | Characterization of the tandem affinity-isolated Staufen1$^{55\,kDa}$ RNPs by western blot and mass spectrometry analysis. (A) Separation of proteins from cell lysates (*Inputs*) before (left panels) and after (right panels) tandem affinity purification (*Staufen1 complexes*) 0.25 mg of total protein obtained from extracts of TAP (control) or Staufen1-TAP expressing cell lines in the absence or presence of HIV-1 were used for affinity purification. Initially, the membrane was blotted with mouse anti-Staufen1 monoclonal antibody shown on the top left and right panels. The star (*) indicates the position of the purified St-CBP protein. **(B)** The proteins from the eluted Staufen1$^{55\,kDa}$ complexes and those from TAP alone (control) were purified from 75 mg of total protein, separated on SDS-PAGE and subsequently stained with Bio-Safe Coomassie Blue. Four bands were excised from gel lanes *(II)* and *(III)* for the identification of potential contaminating proteins. 23 bands from St-TAP and St-TAP HIV-1 (lanes *IV* and *V)* were excised and analyzed with mass spectrometry. Lane *I* represents the molecular weights in kDa of the protein standards. **(C)** Dual affinity purification of Staufen1 complexes derived from Jurkat T St-TAP stable cell lines in the absence or in the presence of HIV-1.

Furthermore, the precursor Gag protein was found in association with Staufen1 but not any of its smaller, mature cleavage products [CA (p24), MA (p17), NC (p7), or p6 (**Figures 2A,C**)]. This result is in accordance with our previous data showing the selective manner in which Staufen1 and Gag interact (Chatel-Chaix et al., 2004). Interestingly, in the majority of the experiments we also detected $pr160^{Gag/Pol}$ (Gag/Pol), probably as a result of its interaction with Staufen1, Gag and the presence of vRNA that facilitates such associations during HIV-1 assembly (Khorchid et al., 2002). The affinity purification was validated by western blotting using antibodies against several proteins that were previously found to associate with Staufen1 such as RHA, ribosomal protein L7a (Villace et al., 2004) and poly-A binding protein (PABP; **Figure 2A**; Miroslav P. Milev and Andrew J. Mouland, data not shown). Western blotting analysis revealed that eukaryotic translation elongation factor-1α (eF1α) is a Staufen1-interacting partner. This is the first time that the association with eF1α with Staufen1 has been reported; it nevertheless interacts with Gag and is incorporated in HIV-1 particles (Cimarelli and Luban, 1999).

Previously, Staufen1 was found to interact with the nucleocytoplasmic shuttling protein, Barentsz (Macchi et al., 2003), a component of exon junction complexes and an important player in nonsense-mediated mRNA decay (NMD) – a surveillance process that degrades aberrant mRNAs containing premature termination codons (Palacios et al., 2004). Staufen1-mediated mRNA decay was also described to involve Staufen1 and the major NMD factor, Upf1 (Kim et al., 2005). Moreover, these two proteins are found in association with APOBEC3G RNPs that might be involved in retroviral restriction (Kozak et al., 2006). These findings provide molecular and biochemical links between mRNA splicing, trafficking and decay. Therefore we wanted to determine the potential association of some of the main NMD factors such as Upf1, Upf2, and Upf3 in Staufen1-containing RNPs in the absence or presence of HIV-1 infection. Our results clearly demonstrate the association of Upf1 with the Staufen1 HIV-1 RNP complexes. When HIV-1 was expressed, we consistently observed approximately threefold more Upf1 eluting from the Staufen1 column compared to that found when HIV-1 was not expressed (**Figures 2A,C**). Upf2 was not detected in any of the experiments using 293T or Jurkat T Staufen1-TAP cell lines (**Figures 2A,C**) indicating that Upf2 is absent or is not stably bound in the Staufen1 RNP (Ajamian et al., 2008). The absence of Upf2 was expected since Staufen1 and Upf2 compete for binding with Upf1. Upf3b was also detected in St-TAP complexes derived from 293T cells as assessed by western blotting (**Figure 2A**).

We have demonstrated an important role for Staufen1 in the process of Gag multimerization, trafficking and viral assembly that could be coordinated with a role in the encapsidation of vRNA (Chatel-Chaix et al., 2007; Abrahamyan et al., 2010; Milev et al., 2010). We wished to verify whether the function of Staufen1 in Gag multimerization, assembly and vRNA encapsidation are linked to the function of other cellular Gag-interacting factors. To this end, we chose the host ATP-binding cassette protein ABCE1 which associates with Gag shortly after its synthesis (Dooher et al., 2007) and is critical for the proper generation of an immature HIV-1 capsid (Zimmerman et al., 2002). As in seen with Staufen1, the NC domain of Gag is a necessary and sufficient determinant for binding ABCE1 (Zimmerman et al., 2002; Lingappa et al., 2006). Equal amounts of ABCE1 were detected in Staufen1 RNPs isolated from cells with or without HIV-1 expression (**Figure 2A**, bottom panel). Several studies have demonstrated that tumor susceptibility gene 101 (TSG101) protein binds the N-terminal p6 region of Gag and is responsible for the release of the virus from the plasma membrane (Sun et al., 1999; Babst et al., 2000; Garrus et al., 2001; VerPlank et al., 2001). We did not find TSG101 in the Staufen1 eluates in any of the cell lines nor could we detect it by mass spectrometry. In fact, other candidate endosomal sorting complex required for transport (ESCRT) proteins were not detected in these Staufen1 RNPs (Miroslav P. Milev and Andrew J. Mouland, data not shown). Thus, despite its interaction with the viral protein Gag, TSG101 appears to be excluded from these particular Staufen1 RNPs suggesting separable functions during HIV-1 replication. Likewise, we did not detect either Vif or Vpr by mass spectrometry and/or western blotting analyses, both well-described interacting partners of Gag (Lavallee et al., 1994; Kondo et al., 1995; Bouyac et al., 1997; Syed and McCrae, 2009). We propose that this negative result could be due to their low abundance in Staufen1 HIV-1 complexes or that these viral proteins interact with distinct subpopulations of Gag that exclude Staufen1 (Klein et al., 2007).

IDENTIFICATION OF PROTEINS ASSOCIATED WITH STAUFEN1 HIV-1 RNPs

After validating our RNP purification protocol by western blotting, we proceeded to mass spectrometry analysis to identify proteins that associate with Staufen1 in these particles both in the absence or presence of HIV-1. For these experiments, stably expressing TAP cells were mock transfected or transfected with a proviral plasmid expressing HIV-1 (pNL4-3), lysed and then used for affinity purification. In the eluates from the control TAP samples [**Figure 2B**, lines (*II*) and (*III*)] we detected a few discrete bands. We sectioned the TAP gel lanes into four pieces (shown with numbers) and analyzed them by mass spectrometry. The proteins that were detected included keratins, immunoglobulins, interferon alpha inducible protein (IFI6), tubulin beta-2 and heat shock protein 90 and since they were found in the control TAP samples, they were considered to be contaminants.

Stable St-TAP cell lines were then mock transfected or transfected with pNL4-3. Lysates were harvested and following SDS-PAGE and Coomassie Blue staining, we observed a similarity in banding pattern between Staufen1-TAP and Staufen1-TAP HIV-1 RNPs [**Figure 2B**, lines (*IV*) and (*V*)]. In a typical experiment, we excised at least 23 bands from the St-TAP lane and corresponding bands from St-TAP HIV-1 lane. Each band was subjected to LC-MS/MS analysis and the data was concatenated and searched against either the NCBI nr human or virus databases as described in Materials and Methods. A separate randomized decoy database search was performed and the search results were filtered to achieve a False Discovery Rate (FDR) of less than 1%. This corresponded to a score cutoff of 48 and 47 for the human and viral databases, respectively.

We typically detected about 200 proteins in both Staufen1-TAP control and Staufen1-TAP HIV-1 RNPs (**Figure 3**; Tables S1 and

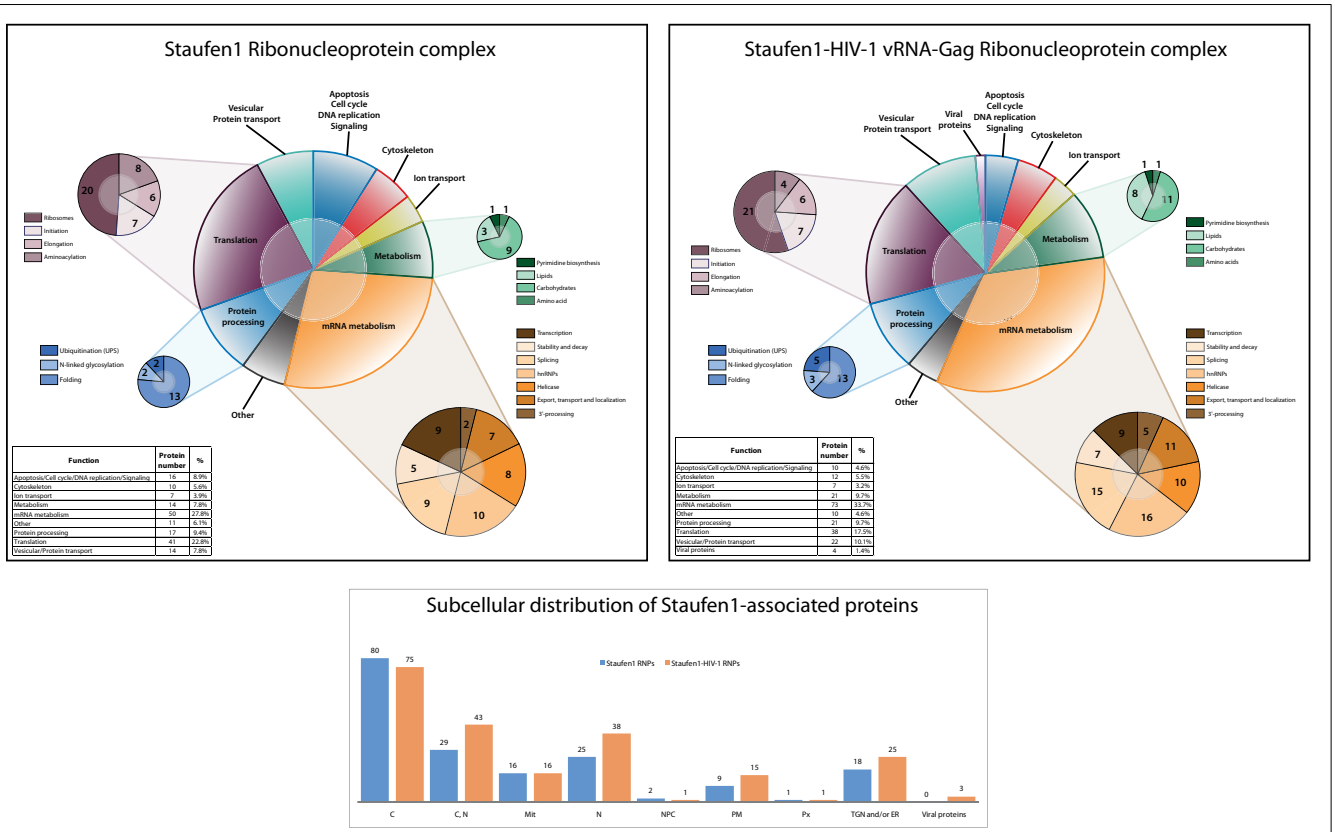

FIGURE 3 | Staufen1 RNPs contain proteins involved in the localization, stabilization and trafficking of mRNAs and HIV-1 vRNA. Graphical representation and comparison of Staufen1-associated proteins isolated from 293T cells in the absence (top panel) and the presence of HIV-1 (middle panel). The newly identified proteins were grouped on the basis of their main function or the process in which they are involved in both control and HIV-1 conditions. The subcellular distribution of proteins found in Staufen1-TAP (blue bars) and Staufen1-TAP HIV-1 (orange bars) RNPs is depicted (bottom panel). The information for each protein was obtained from the UniProt database.

S2 in Supplementary Material). As expected, some of the proteins identified had been previously shown to interact and/or associate with Staufen1, such as hnRNP U, RHA, NFAR, nucleolin, α-tubulin and numerous ribosome subunits (Brendel et al., 2004; Villace et al., 2004). The regulator of nonsense transcripts, Upf1, was also identified (Kim et al., 2005). The majority of the proteins were detected with two or more unique peptides; single peptide hits are also reported in the appended Tables S1 and S2 in Supplementary Material.

We divided all identified proteins from both cohorts into several main categories in respect to their known functions. As shown in the **Figure 3**, we generated 10 functional categories, including viral proteins in the case when HIV-1 was expressed. The largest group encompassed mRNA-binding proteins that participate in different aspects of mRNA metabolism in the cell (RNA transcription, splicing, stability, transport and degradation) and represent ∼29% of the total number of proteins in the Staufen1 RNPs and ∼35% of the total number of proteins in Staufen1-HIV-1 RNPs. These proteins included numerous heterogeneous nuclear ribonucleoproteins (RNP), DEAD-box family helicases and NMD factors Upf1 and Upf3b [detected by western blot in both types RNPs (**Figure 2A**) and by mass spectrometry – only in Staufen1 HIV-1 RNPs (**Table 1**)]. Splicing and mRNA transport factors, such as SFPQ, SF3B2 and endogenous Staufen1 and nucleocytoplasmic shuttling proteins, such as nucleolin, nuclear factor associated with dsRNA, NFAR-1 90 kDa isoform and YB-1 (a universal component of cytoplasmic mRNPs) were also included with this group. Several new mRNA-binding components associated within Staufen1 in both control and HIV-1 conditions. These included leucine-rich protein 130 kDa, LRP130, an RNA-binding protein that accumulates with mRNPs at the nuclear envelope and endoplasmic reticulum (Tsuchiya et al., 2004). Three members of the highly conserved VICKZ family of RNA-binding proteins (Vg1 RBP/Vera, IMP1,2,3, CRD-BP, KOC, ZBP-1) and insulin-like growth factor II mRNA-binding protein 1, 2 and 3 (IMP1 and IMP2 in the native complexes and IMP1 and IMP3 in those purified from HIV-1-expressing cells) were also detected [Reviewed in (Yisraeli, 2005)]. The RNA/DNA-binding protein TDP-43 was detected by mass spectrometry only in HIV-1-containing complexes, but was later confirmed by western blotting analysis in both the presence and absence of HIV-1. Structurally analogous to the hnRNPs, this protein was originally described as a factor that modulates HIV-1 gene expression at the transcriptional level (Ou et al., 1995).

Table 1 | Unique proteins identified by mass spectrometry in Staufen1-HIV-1 RNPs.

Protein name*	UniProt accession number**	Role in HIV-1 replication?	Reference
26S protease regulatory subunit S10B (PSMC6)	P62333	Unknown	N/A
26S proteasome non-ATPase regulatory subunit 2	Q13200	Unknown	N/A
60S ribosomal protein L29 (RPL29)	P47914	Unknown	N/A
7-dehydrocholesterol reductase (DHCR7)	Q9UBM7	Yes	(van't Wout et al., 2005)
Actin-related protein 2/3 complex subunit 4	P59998	Yes	(Komano et al., 2004; Chertova et al., 2006)
ADP-ribosylation factor 4 (ARF4/ARF2)	P18085	Unknown	N/A
ADP-ribosylation factor 6 (ARF6)	P62330	Yes	(Ono et al., 2004)
Alpha-internexin (INA)	Q16352	Unknown	N/A
AP-2 complex subunit mu (AP-2M1)	Q96CW1	Yes	(Le Gall, 1998; Craig et al., 2000; Batonick et al., 2005)
AP-3 complex subunit delta-1 (AP-3D1)	O14617	Yes	(Dong et al., 2005)
CDP-diacylglycerol–inositol 3-phosphatidyltransferase (CDIPT)	O14735	Unknown	N/A
Cleavage and polyadenylation specificity factor subunit 1 (CPSF1)	Q10570	Unknown	N/A
Cleavage and polyadenylation specificity factor subunit 7 (CPSF7)	Q8N684	Unknown	N/A
Coatomer subunit zeta-1 (COPZ1)	P61923	Unknown	N/A
Copine-3	O75131	Unknown	(Chertova et al., 2006)
Delta-1-pyrroline-5-carboxylate synthetase (ALDH18A1)	P54886	Unknown	N/A
Double-stranded RNA-specific adenosine deaminase (ADAR)	P55265	Yes	(Phuphuakrat et al., 2008; Doria et al., 2009)
Dynamin-2 (DNM2)	P50570	Yes	(Pizzato et al., 2007)
E3 ubiquitin-protein ligase (BRE1A)	Q5VTR2	Unknown	N/A
Env	P03377	Yes	(Freed, 2001)
Eukaryotic initiation factor 4A-III (eIF4A3)	P38919	Unknown	N/A
Eukaryotic translation initiation factor 3 subunit E (eIF3E)	P60228	Unknown	N/A
Gag	P12493	Yes	(Freed, 1998)
Gag/Pol	P12493	Yes	(Jacks et al., 1988)
GTP-binding nuclear protein Ran	P62826	Yes	(Askjaer et al., 1998)
Heat shock 70 kDa protein 1L	P34931	Yes	(Rasheed et al., 2008)
Heterogeneous nuclear ribonucleoprotein A/B	Q99729	Yes	(Mouland et al., 2001)
Heterogeneous nuclear ribonucleoprotein F (hnRNP F)	P52597	Unknown	N/A
Heterogeneous nuclear ribonucleoprotein H2	P55795	Unknown	N/A
Heterogeneous nuclear ribonucleoprotein H3 (hnRNP H3)	P31942	Unknown	N/A
Heterogeneous nuclear ribonucleoprotein Q (hnRNP Q)	O60506	Yes	(Hadian et al., 2009)
Heterogeneous nuclear ribonucleoprotein R (hnRNP R)	O43390	Yes	(Hadian et al., 2009)
HIV-1 Rev-binding protein 2	Q13601	Unknown	N/A
Importin-7	O95373	Yes	(Fassati et al., 2003; Zaitseva et al., 2009)
Insulin-like growth factor II mRNA-binding protein-3	O00425	Unknown	N/A
IQ motif containing GTPase activating protein 1	P46940	Unknown	(Chertova et al., 2006)
Leucine-rich repeat-containing protein 59 (LRRC59)	Q96AG4	Unknown	N/A
Long-chain-fatty-acid–CoA ligase 3 (ACSL3)	O95573	Unknown	N/A
Mannosyl-oligosaccharide glucosidase (MOGS)	Q13724	Unknown	N/A
Nef	P05855	Yes	(Arhel and Kirchhoff, 2009)
NF-kappaB repressing factor (NRF)	A3F768	Yes	(Dreikhausen et al., 2005)
Non-POU domain-containing octamer-binding protein (NONO)	Q15233	Yes	(Zolotukhin et al., 2003)
Nuclear pore complex protein 155 (Nup155)	O75694	Yes	(Brass et al., 2008; Lee et al., 2010)
Peroxiredoxin-6	P30041	Unknown	(Chertova et al., 2006)
Phosphatidylserine synthase 1 (PTDSS1)	P48651	Unknown	N/A
Pre-mRNA 3′-end-processing factor FIP1 (FIP1L1)	Q6UN15	Unknown	N/A

(Continued)

Table 1 | Continued

Protein name*	UniProt accession number**	Role in HIV-1 replication?	Reference
Probable ATP-dependent RNA helicase (DDX17)	Q92841	Unknown	N/A***
Probable ATP-dependent RNA helicase (DDX27)	Q96GQ7	Unknown	N/A
Programmed cell death 8 (AIFM1)	O95831	Unknown	N/A
Protein transport protein Sec61 subunit alpha isoform 1 (SEC61A1)	P61619	Unknown	N/A
Protein tyrosine phosphatase-like protein (PTPLAD1)	Q9P035	Unknown	N/A
Putative RNA-binding protein Luc7-like 2	Q9Y383	Unknown	N/A
Pyruvate dehydrogenase E1 component subunit beta (PDHB)	P11177	Unknown	(Ringrose et al., 2008)
Ras-related GTP-binding protein A (RRAGA)	Q7L523	Unknown	N/A
Ras-related protein Rab-10	P61026	Unknown	(Chertova et al., 2006)
Ras-related protein Rab-5C	P51148	Yes	(Vidricaire and Tremblay, 2005; Chertova et al., 2006)
Ras-related protein Rab-8A	P61006	Unknown	(Chertova et al., 2006)
Ribonucleoprotein PTB-binding 1	Q8IY67	Unknown	N/A
Signal recognition particle receptor subunit beta (SRPRB)	Q9Y5M8	Unknown	N/A
Spliceosome RNA helicase (BAT1)	Q13838	Unknown	(Limou et al., 2009)
Splicing factor, arginine/serine-rich 13A (SFRS13A)	O75494	Unknown	N/A
Splicing factor, arginine/serine-rich 4 (SFRS4)	Q08170	Unknown	N/A
Splicing factor, proline- and glutamine-rich (SFPQ)	P23246	Yes	(Zolotukhin et al., 2003)
T-complex protein 1 subunit beta	P78371	Unknown	N/A
THO complex 4 (THOC4)	Q86V81	Unknown	N/A
THO complex subunit 2 (THOC2)	Q8NI27	Unknown	N/A
T-plastin polypeptide (plastin-3)	P13797	Unknown	N/A
Tubulin alpha-4A chain	P68366	Unknown	(Chertova et al., 2006)
V-type proton ATPase subunit d 1	P61421	Unknown	(Chertova et al., 2006)
Zinc finger RNA-binding protein (ZFR)	Q96KR1	Unknown	N/A

Viral proteins are highlighted; **Universal Protein Resource — UniProt database [http://www.uniprot.org/]; * Not applicable.*

The second most predominant category relates to proteins involved in RNA translation (∼23 and ∼18% in the absence and presence of HIV-1, respectively) and includes ribosomal, translation initiation and elongation factors and several aminoacyl-tRNA synthetases. Proteins such as PABP1, eukaryotic translation initiation, and elongation factors – eIF3 (α, β and ε), eIF4A (two isoforms – 1 and 3) and eF1 (α, γ and δ isoforms) were also detected.

Proteins involved in cell metabolism represented ∼8% of the total number of proteins in Staufen1-containing RNPs isolated in the absence of HIV-1 and ∼9% in the presence of HIV-1. These included enzymes that regulate different aspects of the general cellular metabolism of carbohydrates, lipids, amino acids, and nucleotides, such as pyruvate kinase and pyruvate dehydrogenase, lactate dehydrogenase and glyceraldehyde-3-phosphate dehydrogenase, fatty acid synthase, ATP-citrate synthase and others (**Figure 3**; Tables S1 and S2 in Supplementary Material).

Diverse proteins involved in cytoskeleton formation and structure (∼4 and ∼5% in the absence HIV-1 and presence of HIV-1, respectively), including actin, tubulin, vimentin, as well as IQGAP1 were detected (**Figure 3**; Tables S1 and S2 in Supplementary Material). We also placed Matrin 3 in this category as it is a novel Staufen1-binding partner that was originally reported to be one of the major structural proteins of the inner nuclear matrix (Belgrader et al., 1991). An interesting feature of this protein is its ability to retain A–I edited dsRNAs in the nucleus (Reviewed in DeCerbo and Carmichael, 2005). Moreover, it has been shown in association with APOBEC3G RNPs (Kozak et al., 2006) and with 3′-untranslated region (UTR) of the hepatitis C genome (Harris et al., 2006).

Approximately 8% (−HIV-1) and 10% (+HIV-1) of Staufen1-binding partners were vesicular and protein transport proteins. As mentioned earlier, TSG101, a member of ESCRT-I was not detected by western blotting or by mass spectrometry. Instead, we identified some other proteins involved in the control of endosomal dynamics and in intra-Golgi vesicular transport, including vesicle budding from Golgi membranes. These included Ras-related proteins (Rab-5C, Rab8, Rab-10), some of the coatomer protein complex subunits – COP (α, γ and ζ), adaptor proteins – (AP-2, AP-3) and ADP-ribosylation factors (1, 4, 5 and 6). In addition, some cellular factors regulating the processes of protein folding (heat shock proteins, T-complex proteins, Calnexin), ubiquitination and N-linked glycosylation (Ribophorin-1) constitute the protein processing group [∼8% (−HIV) and ∼9% (+HIV-1)].

Finally, the remaining identified proteins included those involved in ion transport (including sodium/potassium-transporting ATPase, several ATP synthases) and apoptosis/cell cycle/DNA replication/signaling (CDC5L, MCM7 and RACK1), while the remaining proteins were grouped under "others" and

included mitochondrial and nucleocytoplasmic transport proteins (Nup155, Importin1, Importin-7, Xpo1, Xpo2 and ADP/ATP translocase; **Figure 3** and see Tables S1 and S2 in Supplementary Material).

We detected 45 proteins from Staufen1 HIV-1 RNPs (including viral proteins such as Gag, Gag/Pol, Env and Nef; Tables S1 and S2 in Supplementary Material) that are virion-associated (Ott, 2002, 2008; Cantin et al., 2005; Komano et al., 2005; Chertova et al., 2006; Goff, 2007) representing 22% of the total number of proteins found in the Staufen1 HIV-1 complexes. Among them were RHA, IQGAP1, actin, vimentin, eF1α, Staufen1, IMP1 and heat shock proteins Hsp60, Hsp70 and Hsc70. The latter three are incorporated within the membrane of the viruses and are important for virus infectivity (Gurer et al., 2002). Upf1, which is found in the HIV-1 RNP, also represents a virion-incorporated protein (Abrahamyan et al., 2010).

CHARACTERIZATION OF INTERACTIONS BETWEEN STAUFEN1 AND SEVERAL NOVEL PARTNERS USING BIOCHEMICAL AND IMMUNOFLUORESCENCE METHODS

We confirmed the association of several proteins with Staufen1 complexes using IP and IF analyses. For the purpose of these experiments, we chose three predominantly nuclear proteins: AU-rich element RNA binding protein 1, AUF1, TAR DNA-binding protein, TDP-43 and chromosomal regional maintenance protein 1 (CRM1 or Xpo1), a factor that mediates the nuclear export and ABCE1 (also known an HP68). IP experiments were performed with lysates derived from HeLa cells. To determine the RNA dependence of these interactions, equal amounts of lysates were treated with or without RnaseA for 30 min on ice before IP. Our results demonstrate the RNA-independent character of Staufen1 interactions with CRM1 and ABCE1 (**Figures 4A,B**, IP panels), whereas those between both Staufen1 and TDP-43 and Staufen1 and AUF1 appeared to be RNA-dependent (**Figures 4C,D**, IP panels). We detected IMP1 in three independent MS analyses and further confirmed its presence in affinity-isolated complexes using polyclonal rabbit anti-IMP1 antibody (**Figure 2A**, bottom panel). IMP1 is a human ortholog of chicken Zipcode binding protein 1 (ZBP-1) and belongs to VICKZ protein family (Yisraeli, 2005). Different studies indicate similar functions for IMP1 and Staufen1 with respect to mRNA transport, translational control and localization. IMP1 binds fragile × mental retardation protein (Rackham and Brown, 2004) and PABP1 (Patel and Bag, 2006) and associates with APOBEC3G (Kozak et al., 2006), YB-1, nucleolin and hnRNP A1 (Jonson et al., 2007), proteins that also associate with Staufen1. Recently, IMP1 has been found to bind to HIV-1 Gag (Roy et al., 2006) and in our own work this protein also associates with lipid raft domains (Milev et al., 2010). We performed IP experiments for IMP1 (**Figure 4E**, IP panel) and observed that its association with Staufen1 was also RNA-independent.

To further demonstrate the interrelationships between Staufen1 and these proteins, we performed laser scanning confocal microscopy to examine their distribution in cells. We transfected HeLa cells with plasmids expressing Staufen1-HA and 24 h later, we fixed and stained the cells with antibodies recognizing the HA-epitope and the endogenous proteins that were used in the IPs, with the exception that we used an anti-GFP to detect IMP1-VenusC (IMP1-VC). We observed co-localization of Staufen1 with ABCE1 and partial co-localization with TDP-43, AUF1 (Lund et al., 2012) and CRM1 [**Figures 4A–D**, co-localization with Staufen1 panels; Manders' coefficients (%) are shown]. As expected, Staufen1 and IMP1 co-localized in cytoplasmic particles, but this was only true for a proportion of these proteins (**Figure 4E**, *co-localization with Staufen1 panel*). Finally, the possible interactions of these novel Staufen1 partners with vRNA and Gag were elucidated by combined FISH and IF co-analyses in HIV-1-expressing cells. We transfected HeLa cells with both pNL4-3 proviral DNA plasmids coding for IMP1-VenusC (**Figures 4A–E**, *distribution + HIV-1 panels*). Cells were fixed and stained with rabbit anti-CRM1, anti-ABCE1 anti-TDP-43, anti-AUF1, or anti-GFP (to detect IMP1-VenusC; all in red, **Figures 4A–E**, *distribution + HIV-1 panels*), along with sheep anti-p17 to detect Gag (shown in blue) and FISH was performed to detect viral RNA (shown in green). The presence of HIV-1 caused the partial accumulation of AUF1 in the cytoplasm. The mechanism, however, that underlines this phenomenon is unclear but could be due to the HIV-1 imposed block on nuclear import (Monette et al., 2009) and the functional significance of this interaction was recently demonstrated (Lund et al., 2012). Importantly, ABCE1, currently implicated in the generation of HIV-1 capsids, co-localized with the vRNA. At present, we do not know if this is via a direct or indirect interaction. The co-localization of IMP1 with viral components was estimated in cells simultaneously transfected with IMP1-VenusC and pNL4-3 plasmids. We noticed that cells overexpressing IMP1-VenusC (**Figure 4E**, shown with white arrows) had an apparent decrease in the signal for vRNA. Cells that did not express or expressed IMP1-VenusC at lower levels showed higher accumulations of vRNA (**Figure 4E**, white arrow head). This negative effect on vRNA in HIV-1 positive cells was observed in more than 55% of the cells.

SUCROSE DENSITY GRADIENT ANALYSIS OF STAUFEN1 HIV-1 RNPs

Sucrose density gradient analyses were then performed to further characterize Staufen1 RNP dynamics when HIV-1 was expressed. The biochemical examination of these RNPs is important since Staufen1 is found in several RNPs relevant to HIV-1 (Chiu et al., 2006; Abrahamyan et al., 2010) but it also selectively associates with the vRNA in complex with Gag and other host proteins (Chatel-Chaix et al., 2004, 2008; Ajamian et al., 2008). Moreover, in our earlier study, we demonstrated that Staufen1 RNPs were plastic in size but co-associated with Gag and vRNA signals (Abrahamyan et al., 2010). We therefore assessed the distribution of Staufen1 RNPs by sucrose density centrifugation to determine how HIV-1 influences this. HA-Staufen1 was transfected into HeLa cells without or with pNL4-3 proviral HIV-1 DNA. Lysates were processed for sucrose density gradient analyses. Fractions were collected from the top of the gradient and HIV-1 vRNA was quantitated by slot blot analysis. An aliquot of each gradient fraction was run on SDS-PAGE and western blotting was performed to identify Staufen1-HA and several of the newly identified members of Staufen1-TAP-containing host proteins (e.g., RP-L7a, TDP-43 and ABCE1, Table S2 in Supplementary Material) and Gag in HIV-1 samples (**Figures 5A,B**). In some cases, lysates were treated with

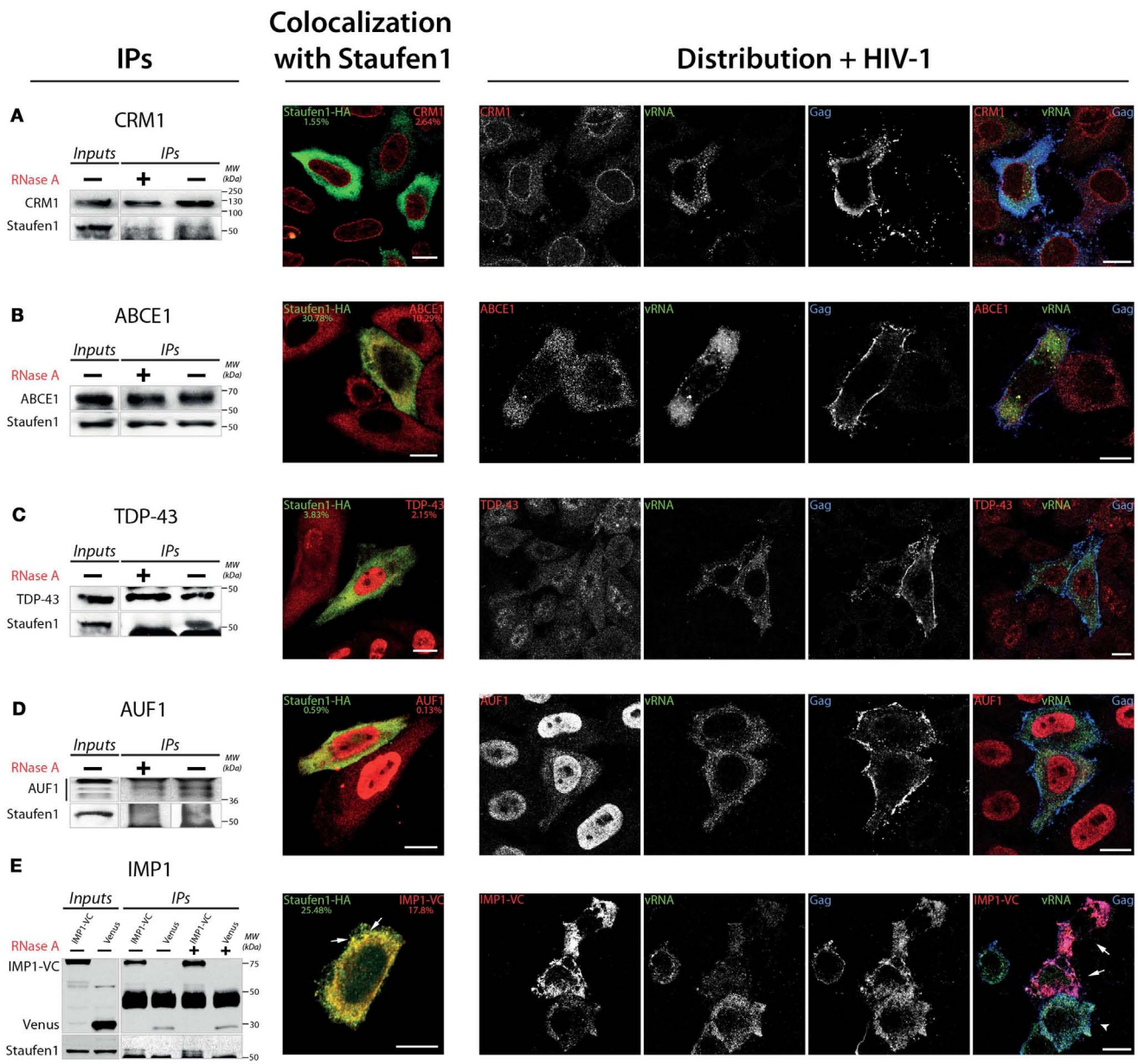

FIGURE 4 | Confirmation of the *in vivo* association of Staufen1 with several of the host factors that were identified in Staufen1-contain RNP complexes. (A–E) CRM1, ABCE1, TDP-43, AUF1 and IMP1 (as IMP1-VenusC) were immunoprecipitated from 500 mg total protein lysate of HeLa cells. For the immunoprecipitation of IMP1 HeLa cells were transfected with IMP1-VenC or Venus-full length (as a control) and immunoprecipitated with a mouse anti-GFP antibody. The images to the immediate right of the IPs show the patterns of co-localization of CRM1, cytoplasmic RNAse L inhibitor (ABCE1), AUF1, TAR DNA-binding protein (TDP-43) and IMP1 with Staufen1-HA. The Manders' coefficients (average from >10 cells per experiment derived from Staufen-HA expressing cells only, in %) are shown to provide an estimate of the co-localization. At the far right, the distribution of each host protein (in red) is shown in relation to Gag (blue) and the viral genomic RNA (vRNA, green) in HIV-1-expressing cells as determined by laser scanning confocal microscopy. Cells overexpressing IMP1-VenusC are indicated with white arrows in **(E)**. Size bars are 10 μm.

RNAse A to determine RNA-dependency. These analyses revealed that there was no consistent shift in the sedimentation profile of Staufen1-HA complexes in mock and HIV-1-expressing cells and they mainly fractionated in denser fractions #11–18 (**Figure 5A**). This was also true for those for the selected Staufen1-associated host proteins. However, Gag sedimented in two regions of the density gradient, in both a light (fractions #1–7) and a more dense region (fractions #12–20; **Figure 5B**), while the vRNA only sedimented in very dense fractions (#16–20) in this assay. RNAse A treatment eliminated the vRNA, but also disrupted the distribution of viral and host proteins in the dense fractions leading to their migration in lighter density fractions, with the exception of the

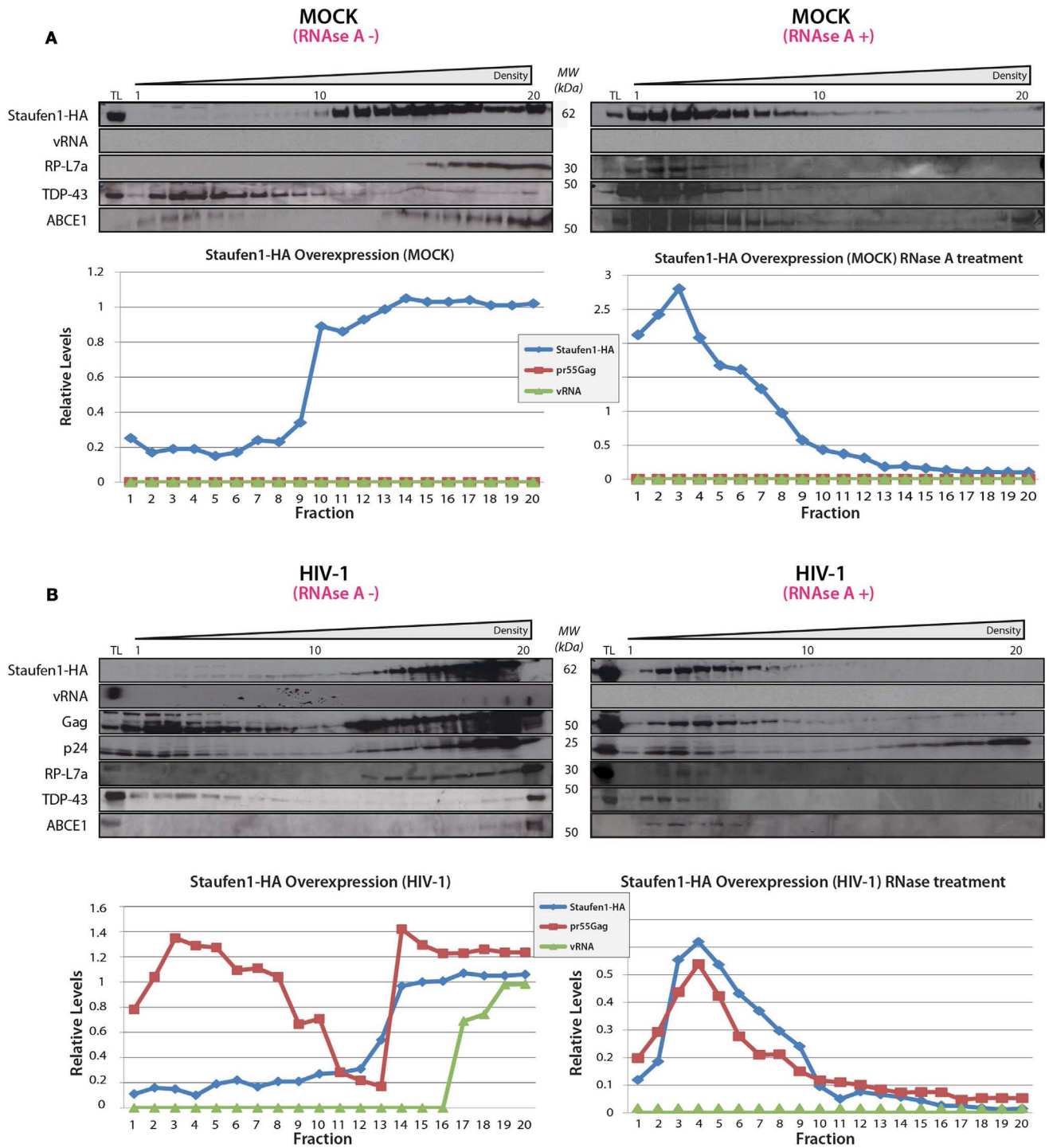

FIGURE 5 | Staufen1 co-fractionates with Gag and vRNA in gradient density fractionation analyses. (A) HeLa cells were either mock transfected with empty vector, pcDNA3, or with a plasmid that expresses Staufen1-HA. The transfected cells were collected 24 h later, lysed and were either mock-treated or treated with RNAse A. The lysates were then fractionated on 5–50% sucrose gradients and 20 fractions were collected for further analysis by western blotting for viral and host proteins, as indicated. HIV-1 viral genomic RNA (vRNA, 9 kb) was assessed in each fraction by slot blot analysis. TL represents the total lysates. **(B)** HeLa cells were co-transfected with pNL 4–3 and Staufen1-HA. The presence of Staufen1-HA, precursor Gag and p24 were assessed in each fraction by western blotting analysis. HIV-1 viral genomic RNA (9 kb, vRNA) was assessed in each fraction by slot blot analysis. Staufen1, Gag and vRNA were quantitated in each fraction by densitometry and relative levels are depicted for each fraction (Blue: Staufen1-HA, Red: Gag, Green-vRNA).

processed form of Gag, p24, which likely represents capsids or virus particles that are membrane-bound (Levesque et al., 2006). The precursor to p24, p25 was also observed in the lighter fractions supporting this notion (**Figure 5** and below). We have shown that the Staufen1-Gag interaction is RNA-independent and in close proximity (Chatel-Chaix et al., 2004) so these results indicate that Gag is recruited to pre-existing Staufen1 RNPs as we demonstrated earlier (Milev et al., 2010) but also, it remains associated to Staufen1 when viral and cellular RNAs are in limiting supply. This notion is also supported in experiments in which a Gag-less pNL4-3 is expressed. This proviral DNA will express all viral proteins and RNAs except for Gag and Gag/Pol (Poon et al., 2002). When expressed alone (**Figure 6A**) or when Staufen1-HA is overexpressed (**Figure 6B**), the sedimentation profiles for vRNA were not appreciably affected in the absence of Gag. This is consistent with our recent findings that showed that Staufen1 and vRNA co-localized significantly in the absence of Gag under the same experimental conditions (Abrahamyan et al., 2010). When Gag expression was rescued by the expression of a Rev-dependent Gag expressor (Lingappa et al., 2006; **Figure 6C**), the distribution of vRNA was consistently found to be shifted toward the lighter fractions, that might be specific to this rescue experiment (i.e., due to *trans* expression of Gag) because the vRNA is found in the penultimate fractions when pNL4-3 is expressed (**Figure 5**). Further experimentation will be required to characterize the function of these lighter RNPs upon Gag rescue in *trans*.

In the experiments above, endogenous Staufen1 is abundantly expressed that could allow the assembly of Staufen1 viral RNPs. In conditions when endogenous Staufen1 is depleted by siRNA, we have shown that large Staufen1 RNPs (SHRNPs) formed in the vicinity of the nucleus and in the cytoplasm. These structures were proposed to be supraphysiologic RNPs that could serve as scaffolds for viral assembly and vRNA encapsidation. We investigated by density gradient analysis whether the SHRNPs represented a super-dense RNP or amalgamations of many smaller RNPs. HeLa cells were transfected with pNL4-3 DNA and either siNS or siStaufen1 siRNAs and lysates were prepared for gradient analyses. While siStaufen1 treatment again resulted in reduced Gag synthesis (Abrahamyan et al., 2010; **Figure 7A**), the sedimentation profiles for vRNA and Gag did not appreciably change (**Figures 7B,C**). However, the relative levels of Gag in light and dense gradient fractions were modulated such that a less abundant signal for Gag in the dense fractions was observed. This could be the populations of Gag influenced by Staufen1 expression levels and functionally relevant for the assembly of dense RNPs or represent a population of Gag with a specific function (Klein et al., 2007). Importantly, these results provide evidence that the larger Staufen1 RNPs observed in Staufen1 depletion conditions likely represent aggregations of

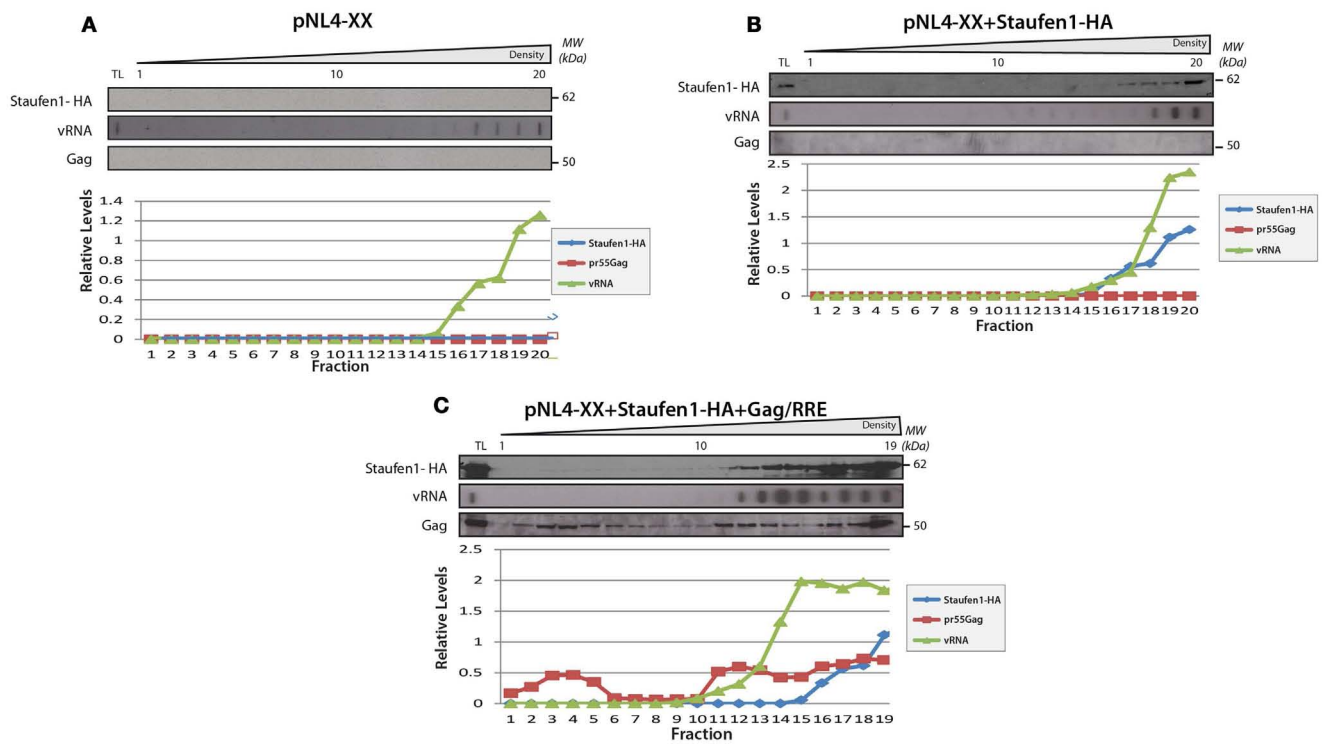

FIGURE 6 | The sedimentation of Staufen1 and vRNA indensitygradientsdid not significantly change in the absence of Gag expression. (A) HeLa cells were co-transfected with pNL4-XX (harboring two mutations in the *gag* open reading frame to prevent Gag synthesis) with either empty vector control **(A)**, Staufen1-HA **(B)**, or Gag-RRE **(C)**. The cells lysates were then fractionated on 5–50% sucrose gradients and 20 fractions were collected for further analysis by western blotting analyses, as indicated. TL represents the total lysates. Staufen1, Gag and vRNA were quantitated in each fraction by densitometry and relative levels are depicted for each fraction (Blue: Staufen1-HA, Red: Gag, Green: vRNA).

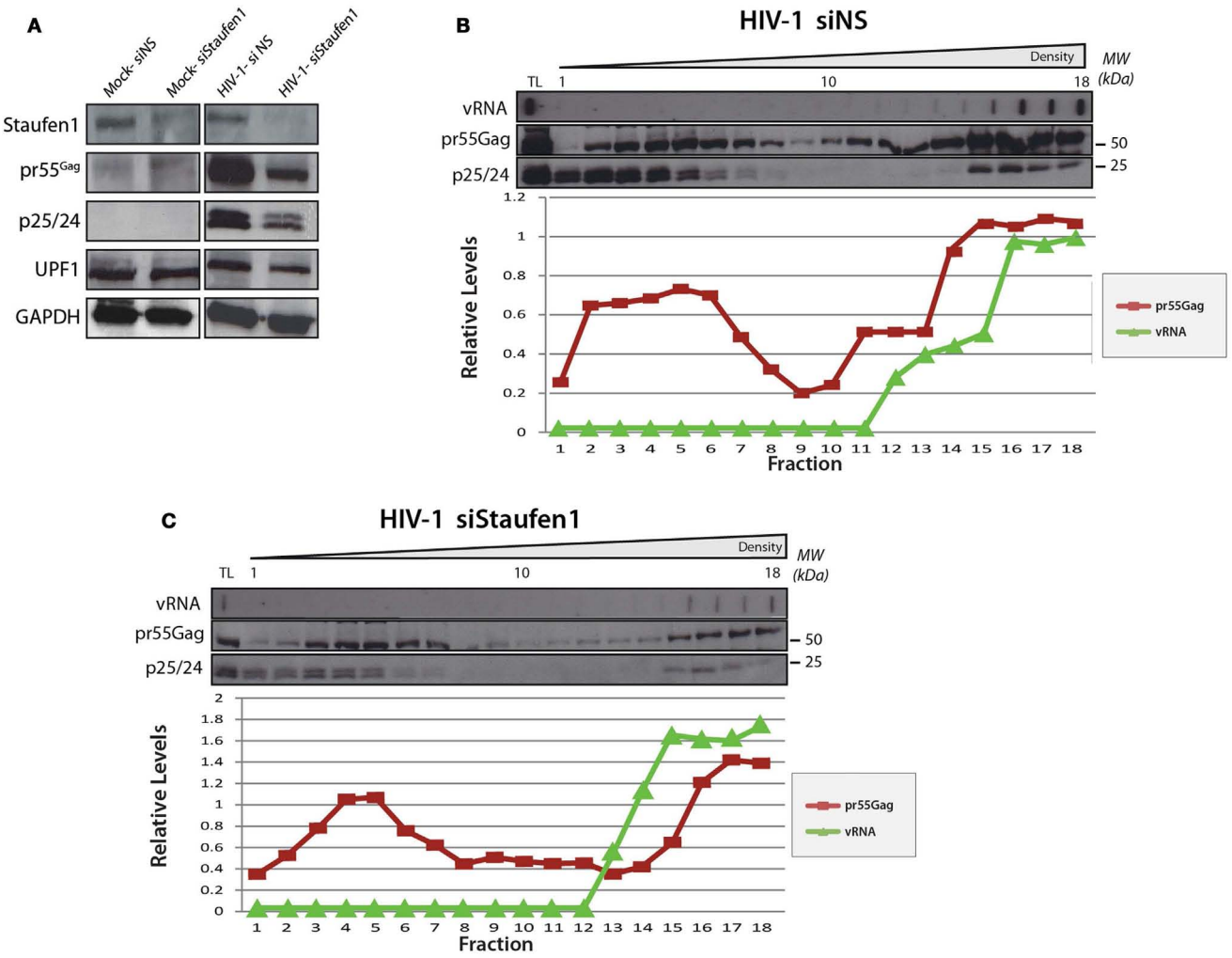

FIGURE 7 | The relative levels of Gag in light and dense gradient fractions are modulatedin Staufen1-depleted cells. HeLa cells were mock transfected or co-transfected with pNL4-3 with either non-silencing control siRNA (siNS) or a siRNA to deplete endogenous Staufen1 (siStaufen1) and were harvested and lysed 36 h later and analyzed by western blotting. Corresponding expression levels for Staufen1, Gag, UPF1 and GAPDH proteins are shown in **(A)**. The cell lysates from siNS-treated **(B)** and siStaufen1-treated **(C)** cells were fractionated on 5–50% sucrose gradients and 19–20 fractions were collected for further analysis by western blotting, as indicated. TL represents the total lysates. HIV-1 viral genomic RNA (9 kb, vRNA) was assessed in each fraction by slot blot analysis. Staufen1, Gag and vRNA were quantitated in each fraction by densitometry and relative levels are depicted for each fraction (Blue: Staufen1-HA, Red: Gag, Green: vRNA).

similar-sized RNPs rather than the assembly of a supraphysiologic RNP (Abrahamyan et al., 2010).

DISCUSSION

The combination of TAP and mass spectrometry has proven to be reliable for the characterization of different protein complexes (reviewed in Xu et al., 2010) including those containing HIV-1 Gag, UPF1 and Staufen1 (Schell et al., 2003; Brendel et al., 2004; Villace et al., 2004; Roy et al., 2006). Here we provide deeper insights into the impact of HIV-1 expression on the composition of Staufen1 RNPs.

While the analyses performed here detected almost all of the previously characterized proteins characterized as components of Staufen1 RNPs (Brendel et al., 2004; Villace et al., 2004), they also revealed that the protein composition of the particles was influenced by the presence of HIV-1. In addition to the viral gene products, Gag, Gag/Pol, Env and Nef, which are all incorporated into Staufen1 RNPs in the presence of HIV-1, generally the number of proteins in the Staufen1 RNP was enhanced in the presence of HIV-1 (**Figure 3**; **Table 1**; Tables S1 and S2 in Supplementary Material). In addition, HIV-1-mediated an increase in the amounts of several other host proteins that were found in smaller amounts in Staufen1-containing RNPs isolated from uninfected 293T cells (**Figure 2A**). The signal intensities of UPF1, eF1α, ribosomal protein L7a and RHA, for example, were approximately threefold greater in western blotting experiments in the presence of HIV-1. Endogenous Staufen1 was also recruited to a higher degree to the complexes isolated from HIV-1-expressing cells (**Figure 2A**,

top panels). This HIV-1-mediated modulation in protein composition of the Staufen1 RNA was indeed selective since equal quantities of several other proteins, such as IMP1, ABCE1 and UPF3 were found between the two treatment groups. The changes to the Staufen1 protein environment described here could invariably be mediated by the presence of the four viral proteins (Gag, Gag/Pol, Env and Nef) and the vRNA within the Staufen1 HIV-1 RNP, thereby recruiting and enriching for a number of host factors. Consistently, Gag can recruit Staufen1 and other host factors (Milev et al., 2010). When this analysis was performed in Jurkat T cell lines, we did not observe some of the same changes to the abundance of proteins (e.g., TDP-43) as judged in western blots (**Figure 2C**). This could possibly be due to lower transfection efficiencies, or more likely, because the compactness of the cytoplasm in Jurkat T cells and the relatively shorter intracellular distances in these mononuclear cells might restrict the protein content of Staufen1 RNPs in general. Overall, it will be important to analyze further the possible functions of the unique proteins found in Staufen1 HIV-1 RNPs and their effects on HIV-1 replication.

CONSTITUENTS OF STAUFEN1 RNPs INVOLVED IN mRNA TRANSLATION, TRAFFICKING AND STABILITY

We identified numerous Staufen1-associated proteins including the small and large ribosomal subunit proteins, translation initiation and elongation factors, tRNA synthetases, some of which are involved in RNA trafficking RNPs (Carson et al., 2008). Most of these proteins were common components that were identified in both native Staufen1 and Staufen1 HIV-1 RNPs as it was in the cases of eIF3α and eIF4A1 (Tables S1 and S2 in Supplementary Material). However, eIF3β was only found in native and eIF3ε was only detected in Staufen1 HIV-1 RNPs (**Table 1**; Tables S1 and S2 in Supplementary Material). In the context of the Staufen1 HIV-1 RNPs, their functions in mRNA translation could be potentially enhanced by the presence of the viral proteins and evidence for this is supported in the literature (Jager et al., 2012). For example, Env, influences RPS6 kinase and upregulates mRNA translation (Barcova et al., 1999). Furthermore, HIV-1 Gag and that of other retroviruses can modulate the translation activity of its cognate mRNA (the vRNA; Sonstegard and Hackett, 1996; Anderson and Lever, 2006).

Proteins involved in mRNA stability were also common to both native Staufen1 and Staufen1 HIV-1 RNPs including Upf1, Upf3b, IMP1 and FUSE-binding protein (refer to Tables S1 and S2 in Supplementary Material for others), but IMP2 and IMP3 were exclusive to native and to Staufen1 HIV-1 complexes, respectively. Although several of these factors have already been shown to alter HIV-1 gene expression (Ajamian et al., 2008; Zhou et al., 2008), additional work will be needed to determine their roles in Staufen1-containing RNPs. Nevertheless, the presence of these proteins suggests that Staufen1 RNPs are involved in the regulation of mRNA translation and stability of both cellular and viral mRNAs. Many components identified as constituents of stress granules (Ohn et al., 2008) were also observed in Staufen1 RNPs including Staufen1 itself, several RNA helicases, translation factors (eIF3, eEF1), IMP1 and ribosomal proteins (Table S2 in Supplementary Material) and their presence or sequestration could be implicated in the abrogation of this stress response in HIV-1- and other virus-infected cells (Abrahamyan et al., 2010; Ruggieri et al., 2012).

STAUFEN1 RNPs: IMPLICATIONS IN TRANSCRIPTION, SPLICING AND mRNA NUCLEAR RETENTION?

Staufen1 RNP also contain a number of proteins implicated in nuclear RNA quality control, a role we have previously characterized for UPF1 (Ajamian et al., 2008). We detected several predominantly nuclear proteins in native Staufen1 and Staufen1 HIV-1 RNPs such as nucleolin (NCL), hnRNPU and RNA helicase (RHA or DDX9; Brendel et al., 2004; Villace et al., 2004) and several transcription and splicing factors as common elements in both control and HIV-1 Staufen1 RNPs (Tables S1 and S2 in Supplementary Material), but there were also significant differences. Staufen1 HIV-1 RNPs appeared to be enriched in splicing factors, RNA helicases and hnRNPs (refer to **Table 1**) that are specifically co-opted by HIV-1 and have established roles in HIV-1 replication (Caputi et al., 1999; Jeang and Yedavalli, 2006; Levesque et al., 2006; Lund et al., 2012). The NF-κB repressing factor (NRF), for instance, binds to a specific negative regulatory element within the HIV-1 LTR and regulates transcription initiation and elongation (Dreikhausen et al., 2005). Two other RNA- and DNA-binding proteins SFPQ (PSF) and Non-POU domain-containing octamer-binding protein (NONO) act in the context of a heterodimer and play essential roles in the transcriptional regulation and in the pre-mRNA splicing. As well, both proteins play a role in HIV-1 replication by binding, with high affinity, the instability (INS) regions in HIV-1 *gag* mRNA suggesting a role in RNA stability or translation (Zolotukhin et al., 2003). Importantly, NONO and PSF form a complex with another common Staufen1 component, nuclear matrix protein Matrin 3, as described above (Zhang and Carmichael, 2001; DeCerbo and Carmichael, 2005). Since Staufen1 can shuttle between the nucleus and cytoplasm (Martel et al., 2006), these potential associations represent potential therapeutic targets in the context of the transporting Staufen1 RNP.

STAUFEN1 RNPs FACTORS INVOLVED IN GENERAL METABOLISM AND CHOLESTEROL BIOGENESIS

Surprisingly and exclusive to Staufen1 HIV-1 RNPs, we detected phosphatidylserine synthase 1 (PTDSS1), long-chain-fatty-acid-CoA ligase 3 (ACSL3) and 7-dehydrocholesterol reductase (DHCR7), the latter catalyzing the generation of cholesterol (**Table 1**). Gag's interaction with Staufen1 on cholesterol-rich membranes could suggest a functional implication in cellular cholesterol biogenesis (Milev et al., 2010) in that rerouting cholesterol-rich membranes toward the periphery promotes virus release and infectivity (Liao et al., 2001; Tang et al., 2009; Coleman et al., 2012). Likewise, Nef was also detected in Staufen1 HIV-1 RNPs and this viral protein could also influence assembly and trafficking since it induces cholesterol biosynthesis genes (**Table 1**; Zheng et al., 2003; van't Wout et al., 2005). These findings favor the idea that the processes of cholesterol biosynthesis, the formation of lipid rafts and the trafficking of viral components might be associated to Staufen1-containing complexes.

STAUFEN1-BINDING PARTNERS INVOLVED IN VESICULAR TRAFFICKING

We identified multiple proteins that regulate vesicle biogenesis and trafficking within Staufen1 RNPs (±HIV-1), with twice the

number of proteins with related functions when HIV-1 was expressed. Several common components were detected and known to be involved in the intracellular vesicular transport between the plasma membrane, endoplasmic reticulum and Golgi membranes including the coatomer subunit alpha (COPA; Beck et al., 2009), vesicle-fusing ATPase (NSF; Zhao et al., 2007) and adaptor protein AP-3S1 (sigma subunit; Tables S1 and S2 in Supplementary Material). The coatomer subunit zeta-1 (COPZ1), ADP-ribosylation factors ARF4 and ARF6, several Rab-related proteins (Rab-5C, -8A and -10), adaptor proteins AP-2M1 (mu subunit), AP-3D1 (delta subunit), which importantly, interact with Nef and Env (i.e., AP-2, mu; Boge et al., 1998; Craig et al., 2000) and Gag (i.e., AP-2, mu; AP-3, delta; Batonick et al., 2005; Dong et al., 2005) all uniquely associated to the Staufen1 HIV-1 RNPs (**Table 1**). We also identified a putative YXXØ (where Ø is a bulky hydrophobic residue) sorting signal in the dsRBD3 of Staufen1 (similar to that found in both Gag and Env; Batonick et al., 2005) that may mediate the mu subunit binding. Likewise, the existence of several di-leucine sorting motifs in Staufen1 could mediate binding to COP1 beta (Ohno et al., 1995; Rapoport et al., 1998). These observations support the notion that the mRNA/HIV-1 vRNA transport pathways are coupled with organized vesicular trafficking in cells (Cohen, 2005; Baumann et al., 2012), that is strengthened by several recent observations that vRNA traffics on endosomal membranes during HIV-1 egress and assembly (Lehmann et al., 2009; Molle et al., 2009).

Most of the biochemical evidence points to a role for Staufen1 RNPs in vRNA fate. The co-sedimentation of several components with Staufen1, using the available antibodies, reveals co-associations that are likely to be functionally relevant in this context and important for HIV-1-mediated disease (e.g., Tosar et al., 2012). Indeed, several of these associations have been characterized previously, for example those that have been characterized between Gag and ABCE1, Staufen1, UPF1, AUF1, IMP1 and RNA helicases. These RNPs appear to be static in size (**Figure 6**), but are mobile since they can aggregate in clusters when Staufen1 is in limiting supply (Abrahamyan et al., 2010). The disruption of all of these protein complexes upon RNAse A treatment reveals the dependence on viral and/or cellular RNA but also indicates that the targeting of RNA-related phenomena will be a suitable therapeutic approach in the future (Radi et al., 2012).

CONCLUSION

Staufen1 has multiple roles during HIV-1 replication including one in Gag multimerization and another in genomic RNA encapsidation. The present study applied tandem affinity immunopurification techniques coupled with mass spectrometry to characterize the composition of Staufen1 RNPs in HIV-1-expressing cells. Our results demonstrate that HIV-1 induces substantial changes to the composition of cellular Staufen1 RNPs. The identification of the associated host and viral factors to the Staufen1 RNP will contribute to a better understanding of how HIV-1 co-opts subcellular RNPs and machineries to achieve intracellular trafficking, efficient gene expression and the correct localization and fate of its genomic RNA.

AUTHORS' CONTRIBUTIONS

Miroslav P. Milev, Mukunthan Ravichandran and Andrew J. Mouland designed the experiments, analyzed the data and drafted the manuscript; Miroslav P. Milev and Mukunthan Ravichandran performed the experiments; Morgan F. Khan and David C. Schriemer performed LC-MS/MS analyses, peptide and protein identifications and analyzed the mass spectrometry results. All authors edited and approved the final manuscript.

ACKNOWLEDGMENTS

We thank Juan Ortin, Luc DesGroseillers, Chris Brown, Jens-Lykke Andersen, Rob Schneider, Finn Nielsen, William Rigby and Jaisri Lingappa for providing constructs and antibodies and Lara Ajamian, Fernando Valiente-Echeverria and Marie-Joelle Miron for comments on the manuscript. Andrew J. Mouland is a recipient of a Fraser, Monat, McPherson McGill University Scholarship and this research was supported by the Canadian Institutes of Health Research (#MOP-38111) to Andrew J. Mouland.

SUPPLEMENTARY MATERIAL

The Supplementary Material (Tables S1 and S2) for this article can be found online at: http://www.frontiersin.org/Virology/10.3389/fmicb.2012.00367/abstract

REFERENCES

Abrahamyan, L. G., Chatel-Chaix, L., Ajamian, L., Milev, M. P., Monette, A., Clement, J. F., et al. (2010). Novel Staufen1 ribonucleoproteins prevent formation of stress granules but favor encapsidation of HIV-1 genomic RNA. *J. Cell. Sci.* 123, 369–383.

Adachi, A., Gendelman, H. E., Koenig, S., Folks, T., Willey, R., Rabson, A., et al. (1986). Production of acquired immunodeficiency syndrome-associated retrovirus in human and nonhuman cells transfected with an infectious molecular clone. *J. Virol.* 59, 284–291.

Ajamian, L., Abrahamyan, L., Milev, M., Ivanov, P. V., Kulozik, A. E., Gehring, N. H., et al. (2008). Unexpected roles for UPF1 in HIV-1 RNA metabolism and translation. *RNA* 14, 914–927.

Anderson, E. C., and Lever, A. M. (2006). Human immunodeficiency virus type 1 Gag polyprotein modulates its own translation. *J. Virol.* 80, 10478–10486.

Arhel, N. J., and Kirchhoff, F. (2009). Implications of Nef: host cell interactions in viral persistence and progression to AIDS. *Curr. Top Microbiol. Immunol.* 339, 147–175.

Arrigo, S. J., Weitsman, S., Zack, J. A., and Chen, I. S. (1990). Characterization and expression of novel singly spliced RNA species of human immunodeficiency virus type 1. *J. Virol.* 64, 4585–4588.

Askjaer, P., Jensen, T. H., Nilsson, J., Englmeier, L., and Kjems, J. (1998). The specificity of the CRM1-Rev nuclear export signal interaction is mediated by RanGTP. *J. Biol. Chem.* 273, 33414–33422.

Babst, M., Odorizzi, G., Estepa, E. J., and Emr, S. D. (2000). Mammalian tumor susceptibility gene 101 (TSG101) and the yeast homologue, Vps23p, both function in late endosomal trafficking. *Traffic* 1, 248–258.

Barcova, M., Speth, C., Kacani, L., Uberall, F., Stoiber, H., and Dierich, M. P. (1999). Involvement of adenylate cyclase and p70 (S6)-kinase activation in IL-10 up-regulation in human monocytes by gp41 envelope protein of human immunodeficiency virus type 1. *Pflugers Arch.* 437, 538–546.

Batonick, M., Favre, M., Boge, M., Spearman, P., Honing, S., and Thali, M. (2005). Interaction of HIV-1 Gag with the clathrin-associated adaptor AP-2. *Virology* 342, 190–200.

Baumann, S., Pohlmann, T., Jungbluth, M., Brachmann, A., and Feldbrugge, M. (2012). Kinesin-3 and dynein mediate microtubule-dependent co-transport of mRNPs and endosomes. *J. Cell. Sci.* 125, 2740–2752.

Beck, R., Rawet, M., Wieland, F. T., and Cassel, D. (2009). The COPI system: molecular mechanisms and function. *FEBS Lett.* 583, 2701–2709.

Belgrader, P., Dey, R., and Berezney, R. (1991). Molecular cloning of matrin 3. A 125-kilodalton protein of the nuclear matrix contains an extensive acidic domain. *J. Biol. Chem.* 266, 9893–9899.

Beriault, V., Clement, J. F., Levesque, K., Lebel, C., Yong, X.,Chabot, B., et al. (2004). A late role for the association of hnRNP A2 with the HIV-1 hnRNP A2 response elements in genomic RNA, Gag, and Vpr localization. *J. Biol. Chem.* 279, 44141–44153.

Boge, M., Wyss, S., Bonifacino, J. S., and Thali, M. (1998). A membrane-proximal tyrosine-based signal mediates internalization of the HIV-1 envelope glycoprotein via interaction with the AP-2 clathrin adaptor. *J. Biol. Chem.* 273, 15773–15778.

Bouyac, M., Courcoul, M., Bertoia, G., Baudat, Y., Gabuzda, D., Blanc, D., et al. (1997). Human immunodeficiency virus type 1 Vif protein binds to the Pr55Gag precursor. *J. Virol.* 71, 9358–9365.

Brass, A. L., Dykxhoorn, D. M., Benita, Y., Yan, N., Engelman, A., Xavier, R. J., et al. (2008). Identification of host proteins required for HIV infection through a functional genomic screen. *Science* 319, 921–926.

Brendel, C., Rehbein, M., Kreienkamp, H. J., Buck, F., Richter, D., and Kindler, S. (2004). Characterization of Staufen 1 ribonucleoprotein complexes. *Biochem. J.* 384, 239–246.

Butsch, M., and Boris-Lawrie, K. (2002). Destiny of unspliced retroviral RNA: ribosome and/or virion? *J. Virol.* 76, 3089–3094.

Cantin, R., Methot, S., and Tremblay, M. J. (2005). Plunder and stowaways: incorporation of cellular proteins by enveloped viruses. *J. Virol.* 79, 6577–6587.

Caputi, M., Mayeda, A., Krainer, A. R., and Zahler, A. M. (1999). hnRNP A/B proteins are required for inhibition of HIV-1 pre-mRNA splicing. *EMBO J.* 18, 4060–4067.

Carson, J. H., Gao, Y., Tatavarty, V., Levin, M. K., Korza, G., Francone, V. P., et al. (2008). Multiplexed RNA trafficking in oligodendrocytes and neurons. *Biochim. Biophys. Acta* 1779, 453–458.

Chatel-Chaix, L., Abrahamyan, L., Frechina, C., Mouland, A. J., and Desgroseillers, L. (2007). The host protein Staufen1 participates in human immunodeficiency virus type 1 assembly in live cells by influencing pr55Gag multimerization. *J. Virol.* 81, 6216–6230.

Chatel-Chaix, L., Boulay, K., Mouland, A. J., and Desgroseillers, L. (2008). The host protein Staufen1 interacts with the Pr55Gag zinc fingers and regulates HIV-1 assembly via its N-terminus. *Retrovirology* 5, 41.

Chatel-Chaix, L., Clement, J. F., Martel, C., Beriault, V., Gatignol, A., Desgroseillers, L., et al. (2004). Identification of Staufen in the human immunodeficiency virus type 1 Gag ribonucleoprotein complex and a role in generating infectious viral particles. *Mol. Cell. Biol.* 24, 2637–2648.

Chertova, E., Chertov, O., Coren, L. V., Roser, J. D., Trubey, C. M., Bess, J. W. Jr., et al. (2006). Proteomic and biochemical analysis of purified human immunodeficiency virus type 1 produced from infected monocyte-derived macrophages. *J. Virol.* 80, 9039–9052.

Chiu, Y. L., Witkowska, H. E., Hall, S. C., Santiago, M., Soros, V. B., Esnault, C., et al. (2006). High-molecular-mass APOBEC3G complexes restrict Alu retrotransposition. *Proc. Natl. Acad. Sci. U.S.A.* 103, 15588–15593.

Cimarelli, A., and Luban, J. (1999). Translation elongation factor 1-alpha interacts specifically with the human immunodeficiency virus type 1 Gag polyprotein. *J. Virol.* 73, 5388–5401.

Clever, J., Sassetti, C., and Parslow, T. G. (1995). RNA secondary structure and binding sites for gag gene products in the 5′ packaging signal of human immunodeficiency virus type 1. *J. Virol.* 69, 2101–2109.

Cochrane, A. W., Mcnally, M. T., and Mouland, A. J. (2006). The retrovirus RNA trafficking granule: from birth to maturity. *Retrovirology* 3, 18.

Cohen, R. S. (2005). The role of membranes and membrane trafficking in RNA localization. *Biol. Cell* 97, 5–18.

Coleman, E. M., Walker, T. N., and Hildreth, J. E. (2012). Loss of Niemann Pick type C proteins 1 and 2 greatly enhances HIV infectivity and is associated with accumulation of HIV Gag and cholesterol in late endosomes/lysosomes. *Virol. J.* 9, 31.

Craig, H. M., Reddy, T. R., Riggs, N. L., Dao, P. P., and Guatelli, J. C. (2000). Interactions of HIV-1 nef with the mu subunits of adaptor protein complexes 1, 2, and 3: role of the dileucine-based sorting motif. *Virology* 271, 9–17.

de Lucas, S., Peredo, J., Marion, R. M., Sanchez, C., and Ortin, J. (2010). Human Staufen1 protein interacts with influenza virus ribonucleoproteins and is required for efficient virus multiplication. *J. Virol.* 84, 7603–7612.

DeCerbo, J., and Carmichael, G. G. (2005). Retention and repression: fates of hyperedited RNAs in the nucleus. *Curr. Opin. Cell Biol.* 17, 302–308.

Doma, M. K., and Parker, R. (2007). RNA quality control in eukaryotes. *Cell* 131, 660–668.

Dong, X., Li, H., Derdowski, A., Ding, L., Burnett, A., Chen, X., et al. (2005). AP-3 directs the intracellular trafficking of HIV-1 Gag and plays a key role in particle assembly. *Cell* 120, 663–674.

Dooher, J. E., Schneider, B. L., Reed, J. C., and Lingappa, J. R. (2007). Host ABCE1 is at plasma membrane HIV assembly sites and its dissociation from Gag is linked to subsequent events of virus production. *Traffic* 8, 195–211.

Doria, M., Neri, F., Gallo, A., Farace, M. G., and Michienzi, A. (2009). Editing of HIV-1 RNA by the double-stranded RNA deaminase ADAR1 stimulates viral infection. *Nucleic Acids Res.* 37, 5848–5858.

Dreikhausen, U., Hiebenthal-Millow, K., Bartels, M., Resch, K., and Nourbakhsh, M. (2005). NF-kappaB-repressing factor inhibits elongation of human immunodeficiency virus type 1 transcription by DRB sensitivity-inducing factor. *Mol. Cell. Biol.* 25, 7473–7483.

Falcon, A. M., Fortes, P., Marion, R. M., Beloso, A., and Ortin, J. (1999). Interaction of influenza virus NS1 protein and the human homologue of Staufen in vivo and in vitro. *Nucleic Acids Res.* 27, 2241–2247.

Fassati, A., Gorlich, D., Harrison, I., Zaytseva, L., and Mingot, J. M. (2003). Nuclear import of HIV-1 intracellular reverse transcription complexes is mediated by importin 7. *EMBO J.* 22, 3675–3685.

Fierro-Monti, I., and Mathews, M. B. (2000). Proteins binding to duplexed RNA: one motif, multiple functions. *Trends Biochem. Sci.* 25, 241–246.

Freed, E. O. (1998). HIV-1 gag proteins: diverse functions in the virus life cycle. *Virology* 251, 1–15.

Freed, E. O. (2001). HIV-1 replication. *Somat. Cell Mol. Genet.* 26, 13–33.

Furic, L., Maher-Laporte, M., and Desgroseillers, L. (2008). A genome-wide approach identifies distinct but overlapping subsets of cellular mRNAs associated with Staufen1- and Staufen2-containing ribonucleoprotein complexes. *RNA* 14, 324–335.

Garrus, J. E., Von Schwedler, U. K., Pornillos, O. W., Morham, S. G., Zavitz, K. H., Wang, H. E., et al. (2001). Tsg101 and the vacuolar protein sorting pathway are essential for HIV-1 budding. *Cell* 107, 55–65.

Goff, S. P. (2007). Host factors exploited by retroviruses. *Nat. Rev. Microbiol.* 5, 253–263.

Gurer, C., Cimarelli, A., and Luban, J. (2002). Specific incorporation of heat shock protein 70 family members into primate lentiviral virions. *J. Virol.* 76, 4666–4670.

Hadian, K., Vincendeau, M., Mäusbacher, N., Nagel, D., Hauck, S. M., Ueffing, M., et al. (2009). Identification of a heterogeneous nuclear ribonucleoprotein-recognition region in the HIV Rev protein. *J. Biol. Chem.* 284, 33384–33391.

Harris, D., Zhang, Z., Chaubey, B., and Pandey, V. N. (2006). Identification of cellular factors associated with the 3′-nontranslated region of the hepatitis C virus genome. *Mol. Cell Proteomics* 5, 1006–1018.

Ho, D. D., Neumann, A. U., Perelson, A. S., Chen, W., Leonard, J. M., and Markowitz, M. (1995). Rapid turnover of plasma virions and CD4 lymphocytes in HIV-1 infection. *Nature* 373, 123–126.

Jacks, T., Power, M. D., Masiarz, F. R., Luciw, P. A., Barr, P. J., and Varmus, H. E. (1988). Characterization of ribosomal frameshifting in HIV-1 gag-pol expression. *Nature* 331, 280–283.

Jager, S., Cimermancic, P., Gulbahce, N., Johnson, J. R., Mcgovern, K. E., Clarke, S. C., et al. (2012). Global landscape of HIV-human protein complexes. *Nature* 481, 365–370.

Jeang, K. T., and Yedavalli, V. (2006). Role of RNA helicases in HIV-1 replication. *Nucleic Acids Res.* 34, 4198–4205.

Jonson, L., Vikesaa, J., Krogh, A., Nielsen, L. K., Hansen, T., Borup, R., et al. (2007). Molecular composition of IMP1 ribonucleoprotein granules. *Mol. Cell Proteomics* 6, 798–811.

Kemler, I., Meehan, A., and Poeschla, E. M. (2010). Live-cell coimaging of the genomic RNAs and Gag proteins of two lentiviruses. *J. Virol.* 84, 6352–6366.

Khan, M. A., Kao, S., Miyagi, E., Takeuchi, H., Goila-Gaur, R., Opi, S., et al. (2005). Viral RNA is required for the association of APOBEC3G with human immunodeficiency virus type 1 nucleoprotein complexes. *J. Virol.* 79, 5870–5874.

Khorchid, A., Halwani, R., Wainberg, M. A., and Kleiman, L. (2002). Role of RNA in facilitating Gag/Gag-Pol interaction. *J. Virol.* 76, 4131–4137.

Kiebler, M. A., and DesGroseillers, L. (2000). Molecular insights into mRNA transport and local translation in the mammalian nervous system. *Neuron* 25, 19–28.

Kiebler, M. A., Hemraj, I., Verkade, P., Kohrmann, M., Fortes, P., Marion, R. M., et al. (1999). The mammalian staufen protein localizes to the somatodendritic domain of cultured hippocampal neurons: implications for its involvement in mRNA transport. *J. Neurosci.* 19, 288–297.

Kim, Y. K., Furic, L., Desgroseillers, L., and Maquat, L. E. (2005). Mammalian Staufen1 recruits Upf1 to specific mRNA 3′UTRs so as to elicit mRNA decay. *Cell* 120, 195–208.

Kim, Y. K., Furic, L., Parisien, M., Major, F., Desgroseillers, L., and Maquat, L. E. (2007). Staufen1 regulates diverse classes of mammalian transcripts. *EMBO J.* 26, 2670–2681.

Klein, K. C., Reed, J. C., and Lingappa, J. R. (2007). Intracellular destinies: degradation, targeting, assembly, and endocytosis of HIV Gag. *AIDS Rev.* 9, 150–161.

Komano, J., Futahashi, Y., Urano, E., Miyauchi, K., Murakami, T., Matsuda, Z., et al. (2005). The interaction of HIV-1 with the host factors. *Jpn. J. Infect. Dis.* 58, 125–130.

Komano, J., Miyauchi, K., Matsuda, Z., and Yamamoto, N. (2004). Inhibiting the Arp2/3 complex limits infection of both intracellular mature vaccinia virus and primate lentiviruses. *Mol. Biol. Cell* 15, 5197–5207.

Kondo, E., Mammano, F., Cohen, E. A., and Gottlinger, H. G. (1995). The p6gag domain of human immunodeficiency virus type 1 is sufficient for the incorporation of Vpr into heterologous viral particles. *J. Virol.* 69, 2759–2764.

Kozak, S. L., Marin, M., Rose, K. M., Bystrom, C., and Kabat, D. (2006). The anti-HIV-1 editing enzyme APOBEC3G binds HIV-1 RNA and messenger RNAs that shuttle between polysomes and stress granules. *J. Biol. Chem.* 281, 29105–29119.

Lavallee, C., Yao, X. J., Ladha, A., Gottlinger, H., Haseltine, W. A., and Cohen, E. A. (1994). Requirement of the Pr55gag precursor for incorporation of the Vpr product into human immunodeficiency virus type 1 viral particles. *J. Virol.* 68, 1926–1934.

Lee, K., Ambrose, Z., Martin, T. D., Oztop, I., Mulky, A., Julias, J. G., et al. (2010). Flexible use of nuclear import pathways by HIV-1. *Cell Host Microbe.* 7, 221–233.

Lehmann, M., Milev, M., Abrahamyan, L., Yao, X. J., Pante, N., and Mouland, A. J. (2009). Intracellular transport of human immunodeficiency virus type 1 genomic RNA and viral production are dependent on dynein motor function and late endosome positioning. *J. Biol. Chem.* 284, 14572–14585.

Lever, A., Gottlinger, H., Haseltine, W., and Sodroski, J. (1989). Identification of a sequence required for efficient packaging of human immunodeficiency virus type 1 RNA into virions. *J. Virol.* 63, 4085–4087.

Levesque, K., Halvorsen, M., Abrahamyan, L., Chatel-Chaix, L., Poupon, V., Gordon, H., et al. (2006). Trafficking of HIV-1 RNA is mediated by heterogeneous nuclear ribonucleoprotein A2 expression and impacts on viral assembly. *Traffic* 7, 1177–1193.

Liao, Z., Cimakasky, L. M., Hampton, R., Nguyen, D. H., and Hildreth, J. E. (2001). Lipid rafts and hiv pathogenesis: host membrane cholesterol is required for infection by hiv type 1. *AIDS Res. Hum. Retroviruses* 17, 1009–1019.

Limou, S., Le Clerc, S., Coulonges, C., Carpentier, W., Dina, C., Delaneau, O., et al. (2009). Genome-wide association study of an AIDS-nonprogression cohort emphasizes the role played by HLA genes (ANRS Genomewide Association Study 02). *J. Infect. Dis.* 199, 419–426.

Lindwasser, O. W., Chaudhuri, R., and Bonifacino, J. S. (2007). Mechanisms of CD4 downregulation by the Nef and Vpu proteins of primate immunodeficiency viruses. *Curr. Mol. Med.* 7, 171–184.

Lingappa, J. R., Dooher, J. E., Newman, M. A., Kiser, P. K., and Klein, K. C. (2006). Basic residues in the nucleocapsid domain of Gag are required for interaction of HIV-1 gag with ABCE1 (HP68), a cellular protein important for HIV-1 capsid assembly. *J. Biol. Chem.* 281, 3773–3784.

Lund, N., Milev, M. P., Wong, R., Sanmuganantham, T., Woolaway, K., Chabot, B., et al. (2012). Differential effects of hnRNP D/AUF1 isoforms on HIV-1 gene expression. *Nucleic Acids Res.* 40, 3663–3675.

Macchi, P., Kroening, S., Palacios, I. M., Baldassa, S., Grunewald, B., Ambrosino, C., et al. (2003). Barentsz, a new component of the Staufen-containing ribonucleoprotein particles in mammalian cells, interacts with Staufen in an RNA-dependent manner. *J. Neurosci.* 23, 5778–5788.

Martel, C., Dugre-Brisson, S., Boulay, K., Breton, B., Lapointe, G., Armando, S., et al. (2010). Multimerization of Staufen1 in live cells. *RNA* 16, 585–597.

Martel, C., Macchi, P., Furic, L., Kiebler, M. A., and Desgroseillers, L. (2006). Staufen1 is imported into the nucleolus via a bipartite nuclear localization signal and several modulatory determinants. *Biochem. J.* 393, 245–254.

Milev, M. P., Brown, C. M., and Mouland, A. J. (2010). Live cell visualization of the interactions between HIV-1 Gag and the cellular RNA-binding protein Staufen1. *Retrovirology* 7, 41.

Molle, D., Segura-Morales, C., Camus, G., Berlioz-Torrent, C., Kjems, J., Basyuk, E., et al. (2009). Endosomal trafficking of HIV-1 gag and genomic RNAs regulates viral egress. *J. Biol. Chem.* 284, 19727–19743.

Monette, A., Ajamian, L., Lopez-Lastra, M., and Mouland, A. J. (2009). Human immunodeficiency virus type 1 (HIV-1) induces the cytoplasmic retention of heterogeneous nuclear ribonucleoprotein A1 by disrupting nuclear import: implications for HIV-1 gene expression. *J. Biol. Chem.* 284, 31350–31362.

Mouland, A. J., Coady, M., Yao, X. J., and Cohen, E. A. (2002). Hypophosphorylation of poly(A) polymerase and increased polyadenylation activity are associated with human immunodeficiency virus type 1 Vpr expression. *Virology* 292, 321–330.

Mouland, A. J., Mercier, J., Luo, M., Bernier, L., Desgroseillers, L., and Cohen, E. A. (2000). The double-stranded RNA-binding protein Staufen is incorporated in human immunodeficiency virus type 1: evidence for a role in genomic RNA encapsidation. *J. Virol.* 74, 5441–5451.

Mouland, A. J., Xu, H., Cui, H., Krueger, W., Munro, T. P., Prasol, M., et al. (2001). RNA trafficking signals in human immunodeficiency virus type 1. *Mol. Cell. Biol.* 21, 2133–2143.

Nathans, R., Chu, C. Y., Serquina, A. K., Lu, C. C., Cao, H., and Rana, T. M. (2009). Cellular microRNA and P bodies modulate host-HIV-1 interactions. *Mol. Cell* 34, 696–709.

Ohn, T., Kedersha, N., Hickman, T., Tisdale, S., and Anderson, P. (2008). A functional RNAi screen links O-GlcNAc modification of ribosomal proteins to stress granule and processing body assembly. *Nat. Cell Biol.* 10, 1224–1231.

Ohno, H., Stewart, J., Fournier, M. C., Bosshart, H., Rhee, I., Miyatake, S., et al. (1995). Interaction of tyrosine-based sorting signals with clathrin-associated proteins. *Science* 269, 1872–1875.

Ono, A., Ablan, S. D., Lockett, S. J., Nagashima, K., and Freed, E. O. (2004). Phosphatidylinositol (4,5) bisphosphate regulates HIV-1 Gag targeting to the plasma membrane. *Proc. Natl. Acad. Sci. U.S.A.* 101, 14889–14894.

Ott, D. E. (2002). Potential roles of cellular proteins in HIV-1. *Rev. Med. Virol.* 12, 359–374.

Ott, D. E. (2008). Cellular proteins detected in HIV-1. *Rev. Med. Virol.* 18, 159–175.

Ou, S. H., Wu, F., Harrich, D., Garcia-Martinez, L. F., and Gaynor, R. B. (1995). Cloning and characterization of a novel cellular protein, TDP-43, that binds to human immunodeficiency virus type 1 TAR DNA sequence motifs. *J. Virol.* 69, 3584–3596.

Palacios, I. M., Gatfield, D., St Johnston, D., and Izaurralde, E. (2004). An eIF4AIII-containing complex required for mRNA localization and nonsense-mediated mRNA decay. *Nature* 427, 753–757.

Patel, G. P., and Bag, J. (2006). IMP1 interacts with poly(A)-binding protein (PABP) and the autoregulatory translational control element of PABP-mRNA through the KH III-IV domain. *FEBS J.* 273, 5678–5690.

Phuphuakrat, A., Kraiwong, R., Boonarkart, C., Lauhakirti, D., Lee, T. H., and Auewarakul, P. (2008). Double-stranded RNA adenosine deaminases enhance expression of human immunodeficiency virus type 1 proteins. *J. Virol.* 82, 10864–10872.

Pizzato, M., Helander, A., Popova, E., Calistri, A., Zamborlini, A., Palù, G., et al. (2007). Dynamin 2 is required for the enhancement of HIV-1 infectivity by Nef. *Proc. Natl. Acad. Sci. U.S.A.* 104, 6812–6817.

Poole, E., Strappe, P., Mok, H. P., Hicks, R., and Lever, A. M. (2005). HIV-1 Gag-RNA interaction occurs

at a perinuclear/centrosomal site; analysis by confocal microscopy and FRET. *Traffic* 6, 741–755.

Poon, D. T., Chertova, E. N., and Ott, D. E. (2002). Human immunodeficiency virus type 1 preferentially encapsidates genomic RNAs that encode Pr55 (Gag): functional linkage between translation and RNA packaging. *Virology* 293, 368–378.

Puig, O., Caspary, F., Rigaut, G., Rutz, B., Bouveret, E., Bragado-Nilsson, E., et al. (2001). The tandem affinity purification (TAP) method: a general procedure of protein complex purification. *Methods* 24, 218–229.

Purcell, D. F., and Martin, M. A. (1993). Alternative splicing of human immunodeficiency virus type 1 mRNA modulates viral protein expression, replication, and infectivity. *J. Virol.* 67, 6365–6378.

Rackham, O., and Brown, C. M. (2004). Visualization of RNA-protein interactions in living cells: FMRP and IMP1 interact on mRNAs. *EMBO J.* 23, 3346–3355.

Radi, M., Falchi, F., Garbelli, A., Samuele, A., Bernardo, V., Paolucci, S., et al. (2012). Discovery of the first small molecule inhibitor of human DDX3 specifically designed to target the RNA binding site: towards the next generation HIV-1 inhibitors. *Bioorg. Med. Chem. Lett.* 22, 2094–2098.

Rapoport, I., Chen, Y. C., Cupers, P., Shoelson, S. E., and Kirchhausen, T. (1998). Dileucine-based sorting signals bind to the beta chain of AP-1 at a site distinct and regulated differently from the tyrosine-based motif-binding site. *EMBO J.* 17, 2148–2155.

Rasheed, S., Yan, J. S., Lau, A., and Chan, A. S. (2008). HIV replication enhances production of free fatty acids, low density lipoproteins and many key proteins involved in lipid metabolism: a proteomics study. *PLoS One* 3, e3003.

Ringrose, J. H., Jeeninga, R. E., Berkhout, B., and Speijer, D. (2008). Proteomic studies reveal coordinated changes in T-cell expression patterns upon infection with human immunodeficiency virus type 1. *J. Virol.* 82, 4320–4330.

Roegiers, F., and Jan, Y. N. (2000). Staufen: a common component of mRNA transport in oocytes and neurons? *Trends Cell Biol.* 10, 220–224.

Roy, B. B., Hu, J., Guo, X., Russell, R. S., Guo, F., Kleiman, L., et al. (2006). Association of RNA helicase a with human immunodeficiency virus type 1 particles. *J. Biol. Chem.* 281, 12625–12635.

Ruggieri, A., Dazert, E., Metz, P., Hofmann, S., Bergeest, J. P., Mazur, J., et al. (2012). Dynamic oscillation of translation and stress granule formation mark the cellular response to virus infection. *Cell Host Microbe* 12, 71–85.

Saunders, L. R., and Barber, G. N. (2003). The dsRNA binding protein family: critical roles, diverse cellular functions. *FASEB J.* 17, 961–983.

Schell, T., Kocher, T., Wilm, M., Seraphin, B., Kulozik, A. E., and Hentze, M. W. (2003). Complexes between the nonsense-mediated mRNA decay pathway factor human upf1 (up-frameshift protein 1) and essential nonsense-mediated mRNA decay factors in HeLa cells. *Biochem. J.* 373, 775–783.

Schwartz, S., Felber, B. K., Benko, D. M., Fenyo, E. M., and Pavlakis, G. N. (1990). Cloning and functional analysis of multiply spliced mRNA species of human immunodeficiency virus type 1. *J. Virol.* 64, 2519–2529.

Sonstegard, T. S., and Hackett, P. B. (1996). Autogenous regulation of RNA translation and packaging by Rous sarcoma virus Pr76gag. *J. Virol.* 70, 6642–6652.

Sun, Z., Pan, J., Hope, W. X., Cohen, S. N., and Balk, S. P. (1999). Tumor susceptibility gene 101 protein represses androgen receptor transactivation and interacts with p300. *Cancer* 86, 689–696.

Syed, F., and McCrae, M. A. (2009). Interactions in vivo between the Vif protein of HIV-1 and the precursor (Pr55 (GAG)) of the virion nucleocapsid proteins. *Arch. Virol.* 154, 1797–1805.

Tang, Y., Leao, I. C., Coleman, E. M., Broughton, R. S., and Hildreth, J. E. (2009). Deficiency of niemann-pick type C-1 protein impairs release of human immunodeficiency virus type 1 and results in Gag accumulation in late endosomal/lysosomal compartments. *J. Virol.* 83, 7982–7995.

Thomas, M. G., Martinez Tosar, L. J., Loschi, M., Pasquini, J. M., Correale, J., Kindler, S., et al. (2005). Staufen recruitment into stress granules does not affect early mRNA transport in oligodendrocytes. *Mol. Biol. Cell* 16, 405–420.

Tian, B., Bevilacqua, P. C., Egelman-Parente, A., and Mathews, M. B. (2004). The double-stranded-RNA-binding motif: interference and much more. *Nat. Rev. Mol. Cell Biol.* 5, 1013–1023.

Tosar, L. J., Thomas, M. G., Baez, M. V., Ibanez, I., Chernomoretz, A., and Boccaccio, G. L. (2012). Staufen: from embryo polarity to cellular stress and neurodegeneration. *Front. Biosci. (Schol. Ed.)* 4, 432–452.

Tsuchiya, N., Fukuda, H., Nakashima, K., Nagao, M., Sugimura, T., and Nakagama, H. (2004). LRP130, a single-stranded DNA/RNA-binding protein, localizes at the outer nuclear and endoplasmic reticulum membrane, and interacts with mRNA in vivo. *Biochem. Biophys. Res. Commun.* 317, 736–743.

van't Wout, A. B., Swain, J. V., Schindler, M., Rao, U., Pathmajeyan, M. S., Mullins, J. I., et al. (2005). Nef induces multiple genes involved in cholesterol synthesis and uptake in human immunodeficiency virus type 1-infected T cells. *J. Virol.* 79, 10053–10058.

VerPlank, L., Bouamr, F., Lagrassa, T. J., Agresta, B., Kikonyogo, A., Leis, J., et al. (2001). Tsg101, a homologue of ubiquitin-conjugating (E2) enzymes, binds the L domain in HIV type 1 Pr55(Gag). *Proc. Natl. Acad. Sci. U.S.A.* 98, 7724–7729.

Vidricaire, G., and Tremblay, M. J. (2005). Rab5 and Rab7, but not ARF6, govern the early events of HIV-1 infection in polarized human placental cells. *J. Immunol.* 175, 6517–6530.

Villace, P., Marion, R. M., and Ortin, J. (2004). The composition of Staufen-containing RNA granules from human cells indicates their role in the regulated transport and translation of messenger RNAs. *Nucleic Acids Res.* 32, 2411–2420.

Vyboh, K., Ajamian, L., and Mouland, A. J. (2012). Detection of viral RNA by fluorescence in situ hybridization (FISH). *J. Vis. Exp.* 63, e4002. doi:10.3791/4002

Wang, W. K., Chen, M. Y., Chuang, C. Y., Jeang, K. T., and Huang, L. M. (2000). Molecular biology of human immunodeficiency virus type 1. *J. Microbiol. Immunol. Infect.* 33, 131–140.

Wickham, L., Duchaine, T., Luo, M., Nabi, I. R., and Desgroseillers, L. (1999). Mammalian staufen is a double-stranded-RNA- and tubulin-binding protein which localizes to the rough endoplasmic reticulum. *Mol. Cell. Biol.* 19, 2220–2230.

Wilhelm, J. E., and Vale, R. D. (1993). RNA on the move: the mRNA localization pathway. *J. Cell Biol.* 123, 269–274.

Xu, X., Song, Y., Li, Y., Chang, J., Zhang, H., and An, L. (2010). The tandem affinity purification method: an efficient system for protein complex purification and protein interaction identification. *Protein Expr. Purif.* 72, 149–156.

Yao, X. J., Mouland, A. J., Subbramanian, R. A., Forget, J., Rougeau, N., Bergeron, D., et al. (1998). Vpr stimulates viral expression and induces cell killing in human immunodeficiency virus type 1-infected dividing Jurkat T cells. *J. Virol.* 72, 4686–4693.

Yi, R., Bogerd, H. P., and Cullen, B. R. (2002). Recruitment of the Crm1 nuclear export factor is sufficient to induce cytoplasmic expression of incompletely spliced human immunodeficiency virus mRNAs. *J. Virol.* 76, 2036–2042.

Yisraeli, J. K. (2005). VICKZ proteins: a multi-talented family of regulatory RNA-binding proteins. *Biol. Cell* 97, 87–96.

Yoon, Y. J., and Mowry, K. L. (2004). Xenopus Staufen is a component of a ribonucleoprotein complex containing Vg1 RNA and kinesin. *Development* 131, 3035–3045.

Zaitseva, L., Cherepanov, P., Leyens, L., Wilson, S. J., Rasaiyaah, J., and Fassati, A. (2009). HIV-1 exploits importin 7 to maximize nuclear import of its DNA genome. *Retrovirology* 6, 11.

Zhang, Z., and Carmichael, G. G. (2001). The fate of dsRNA in the nucleus: a p54(nrb)-containing complex mediates the nuclear retention of promiscuously A-to-I edited RNAs. *Cell* 106, 465–475.

Zhao, C., Slevin, J. T., and Whiteheart, S. W. (2007). Cellular functions of NSF: not just SNAPs and SNAREs. *FEBS Lett.* 581, 2140–2149.

Zheng, Y. H., Plemenitas, A., Fielding, C. J., and Peterlin, B. M. (2003). Nef increases the synthesis of and transports cholesterol to lipid rafts and HIV-1 progeny virions. *Proc. Natl. Acad. Sci. U.S.A.* 100, 8460–8465.

Zhou, H., Xu, M., Huang, Q., Gates, A. T., Zhang, X. D., Castle, J. C., et al. (2008). Genome-scale RNAi screen for host factors required for HIV replication. *Cell Host Microbe* 4, 495–504.

Zimmerman, C., Klein, K. C., Kiser, P. K., Singh, A. R., Firestein, B. L., Riba, S. C., et al. (2002). Identification of a host protein essential for assembly of immature V-1 capsids. *Nature* 415, 88–92.

Zolotukhin, A. S., Michalowski, D., Bear, J., Smulevitch, S. V., Traish, A. M.,

Peng, R., et al. (2003). PSF acts through the human immunodeficiency virus type 1 mRNA instability elements to regulate virus expression. *Mol. Cell. Biol.* 23, 6618–6630.

Conflict of Interest Statement: The authors declare that the research was conducted in the absence of any commercial or financial relationships that could be construed as a potential conflict of interest.

Received: 31 July 2012; accepted: 27 September 2012; published online: 25 October 2012.
Citation: Milev MP, Ravichandran M, Khan MF, Schriemer DC and Mouland AJ (2012) Characterization of Staufen1 ribonucleoproteins by mass spectrometry and biochemical analyses reveal the presence of diverse host proteins associated with human immunodeficiency virus type 1. Front. Microbio. ***3****:367. doi: 10.3389/fmicb.2012.00367*
This article was submitted to Frontiers in Virology, a specialty of Frontiers in Microbiology.

frontiers in
MICROBIOLOGY

ORIGINAL RESEARCH ARTICLE
published: 10 December 2012
doi: 10.3389/fmicb.2012.00411

Global analysis of viral infection in an archaeal model system

Walid S. Maaty[1], Joseph D. Steffens[1], Joshua Heinemann[1], Alice C. Ortmann[2], Benjamin D. Reeves[1], Swapan K. Biswas[1], Edward A. Dratz[1], Paul A. Grieco[1], Mark J. Young[3,4] and Brian Bothner[1]*

[1] Department of Chemistry and Biochemistry, Montana State University, Bozeman, MT, USA
[2] Department of Marine Science, University of South Alabama, Mobile, AL, USA
[3] Department of Microbiology, Montana State University, Bozeman, MT, USA
[4] Department of Plant Sciences, Montana State University, Bozeman, MT, USA

Edited by:
Kevin Coombs, University of Manitoba, Canada

Reviewed by:
Ben Berkhout, University of Amsterdam, Netherlands
Peter Uetz, Virginia Commonwealth University, USA

***Correspondence:**
Brian Bothner, Department of Chemistry and Biochemistry, Montana State University, 111 CBB, Bozeman, MT 59715, USA.
e-mail: bbothner@chemistry.montana.edu

The origin and evolutionary relationship of viruses is poorly understood. This makes archaeal virus-host systems of particular interest because the hosts generally root near the base of phylogenetic trees, while some of the viruses have clear structural similarities to those that infect prokaryotic and eukaryotic cells. Despite the advantageous position for use in evolutionary studies, little is known about archaeal viruses or how they interact with their hosts, compared to viruses of bacteria and eukaryotes. In addition, many archaeal viruses have been isolated from extreme environments and present a unique opportunity for elucidating factors that are important for existence at the extremes. In this article we focus on virus-host interactions using a proteomics approach to study *Sulfolobus* Turreted Icosahedral Virus (STIV) infection of *Sulfolobus solfataricus P2*. Using cultures grown from the ATCC cell stock, a single cycle of STIV infection was sampled six times over a 72 h period. More than 700 proteins were identified throughout the course of the experiments. Seventy one host proteins were found to change their concentration by nearly twofold ($p < 0.05$) with 40 becoming more abundant and 31 less abundant. The modulated proteins represent 30 different cell pathways and 14 clusters of orthologous groups . 2D gel analysis showed that changes in post-translational modifications were a common feature of the affected proteins. The results from these studies showed that the prokaryotic antiviral adaptive immune system CRISPR-associated proteins (CAS proteins) were regulated in response to the virus infection. It was found that regulated proteins come from mRNAs with a shorter than average half-life. In addition, activity-based protein profiling (ABPP) profiling on 2D-gels showed caspase, hydrolase, and tyrosine phosphatase enzyme activity labeling at the protein isoform level. Together, this data provides a more detailed global view of archaeal cellular responses to viral infection, demonstrates the power of quantitative two-dimensional differential gel electrophoresis and ABPP using 2D gel compatible fluorescent dyes.

Keywords: archaea, virus infection, *S. solfataricus P2*, proteomics, virus–host interaction, differential gene expression, activity probes, caspase

INTRODUCTION

Identifying and understanding the interplay of viral and host factors during cell entry, replication, and egress is critical to deciphering the events that determine the fate of infection. Such studies have historically played an important role in elucidating fundamental aspects of molecular and cellular mechanisms. Archaeal host-virus interactions are just beginning to be explored and the current understanding of archaeal virus mechanisms is rudimentary at best. This is especially true of viruses that infect members of the crenarchaea. Even for the first viruses described that infect the crenarachaeal host *Sulfolobus* species, such as *Sulfolobus* spindle-shaped virus (SSV; Wiedenheft et al., 2004) and *Sulfolobus islandicus* rod-shaped virus (SIRV; Kessler et al., 2004), the viral replication cycle is just beginning to be understood. The recently described *Sulfolobus* Turreted Icosahedral Virus (STIV; Rice et al., 2004; Maaty et al., 2006) has emerged as a model crenarchaeal virus system due to the availability of a sequenced genome (Rice et al., 2004), infectious clones which facilitate genetic manipulations (Wirth et al., 2011), and detailed structural information on the STIV virion (Larson et al., 2006, 2007a; Khayat et al., 2010) and many of the structural and non-structural components (Maaty et al., 2006). Major findings include an icosahedral virion architecture with an internal lipid membrane, turret structures on the surface, and the discovery that STIV has evolved a novel release mechanism that involves the creation of pyramidal structures on the surface of infected cells (Brumfield et al., 2009; Snyder et al.,

Abbreviations: ABPP, activity-based protein profiling; LCMS, liquid chromatography-mass spectrometry; STIV, *Sulfolobus* turreted icosahedral virus.

2011; Fu and Johnson, 2012). Most strikingly, there appears to be a evolutionary relationship at the structural level with prokaryotic and eukaryotic viruses (Khayat et al., 2005; Maaty et al., 2006). STIV has arguably become one of the most studied crenarchaeal archaeal virus systems.

Crenarchaeal viruses form a distinct yet highly diverse group. The description of less than 50 viruses has led to at least seven new families (Globuloviridae, Guttaviridae, Fuselloviridae, Bicaudaviridae, Ampullaviridae, Rudiviridae, and Lipothrixviridae) with viruses such as STIV still awaiting assignment (Lawrence et al., 2009). All have circular double-stranded DNA genomes except for the Rudiviridae and Lipothrixviridae which are the only known viruses to have linear dsDNA. To date, there is no description of ssDNA or ssRNA archaeal viruses, however, recent evidence from metagenomic analysis of archaeal dominated hot springs in Yellowstone National Park (YNP) identified novel positive-strand RNA viruses (Bolduc et al., 2012). While most archaea possess CRISPR/Cas antiviral systems, the mechanism of this or other viral counter measures have yet to be worked out. Originally, a number of the crenarchaeal viruses, including STIV and SIRV2, were not believed to cause cell lysis (Prangishvili and Garrett, 2005). It was later revealed that both of these viruses have very narrow host ranges and are only able to infect a sub-population of cells in a stock culture (Ortmann et al., 2008; Quax et al., 2011). The ability of STIV and SIRV2 to cause cell lysis was clearly demonstrated when both were shown to produce viral associated pyramids (VAPs) on the surface of host cells that opened to release mature particles (Brumfield et al., 2009; Prangishvili and Quax, 2011). Previously only eukaryotic viruses were known to produce replication structures and nothing like the VAPs had ever been described before.

Sulfolobus Turreted Icosahedral Virus was isolated from enrichment cultures of a high temperature (∼80°C) acidic (∼pH 2.9–3.9) hot spring in YNP (Rice et al., 2001). This was the first icosahedral virus described with an archaeal host. It has been shown to infect *S. solfataricus* (P2), originally isolated from Italy, as well as several *Sulfolobus* species found in YNP. Structural models based on cryo-electron microscopy and image reconstruction revealed that the STIV capsid has pseudo $T = 31$ symmetry, turret structures at each of the fivefold axes, and an internal lipid monolayer (Rice et al., 2004; Khayat et al., 2005). Subsequent analysis determined that the capsid is composed of nine viral proteins and an internal cyclic tetraether lipid layer, which is selected from the host lipid compliment (Maaty et al., 2006). The 17.6 kb dsDNA genome has 38 recognized open reading frames (Maaty et al., 2012). Functional and evolutionary insight for the gene products of 4 open reading frames has come from crystal structures of A197, F93, B116, and the major coat protein (Larson et al., 2006, 2007a,b).

Global untargeted analyses of gene and protein expression profiles are powerful approaches for examining viral infection (Der et al., 1998). An advantage of untargeted approaches is the ability to detect novel and unexpected connections that would be missed with a more focused approach. Proteomics approaches including methods such as shot-gun liquid chromatography-mass spectrometry, differential gel electrophoresis (DIGE), and isotope coding facilitate quantitative analyses of whole proteomes. DIGE, which is based on 2-dimensional electrophoresis (2D), allows differences between independent samples labeled with different fluorescent dyes to be detected on a single gel. This differential approach improves reproducibility and facilitates comparison based on statistically significant changes between thousands of proteins in parallel (Tonge et al., 2001; Gharbi et al., 2002; Van den Bergh et al., 2003). Fluorescence-based DIGE is quantitative over a large range of protein concentrations and has an inherent ability to detect post-translational modifications (PTMs) and changes in PTMs based on changes in protein mobility. A limiting factor with the 2D-DIGE approach is that generally only ∼1000 proteins can be separated on a single gel. For complex eukaryotic samples, prefractionation or the use of narrow pH range isoelectric focusing strips may be required. With prokaryotic species such as *Sulfolobus* (∼3,000 genes), a single wide pI range 2D gel provides a high degree of proteome coverage of the expressed proteins.

While measurements of changes in mRNA, protein, and protein PTMs are powerful approaches and are the foundation of functional genomics, they are only proxies for biological activity. Activity-based protein profiling (ABPP) on the other hand, is a direct read-out of protein function. ABPP uses semi-targeted probes to covalently label enzymes in specific catalytic classes by taking advantage of active site chemistry. Probes have been developed for a wide range of enzyme classes. A distinct advantage of ABPP is that changes in enzyme activity provides a direct read-out of biological change, yet can be followed at the level of the proteome (Speers and Cravatt, 2004; Sadaghiani et al., 2007). This approach overcomes the problem that abundance of mRNA or protein frequently does not directly correlate with protein activity. The application of ABPP to cancer and viral infection has already led to significant findings (Furman et al., 2009; Wang et al., 2009; Blais et al., 2010; Nomura et al., 2010; Singaravelu et al., 2010). In this study we used three new types of aqueous soluble rhodamine dyes derivatized with different activity-based probes to extend ABPP to use with 2D-DIGE.

The goal of this study was to expand what is known about host-virus interactions in archaea using untargeted 2D-DIGE and ABPP. Specifically that study was interested in how cultures of *S. solfataricus* (P2; ATCC) stock cells respond to virus. Based on cell counts of infected/non-infected cells, it was previously reported that 10% of cells in ATCC stock cultures support STIV replication (Ortmann et al., 2008). In contrast to a recent report that followed the *S. solfataricus* P2-2-12 substrain that is readily infected by STIV (∼100% of the cells) and showed a rather weak host response in the proteome (Maaty et al., 2012), the *S. solfataricus P2* cultures had a strong proteomic response to virus. *S. solfataricus* P2-2-12 is a susceptible strain isolated by single colony plating (Ortmann et al., 2008). The analysis followed a time course of STIV inoculated *S. solfataricus P2* cultures. Because only a small percentage of cells appear to become infected in such cultures, it was expected that changes at the proteome level would be minimal. Surprisingly, a relatively strong change in protein abundance occurred across the cell population with 40 increasing and 31 decreasing in abundance over the course of 72 h. More than half of these proteins were assigned to just five [clusters of orthologous groups (COG)]. In addition to simple changes in protein concentration, numerous examples of host proteins that were altered post-translationally were detected. This represents the first wide-scale application of

activity probes in Archaea and ABPP of serine hydrolases, tyrosine phosphatases, and caspase-like active sites revealed the responsiveness of archaeal enzymes to the probes. A comparison of the regulated proteins to their mRNA half-life revealed that proteins showing changes in abundance came from mRNAs with shorter than average half-lives. *S. solfataricus* (P2) cells clearly respond to STIV, this can be seen across the proteome and includes changes in CAS proteins believed to be part of a CRISPR antiviral system, without significant change to growth rate or morphology.

MATERIALS AND METHODS

VIRUS PURIFICATION AND INFECTION

Production of the virus was carried out by growing the *S. solfataricus* (P2) cells in Medium 182 (http://www.dsmz.de/microorganisms/medium/pdf/DSMZ_Medium182.pdf) at pH 2.5 as previously described (Ortmann et al., 2008). Briefly, infected cultures were monitored for virus production using an immunodot blot assay for the major capsid protein. Cultures were harvested between 48 and 60 h post-infection (hpi). Cells were removed by centrifugation ($4000 \times g$ for 10 min), and the supernatant containing the virus was filtered through a 0.22-μm Seritop filter (Millipore). The filtrate was concentrated over Amicon membranes (Millipore) with a molecular mass cutoff of 100 kDa until the retained volume was ∼15 mL. For this study, three independent 1 L cultures of *S. solfataricus* (P2) were inoculated with 0.1 mL concentrated STIV (10^{11} virus mL). Preliminary experiments were conducted to determine the amount of virus required to achieve maximal infection and addition of larger volumes of virus did not change culture growth curves or result in greater virus production. Infected cells from 100 mL were recovered at 12 h intervals post-infection (12, 24, 36, 48, 60, and 72 hpi). Uninfected control cultures were grown and sampled in parallel. Epifluorescence performed as previously described (Ortmann and Suttle, 2009).

2-D DIGE SAMPLE PREPARATION

Sample extracts were prepared from cell suspensions washed with PBS. Pelleted cells were broken by freeze-thaw then mixed in lysis buffer (30 mM Tris-HCl pH 8.5 (4˚C), 7 M urea, 2 M thiourea, 4% CHAPS, 50 mM DTT, 0.5% IPG carrier ampholytes and a cocktail of protease inhibitors) for 1 h and the supernatant was clarified by centrifugation. Proteins were purified and concentrated by precipitation with a fivefold volume of cooled acetone, and re-suspended for 1 h. in lysis buffer without DTT. Protein concentration was measured with the RC/DC Protein Assay Kit (Bio-Rad). Samples were kept frozen until use. *S. solfataricus* (P2) protein samples were prepared and labeled with CyDyes according to the manufacturer's protocol. Briefly, 50 μg of each protein extract was labeled separately at 0˚C in the dark for 30 min with 400 pM of the *N*-hydroxysuccinimide esters of cyanine dyes (Cy3 and Cy5 CyDyes; GE Healthcare) dissolved in 99.8% DMF (Sigma). The internal standard, an equimolecular mixture of all the protein extracts, was labeled with Cy2. Labeling reactions were quenched by the addition of 1 μL of a 10-mM L-lysine solution (Sigma) and left on ice for 10 min. Cy2, Cy3, and Cy5 for appropriate control or infected samples were combined and mixed with rehydration buffer (7 M urea, 2 M thiourea, 4% CHAPS) containing 50 mM DTT and 0.5% IPG.

2-DE WITH IPG STRIPS

2-DE was performed as described elsewhere (Gorg et al., 2004), using precast IPG strips (pH 3–11 NL, non-linear, 24 cm length; GE Healthcare) in the first dimension (IEF). Labeled samples were combined with up to 450 μL rehydration buffer (7 M urea, 2 M thiourea, 4% CHAPS, 0.5% IPG buffer pH 3–11 NL, 40 mM DTT, and traces of bromophenol blue) and loaded onto IPG strips. Typically, 150 μg proteins were loaded on each IPG strip and IEF was carried out with the IPGPhor II (GE Healthcare). Focusing was carried out at 20˚C, with a maximum of 50 μA/strip. Active rehydration was achieved by applying 50 V for 12 h. This was followed by a stepwise progression of 500 V for 500 Vh, gradient ramp from 500 to 1000 V for 1 h, gradient ramp from 1000 to 3000 V for 1 h, gradient ramp from 3000 to 5000 V for 1 h, gradient ramp from 5000 to 8000 V for 1 h, gradient ramp to 8000 V over 1 h, then 8000 V constant for a total of 44,000 Vh. After IEF separation, the strips were equilibrated twice for 15 min with 50 mM Tris-HCl, pH 8.8, 6 M Urea, 30% glycerol, 2% SDS, and a trace of bromophenol blue. The first equilibration solution contained 65 mM DTT, and 53 mM iodoacetamide was added in the second equilibration step instead of DTT. The strips were sealed on the top of the gels using a sealing solution (0.5% agarose, 0.5% SDS, 0.5 M Tris-HCl). Second-dimension SDS-PAGE was performed in Dalt II (GE Healthcare) using 1 mm-thick, 24-cm, 13% polyacrylamide gels, and electrophoresis was carried out at a constant current (45 min at 2 mA/gel, then at 15 mA/gel for ∼16 h at 20˚C). Electrophoresis was completed once the bromophenol blue dye front reached the bottom of the gel. When relevant, gels were stained with ProQ Diamond (Invitrogen), a phosphorylation specific fluorescent stain or with SYPRO® Ruby, and Coomassie® Brilliant Blue stains for spot picking.

IMAGE ACQUISITION AND ANALYSIS

After electrophoresis, gels were scanned using the Typhoon Trio Imager according to the manufacturer's protocol (GE Healthcare). Scans were acquired at 100 μm resolution. Images were subjected to automated difference in-gel analysis using Progenesis SameSpots software version 2.0.2 (Non-linear Dynamics Ltd.). The Cy3 gel images were scanned at an excitation wavelength of 540 nm with an emission wavelength of 590 nm, Cy5 gel images were scanned at an excitation wavelength of 620 with an emission wavelength of 680 nm, while the Cy2 gel images were scanned at an excitation wavelength of 532 nm with 526 nm emission filter. Gel spots were co-detected as DIGE image pairs, which were linked to the corresponding in-gel Cy2 standard. Between gels comparisons were performed utilizing the in-gel standard from each image pair using Progenesis SameSpots. All seven groups (12, 24, 36, 48, and 72 hpi of infected and normal samples were compared with each other; and fold values, as well as *p*-values of all spots, were computed with the Progenesis software, using one way ANOVA analysis. All spots were manually checked before applying the statistical criteria (ANOVA $p < 0.05$ and fold ≥ 1.5). The normalized spot volumes were used in statistical processing. The gels were then stored in 1% acetic acid at 4˚C until spot excision.

PROTEIN IDENTIFICATION

Protein spots of interest were excised from the gels, washed, in-gel reduced and S-alkylated, followed by digestion with porcine trypsin (Promega) overnight at 37°C (Shevchenko et al., 1996). The solution containing peptides released during in-gel digestion were transferred to sample analysis tube prior to mass analysis. LC/MS/MS used an integrated Agilent 1100 liquid chromatography–mass-selective detection (LC-MSD) trap (XCT-Ultra 6330) controlled with ChemStation LC 3D (Rev A.10.02). The Agilent XCT-Ultra ion trap mass spectrometer is fitted with an Agilent 1100 CapLC and nano-LC sprayer under the control of MSD trap control version 5.2 Build no. 63.8 (Bruker Daltonic GmbH). Injected samples were first trapped and desalted on the Zorbax 300SB-C18 Agilent HPLC-Chip enrichment column (40 NL volume) for 3 min with 0.1% formic acid delivered by the auxiliary pump at 4 μl/min. The peptides were then reverse eluted and loaded onto the analytical capillary column (43 mm × 75 μm ID, also packed with 5 μm Zorbax 300SB-C18 particles) connected in-line to the mass spectrometer with a flow of 600 NL/min. Peptides were eluted with a 5 to 90% acetonitrile gradient over 16 min. Data-dependent acquisition of collision induced dissociation tandem mass spectrometry (MS/MS) was utilized. Parent ion scans were run over the *m/z* range of 400–2200 at 24,300 *m/z-s*. MGF compound list files were used to query an in-house database using Biotools software version 2.2 (Bruker Daltonic) with 0.5 Da MS/MS ion mass tolerance. Protein identification was accomplished by database search using MASCOT (Matrix science, London, UK). Protein identifications were considered to be positive when the protein score was >50 ($p < 0.05$).

ACTIVITY-BASED PROTEIN LABELING

S. solfataricus proteins were labeled with previously synthesized aqueous soluble rhodamine dyes (Dratz and Grieco, 2009, 2010) coupled to (1) a phenyl vinyl sulfonate (ZG-PVS) for Tyrosine phosphatase labeling (Liu et al., 2008), (2) a fluorophosphonate (ZG-FP) for Serine hydrolase labeling (Liu et al., 1999), and (3) acyloxymethyl ketone (ZG-AOMK) with a DVED peptide sequence for caspase labeling (Kato et al., 2005). Structures are shown in **Figure 5**. A publication detailing synthesis and properties of the dye is forth coming. The labeling reactions were performed using each corresponding dye at a final concentration of 5 μM in PBS, pH 7.0, for 20 min at room temperature. Reactions were quenched with four-volumes of cold to precipitate the proteins. The sample precipitates were solubilized in 2D gel-loading buffer containing 40 mM DTT then loaded onto 24 cm, 3-11 NL isoelectric focusing gel strips. ABPP labeled 2D-gels were scanned on the Typhoon fluorescence imager using a standard 532/580 nm filter set. Gels were then stained with SyproRuby (Molecular Probes) to confirm equal protein loading before DIGE analysis.

RESULTS

Batch cultures of *S. solfataricus* (P2) grown at 80°C, pH 2.5, were infected during early log phase with STIV at a multiplicity of infection (MOI) of ∼10. Infected and control cultures were treated identically and subsamples were removed at 12, 24, 36, 48, 60, and 72 h post inoculation (hpi). Cell growth rate was only moderately slower in the inoculated cultures as monitored by optical density (Figure S1 in Supplementary Material). Epifluorescent viral counts (Figure S1 in Supplementary Material), qPCR for the viral genome, and an ELISA specific for the major capsid protein of STIV (data not shown) were used to confirm viral replication (Ortmann et al., 2008). Together this data suggested that a single round of viral replication occurred. Cell counts and electron microscopy indicated that approximately 10% of the SsP2 cells became infected (Ortmann et al., 2008).

Cells from three biological replicates of infected and control cultures were subjected to standard minimal CyDye labeling and then analyzed by 2D-DIGE (Tannu and Hemby, 2006). Greater than 1000 spots were found on each gel and after filtering to remove irregularities, 700 were used in the analysis across all gels (Figure S2 in Supplementary Material). Using an approximate twofold change cutoff, there were 71 regulated proteins with 40 being more abundant and 31 less abundant in the infected samples. Changes in protein abundance began at 12 hpi and peaked near 48 hpi. The general trend was an immediate down regulation of host proteins followed by increasing up regulation over the course of the infection. Proteins spots were identified using in-gel digestion and LCMS/MS analysis, followed by searching of a local MASCOT database containing all viral and host ORFs greater than 50 amino acids. This expands the database slightly beyond what has been annotated in TIGR and NCBI. Previous experience with STIV indicated that non-annotated reading frames can be used (Maaty et al., 2006), therefore, this approach was adopted to minimize false negatives in the preliminary IDs. A list of the time points, identified host proteins, and associated COG groups is shown in **Table 1**. More detailed information including spot location, fold change, sequences, scores, percent coverage, and links to genome databases and annotation is provided in Table S1 in Supplementary Material.

Based on the COG partitioning, the regulated proteins fell into 14 of the 26 groups (**Figure 1**; **Table 1**). More than one-half of the regulated proteins were in just five of the COG groups (Transcription K; Translation J; PTM, protein turnover, chaperones O; Energy production and conversion C; Amino acid transport, and metabolism E). These five COG groups account for only 25.4% of the *S. solfataricus* (P2) genome; therefore they are over-represented in the regulated protein fraction. Eight of the 71 proteins (SSO: 0286, 730, 1098, 1442, 2749, 1443, 1988, and 2569) fell into the unknown function (COG = S) and unclassified categories. At the genome level 49% of *S. solfataricus* (P2) genes are currently assigned to a specific category while 27% of the open reading frames have no assigned functional role and are listed as hypothetical genes. The remaining 24% are listed as conserved hypothetical genes. Therefore, the proteins regulated during viral infection tend to be in familiar COG groups or have sequence homology with known proteins, rather than being novel proteins unique to *Sulfolobus* or Archaea.

A number of protein functional categories displayed a mixed response to infection with some members increasing in abundance and others decreasing (**Figure 1**; **Table 1**). For example, proteins with a role in transcription and translation were split between up and down categories. Of particular interest is ribosomal protein L7Ae. It plays a critical role in binding and folding of small RNAs (Dennis and Omer, 2005; Omer et al., 2006), which are playing an ever expanding biological role. Another

Table 1 | 2D-DIGE identified proteins organized within COGs.

COG functional category	Protein and regulation
Unclassified	CRISPR-associated regulatory protein, Csa2 family (csa2), SSO1442 (48)↑; CRISPR-associated protein, Csa5, SSO1443 (36,48)↓; CRISPR-associated protein, TM1791.1, SSO1988 (36,48)↓
§Energy production and conversion	Acetyl-CoA synthetase, SSO1111 (36,72)↑; Heterodisulfite reductase subunit B, SSO1129 (72)↑; Heterodisulfide reductase subunit C, SSO1134 (48, 72)↑; FkbR2, putative, SSO1135 (48,72)↓; Carbon monoxide dehydrogenase small chain, SSO2433 (12,24,36,48,72)↓; Succinyl-CoA synthetase alpha subunit, SSO2482 (36)↑; Succinyl-CoA synthetase beta subunit, SSO2483 (12, 24, 48, 72)↓; Rubrerythrin, SSO2642 (12,24,36)↓; Electron transfer flavoprotein, SSO2817 (48)↑
Amino acid transport and metabolism	X-pro aminopeptidase, SSO0010 (12,24)↓; Prolidase, SSO0363 (48,72)↓; d-3-phosphoglycerate dehydrogenase, SO0905 (36)↑; FkbR2, putative, SSO1154 (12,24,36,48)↓; *O*-succinylhomoserine (thiol)-lyase, SSO2368 (72)↑; 3-isopropylmalate dehydratase, SSO2471 (36)↑
Nucleotide transport and metabolism	Uracil phosphoribosyltransferase, SSO0231 (48)↑, Glutamine amidotransferase, SSO0571 (72)↑
Carbohydrate transport and metabolism	Phosphomannomutase, SSO0207 (12, 24)↓(48)↑, phosphoenolpyruvate synthase, SSO0883 (12,24)↓; bifunctional phosphoglucose/phosphomannose isomerase, SSO2281(72)↑; ABC transporter, SSO2850 (72)↑; Fructokinase, SSO3195 (36, 48)↑
Lipid transport and metabolism	Acetyl-CoA acetyltransferase, SSO2061 (12, 24)↓(48)↑, Lipase, SSO2493 (36,48)↑, Acyl-CoA dehydrogenase, SSO2511 (72)↑
§Translation	50S ribosomal protein L7Ae,SSO0091(48)↑; Methionine aminopeptidase, SSO0098 (36,48)↑; Aspartyl-tRNA synthetase, SSO0173 (72)↑; LSU ribosomal protein L12AB, SSO0342 (48)↓; LSU ribosomal protein L11AB, SSO0346 (48)↓; Threonyl-tRNA synthetase homolog, SSO0384 (72)↑; SSU ribosomal, SSO0411 (48)↑; prolyl (glutamyl) tRNA synthetase, SSO0569 (72)↑; ribosomal protein S5, SSO0698 (48)↑
§Transcription	30S ribosomal protein S14 homolog, SSO0049 (12)↓; transcription elongation factor NusA-like protein, SSO0172 (72)↓; Transcription factor E , SSO0266 (12,24,72)↓; DNA binding protein SSO10b, SSO0962 (36)↓; Transcriptional regulator marR family, SSO1082 (12)↑; transcriptional regulator Lrs14, SSO1108 (36)↓; Regulatory protein; AsnC family, SSO5522 (12)↑
Replication, recombination, and repair	DNA repair protein radA, SSO0250 (36,48)↑; Endonuclease IV-like protein, SSO2156 (48)↑, Single-stranded DNA binding protein, SSO2364 (48,72)↓
§Post-translational modification, protein turnover, chaperones	Thermosome beta subunit, SSO0282 (12,24)↓(48)↑; prefoldin subunit alpha, SSO0349 (72)↓; Prefoldin beta subunit, SSO0730 (12,24)?; proteasome alpha subunit, SSO0738 (36,48)↑; thermosome subunit alpha, SSO0862 (36,72)↑; Peroxiredoxin, SSO2613 (36,48,72)↓; Thermosome gamma subunit, SSO3000 (12,72)↓
Inorganic ion transport and metabolism	Superoxide dismutase, SSO0316 (12,24)↓(36,48)↑
General function prediction only	Molybdenum transport protein ModA related protein, SSO1066 (36)↑; Carbon monoxide dehydrogenase, large chain, SSO1209 (24)↓; 3-oxoacyl-(acyl carrier protein) reductase (fabG-4), SSO2205 (72)↑; 3-oxoacyl-(acyl carrier protein) reductase (fabG-5), SSO2276 (48)↑; MoxR-like ATPases, SSO2363 (12,24)?; Carbon monoxide dehydrogenase, medium chain, SSO2434 (36, 48)↑; NAD-dependent alcohol dehydrogenase, SSO2536 (72)↑, INOSINE-5-MONOPHOSPHATE DEHYDROGENASE putative, SSO2588 (12,24)↓; Carbon monoxide dehydrogenase, medium chain, SSO2636 (36)↑; Alcohol dehydrogenase (adh-13), SSO2878 (36)↑; Tryptophan repressor binding protein, SSO3155 (72)↑
Function unknown	Hypothetical protein, SSO0276 (12)↑, Hypothetical protein, SSO0286 (36)↑; Conserved hypothetical protein, SSO1098 (12,24,36,48)↑; Hypothetical protein, SSO2569 (48)?; Conserved hypothetical protein, SSO2749 (12,24)↓
Signal transduction mechanisms	Universal stress protein, SSO1865 (12,24,36,48)↓

Numbers in parenthesis designate time points (hpi). § *Majority of regulated proteins belongs to those COG groups.* ↑↓ *Arrows indicates direction of regulation. The following COG functional categories are not detected in this study. RNA processing and modification, coenzyme transport and metabolism, chromatin structure, and dynamics, cell cycle control, mitosis, and meiosis, cell wall/membrane biogenesis, cell motility, secondary metabolites biosynthesis, transport, and catabolism, intracellular trafficking and secretion, defense mechanisms, extracellular structures, nuclear structure and cytoskeleton.*

functional group of proteins with both up and down regulation were those involved with carbohydrate metabolism and transport, two processes important to STIV replication (Larson et al., 2006; Maaty et al., 2012).

Only two STIV proteins, B345 (major capsid protein) and C92 (formation of VAPs) were detected by the DIGE analysis, both at 36 hpi. B345 and C92 are expressed in large quantities during viral replication (Maaty et al., 2012), so it is reasonable that when viral replication is occurring in 10% of the population, only the most abundant virus proteins would be detected. B345 was identified in more than one horizontally displaced spot on the gels, indicative of several different PTM isoforms. Similar multiple isoforms were

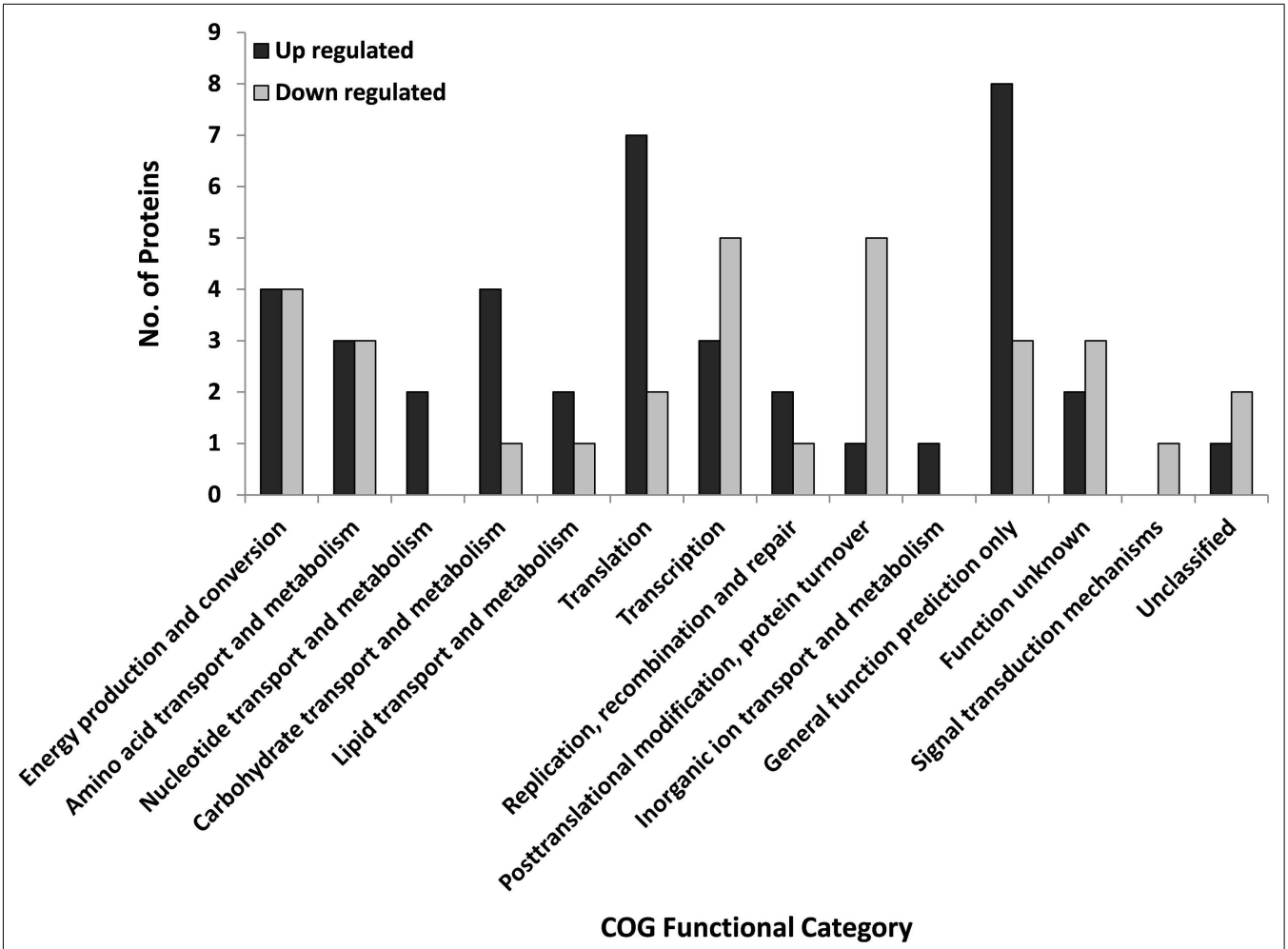

FIGURE 1 | Regulated *S. solfataricus* (P2) proteins by COG designation that were regulated during STIV infection. Proteins were classified as regulated if the fold change at any time point was ∼twofold and $p < 0.05$ (ANOVA). There were 40 up-regulated and 31 down regulated proteins.

found in purified STIV particles (Maaty et al., 2006) and from studies using the readily infectable isolate, SsP2-2-12 (Maaty et al., 2012). The other viral protein, C92 (9.8 kDa, pI 5.19) is a small membrane protein that assembles into the large VAPs that have been described recently (Brumfield et al., 2009; Snyder et al., 2011). The mechanism behind this polymerization is currently unknown and no similar structures have ever been reported beyond STIV and SIRV2.

As the number of genomic and proteomic studies characterizing cellular response to various perturbations have accumulated, features of a general response have emerged. Common participants in the stress response include heat shock proteins, chaperones, and mediators of oxidation/reduction (Macario et al., 1999; Kvint et al., 2003; Casado-Vela et al., 2006; Chertova et al., 2006). A number of the regulated proteins found in this study are consistent with a general stress response following infection. Superoxide dismutase (SSO0316) participates in the scavenging of reactive oxygen species and has been shown to be up-regulated in animal and plant cells during viral infection (Alfonso et al., 2004; Casado-Vela et al., 2006). In contrast, down regulated proteins include SSO1865, which is homologous to universal stress protein (USP), and Rubrerythrin (SSO2642), a non-heme iron binding protein found in many air-sensitive Bacteria and Archaea that is a member of a broad superfamily of ferritin-like diiron-carboxylate proteins (Andrews, 1998; Kurtz, 2006).

ANTIVIRAL SYSTEMS

Inoculation of *S. solfataricus* P2 cultures with high MOI of STIV leads to viral production and eventual cell lysis only in a limited number of cells, ∼10% (Ortmann et al., 2008). The reason for this is unknown, although such fractional susceptibility to infections has also been confirmed with other archaeal virus/host systems (Prangishvili et al., 1999; Kessler et al., 2004; Peng et al., 2004). Plausible explanations include, but are not limited to (i) not all of the cells express the viral receptor, (ii) cellular host factors required for replication are at low levels or possibly are missing, or (iii) an antiviral defense system is functioning in most but not all cells. Members of the CAS family were among the regulated host proteins. These CAS family are part of the CRISPR/Cas (clusters of regularly interspaced short palindromic repeat) prokaryotic

adaptive immune system which help prokaryotes resist viral infection (Barrangou et al., 2007). CRISPR regions have been identified in *Sulfolobus* spp. DNA (Mojica et al., 2005; Kunin et al., 2007) and specific matches to viral sequences, including STIV, are present (Mojica et al., 2005). Three CRISPR-associated proteins (CAS proteins) SSO 1442, 1443, 1988 were the significantly regulated group of proteins. The presence of six additional CAS proteins was confirmed by survey-based spot picking (SSO: 1398, 1399, 1401, 1441, 1514, and 1991) bringing the total to nine. Recent studies of the CRISPR/Cas system in *S. solfataricus* (Garrett et al., 2011a,b), including structural studies of the (CRISPR)-associated complex for antiviral defense (CASCADE) that targets invading DNA (Lintner et al., 2011b), the CMR complex that targets invading RNA (Zhang et al., 2012), and potential transcriptional regulators of CRISPR/Cas (Lintner et al., 2011b) are beginning to shed light on how this system works in Archaea. It is interesting to note that prior study using a fully STIV susceptible strain of *S. solfataricus* did not detect expression of any CAS proteins (Maaty et al., 2012).

POST-TRANSLATIONAL MODIFICATION OF HOST PROTEINS

Protein synthesis and degradation are not the only ways in which protein activity can be regulated. PTMs are a common and often rapid way in which protein activity can be altered. Based on gene annotation and functional characterization, the presence of enzymes involved with the addition and removal of PTMs such as methylation, acetylation, phosphorylation, glycosylation, and N-terminal processing are present in *S. solfataricus* (P2; Krishna and Wold, 1993; She et al., 2001; Chaban et al., 2006). Finding the targets and frequency of PTM is a challenging task and currently, little is known about the use of PTM in Archaea (Barry et al., 2006). The ability to detect PTMs and changes in PTMs globally, at the level of the proteome, without limiting the scope of the experiment, is a major strength of the 2D-DIGE approach. Changes in protein pI and/or MW are caused by most PTMs leading to altered isoform positions on the gel and changes in spot intensities. Proteins with less than complete modification at a specific site will be found in more than one spot and the spot intensity ratios can be used to follow the fraction of modification and the kinetics of modification. Of the 71 regulated proteins, 23 were identified in more than one spot, suggesting that regulation may be the result of changes in PTMs and corresponding shifts on the gels (see **Figure 2**). A number of proteins appear in 2–6 horizontally shifted spots, indicating the presence of multiple modifications.

Protein phosphorylation is a common PTM that changes the pI of the intact protein and shifts the protein position on the 2D gel. The detailed characterization of specific protein phosphorylation has only been described for a few *Sulfolobus* proteins. Interestingly, one of these, phosphohexomutase (SSO0207; Ray et al., 2005) was among the regulated proteins. Phosphohexomutase was found in six different gel spots and exhibited a complex pattern of regulation (**Figure 2B**). Rubrerythrin, the putative stress response factor discussed above, was found in multiple horizontal spots that were down regulated at 12 and 24 hpi in addition to vertical shifts. Shifts in the vertical migration (molecular weight dimension) can be minor as seen with USP (**Figure 2D**), or major as in the case of the thermosome beta subunit (**Figure 2C**). Another protein known to be regulated by phosphorylation is D-gluconate dehydratase (SSO3198), a key enzyme in the non-phosphorylated Entner–Doudoroff pathway (Kim and Lee, 2005). We found this to be up-regulated at 48 h and to appear in multiple positions on the gels. All of these PTM were detected using standard CyDye DIGE analysis, illustrating a strength of the 2D-DIGE method.

Directed PTM experiments using ProQ Diamond, a phosphorylation specific fluorescent stain were conducted to look specifically for phosphorylated proteins. 2D-gels of control and infected cells at 36 and 48 hpi were analyzed after ProQ Diamond

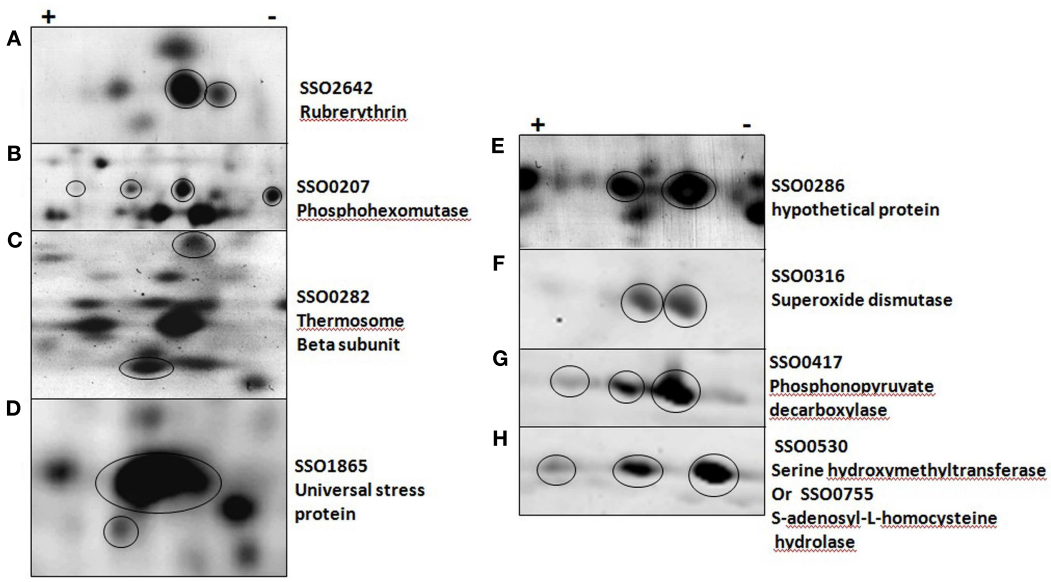

FIGURE 2 | Post-translationally modified proteins in five *solfataricus* (P2). (A–D) were imaged with a general protein stain, **(E–H)** with a phosphoprotein specific stain. Circles indicate protein of interest in each panel.

staining and ∼100 protein spots could be detected, 18 of which were intense (**Figure 3**). The reported detection limit for this dye is 1–16 ng/band (Invitrogen). Fifteen of the 18 intense spots contained a single protein (Table S3 in Supplementary Material). The other three spots contained more than one protein, each with good sequence coverage, so the specific protein responsible for ProQ Diamond staining of the spot could not be determined. Two of the 18 intense ProQ Diamond staining spots appeared only after infection; ribosomal protein L22AB (SSO0713) and geranylgeranyl hydrogenase (SSO2353). The latter protein was also found in one of the only other proteomic surveys of *S. solfataricus* (P2), however the presence of phosphorylation was not addressed (Barry et al., 2006). The only other documented report of phosphorylation for one of the regulated proteins concerned the conserved hypothetical protein (SSO0286), which was found here in two spots and has 93% sequence similarity to Fructose-1,6-Bisphosphatase from *S. tokodaii* (Nishimasu et al., 2004). Phosphorylation of Fructose-1,6-Bisphosphatase is typically involved in switching between glycolysis and gluconeogenesis, which can be of value when cellular energy is needed but the glucose level in the medium is low. Five of the proteins with significant phosphorylation were also in the group of 71 regulated proteins discussed above.

NETWORK REGULATION

The analysis of the STIV-*S. solfataricus* (P2) interaction has focused on specific proteins and pathways above. A more general analysis of the data may also be useful for putting the data in perspective with other organisms and approaches. Data on mRNA half-life in *S. solfataricus* and *S. acidocaldarius* were previously measured in a genome-wide study (Andersson et al., 2006). The results were essentially the same for the two species, with a median half-life of ∼5.3 min and ∼50% of the mRNA lifetimes between 4–8 min. We compared the half-life of mRNAs corresponding to proteins that were differentially regulated following virus infection with the genome-wide values (**Figure 4A**). The observed pattern shows that regulated proteins come from mRNAs with a shorter than average half-life. Analysis of the lifetime data based on the 62 regulated proteins for which mRNA half-lives were known and 1961 half-life values from *S. solfataricus* using the Kolmogorov–Smirnov test, confirmed that the distributions

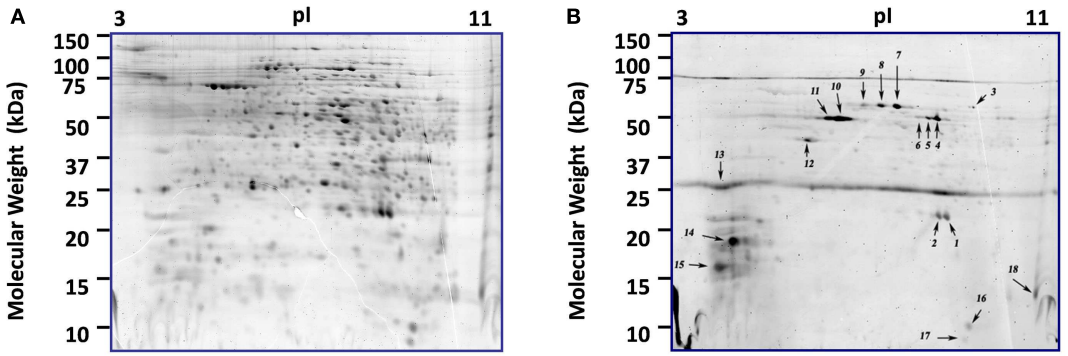

FIGURE 3 | Comparison of phosphorylated and total proteome of *S. solfataricus* (P2). 2D-gels at 36 h post-infection. **(A)** Proteome staining with the fluorescent dye Sypro Ruby. **(B)** Same gel using the phosphoprotein specific stain, ProQ diamond. Each of the numbered spots was picked and the proteins were identified by LCMS and results are shown in Table S4 in Supplementary Material.

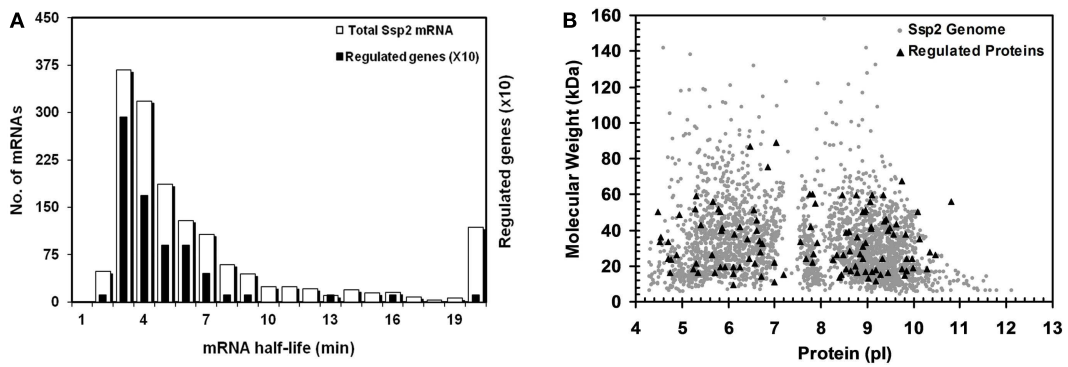

FIGURE 4 | mRNA half-life and MW/pI distribution of proteins with altered abundance. (A) Half-life of 1880 *S. solfataricus* (P2) mRNAs (white bars) and those for regulated proteins (black bars). Regulated proteins have RNA half-lives that are significantly biased against slow turnover based on a Kolmogorov–Smirnov test (p=0.0002). Bars for the regulated proteins are shown 10X for clarity; **(B)** Virtual 2D gel of *S. solfataricus* (P2) proteome. Calculated MW and pi distribution for the regulated proteins (triangles) and all predicted *S. solfataricus* (P2) genes (grey circles). The regulated proteins were found to be biased with respect to pi (p=0.001) but not MW (p=0.41) based on a Kolmogorov–Smirnov test.

were different ($p = 0.0002$). The study by Andersson et al. found that functional categories for translation, metabolism, and energy production were over-represented in the shortest half-life group of mRNAs. This is consistent with the population of proteins that were found to be regulated in the present study. The bias toward proteins that come from mRNAs with rapid turnover being regulated proteins is also consistent with computational models using a cost-benefit analysis for interpreting gene network regulation (Carlson, 2007).

An important consideration with any "omics" approach is data bias. It is commonly assumed that 2D gel analysis is biased against proteins at the pI and MW extremes. To test this, we compared the isoelectric point and apparent mass of the regulated *S. solfataricus* (P2) proteins to those of the predicted proteome. For visualization, the pI and MW of all annotated *S. solfataricus* (P2) genes were plotted as a virtual 2D gel, overlayed with darker spots for the regulated proteins (**Figure 4B**). Analysis of the 71 regulated proteins and the ∼3000 predicted genes, using the Kolmogorov–Smirnov test, revealed that there was no bias of the regulated proteins with respect molecular weight ($p = 0.41$). However, the regulated proteins did show a bias with respect to pI ($p = 0.001$). At this point, it is not known whether this is due to technical issues related to the 2D gel process or is a reflection of the chemical properties of regulated proteins. However, this result is interesting because, while there is no inherent cost-benefit basis for selectively altering the turnover of mRNA's that encode for proteins with different pIs, there clearly is for extremes in MW. This is because the synthesis of short and long mRNAs and proteins require different resource commitments that will be allocated differently during stress response (Andersson et al., 2006; Carlson, 2007).

ACTIVITY-BASED PROTEIN PROFILING

A commonality of genomic and proteomic methods is that each measures the amount of a biomolecule present in a cell at a given time. While this can be highly informative and is the basis for nearly all studies looking at mRNA and proteins, the amount of mRNA and protein are proxies for biological activity. In contrast, ABPP is a powerful analytical method to detect and compare protein activities across proteomes. The use of ABPP in general is increasing rapidly, but few probes have been synthesized that demonstrate compatibility with 2D-Gel analysis (Schicher et al., 2010). The majority of standard fluorescent dyes behave poorly on 2D-gels because they alter protein pI, decrease solubility, and/or result in smearing. We have synthesized a series of dyes specifically designed for optimal 2D gel analysis, that exhibit high aqueous solubility and do not perturb protein pI (Dratz and Grieco, 2009, 2010), three of which are presented here as activity-based probes for the first time (**Figure 5**). This is also the first survey of caspases, serine hydrolases, and tyrosine phosphatases in an archaeal organism.

Caspase-like enzymes

Caspases are a family of cysteine proteases that regulate programmed cell death (apoptosis) and other functions in eukaryotic cells. Caspases are present in cells as zymogens that require activation cascades (Boatright and Salvesen, 2003). The presence of caspase-like proteins in Archaea was unknown until a report of caspase eight antibody cross-reactivity in *Haloferax volcanii* (Bidle et al., 2010). Genomic analysis of *H. volcanii* identified a subset of 18 potential target proteins containing the signature tetrapeptide caspase cleavage motif (IETD), however caspase-like function was not assessed in the study. Therefore, we used a fluorescently tagged caspase specific probe (ZG-AOMK) to screen for caspase-like enzyme activity. Incubation of total soluble proteins from infected *S. solfataricus* (P2) cells with ZG-AOMK followed by 2D gel analysis, revealed groups of spots between 30–75 kDa with significant labeling (**Figure 6A**).

Protein staining of the gel (**Figure 6B**) showed that the labeling was highly discrete, because the activity and protein abundance patterns were quite distinct. Six spots were selected for in-gel proteolysis and LCMS identification, four of which contained proteins known to have reactive cysteines. Thiosulfate sulfurtransferase (cysA-2), SSO1817, was in spot 4. This enzyme contains a Rhodanese Homology Domain with a catalytically active cysteine residue. Spot 6 had 5-Oxo-L-prolinase, which has a sulfhydryl involved with NTPase and prolinase activities (Williamson and Meister, 1982). Adenosylhomocysteinase, spot 5, has a cysteine in the catalytic center that is reported to maintain reduction potential for effective release of the reaction products and regeneration of the active form (NAD+ form) of the enzyme (Yuan et al., 1996). Lastly, 4-aminobutyrate aminotransferase, spot 1, has a pair of cysteines that mediate dimerization (Kim and Churchich, 1989). Caspase inhibitors are well known to be promiscuous, reacting with enzymes having cysteines in the active site (Furman et al., 2009). The labeling of 4-aminobutyrate aminotransferase was a bit more puzzling, however, on closer inspection, it was noted that a cysteine is involved with dimerization. Specificity of the protein–protein interaction must then be an inherent part of the region surrounding the active cysteine. Making it much like a caspase in that it recognizes a specific amino acid sequence and places a reactive cysteine in position to react. A detailed list of the proteins labeled with the caspase probe can be found in Table S4 in Supplementary Material.

Serine hydrolases

The second activity probe used targeted serine hydrolases which are one of the largest and most widely distributed enzyme classes in all three kingdoms of life. This class of enzymes utilizes a conserved serine nucleophile to hydrolyze amide, ester, and thioester bonds in both protein and small molecule (metabolite) substrates. A broad spectrum fluorophosphonate probe has been shown to effectively modify the serine hydrolase superfamily including proteases, lipases, esterase, acetylcholinesterase, thioesterases, some phospholipases, and amidases (Liu et al., 1999; Simon and Cravatt, 2010). Biochemical, structural, and *in silico* studies have confirmed the presence of the serine hydrolase superfamily members mentioned above as well as α-amylases (Janecek and Blesak, 2011) and prolyl oligopeptidases (Bartlam et al., 2004) in Archaea. We used the fluorophosphonate (ZG-FP) probe (**Figure 5**) to test for such activity, and labeled total soluble protein during viral infection. *S. sulfolobus* (P2) samples at 32 control and 32 hpi were incubated with ZG-FP and then analyzed by 2D-gels with differential labeling of total protein. Approximately ∼15 spots at both control and 32 hpi were specifically tagged (**Figures 6C,D**),

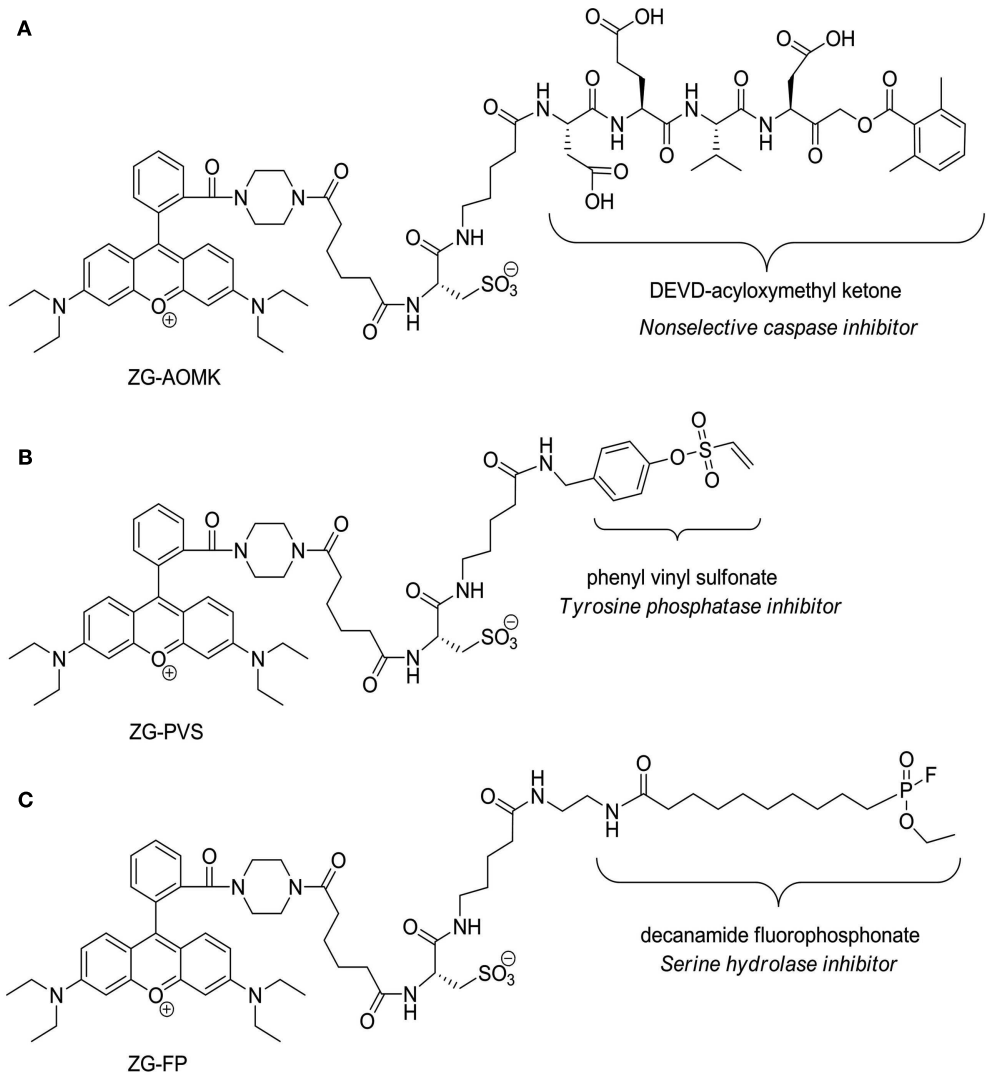

FIGURE 5 | Structures of the zwitterionic ABPP probes. (A) Acyloxymethyl ketone probe (ZG-AOMK) for caspase. **(B)** Phenyl vinyl sulfonate probe (ZG-PVS) for Tyrosine phosphatase. **(C)** Fluorophosphonate (ZG-FP) for Serine hydrolase. Note that the protein reactive functional groups are labeled and the protein classes to which they inhibit are denoted below.

the pattern was significantly different between the two gels. The protein spots were identified by in-gel digestion and LC/MS/MS. Fifteen different proteins were identified including gene annotated as metal-dependent hydrolase, serine hydroxymethyltransferase; *S*-adenosylhomocysteine hydrolase (see Table S4 in Supplementary Material for complete list). This approach promises to be a widely applicable tool for better understanding pathways that are regulated during infection and for many other functional protein annotation projects.

Tyrosine phosphatases

The third probe addresses protein dephosphorylation. The level of protein phosphorylation is balanced by the antagonistic functions of protein kinases and phosphatases (Denu et al., 1996). Tyrosine phosphatases remove phosphate groups from the amino acid tyrosine and are very important component in eukaryotic and bacterial signaling pathways (Li and Dixon, 2000; Tonks and Neel, 2001). *In silico* analysis of archaeal organisms found several candidate phosphatases (Stravopodis and Kyrpides, 1999), and the18 kDa tyrosine/serine phosphatase SSO2453 which was previously described in *Thermoeoeeus kodakaraensis* (Jeon et al., 2002). Another group of low molecular weight protein-tyrosine phosphatase are VH1-like phosphatases which have been found in Bacteria, Archaea, plants, yeast, insects, worms, and mammals. A homolog to this phosphatase is annotated in *S. solfataricus P2* as tyrosine phosphatase (SSO2453). Their average size of 16 kDa, is close to the major low molecular weight spots 29 and 30 in **Figures 6E,F**. The presence of phosphorylated proteins (**Figure 3**) suggested that phosphatases may play a role in signaling during STIV infection. To conduct a biochemical test, control and STIV infected cells were compared using 2D-gels with differential labeling of protein and enzyme activity 24 and 32 hpi after reaction

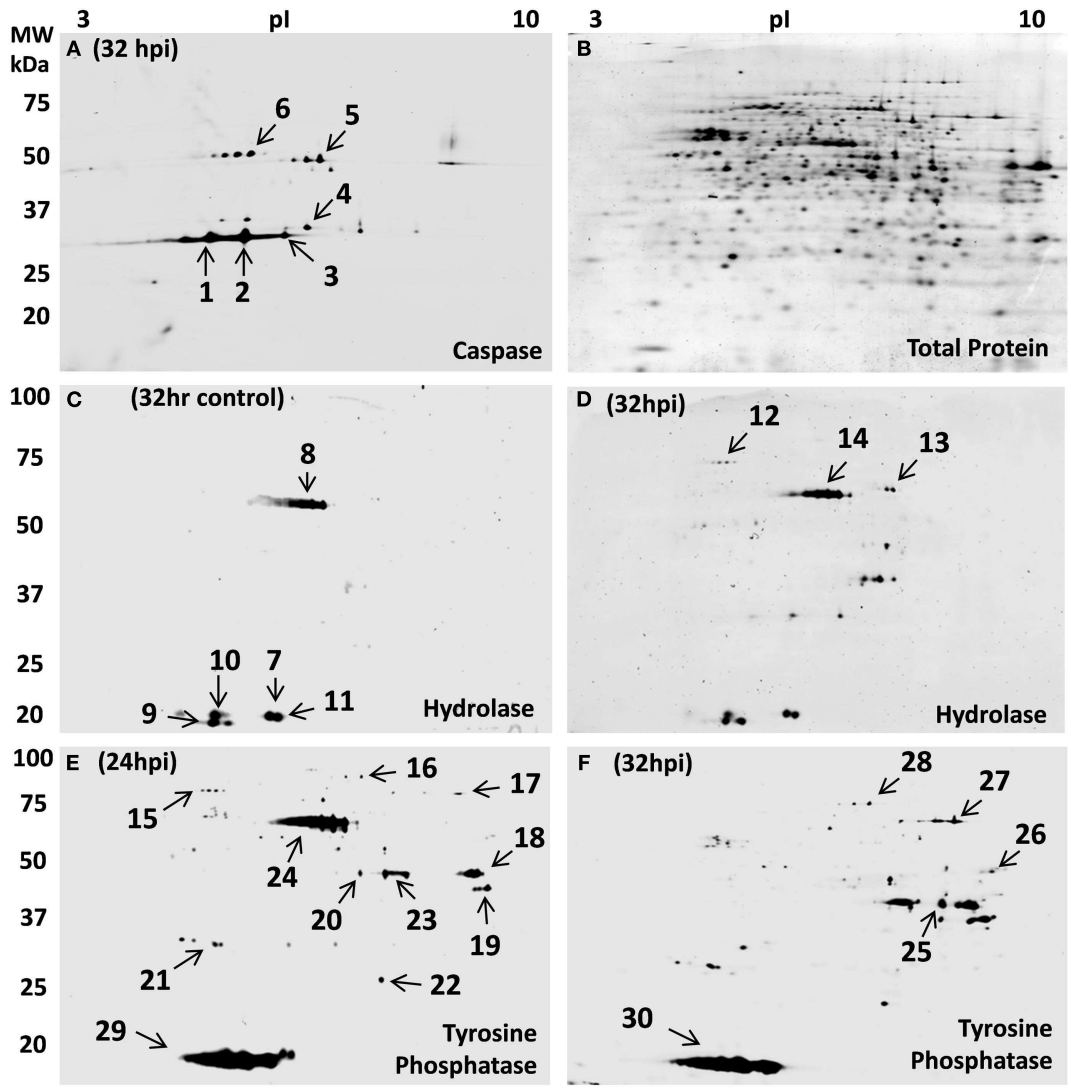

FIGURE 6 | Host protein activity-based reactivity changes during STIV infection. (A) Novel zwitterionic acyloxymethyl ketone probe (ZG-AOMK) for caspase as described in the text, was reacted with total soluble protein from 32 h infected *S. solfataricus*. Approximately 27 protein spots were labeled with the caspase specific probe. **(B)** Subsequent staining for total protein, using SyproRuby, showed ∼800 spots. Zwitterionic fluorophosphonate (ZG-FP) for Serine hydrolase was reacted with total soluble protein from *S. solfataricus* control **(C)** and 32 hpi **(D)**. Approximately 15 protein spots were labeled with the Serine hydrolase specific probe. Phenyl vinyl sulfonate probe (ZG-PVS) for Tyrosine phosphatase was reacted with total soluble protein from virus infected *S. solfataricus* 24 hpi **(E)** and 32 hpi **(F)**. Subsequent staining of gels in **(C–F)** for total protein, using SyproRuby, showed ∼800 spots (as shown in **B**).

with ZG-PVS. As with the other two probes, selective labeling of proteins was evident and differences were observed between the samples. Two regions showed very strong labeling (spots 24 and 29, **Figure 6E**). Protein identification of spot 29 from three gels consistently revealed rubrerythrin (SSO2642) and prefoldin (SSO0730). In addition, an 11.5 kDa acylphosphatase, SSO0887, which closely matches the position on the gel was identified. The signal from the probe was very strong (**Figure 6E**), even though the amount of protein was low, indicating that the reactivity was high. In-gel proteolysis and mass spectrometry analysis only found a single peptide, but it occurs at the pI and MW expected, the identification score for the peptide was highly significant, and the protein is small, limiting possible peptides to be detected. Therefore, we propose the SSO0887 is the actual protein being labeled.

The other region with intense labeling (spot 24) contained three proteins (2-methylcitrate dehydratase, serine hydroxymethyltransferase, and *S*-adenosyl-homocysteine hydrolase) none of which would be expected to react. There could be a mis-annotation, or we failed to detect the protein responsible for the labeling. None of the other spots provided hits to proteins with direct linkage to phosphatases (the complete list of identified proteins can be found in Table S4 in Supplementary Material). This inspired a second sequence-based check for potential phosphatases

in *S. solfataricus* P2. Blast alignments of phosphatase sequences from other archaeal organisms lead to the putative identification of four additional phosphatases (NagD-like sugar phosphatase SSO2355, phosphoglycolate phosphatase SSO0094, phosphohexomutase SSO0481, and a tyrosine phosphatase SSO2453). The question now is what biological role is being carried out by the acylphosphatase in spot 29 and also, which protein is being labeled in spot 24 that is highly reactive at 24 hpi, yet disappears entirely 8 h later. What is clear is how this probe quickly revealed that proteins with phosphatase-like activity were present and that the use of such probes can help to focus bioinformatics searches.

DISCUSSION

Despite widespread interest in archaeal organisms and more recently the viruses that infect them, many basic questions remain to be answered regarding their biology and biochemistry. Here we have coupled the well tested approach of following a host during viral infection/replication with multi-tiered "omics" experiments to learn more about the virus and it's interaction with the host. Combining data on mRNA lifetime and protein abundance, protein PTMs, and protein activities, provided insights into host and virus biology. Specifically, the interplay between STIV and *S. solfataricus* (P2) was characterized during a single round of replication. The majority of the cells in this ATCC stock were resistant to infection. This was confirmed visually and with growth curves (Figure S1 in Supplementary Material). Similar findings have been reported for other archaeal viruses and specific host species (Kessler et al., 2004; Peng et al., 2004; Happonen et al., 2010). Currently, it is unclear why many of the cells in these populations appear to be refractory to viral infection and this is the first report to address infection in a population of archaeal cells in which the majority does not show signs of viral burden. Unexpectedly, a stronger host response to viral infection at the proteome level was measured when infection rate was low, compared to the clonal isolate SsP2-2-12 that is highly susceptible to infection (Maaty et al., 2012).

Viral production is much greater from a culture of the highly susceptible *S. solfataricus* (SsP2-2-12) compared to the stock *S. solfataricus* (P2) ATCC strain used in this study. Comparative proteomics confirms this, as viral proteins were readily detected on 2D-gels using DIGE analysis at 24 and 32 h post exposure (Maaty et al., 2012), in contrast to the data presented here where only the two most highly expressed viral proteins, B345 (major capsid protein) and C92 (VAP), were detected on the gels. In stark contrast to viral protein production, only ten host proteins changed in abundance in the susceptible isolate, whereas 71 host proteins from 33 different pathways (Table S2 in Supplementary Material) changed in abundance across the time course shown here for *S. solfataricus* (P2; Table S1 in Supplementary Material). This discrepancy cannot be attributed to variation in the biological replicates, or dramatically different numbers of virus per cell (Ortmann et al., 2008). Together, these results indicate that the proteomic response observed here is predominantly coming from cells that are not showing visual or growth related signs of infection suggesting that an active response to STIV may be occurring.

HOST REGULATED PROTEINS

In the regulated protein pool, known stress response proteins were found, but the most intriguing host proteins; SSOs 1442, 1443, and 1988; are those from the CAS family. Proteins SSO1442 and perhaps 1443 (csa2 and csa5 respectively) are part of the CASCADE complex in *S. solfataricus* (P2) and thus play an important role in the newly characterized antiviral response in Archaea (Lintner et al., 2011b). This antiviral system uses CRISPRs as part of a double-stranded DNA monitoring system in prokaryotes (Barrangou et al., 2007). In addition to the regulated CAS proteins, six others were detected, with SSO1399, 1401, and 1441 being part of the same CASCADE complex (Lintner et al., 2011b). It has been suggested that Csa3 (Sso1445), may act as a transcription factor to regulate expression of these other CRISPR/Cas components, and that this may occur in response to viral infection (Lintner et al., 2011a), which is consistent with our results. Significantly, no regulated or constitutively expressed CAS proteins were found in the study using the readily infected SsP2-2-12 isolate (Maaty et al., 2012). This is a particularly exciting finding in that we now have a viral system and specific protein targets to test the mechanism of CASCADE *in vivo*.

POST TRANSLATION MODIFICATIONS

Our initial proteomics approach focused on changes in protein abundance, leading to the identification of a number of proteins and pathways found to be important in prokaryotic and eukaryotic response to viral infection (Table S1 in Supplementary Material). A distinct advantage of the 2D-DIGE approach over strictly mass spectrometry-based methods (on protein digests), is the ease with which PTMs and changes in PTMs can be detected and accurately quantified on intact proteins. Complex changes in the level of even multiple PTMs can be tracked on intact proteins and measured globally in a straight-forward manner using protein isoform abundances (**Figure 2**) or specific tagging for a PTM (**Figure 3**). It is worth stressing the point that without prior knowledge and focused methods, obtaining data on the relative populations of given protein isoforms, such as shown for phosphohexomutase and phosphonopyruvate decarboxylase (**Figures 2B,G**) would be extremely challenging. A clear direction for future investigation is to characterize specific targeted PTMs that are associated with biological mechanisms of interest and their functional outcomes.

PROTEIN TO MRNA CORRELATION

A large number of studies, including our own work on *S. solfataricus,* have detailed the lack of correlation between changes in mRNA and protein levels (Lee et al., 2003; Mehra et al., 2003; Neumann et al., 2004; Maaty et al., 2009, 2012). This is due in part to differences in the turnover rates (half-life) of a given mRNA and the protein it codes for (Taniguchi et al., 2010). Genes encoding proteins that require tight regulation, such as signaling or metabolic pathways, generally have mRNAs with shorter than average half-life (Andersson et al., 2006). Using the work of Anderson et al. as a reference, we show that the regulated proteins come from mRNAs with a shorter than average half-life. This observation could be considered within the context of a cost-benefit analysis of biomolecule synthesis (Carlson, 2007) and systems biology modeling

of regulatory networks and theory (Singh and Hespanha, 2009; Babu, 2010). Broadly, this indicates that regulation in *S. solfataricus* is controlled at multiple levels and that the overall network structure is consistent with that in Bacteria such as *E. coli*.

A significant challenge in studies using transcriptomics and proteomics approaches is connecting the data to biological mechanisms. For example, as discussed above, mRNA and protein abundance have only a weak correlation in most cases. An additional separation is that protein abundance is only a very imperfect proxy for activity, as other levels of regulation exist as well. This is what makes the chemical biology approach of ABPP so exciting. For the classes of enzymes that can be targeted with this approach, the read-out is a direct measure of biological activity. When ABPP is conducted with proteomics, enzyme class screening becomes a way to broadly screen activity yet retain specificity down to the level of isozymes. Until now, the ABPP proteomics connection has relied almost entirely on 1D SDS-PAGE or affinity purification using biotinylated probes. We have adapted 2D gel-friendly dyes (Dratz and Grieco, 2009, 2010) to 2D ABPP and this allows much higher resolution analysis of ABPP at the individual protein and protein isoform level, which should facilitate an even more effective use of activity probes.

HOST CELL ENZYME ACTIVITY

This study marks the first use of these three classes of activity probes in Archaea. Two of the enzyme classes, serine hydrolase, and phosphatase, were expected to be present in *S. solfataricus* based on amino acid homology. Caspase-like activity had been suggested but never demonstrated. All three probes reacted with discrete protein spots and performed well using standard 2D gel running conditions (**Figure 6**). The benefit to this work was multifold. First, we have shown that standard activity probes can be effective with proteins from extremophiles, activity changes in specific biological pathways involved with viral infection could be targeted, and the identification of proteins that were targeted can be used to assist in gene annotation and establish cross-reactivity with other enzyme classes. When ABPP probes are coupled with 2D gel-based proteomics, enzyme cross-reactivity is actually an advantage. Up to a point, the more cross-reactivity a probe has, the wider the window of biological change that can be assessed. Specific to this work, phosphatases are clearly a part of the signaling during STIV infection, a number of proteins have cysteine residues with a nucleophilicity and selectivity similar to caspases, and ABPP expanded the accessible dynamic range in our experiments. In the big picture, these findings demonstrate the practicality and versatility of semi-directed ABPP to complement other omics methods and accelerate the discovery of altered protein activities.

We are just beginning to scratch the surface and see into the world of archaeal viruses and have glimpses of how they interact with their hosts. As these studies progress, the list of commonalities and differences between the three domains of life will surely continue to grow as will the potential for cross fertilization between mechanistic studies of Archaea, Eukarya, and Bacteria. The relatively small size of the *Sulfolobus* genome, the mix of eukaryotic and bacterial features, and the evolutionary relationship of STIV with viruses in all three domains makes this an ideal system to investigate viral host interactions.

ACKNOWLEDGMENTS

We would like to thank Jim Robison-Cox, Benjamin Sharp, and Rebecca Taylor for assistance with statistical analysis. C. M. Lawrence for critical reading of the manuscript. BB is funded by MCB 0646499 from the National Science Foundation, the Center for Bio-Inspired Nanomaterials (Office of Naval Research grant #N00014-06-01-1016), and the Thermal Biology Institute (NASA grant NNG04GR46G) We would like to thank the Murdock Charitable Trust and NIH cobre 5P20RR02437 for support of the Mass Spectrometry Facility at MSU.

SUPPLEMENTARY MATERIAL

The Supplementary Material for this article can be found online at http://www.frontiersin.org/Virology/10.3389/fmicb.2012.00411/abstract

Table S1 | Regulated *S. solfataricus* (P2) proteins.

Table S2 | Sulfolobus pathways.

Table S3 | Identified proteins from phospho-stained spots.

Table S4 | Identifed ABPP labeled proteins.

REFERENCES

Alfonso, P., Rivera, J., Hernaez, B., Alonso, C., and Escribano, J. M. (2004). Identification of cellular proteins modified in response to African swine fever virus infection by proteomics. *Proteomics* 4, 2037–2046.

Andersson, A. F., Lundgren, M., Eriksson, S., Rosenlund, M., Bernander, R., and Nilsson, P. (2006). Global analysis of mRNA stability in the archaeon Sulfolobus. *Genome Biol.* 7, R99.

Andrews, S. C. (1998). Iron storage in bacteria. *Adv. Microb. Physiol.* 40, 281–351.

Babu, M. M. (2010). Structure, evolution and dynamics of transcriptional regulatory networks. *Biochem. Soc. Trans.* 38, 1155–1178.

Barrangou, R., Fremaux, C., Deveau, H., Richards, M., Boyaval, P., Moineau, S., et al. (2007). CRISPR provides acquired resistance against viruses in prokaryotes. *Science* 315, 1709–1712.

Barry, R. C., Young, M. J., Stedman, K. M., and Dratz, E. A. (2006). Proteomic mapping of the hyperthermophilic and acidophilic archaeon Sulfolobus solfataricus P2. *Electrophoresis* 27, 2970–2983.

Bartlam, M., Wang, G. G., Yang, H. T., Gao, R. J., Zhao, X. D., Xie, G. Q., et al. (2004). Crystal structure of an acylpeptide hydrolase/esterase from Aeropyrum pernix K1. *Structure* 12, 1481–1488.

Bidle, K. A., Haramaty, L., Baggett, N., Nannen, J., and Bidle, K. D. (2010). Tantalizing evidence for caspase-like protein expression and activity in the cellular stress response of Archaea. *Environ. Microbiol.* 12, 1161–1172.

Blais, D. R., Brulotte, M., Qian, Y. M., Belanger, S., Yao, S. Q., and Pezacki, J. P. (2010). Activity-based proteome profiling of hepatoma cells during hepatitis C virus replication using protease substrate probes. *J. Proteome Res.* 9, 912–923.

Boatright, K. M., and Salvesen, G. S. (2003). Mechanisms of caspase activation. *Curr. Opin. Cell Biol.* 15, 725–731.

Bolduc, B., Shaughnessy, D. P., Wolf, Y. I., Koonin, E. V., Roberto, F. F., and Young, M. (2012). Identification of novel positive-strand RNA viruses by metagenomic analysis of archaea-dominated yellowstone hot springs. *J. Virol.* 86, 5562–5573.

Brumfield, S. K., Ortmann, A. C., Ruigrok, V., Suci, P., Douglas, T., and Young, M. J. (2009). Particle assembly and ultrastructural features associated with replication of the lytic archaeal virus Sulfolobus turreted icosahedral virus. *J. Virol.* 83, 5964–5970.

Carlson, R. P. (2007). Metabolic systems cost-benefit analysis for interpreting network structure and regulation. *Bioinformatics* 23, 1258–1264.

Casado-Vela, J., Selles, S., and Martinez, R. B. (2006). Proteomic analysis of tobacco mosaic virus-infected tomato (Lycopersicon esculentum M.) fruits and detection of viral coat protein. *Proteomics* 6(Suppl. 1), S196–S206.

Chaban, B., Voisin, S., Kelly, J., Logan, S. M., and Jarrell, K. F. (2006). Identification of genes involved in the biosynthesis and attachment of Methanococcus voltae N-linked glycans: insight into N-linked glycosylation pathways in Archaea. *Mol. Microbiol.* 61, 259–268.

Chertova, E., Chertov, O., Coren, L. V., Roser, J. D., Trubey, C. M., Bess, J. W. Jr., et al. (2006). Proteomic and biochemical analysis of purified human immunodeficiency virus type 1 produced from infected monocyte-derived macrophages. *J. Virol.* 80, 9039–9052.

Dennis, P. P., and Omer, A. (2005). Small non-coding RNAs in Archaea. *Curr. Opin. Microbiol.* 8, 685–694.

Denu, J. M., Stuckey, J. A., Saper, M. A., and Dixon, J. E. (1996). Form and function in protein dephosphorylation. *Cell* 87, 361–364.

Der, S. D., Zhou, A., Williams, B. R., and Silverman, R. H. (1998). Identification of genes differentially regulated by interferon alpha, beta, or gamma using oligonucleotide arrays. *Proc. Natl. Acad. Sci. U.S.A.* 95, 15623–15628.

Dratz, E.A., and Grieco, P.A. (2009). *Novel Zwitterionic Fluorescent Dyes for Labeling in Proteomic and Other Biological Analyses.* USA patent application.

Dratz, E.A., and Grieco, P.A. (2010). *Novel Zwitterionic Fluorescent Dyes for Labeling in Proteomic and Other Biological Analyses.* USA patent application.

Fu, C. Y., and Johnson, J. E. (2012). Structure and cell biology of archaeal virus STIV. *Curr. Opin. Virol.* 2, 122–127.

Furman, L. M., Maaty, W. S., Petersen, L. K., Ettayebi, K., Hardy, M. E., and Bothner, B. (2009). Cysteine protease activation and apoptosis in murine norovirus infection. *Virol. J.* 6.

Garrett, R. A., Shah, S. A., Vestergaard, G., Deng, L., Gudbergsdottir, L., Kenchappa, C. S., et al. (2011a). CRISPR-based immune systems of the sulfolobales: complexity and diversity. *Biochem. Soc. Trans.* 39, 51–57.

Garrett, R. A., Vestergaard, G., and Shah, S. A. (2011b). Archaeal CRISPR-based immune systems: exchangeable functional modules. *Trends Microbiol.* 19, 549–556.

Gharbi, S., Gaffney, P., Yang, A., Zvelebil, M. J., Cramer, R., Waterfield, M. D., et al. (2002). Evaluation of two-dimensional differential gel electrophoresis for proteomic expression analysis of a model breast cancer cell system. *Mol. Cell Proteomics* 1, 91–98.

Gorg, A., Weiss, W., and Dunn, M. J. (2004). Current two-dimensional electrophoresis technology for proteomics. *Proteomics* 4, 3665–3685.

Happonen, L. J., Redder, P., Peng, X., Reigstad, L. J., Prangishvili, D., and Butcher, S. J. (2010). Familial relationships in hyperthermo- and acidophilic Archaeal viruses. *J. Virol.* 84, 4747–4754.

Janecek, S., and Blesak, K. (2011). Sequence-structural features and evolutionary relationships of family GH57 alpha-amylases and their putative alpha-amylase-like homologues. *Protein J.* 30, 429–435.

Jeon, S. J., Fujiwara, S., Takagi, M., Tanaka, T., and Imanaka, T. (2002). Tk-PTP, protein tyrosine/serine phosphatase from hyperthermophilic archaeon Thermoeoeeus kodakaraensis KOD1: enzymatic characteristics and identification of its substrate proteins. *Biochem. Biophys. Res. Commun.* 295, 508–514.

Kato, D., Boatright, K. M., Berger, A. B., Nazif, T., Blum, G., Ryan, C., et al. (2005). Activity-based probes that target diverse cysteine protease families. *Nat. Chem. Biol.* 1, 33–38.

Kessler, A., Brinkman, A. B., Van Der Oost, J., and Prangishvili, D. (2004). Transcription of the rod-shaped viruses SIRV1 and SIRV2 of the hyperthermophilic archaeon Sulfolobus. *J. Bacteriol.* 186, 7745–7753.

Khayat, R., Fu, C. Y., Ortmann, A. C., Young, M. J., and Johnson, J. E. (2010). The architecture and chemical stability of the archaeal Sulfolobus turreted icosahedral virus. *J. Virol.* 84, 9575–9583.

Khayat, R., Tang, L., Larson, E. T., Lawrence, C. M., Young, M., and Johnson, J. E. (2005). Structure of an archaeal virus capsid protein reveals a common ancestry to eukaryotic and bacterial viruses. *Proc. Natl. Acad. Sci. U.S.A.* 102, 18944–18949.

Kim, S., and Lee, S. B. (2005). Identification and characterization of Sulfolobus solfataricus D-gluconate dehydratase: a key enzyme in the non-phosphorylated Entner–Doudoroff pathway. *Biochem. J.* 387, 271–280.

Kim, Y. T., and Churchich, J. E. (1989). Sequence of the cysteinyl-containing peptides of 4-aminobutyrate aminotransferase – identification of sulfhydryl residues involved in intersubunit linkage. *Eur. J. Biochem.* 181, 397–401.

Krishna, R. G., and Wold, F. (1993). Post-translational modification of proteins. *Adv. Enzymol. Relat. Areas Mol. Biol.* 67, 265–298.

Kunin, V., Sorek, R., and Hugenholtz, P. (2007). Evolutionary conservation of sequence and secondary structures in CRISPR repeats. *Genome Biol.* 8, R61.

Kurtz, D. M. Jr. (2006). Avoiding high-valent iron intermediates: superoxide reductase and rubrerythrin. *J. Inorg. Biochem.* 100, 679–693.

Kvint, K., Nachin, L., Diez, A., and Nystrom, T. (2003). The bacterial universal stress protein: function and regulation. *Curr. Opin. Microbiol.* 6, 140–145.

Larson, E. T., Eilers, B., Menon, S., Reiter, D., Ortmann, A., Young, M. J., et al. (2007a). A winged-helix protein from Sulfolobus turreted icosahedral virus points toward stabilizing disulfide bonds in the intracellular proteins of a hyperthermophilic virus. *Virology* 368, 249–261.

Larson, E. T., Eilers, B. J., Reiter, D., Ortmann, A. C., Young, M. J., and Lawrence, C. M. (2007b). A new DNA binding protein highly conserved in diverse crenarchaeal viruses. *Virology* 363, 387–396.

Larson, E. T., Reiter, D., Young, M., and Lawrence, C. M. (2006). Structure of A197 from Sulfolobus turreted icosahedral virus: a crenarchaeal viral glycosyltransferase exhibiting the GT-A fold. *J. Virol.* 80, 7636–7644.

Lawrence, C. M., Menon, S., Eilers, B. J., Bothner, B., Khayat, R., Douglas, T., et al. (2009). Structural and functional studies of archaeal viruses. *J. Biol. Chem.* 284, 12599–12603.

Lee, P. S., Shaw, L. B., Choe, L. H., Mehra, A., Hatzimanikatis, V., and Lee, K. H. (2003). Insights into the relation between mRNA and protein expression patterns: II. Experimental observations in Escherichia coli. *Biotechnol. Bioeng.* 84, 834–841.

Li, L. W., and Dixon, J. E. (2000). Form, function, and regulation of protein tyrosine phosphatases and their involvement in human diseases. *Semin. Immunol.* 12, 75–84.

Lintner, N. G., Frankel, K. A., Tsutakawa, S. E., Alsbury, D. L., Copie, V., Young, M. J., et al. (2011a). The structure of the CRISPR-associated protein Csa3 provides insight into the regulation of the CRISPR/Cas system. *J. Mol. Biol.* 405, 939–955.

Lintner, N. G., Kerou, M., Brumfield, S. K., Graham, S., Liu, H. T., Naismith, J. H., et al. (2011b). Structural and functional characterization of an archaeal clustered regularly interspaced short palindromic repeat (CRISPR)-associated complex for antiviral defense (CASCADE). *J. Biol. Chem.* 286, 21643–21656.

Liu, S. J., Zhou, B., Yang, H. Y., He, Y. T., Jiang, Z. X., Kumar, S., et al. (2008). Aryl vinyl sulfonates and sulfones as active site-directed and mechanism-based probes for protein tyrosine phosphatases. *J. Am. Chem. Soc.* 130, 8251–8260.

Liu, Y. S., Patricelli, M. P., and Cravatt, B. F. (1999). Activity-based protein profiling: the serine hydrolases. *Proc. Natl. Acad. Sci. U.S.A.* 96, 14694–14699.

Maaty, W. S., Selvig, K., Ryder, S., Tarlykov, P., Hilmer, J. K., Heinemann, J., et al. (2012). Proteomic analysis of Sulfolobus solfataricus during Sulfolobus turreted icosahedral virus infection. *J. Proteome Res.* 11, 1420–1432.

Maaty, W. S., Wiedenheft, B., Tarlykov, P., Schaff, N., Heinemann, J., Robison-Cox, J., et al. (2009). Something old, something new, something borrowed; how the thermoacidophilic archaeon Sulfolobus solfataricus responds to oxidative stress. *PLoS ONE* 4:e6964. doi:10.1371/journal.pone.0006964

Maaty, W. S. A., Ortmann, A. C., Dlakic, M., Schulstad, K., Hilmer, J. K., Liepold, L., et al. (2006). Characterization of the archaeal thermophile Sulfolobus turreted icosahedral virus validates an evolutionary link among double-stranded DNA viruses from all domains of life. *J. Virol.* 80, 7625–7635.

Macario, A. J., Lange, M., Ahring, B. K., and De Macario, E. C. (1999). Stress genes and proteins in the archaea. *Microbiol. Mol. Biol. Rev.* 63, 923–967. (Table of contents).

Mehra, A., Lee, K. H., and Hatzimanikatis, V. (2003). Insights into the relation between mRNA and protein expression patterns: I. Theoretical considerations. *Biotechnol. Bioeng.* 84, 822–833.

Mojica, F. J., Diez-Villasenor, C., Garcia-Martinez, J., and Soria, E. (2005). Intervening sequences of regularly spaced prokaryotic repeats derive from foreign genetic elements. *J. Mol. Evol.* 60, 174–182.

Neumann, S., Schuchardt, K., Reske, A., Reske, A., Emmrich, P., and Paschke, R. (2004). Lack of correlation for

sodium iodide symporter mRNA and protein expression and analysis of sodium iodide symporter promoter methylation in benign cold thyroid nodules. *Thyroid* 14, 99–111.

Nishimasu, H., Fushinobu, S., Shoun, H., and Wakagi, T. (2004). The first crystal structure of the novel class of fructose-1,6-bisphosphatase present in thermophilic archaea. *Structure* 12, 949–959.

Nomura, D. K., Dix, M. M., and Cravatt, B. F. (2010). Activity-based protein profiling for biochemical pathway discovery in cancer. *Nat. Rev. Cancer* 10, 630–638.

Omer, A. D., Zago, M., Chang, A., and Dennis, P. P. (2006). Probing the structure and function of an archaeal C/D-box methylation guide sRNA. *RNA* 12, 1708–1720.

Ortmann, A. C., Brumfield, S. K., Walther, J., McInnerney, K., Brouns, S. J. J., Van De Werken, H. J. G., et al. (2008). Transcriptome analysis of infection of the Archaeon Sulfolobus solfataricus with Sulfolobus turreted icosahedral virus. *J. Virol.* 82, 4874–4883.

Ortmann, A. C., and Suttle, A. S. (2009). Determination of virus abundance by epifluorescence microscopy. *Methods Mol. Biol.* 501, 87–95.

Peng, X., Kessler, A., Phan, H., Garrett, R. A., and Prangishvili, D. (2004). Multiple variants of the archaeal DNA rudivirus SIRV1 in a single host and a novel mechanism of genomic variation. *Mol. Microbiol.* 54, 366–375.

Prangishvili, D., Arnold, H. P., Gotz, D., Ziese, U., Holz, I., Kristjansson, J. K., et al. (1999). A novel virus family, the rudiviridae: structure, virus-host interactions and genome variability of the Sulfolobus viruses SIRV1 and SIRV2. *Genetics* 152, 1387–1396.

Prangishvili, D., and Garrett, R. A. (2005). Viruses of hyperthermophilic crenarchaea. *Trends Microbiol.* 13, 535–542.

Prangishvili, D., and Quax, T. E. F. (2011). Exceptional virion release mechanism: one more surprise from archaeal viruses. *Curr. Opin. Microbiol.* 14, 315–320.

Quax, T. E. F., Lucas, S., Reimann, J., Pehau-Arnaudet, G., Prevost, M. C., Forterre, P., et al. (2011). Simple and elegant design of a virion egress structure in archaea. *Proc. Natl. Acad. Sci. U.S.A.* 108, 3354–3359.

Ray, W. K., Keith, S. M., Desantis, A. M., Hunt, J. P., Larson, T. J., Helm, R. F., et al. (2005). A phosphohexomutase from the archaeon Sulfolobus solfataricus is covalently modified by phosphorylation on serine. *J. Bacteriol.* 187, 4270–4275.

Rice, G., Stedman, K., Snyder, J., Wiedenheft, B., Willits, D., Brumfield, S., et al. (2001). Viruses from extreme thermal environments. *Proc. Natl. Acad. Sci. U.S.A.* 98, 13341–13345.

Rice, G., Tang, L., Stedman, K., Roberto, F., Spuhler, J., Gillitzer, E., et al. (2004). The structure of a thermophilic archaeal virus shows a double-stranded DNA viral capsid type that spans all domains of life. *Proc. Natl. Acad. Sci. U.S.A.* 101, 7716–7720.

Sadaghiani, A. M., Verhelst, S. H. L., and Bogyo, M. (2007). Tagging and detection strategies for activity-based proteomics. *Curr. Opin. Chem. Biol.* 11, 20–28.

Schicher, M., Morak, M., Birner-Gruenberger, R., Kayer, H., Stojcic, B., Rechberger, G., et al. (2010). Functional proteomic analysis of lipases and esterases in cultured human adipocytes. *J. Proteome Res.* 9, 6334–6344.

She, Q., Singh, R. K., Confalonieri, F., Zivanovic, Y., Allard, G., Awayez, M. J., et al. (2001). The complete genome of the crenarchaeon Sulfolobus solfataricus P2. *Proc. Natl. Acad. Sci. U.S.A.* 98, 7835–7840.

Shevchenko, A., Jensen, O. N., Podtelejnikov, A. V., Sagliocco, F., Wilm, M., Vorm, O., et al. (1996). Linking genome and proteome by mass spectrometry: large-scale identification of yeast proteins from two dimensional gels. *Proc. Natl. Acad. Sci. U.S.A.* 93, 14440–14445.

Simon, G. M., and Cravatt, B. F. (2010). Activity-based proteomics of enzyme superfamilies: serine hydrolases as a case study. *J. Biol. Chem.* 285, 11051–11055.

Singaravelu, R., Blais, D. R., McKay, C. S., and Pezacki, J. P. (2010). Activity-based protein profiling of the hepatitis C virus replication in Huh-7 hepatoma cells using a non-directed active site probe. *Proteome Sci.* 8, 1–15.

Singh, A., and Hespanha, J. P. (2009). Evolution of gene auto-regulation in the presence of noise. *IET Syst. Biol.* 3, 368–378.

Snyder, J. C., Brumfield, S. K., Peng, N., She, Q. X., and Young, M. J. (2011). Sulfolobus turreted icosahedral virus c92 protein responsible for the formation of pyramid-like cellular lysis structures. *J. Virol.* 85, 6287–6292.

Speers, A. E., and Cravatt, B. F. (2004). Profiling enzyme activities in vivo using click chemistry methods. *Chem. Biol.* 11, 535–546.

Stravopodis, D. J., and Kyrpides, N. C. (1999). Identification of protein-tyrosine phosphatases in archaea. *J. Mol. Evol.* 48, 625–627.

Taniguchi, Y., Choi, P. J., Li, G. W., Chen, H. Y., Babu, M., Hearn, J., et al. (2010). Quantifying E-coli proteome and transcriptome with single-molecule sensitivity in single cells. *Science* 329, 533–538.

Tannu, N. S., and Hemby, S. E. (2006). Two-dimensional fluorescence difference gel electrophoresis for comparative proteomics profiling. *Nat. Protoc.* 1, 1732–1742.

Tonge, R., Shaw, J., Middleton, B., Rowlinson, R., Rayner, S., Young, J., et al. (2001). Validation and development of fluorescence two-dimensional differential gel electrophoresis proteomics technology. *Proteomics* 1, 377–396.

Tonks, N. K., and Neel, B. G. (2001). Combinatorial control of the specificity of protein tyrosine phosphatases. *Curr. Opin. Cell Biol.* 13, 182–195.

Van den Bergh, G., Clerens, S., Cnops, L., Vandesande, F., and Arckens, L. (2003). Fluorescent two-dimensional difference gel electrophoresis and mass spectrometry identify age-related protein expression differences for the primary visual cortex of kitten and adult cat. *J. Neurochem.* 85, 193–205.

Wang, Q. Y., Patel, S. J., Vangrevelinghe, E., Xu, H. Y., Rao, R., Jaber, D., et al. (2009). A small-molecule dengue virus entry inhibitor. *Antimicrob. Agents Chemother.* 53, 1823–1831.

Wiedenheft, B., Stedman, K., Roberto, F., Willits, D., Gleske, A. K., Zoeller, L., et al. (2004). Comparative genomic analysis of hyperthermophilic archaeal fuselloviridae viruses. *J. Virol.* 78, 1954–1961.

Williamson, J. M., and Meister, A. (1982). Effect of sulfhydryl-group modification on the activities of 5-Oxo-L-prolinase. *J. Biol. Chem.* 257, 9161–9172.

Wirth, J. F., Snyder, J. C., Hochstein, R. A., Ortmann, A. C., Willits, D. A., Douglas, T., et al. (2011). Development of a genetic system for the archaeal virus Sulfolobus turreted icosahedral virus (STIV). *Virology* 415, 6–11.

Yuan, C. S., Aultriche, D. B., and Borchardt, R. T. (1996). Chemical modification and site-directed mutagenesis of cysteine residues in human placental S-adenosylhomocysteine hydrolase. *J. Biol. Chem.* 10, 581–581.

Zhang, J., Rouillon, C., Kerou, M., Reeks, J., Brugger, K., Graham, S., et al. (2012). Structure and mechanism of the CMR complex for CRISPR-mediated antiviral immunity. *Mol. Cell* 45, 303–313.

Conflict of Interest Statement: The authors declare that the research was conducted in the absence of any other commercial or financial relationships that could be construed as a potential conflict of interest. E.A. Dratz and P.A. Grieco are principles in Zdye LLC that has been developing zwitterionic dyes for proteomic analysis.

Received: 18 June 2012; accepted: 14 November 2012; published online: 10 December 2012.

Citation: Maaty WS, Steffens JD, Heinemann J, Ortmann AC, Reeves BD, Biswas SK, Dratz EA, Grieco PA, Young MJ and Bothner B (2012) Global analysis of viral infection in an archaeal model system. Front. Microbio. ***3****:411. doi: 10.3389/fmicb.2012.00411*

This article was submitted to Frontiers in Virology, a specialty of Frontiers in Microbiology.